Durham E-Theses

Transcriptional Regulation of Metabolic Genes by the Basic Leucine Zipper Transcription Factor Hac1ip and Nutrient Stimuli

PARMAR, VIPULKUMAR,MOHANLAL

Transcriptional Regulation of Metabolic Genes by the Basic Leucine Zipper Transcription Factor Hac1^{i}p and Nutrient Stimuli

Vipulkumar Mohanlal Parmar

This thesis is submitted as part of the requirements for the
award of the
Degree of Doctor of Philosophy
of the
University of Durham

2012

ABSTRACT

Saccharomyces cerevisiae cells respond to nutrients in their environment by altering their metabolic and transcriptional state in order to optimise the use of available nutrients and decide which of the several developmental pathways to pursue. In the yeast *S. cerevisiae*, meiosis and pseudohyphal growth are two major differentiation outcomes in response to nitrogen starvation. A central component of unfolded protein response pathway, the bZIP transcription factor Hac1[i]p, negatively regulates meiosis and pseudohyphal growth. The present study investigates this negative regulatory mechanism at early meiotic genes by Hac1[i]p in nitrogen-rich conditions. Regulation of transcription by Ume6p transcriptional regulator, Rpd3p-Sin3p histone deacetylase complex and Isw2p-Itc1p chromatin remodelling complex at URS1 was also investigated here. We also tested for induction of pseudohyphal growth in diploids from SK1 genetic background in response to nitrogen starvation conditions known to induce meiosis.

I constructed destabilised β-galactosidase reporters expressed from URS1-*CYC1*-Ub-X-*lacZ* reporters to analyze transcriptional activity at URS1 site of early meiotic genes in nutrient rich conditions. The data presented here successfully demonstrates Hac1[i]p-mediated repression at URS1 sites in nitrogen-rich conditions. URS1-*CYC1*-Ub-X-*lacZ* reporters were expressed in mitotic repression machinery mutants (*ume6Δ*, *rpd3Δ*, *sin3Δ*, *isw2Δ* and *itc1Δ*) under nitrogen rich conditions. The data presented here from these experiments not only corroborates their known role in repression at URS1 but also suggested regulation at additional sites in the minimal *CYC1* promoter. Deletion of Sin3p suggested independent repression function separable from Rpd3p. Isw2p also acts independently of Itc1p at sites other than URS1. We also show that pseudohyphal growth was stimulated by non-fermentable carbon sources in sporulation efficient SK1 genetic background. The data also indicates that stimulation of pseudohyphal growth by non-fermentable carbon sources does not require respiration function or functional mitochondrial RTG pathway.

Ime1 and Ime2 are required for pseudohyphal growth of
***Saccharomyces cerevisiae* on nonfermentable carbon sources.**

Strudwick N, Brown M, **Parmar VM**, Schröder M.

Durham University, School of Biological and Biomedical Sciences, Durham DH1 3LE, United Kingdom.

Abstract

Pseudohyphal growth and meiosis are two differentiation responses to nitrogen starvation of diploid Saccharomyces cerevisiae. Nitrogen starvation in the presence of fermentable carbon sources is thought to induce pseudohyphal growth, whereas nitrogen and sugar starvation induces meiosis. In contrast to the genetic background routinely used to study pseudohyphal growth (Σ1278b), nonfermentable carbon sources stimulate pseudohyphal growth in the efficiently sporulating strain SK1. Pseudohyphal SK1 cells can exit pseudohyphal growth to complete meiosis. Two stimulators of meiosis, Ime1 and Ime2, are required for pseudohyphal growth of SK1 cells in the presence of nonfermentable carbon sources. Epistasis analysis suggests that Ime1 and Ime2 act in the same order in pseudohyphal growth as in meiosis. The different behaviors of strains SK1 and Σ1278b are in part attributable to differences in cyclic AMP (cAMP) signaling. In contrast to Σ1278b cells, hyperactivation of cAMP signaling using constitutively active Ras2(G19V) inhibited pseudohyphal growth in SK1 cells. Our data identify the SK1 genetic background as an alternative genetic background for the study of pseudohyphal growth and suggest an overlap between signaling pathways controlling pseudohyphal growth and meiosis. Based on these findings, we propose to include exit from pseudohyphal growth and entry into meiosis in the life cycle of S. cerevisiae.

ACKNOWLEDGEMENTS

I would like to thank Dr Martin Schröder for providing me the opportunity to work in this exciting research area. I am also indebted to Dr D.J.Mohan and Rakesh Sir for introducing me to the wonderful field of biology and making it interesting. Many thanks to Natalie, Sergej, Claire, Saeed, Ewa, Monika, Louise, David, Sid, Adina and Max from lab 2 for their good company and tolerating me and also a word of thanks for Lesley, Prashant, Usha and Paud. It was great working with you guys.

I am very grateful to all my family who have constantly supported me during this research journey. Thanks to my nieces and nephews Ishii, Abeer, Vishwanshi, Dheeya and Mitul and cousins Manya and Maitry, who have always cheered me up. I would also like to thank my dear friends Jignesh, Paramjeet, Priya, Kshitish and Sapan and their family. A special thanks to my Late Father-in-law Mr. Tilak Raj Bajaj, whose humor, words of encouragement and constant support have boosted me from time to time.

A very special word for my dear Wife Tanu, who has constantly and unconditionally supported me in all my ups and downs, put up with my odd hours and has been my inspiration. This work is dedicated to my wife and my parents.

This acknowledgement would also be incomplete if I did not thank millions of yeasts who sacrificed their life in the process of generating data this thesis. Thank you yeast.

Declaration

No material contained herein has been previously submitted for any other degree.Except where acknowledged, all material is the work of the author.

Statement of Copyright

The copyright of this thesis rests with author. No quotation from it should be published without his prior written consent and information derived from it should be acknowledged.

TABLE OF CONTENTS

Chapter 1 INTRODUCTION

Chapter 2 MATERIALS AND METHODS

Chapter 3 DESTABILISED β-GALACTOSIDASE REPORTERS: CONSTRUCTION, VALIDATION AND TRANSCRIPTIONAL REGULATION OF URS1 CONTROLLED EARLY MEIOTIC GENES

Chapter 4 TRANSCRIPTIONAL REGULATION OF METABOLIC GENES UNDER NUTRIENT RICH CONDITIONS

Chapter 5 PSEUDOHYPHAL GROWTH ON NON-FEREMENTABLE CARBON SOURCES

Chapter 6 CONCLUSIONS AND FUTURE WORK

LIST OF FIGURES

x

LIST OF TABLES

LIST OF ABBREVIATIONS

A_{600}nm	Absorbance measured at 600nm wavelength
ATP	Adenosine 5'-triphosphate
BSA	bovine serum albumin
$CHCl_3$	Chloroform
CIAP	Calf intestine alkaline phosphatase
C-SPO medium	Complete sporulation medium
DAG	Diacylglycerol
DNA	deoxyribonucleic acid
dNTP	deoxynucleoside triphosphate
DOC	Deoxycorticosterone
EDTA	Ethylenediamine tetraacetic acid
ER	Endoplasmic reticulum
EtOH	Ethanol
GRE	Glucocorticoid response elements
H_2O	Hydrogen dioxide or water
IPTG	isopropyl-β-D-thiogalactopyranoside
Kb	Kilobases
kDa	kilo Dalton (unit in mass)
KOAc	Potassium acetate
LB	Lennox broth or lysogeny broth
LiOAc	Lithium acetate
M	Molar
mM	millimolar
mg	milligrams
$MgCl_2$	Magnesium chloride
min	minutes
ml	millilitre
NAD^+	nicotinamide adenine dinucleotide
Na_2CO_3	Sodium carbonate
ng	nanogram
Ø	diameter
ºC	degree celsius
PCR	Polymerase chain reaction
PEG4000	Polyethylene glycol 4000
PSP2	Presporulation medium
RAS2	GTP binding protein
RLB	Reporter lysis buffer
RNA	Ribonucleic acid
RNase A	Ribonuclease A
RPI	Roche protease inhibitor
rpm	revolutions per minute
RT	Room temperature
s	Seconds
SD	Synthetic dextrose meduium
SDS	Sodium dodecyl sulfate
SLA	synthetic low ammonium
TE	Tris ethylene diaminetetratetraacetic acid

Tris	tris(hydroxymethyl)aminomethane
Tris·HOAc	tris acetic acid
Tris-HCl	tris hydrochloric acid
Tween 20	Polysorbate 20
U	Units
Ub	Ubiquitin
X-gal	5-bromo4-chloro-3-indolyl-β-D-galactopyranoside
YPAc	Yeast extract peptone Acetate medium
μgm	microgram
μM	micromolar
μm	micrometer or micron or 1×10^{-6} of a meter
YNB	Yeast nitrogen base
YPAc	Yeast extract peptone acetate medium
YPD	Yeast extract peptone dextrose medium
β-gal	β-galactosidase
Δ	Deletion
λ	wavelength
μl	microlitre

Genes and pathways

CYC1	Cytochrome *c,* isoform 1
GPCR	G protein coupled receptor
HAC1	Homologue of ATF/CREB1
HOG	High osmolarity gylcerol
IME1	Initiator of meiosis 1
IRE1	Inositol requiring enzyme 1
ISW2	Imitation switch protein 2
ITC1	Isw2 complex subunit
MAPK	Mitogen activated protein kinase
PKA	Protein kinase A
RPD3	Histone deacetylase of *RPD3-SIN3* complex
SIN3	Switch Independent 3, transcriptional regulator
UAS	Upstream activating sequence
UPR	Unfolded protein response
UPRE	Unfolded protein response element
URS1	Upstream repressing site 1

Chapter 1

Introduction

INTRODUCTION

Organisms respond to a number of stimuli in their environment ranging from temperature, osmolarity, pH, nutrition, etc. The budding yeast *Saccharomyces cerevisiae* also responds to its nutritional environment in different ways to a number of different nutritional cues. Limitation of one or more key nutrients can trigger a variety of developmental responses. *S. cerevisiae* diploids undergo meiosis in response to nutrient starvation and form spores which stay dormant until they germinate in favourable conditions. Alternatively the diploid cells can form pseudohyphae, which are synchronously growing elongated cells branching out from an edge of the colony to forage for nutrients. Similar responses in haploids are termed as filamentation, which is marked by invasive growth that is capable of invading the underlying medium and increased cell-cell adhesion. Haploid or diploid cells can stop mass accumulation, arrest cell cycle progression and enter G_0 state. These differentiation events require a lot of metabolic, transcriptional and morphological, reprogramming. The role of nutrient sensing and signalling is to sense the nutritional state of the cell and its environment and initiate signalling that would allow accumulation of cell mass. Nutrient signalling pathways also optimize the nutrient conversion to cell mass and indirectly regulate cell proliferation and developmental pathways. These processes are performed by various signalling cascades initiated in response to specific nutritional niches and cross talk between these pathways executes the cell's response. There has been considerable advance in understanding of the components of different signalling pathways but we do not, as of yet, understand completely the molecular mechanisms behind how cells sense nutrients and respond into signals to decide its cell fate.

1.1 Nutrient signalling pathways in *S. cerevisiae*:

Diploid *S. cerevisiae* cells respond to nutrients in their environment by altering their metabolic and transcriptional state to optimise the use of available nutrients and to decide which of the several developmental pathways to pursue. There are number of signalling pathways that respond to availability and type of carbon source, nitrogen source, amino acids and other nutritional cues and mediate cell's response (**Figure 1.1**). The first step towards signalling is sensing of cell's extracellular nutritional

environment and intracellular concentration of nutrients. Carbon source, nitrogen source and amino acid as nutrients have been discussed here.

1.1.1 Carbon source

S. cerevisiae can grow readily on fermentable carbon sources by fermentation and utilise non-fermentable carbon sources by respiration. Glucose is preferred over other fermentable carbon source sources and more so over non-fermentable carbon sources. This repression of utilization of other carbon sources including the non-fermentable carbon sources is called glucose repression (Gancedo, 1998). Glucose sensing occurs through the G-protein coupled receptor (GPCR) Gpr1p, which interacts with the G protein α-subunit Gpa2p and transmits the signal [**Figure 1.1** and (Kraakman et al., 1999; Xue et al., 1998; Yun et al., 1997; Yun et al., 1998)]. Besides GPCRs, *S. cerevisiae* also express a family of hexose transporters that are involved in sugar sensing or transport. *RGT2* and *SNF3* are members of this family, which encode transmembrane proteins that act as low affinity and high affinity sensors of glucose and initiate signalling of a pathway that controls the expression of hexose transporter genes (Özcan et al., 1996). However, direct binding of glucose has not been shown for both the proteins. Hexose kinases Hxk1p, Hxk2p and Glk1p are intracellular proteins that bind to glucose and phosphorylate it at C6 (Bianconi, 2003; Clifton et al., 1993; Lobo and Maitra, 1977; Walsh et al., 1983). This is the first step in metabolism of glucose to form glucose 6-phosphate (Rose et al., 1991). Two signalling pathways respond to glucose, the first through PKA mediated monomeric Ras GTPases and a second using a Gα homolog, Gpa2p and a putative G-protein coupled receptor, Gpr1p (Batlle et al., 2003; Broach and Deschenes, 1990; Harashima et al., 2006; Rolland et al., 2002). Snf1p kinase is essential for growth on less preferred fermentable carbon sources such as sucrose, galactose and maltose or non-fermentable carbon sources like glycerol and ethanol. Besides its requirement for growth in the absence of glucose, Snf1p is also required in a number of processes such as meiosis, ageing, glycogen accumulation, inositol growth and pseudohyphal growth (Ashrafi et al., 2000; Honigberg and Purnapatre, 2003; Kuchin et al., 2002; Shirra and Arndt, 1999). Snf1p is a member of the AMP-activated protein kinase family that responds to AMP:ATP ratio. In the absence of glucose, the Snf1p

serine/threonine protein kinase activates Cat8p and Sip4p and represses Mig1p regulating transcriptional changes associated with glucose derepression (Hong et al., 2003; Lesage et al., 1996; Nath et al., 2003; Rahner et al., 1996; Randez-Gil et al., 1997). Protein kinase A (PKA), Snf1p, and the Rgt2p-Snf3p glucose sensors play redundant and overlapping roles in carbon source signalling (Rolland et al., 2002).

1.1.2 Nitrogen source

Yeast cells respond to the availability and type of nitrogen source. Preferred nitrogen sources are metabolised over less preferred nitrogen sources. These favourable nitrogen sources enhance growth rate and repress metabolism of less preferred nitrogen source. Ammonium and glutamine are preferred nitrogen sources and their addition to cells growing on alternate nitrogen source results in repression of large collection of genes involved in the nitrogen catabolism. This is also called nitrogen discrimination pathway (NDP) or nitrogen catabolite repression (NCR) (Hofman-Bang, 1999). The quality of nitrogen sources and their availability informs metabolic processes and influences the developmental decisions of the cell. The presence of high quality nitrogen sources prevents pseudohyphal growth or invasive growth and the presence of any nitrogen source prevents meiosis and sporulation. Mep1p, Mep2p and Mep3p are the ammonium transporters in *S. cerevisiae* that sense extracellular nitrogen (**Figure 1.1**). Mep2p, and Mep1p are required for nitrogen sensing and activation of cAMP-PKA pathway following addition of nitrogen source to nitrogen starved cells (Van Nuland et al., 2006). Overexpression of Mep2p under nitrogen replete condition activates transcriptional profile consistent with activation of MAPK pathway (Lorenz and Heitman, 1998a; Rutherford et al., 2008). The activity of Mep2p, but not Mep1p or Mep3p is required for induction of pseudohyphal growth (Lorenz and Heitman, 1997). However the details of Mep2p signalling are not fully elucidated. Nitrogen starvation induces *GPR1* transcription and Gpa2p-Gpr1p has been implicated in nitrogen sensing as *gpa2* and *gpr1* strains show a defect in pseudohyphal differentiation (Kübler et al., 1997; Lorenz and Heitman, 1997; Lorenz et al., 2000b; Tamaki et al., 2000). But the primary function of Gpr1p is glucose sensing as Gpr1p binds to glucose with low affinity and Gpr1p may be integrating glucose and nitrogen signals in the pseudohyphal pathway.
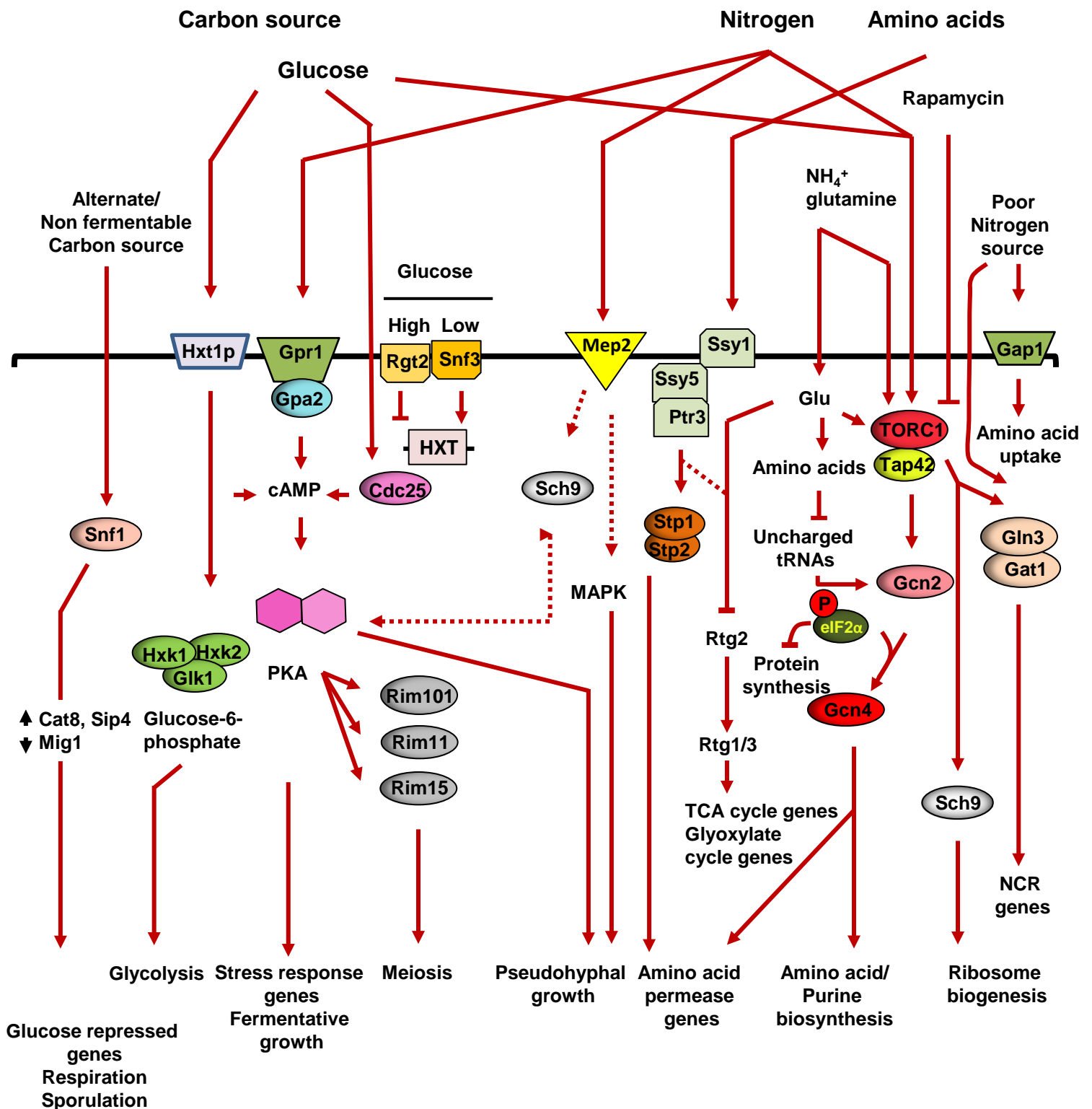
Figure 1.1 Nutritional signalling pathways in *S cerevisiae*. Nutrients are sensed by *S. cerevisiae* through different sensors to initiate signalling pathways that may function separately or communicate with each other and may converge evoking a specific response. Carbon and nitrogen sources form major signalling pathways that regulate growth, metabolism, stress response and developmental pathways. Sensing and subsequent response to change in carbon sources are shown here. In presence of glucose plasma membrane sensing proteins Snf3p, Rgt2p, Gpr1p and Hxk2p lead to metabolic changes like glycolysis, induce differentiation pathways like meiosis or

4

pseudohyphal growth. Snf1p is activated in presence of alternate carbon source or non fermentable carbon sources to induce expression of glucose repressed genes. Nitrogen sources are sensed through ammonium permease Mep2p and possibly through Gpa2p-Gpr1p. The SPS (Ssy1p-Ptr3p-Ssy5p) system senses extracellular amino acid concentration and upregulates amino acid permease gene expression, while the intracellular amino acid is sensed by a mechanism involving uncharged tRNAs and Gcn2p thereby activating GCN pathway. As a result general protein synthesis is repressed by phosphorylated eIF2α with the selective exception of Gcn4p to upregulate amino acid biosynthesis. General amino acid permease Gap1p is stabilised in absence of a high quality nitrogen source to induce uptake of amino acids. Growth on poor nitrogen sources also activates Gln3p and Gat1p to induce nitrogen catabolite repression (NCR) genes. Under nutrient-rich conditions, TORC1 inhibits the function of transcriptional activators that are involved in nitrogen catabolite-repression (Gat1p, Gln3p), retrograde response (Rtg1p, Rtg3p) while activates those involved in ribosome biosynthesis (Sch9p). Black arrows indicate transcriptional upregulation or downregulation. See text for further details.

1.1.3 Amino acid

The sensing of amino acid availability both for incorporation into protein and as nitrogen source in biosynthetic reactions occurs through signalling cascades in yeast. The SPS (Ssy1p-Ptr3p-Ssy5p) signalling system senses external amino acid concentrations (Forsberg and Ljungdahl, 2001). The Ssy1p sensor protein, which resembles an amino acid permease, signals to two transcription factors Stp1p and Stp2p, targeting mainly genes that encode amino acid metabolizing enzymes and amino acid transporters (Andreasson and Ljungdahl, 2002). Internal amino acids are sensed by general control of amino acid biosynthesis (GCN). This intracellular nitrogen sensing mechanism involves association of uncharged tRNA and Gcn2p kinase leading to its activation. Gcn2p phosphorylates eIF2α in response to amino acid starvation and other stimuli, reducing global protein synthesis (Cherkasova and Hinnebusch, 2003; Dever, 2002; Hinnebusch, 2005; Hinnebusch and Natarajan, 2002). However, *GCN4* mRNA is upregulated by Gcn2p through upstream open reading frames (Mueller and Hinnebusch, 1986) and Gcn4p upregulates genes for biosynthesis of amino acids, the nitrogen source in the medium. The presence of preferable nitrogen source or high concentration of amino acids represses general amino acid permease Gap1p (Magasanik and Kaiser, 2002). Upon nitrogen limitation Gap1p expression is induced by two GATA transcription factors Gln3p and Gat1p (Stanbrough and Magasanik, 1996; Stanbrough et al., 1995). Gap1p is also implicated in activation of the PKA pathway that involves the protein Sch9p kinase on addition of amino acids to nitrogen starved cells (Donaton et al., 2003; Thevelein et al., 2005). Gln3p is a master regulator under alternative nitrogen sources along with Gat1p acting as transcriptional activators while Dal80p and Gzf3p acting as transcriptional repressors of NCR sensitive genes (Coffman et al., 1996; Cooper, 2002; Magasanik and Kaiser, 2002; Scherens et al., 2006). Limiting glutamine and TOR inhibitor rapamycin also activate Gln3p (Beck and Hall, 1999; Crespo et al., 2002). Glutamate and α-ketoglutarate are very important for nitrogen assimilation and therefore the pathways regulating the levels of glutamate are closely related to nitrogen regulation. The Retrograde (RTG) signalling pathway is one such pathway that regulates the genes of TCA cycle maintaining glutamate homeostasis in the cell. It is activated in response to mitochondrial defects or inactivation of key tricarboxylic acid (TCA) cycle enzymes (Butow and Avadhani, 2004; Liu and Butow, 1999) This

way yeast cells can assimilate nitrogen by conversion to ammonium and then condensation with α-ketoglutarate to form glutamate. Exogenous glutamate levels sensed by SPS-system negatively regulate Rtg2p (**Figure 1.1**). Cells utilising glucose repress citric acid cycle genes and maintain α-ketoglutarate levels from pyruvate and acetyl-CoA by the RTG signalling pathway. The citric acid cycle enzymes are responsive to heme-dependent Hap1p and heme independent Hap2-3-4-5p complex in the presence of alternative carbon sources (Liu and Butow, 1999). The RTG pathway consists of *RTG1* and *RTG3* encoding basic helix-loop-helix leucine zipper-(b-HLH/Zip) type transcription factors. Rtg1p and Rtg3p form a heterodimer to bind to target gene promoters. *RTG2* encodes a cytosolic protein with an N-terminal ATP-binding domain. Integrity of ATP-binding domain of Rtg2p is essential for its function. Rtg2p is required for Rtg3p dephosphorylation and nuclear translocation of Rtg1/3p. Rtg1/3p activates several genes of the TCA cycle, *CIT2* (encodes the peroxisomal isoform of citrate synthase) and *DLD3* (encodes cytosolic isoform of D-lactate dehydrogenase). Besides Rtg1p, Rtg2p and Rtg3p, Grrr1p also acts positively, while Mks1p, Lst8p and Bmh1-2p negatively regulate the RTG signalling pathway of mitochondria (Liu and Butow, 2006). Therefore RTG pathway provides a means to grow on poor nitrogen sources and maintains glutamate levels in the absence of mitochondrial function. The RTG pathway also regulates genes of the glyoxylate cycle, genes involved in β-oxidation of fatty acids and genes encoding enzymes of lysine biosynthesis (Chelstowska and Butow, 1995; Dilova et al., 2002).

1.1.4 The TOR signalling pathway

The TOR signalling pathway is a major integrator of nutrient-derived signals that in co-ordination with other signalling pathways controls cell growth and proliferation. Crosstalk of TOR signalling pathway and other pathways has been proposed to regulate responses to nitrogen/amino acid availability. Treatment of cells with rapamycin results in physiological changes like G1 cell cycle arrest, protein synthesis inhibition, glycogen accumulation and autophagy which closely resemble those observed in cells deprived of nutrients. TOR signalling is controlled by two distinct evolutionarily conserved multimeric protein complexes known as TORC1 and TORC2. Tor1p and Tor2p associate with Kog1, Tco89p and Lst8p in the protein

complex TORC1. In TORC2, Tor2p associates with Lst8p, Avo1p, Avo2p, Avo3p, Bit61p and Bit2p as a separate complex (Chen and Kaiser, 2003; Loewith et al., 2002; Reinke et al., 2004; Wedaman et al., 2003). TORC1 is rapamycin sensitive and is involved in nutrient signalling, while TORC2 is rapamycin insensitive and is involved in spatial control of cell growth, but a clear distinction of separate functions is not possible as the TORC1 component Kog1p also regulates actin polarization (Aronova et al., 2007; Loewith et al., 2002; Wang and Jiang, 2003). Tap42p is a direct target of TORC1 phosphorylation and regulates repression of stress regulated genes, nitrogen catabolite repression and retrograde signalling as well as crosstalk between TORC1 and general amino acid control (GAAC) response [**Figure 1.1** and (Cherkasova and Hinnebusch, 2003; Duvel et al., 2003; Rohde et al., 2004)]. During growth in preferred nitrogen sources, Gln3p is cytosolic but translocates to the nucleus by Sit4p-dependent phosphorylation when cells are shifted to poor nitrogen sources or upon rapamycin treatment and activates transcription of genes required for utilisation of less preferable nitrogen sources (Beck and Hall, 1999; Cardenas et al., 1999). Sit4p and Tap42p act in concert to dephosphorylate downstream targets in response to rapamycin, thus making Tap42p a positive regulator of phosphatase activity. Tap42p also acts in a similar fashion in rapamycin activation of RTG target genes (Duvel et al., 2003). The TORC1 protein kinase phosphorylates Sch9p and phosphorylation is required for activation of Sch9p (Urban et al., 2007). Sch9p plays a significant role in connecting TOR-dependent nutrient sensing to ribosome biogenesis and a major role in coupling the cell size to cell division (**Figure 1.1**). Sch9p is a protein kinase that induces ribosome biogenesis and represses genes involved in carboxylic acid metabolism when overexpressed and regulates a similar set of functions as Ras-PKA (Jorgensen et al., 2004; Zaman et al., 2009). Sch9p is rapidly dephosphorylated in response to rapamycin, carbon or nitrogen starvation, while Sch9p restores phosphorylation when shifted from ammonium to urea and addition of missing nutrient rapidly (Urban et al., 2007). Diminished Sch9p activity or deletion of *GPR1* induces genes required for sterol and cell wall biosynthesis. It has also been suggested that Sch9p mitigates the signalling activity of Gpa2p (Zaman et al., 2009). These results hint a possible crosstalk between TOR pathway and Gpa2p-PKA pathway through Sch9p. The Tor pathway often works in parallel with the cAMP-PKA pathway to control common targets and also intersects with other signalling networks, such as the GAAC response (Chen and Fink, 2006; Hinnebusch,

2005; Marion et al., 2004; Roosen et al., 2005; Urban et al., 2007; Zurita-Martinez and Cardenas, 2005). Several newly identified Tor substrates, Sch9p, Ypk1p and Slm1p, Slm2p, further link TOR function to amino acid signalling, actin organization, control of cell integrity and stress responses (Audhya et al., 2004; Bultynck et al., 2006; Daquinag et al., 2007; Fadri et al., 2005; Kamada et al., 2005; Mulet et al., 2006; Urban et al., 2007).

1.2   Differentiation responses in *Saccharomyces cerevisiae*:

Differentiation responses in *S. cerevisiae* are heavily regulated by the extracellular and intracellular nutrient environment. *S. cerevisiae* produce mitotic daughters when the nutrients are plentiful. However when the nutrients are scarce normal cell growth and mitosis ceases. The nitrogen starvation can induce two different responses in **a**/α diploid *S. cerevisiae*. In the presence of fermentable carbon sources yeast form can undergo morphological change to form pseudohyphae (Gimeno et al., 1992), while non-fermentable carbon source induces the **a**/α diploid cell to undergo meiosis and form an ascus (Herskowitz, 1988), which can again germinate when the nutrients are plentiful (Herman and Rine, 1997). Meiosis or sporulation plays an important role in the sexual life cycle of budding yeast S. *cerevisiae* and it is critical in generating genetic diversity while conserving the functional genome (Marston and Amon, 2004) and surviving nutrient starvation (Kupiec et al., 1997). Pseudohyphal growth allows immobile cells to forage for nutrients and escape nitrogen limiting conditions. When cells in pseudohyphal growth form face severe starvation, the cells can undergo sporulation. The **a** and α haploid cells on depletion of nutrients enter into a no-metabolic and quiescent stage with G1 arrest in the mitotic cycle. When carbon source is limiting, haploid cells can form filamentous growth known as haploid-invasive growth, which is characterised by elongated cell morphology, altered budding pattern and invasion of agar. Thus the differentiation responses are regulated depending on cell type and nutritional availability at each stage of yeast life cycle, except for mating (**Figure 1.2A**).
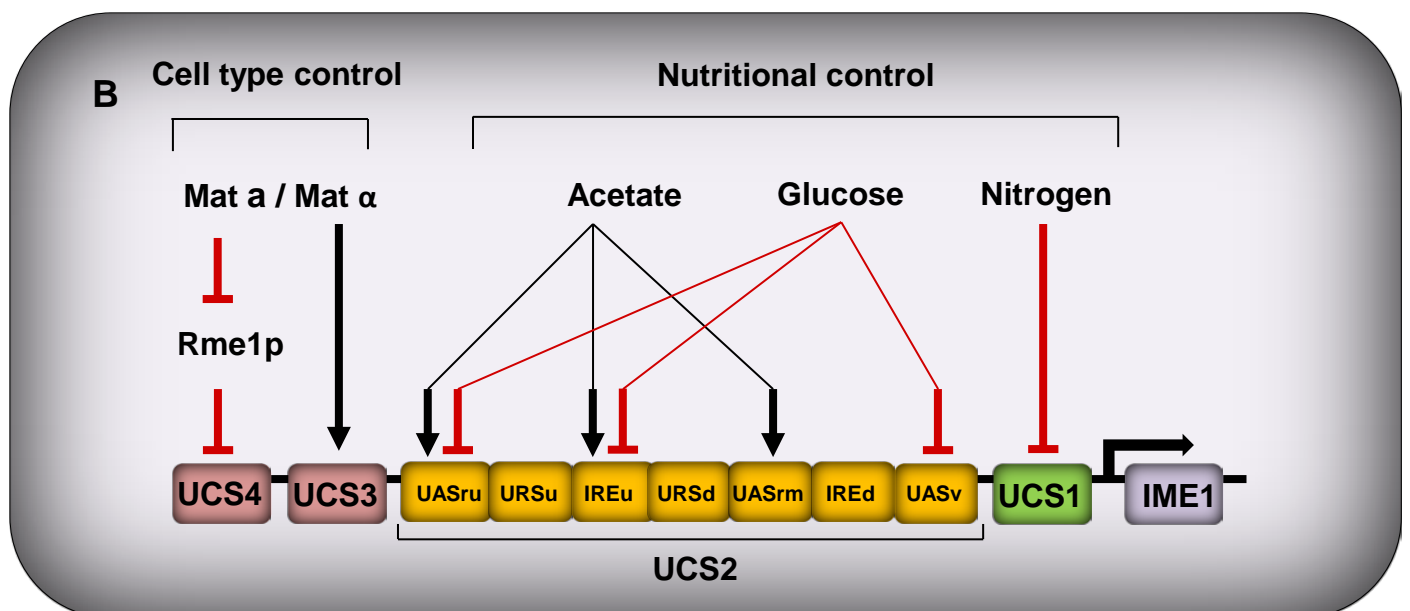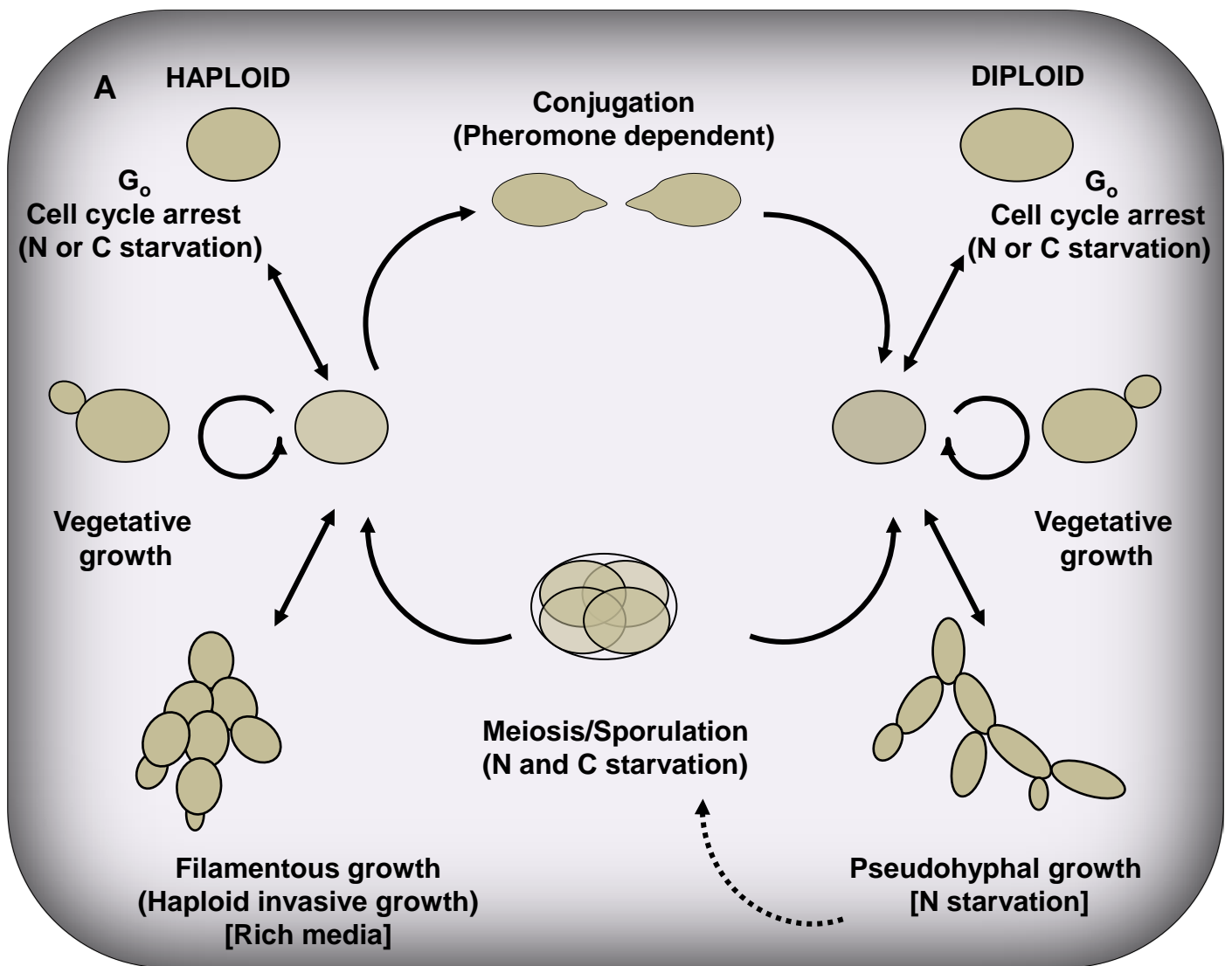
Figure 1.2 Yeast growth, development and regulation of *IME1* promoter. **A** - Once every cycle, haploid and diploid cells must choose to enter into one of the four developmental pathways. All of the developmental outcomes, with the exception of mating pathway are regulated by nutrition and cell type. **B -** The cell type and nutritional signals mediate the transcriptional regulation of *IME1*.

1.2.1 Meiosis

Meiosis is the cellular program that transforms diploid **a**/α cell into four haploid progenies (**a** or α) in an ascus. The process of meiosis requires a transcriptional program of approximately 1000 genes and can be divided roughly in three stages: early, middle and late stage depending on temporal expression of genes required for meiosis (Chu et al., 1998; Primig et al., 2000). Firstly, the key meiotic regulatory genes are expressed as cells exit the G1 phase of mitotic growth and enter the meiotic program. Secondly, on activation of early meiotic genes the cells undergo DNA replication, meiotic recombination and lastly, two sequential rounds of chromosome segregation to form four haploid products. During meiotic prophase, pair of homologous chromosomes become physically associated along the length by a large protein structure referred to as synaptonemal complexes (Page and Hawley, 2004). The process of meiosis and spore formation combined is called sporulation. The entry into meiosis is regulated by the *IME1* gene (<u>I</u>nitiator of <u>Me</u>iosis 1) in response to nutritional and cell type controls. The master regulator of meiosis Ime1p is induced in *MAT***a**/*MAT*α cells under nitrogen starvation in the presence of a non-fermentable carbon source starting a transcriptional programme to ensue meiosis (Sagee et al., 1998). The positive and negative regulatory sequences in the *IME1* promoter control *IME1* transcription in response to nutritional cues and cell type control. Presence of even low levels of glucose represses sporulation while non-fermentable carbon source like acetate induce sporulation in nitrogen starved diploids (Kassir et al., 2003).

1.2.1.1 Nutritional regulation of meiotic induction

Meiotic induction of *S. cerevisiae* depends on nutritional control and cell type control. For cells to enter the meiotic program they need two specific nutritional cues. One, the environment must lack one essential growth nutrient, mainly nitrogen limitation, which causes G1 arrest in the mitotic cycle. Second, is the absence of glucose, as this can inhibit meiotic initiation and promote differentiation into pseudohyphal growth. The cell type control means that only diploid yeast undergoes meiosis while haploids are prevented from undergoing meiosis. Upon nitrogen and glucose

starvation, the master regulator of meiosis, *IME1* is expressed to induce set of early meiotic genes.

The level of nitrogen and the type of carbon source is sensed by the *IME1* promoter to induce transcription of *IME1*. *IME1* is repressed in growing cells, but once cells cease growth, it is expressed at a moderate level (Kassir et al., 1988; Smith and Mitchell, 1989). Further induction of *IME1* is inhibited in the presence of glucose or in the absence of non-fermentable carbon source (Purnapatre and Honigberg, 2002). *IME1* transcription requires the function of respiratory metabolism of non-fermentable carbon source (Treinin and Simchen, 1993). However the requirement for a non-fermentable carbon source can be bypassed by overexpression of *IME1*. *IME1* has a large (~2kb) promoter region (Granot et al., 1989; Rupp et al., 1999) at which the cell type and nutritional signals converge to regulate the entry into meiosis. The *IME1* promoter is divided into four contiguous regions, upstream control regions (UCS1-4) and contains other regulatory elements within this region [**Figure 1.2B** and (Sagee et al., 1998)].

Regulation of *IME1* by nitrogen source

The UCS1 element in the *IME1* promoter responds to nitrogen levels, as deletion of UCS1 leads to inappropriate activation of *IME1* in vegetatively growing cells (**Figure 1.2B**). In addition mutants lacking cAMP or AMP dependent PKA also sporulate in the absence of nitrogen limitation (Matsumoto et al., 1983). Cdc25p is a known PKA and MAP kinase activator and has been suggested to transmit nitrogen signals to UCS1 (Matsumoto et al., 1983). Induction of meiosis in laboratory strains is mainly studied by nitrogen limitation, but it is not certain that nitrogen starvation represses meiosis or nitrogen starvation causes G1 arrest and indirectly promotes meiosis. However when nitrogen is present in absence of other essential nutrients, *S. cerevisiae* still induces meiosis supporting the notion that nitrogen starvation indirectly induces meiosis by G1 arrest.

Regulation of *IME1* by glucose

The meiotic program is inhibited in the presence of glucose even at relatively low concentrations. The *IME1* promoter senses glucose through UCS2. Three main elements UASru, UASrm and IREu, repress in the presence of glucose, but activate in the absence of glucose and/or presence of acetate (Kassir et al., 2003). The

elements UCS1, UASru, IREu and UASv (UAS activity in vegetative growth) integrate several signalling pathways to repress *IME1* transcription in the presence of glucose (**Figure 1.2B**). Thus the block on meiosis by glucose is mediated by a number of signalling pathways. Snf1p kinase, which is inhibited by glucose under the glucose repression pathway, is required for expression of *IME1* and *IME2*, an early meiotic gene. The glucose sensors Rgt2p and Snf3p act upstream of Snf1p and are required for repression of *IME1* in the presence of glucose. Activated PKA inhibits *IME1* and *IME2* and promotes growth. Gpa2p also binds directly to Ime2p to inhibit its kinase activity (Donzeau and Bandlow, 1999). Also transient activation of Ras pathway has also been suggested to repress meiotic initiation indirectly through activation of PKA pathway. The Rim15p kinase promotes the association of Ime1p to Ume6p (transcriptional activator of EMGs) to induce the early meiotic genes. But glucose represses *RIM15* expression and PKA directly inhibits Rim15p by phosphorylation. *IME1* may also be repressed by the PKA pathway through the Msn2p-Msn4p transcription complex inhibition by phosphorylation (Garreau et al., 2000). Msn2p-Msn4p activates transcription of many stress responsive genes by binding to stress responsive element (STRE) present in the promoters of these genes. *TPS1* (trehalose phosphate synthethase 1), one such stress responsive gene is required for induction of *IME1* (De Silva-Udawatta and Cannon, 2001). Also a STRE site is present in the *IME1* promoter region. PKA may also regulate the Msn2p-Msn4p complex by phosphorylating Sok2p, which is thought to bind to Msn2p-Msn4p and convert it to a transcriptional repressor (Shenhar and Kassir, 2001). The regulation of *IME1* is very important as is evident from the complex *IME1* promoter and interplay of negative and positive regulatory proteins. Thus, there are a number of pathways that regulate the expression of *IME1*, but complete mechanism of meiotic initiation is partially known.

Regulation of IME1 by non-fermentable carbon source

In the presence of non-fermentable carbon source *IME1* is expressed at low levels, resulting from the competition of the repressive action of UCS1, URSu, URSd, IREd and positive action of UASru, IREu, UASrm and UASv (**Figure 1.2B**). Upon nitrogen depletion, relief of UCS1 repression promotes the increase of transcription (Kassir et al., 2003). Meiotic induction has also been shown to be dependent on the alkalization

of the media. Metabolism of non-fermentable carbon sources produce CO_2, which creates alkaline conditions in the medium (Ohkuni and Yamashita, 2000). Further *RIM101* is required both for adaptation to extracellular alkalization and for *IME1* transcription (Lamb et al., 2001).

Activation of meiosis by G1 arrest and *CLN3*

In *S. cerevisiae* the cells require G1 arrest to undergo meiosis (Hirschberg and Simchen, 1977). Cln3p, a G1 cyclin is present at constant levels during cell cycle and functions primarily to promote transition from G1 to S phase. When G1 arrest occurs, Cln3p levels decline rapidly and this decline is required partly for meiotic induction because Cln3p inhibits *IME1* expression and Ime1p localization to nucleus (Colomina et al., 1999; Gallego et al., 1997; Parviz and Heideman, 1998).

Return to growth

Nitrogen and glucose starvation is not only required to initiate meiosis, but also to complete the process because addition of rich media can inhibit sporulation even after meiotic S phase, meiotic recombination, and synapotenemal complex formation have taken place (Esposito and Esposito, 1974; Friedlander et al., 2006; Honigberg et al., 1992; Honigberg and Esposito, 1994; Sherman and Roman, 1963; Simchen et al., 1972; Zenvirth et al., 1997). Moreover such refed cells can exit the sporulation program and return to mitotic growth as long as the commitment point has not passed. Commitment occurs after premeiotic DNA replication and recombination, but before meiosis I and cells cannot return to vegetative growth after this point. Overproduction of *IME1* in stationary phase cultures can induce meiotic recombination and synaptonemal complex formation, but glucose can stall further progression into late prophase, suggesting that nutritional signals can control later steps in the program through an *IME1*-independent pathway (Lee and Honigberg, 1996).

1.2.1.2 Cell type control

Cell type control ensures that *IME1* is not induced in haploid cells under any nutritional condition. *RME1* (Repressor of *IME1*) represses transcription of *IME1* in haploids and inhibits meiosis so haploids cannot undergo meiosis. Rme1p is expressed at much higher levels in haploids than diploids and represses *IME1* by binding to Rme1p repressor element (RRE1) site in UCS4 of *IME1* [**Figure 1.2B,** (Covitz et al., 1991; Covitz and Mitchell, 1993)]. Rme1p also binds to a similar site in the promoter of *CLN2,* which encodes a G1 cyclin, to activate its transcription and Cln2p inhibits *IME1* expression (Purnapatre et al., 2002). Only *MATa*/*MATα* cells can undergo meiosis as **a1**-α2, the heterodimer produced in diploids binds to an operator site in the *RME1* promoter repressing its transcription (Covitz and Mitchell, 1993; Herskowitz et al., 1992). In addition to repression of *RME1*, **a1**-α2 also promotes *IME1* expression by activation of *IME4* (Shah and Clancy, 1992). *IME4* is also a positive regulator of meiosis and is only expressed in **a**/α diploid cells. Though *IME4* is an early meiotic gene it is not under the regulation of Ime1p. *IME4* encodes a putative mRNA N6-adenosine methyltransferase required for entry into meiosis (Clancy et al., 2002). Expression of *IME4* is induced under starvation conditions (Shah and Clancy, 1992) and *IME4* can transcribe sense and antisense mRNA. The antisense promoter of *IME4* is stronger than the sense promoter in haploids and causes inhibition of sense transcript by antisense transcript thereby inhibiting entry into meiosis. Conversely in diploids the sense *IME4* transcript is produced as the antisense promoter is inhibited by **a1**-α2 heterodimer (Hongay et al., 2006). *IME4* is essential for *IME1* accumulation and sporulation (Shah and Clancy, 1992). An *rme1* mutation does not alter the regulation of *IME4* expression by **a1**-α2 but the *rme1* mutation can suppress an *ime4* insertion mutation to permit expression of *IME1*. Moreover **a1**-α2 represses *RME1* expression directly. These data suggest that *RME1* and *IME4* may act in parallel pathways to activate *IME1* (Covitz et al., 1991; Shah and Clancy, 1992).

1.2.1.3 Regulation of early meiotic genes

IME1 encodes a transcriptional activator, which once induced is required for transcription of early meiotic genes (EMGs) (Kassir et al., 2003; Mandel et al., 1994; Smith et al., 1993). An *IME1* null mutation leads to loss of expression of all meiotic genes except *IME4* (Kassir et al., 2003; Kupiec et al., 1997). Ime1p associates with Ume6p, a transcriptional repressor of early meiotic genes under vegetative growth and a transcriptional activator under meiosis inducing conditions. Ume6p interaction with Ime1p leads to expression of early meiotic genes like *IME2*, *SPO13* and *HOP1* (Malathi et al., 1997; Rubin-Bejerano et al., 1996). Rim11p, GSK3 family protein kinase activated in response to starvation by nitrogen limitation (Xiao and Mitchell, 2000) phosphorylates Ime1p to stabilise Ime1p-Ume6p association (Malathi et al., 1997; Malathi et al., 1999).This association can be destabilised by presence of glucose through repressing expression of Rim15p (Vidan and Mitchell, 1997). Ume6p is a C6-zinc cluster DNA binding protein that binds to 9-bp upstream repressing site 1 (URS1) present in promoters of early meiotic and non-meiotic genes (Anderson et al., 1995; Strich et al., 1994). Deletion of *UME6* induces the expression of genes containing URS1 in vegetative growth conditions (Bowdish and Mitchell, 1993; Strich et al., 1994). *ume6Δ* cells arrest during prophase early in meiosis and display delay in induction of mid and late genes (Steber and Esposito, 1995). These data show that Ume6p is not only a repressing factor in mitotic growth, but also promotes the meiotic process induction. It has also been suggested that repression by Ume6 is relieved by *in vivo* interaction of Ume6p and Cdc20p, an activator of anaphase promoting complex/cyclosome (APC/C) ubiquitin ligase. Ume6p degrades partially after ubiquitination and Ime1p association is required for complete destruction and entry into meiosis by induction of EMGs (Mallory et al., 2007). Under mitotic growth conditions Ume6p is not degraded as Cdc20p is inactive due to its phosphorylation by PKA. Early meiotic genes are transcribed following histone acetylation by Gcn5p histone acetyl transferase (**Figure 1.3A**) (Burgess et al., 1999).

Ume6p interacts with Sin3p and recruits the Rpd3p histone deacetylase to bring about repression under vegetative growth conditions (Kadosh and Struhl, 1997) by denying access to SAGA histone acetyl transferase complex (**Figure 1.3B**). Sin3p is a co-repressor which is recruited by Ume6p to the promoters of early meiotic genes and Rpd3p functions as a histone deacetylase (Kadosh and Struhl, 1997).
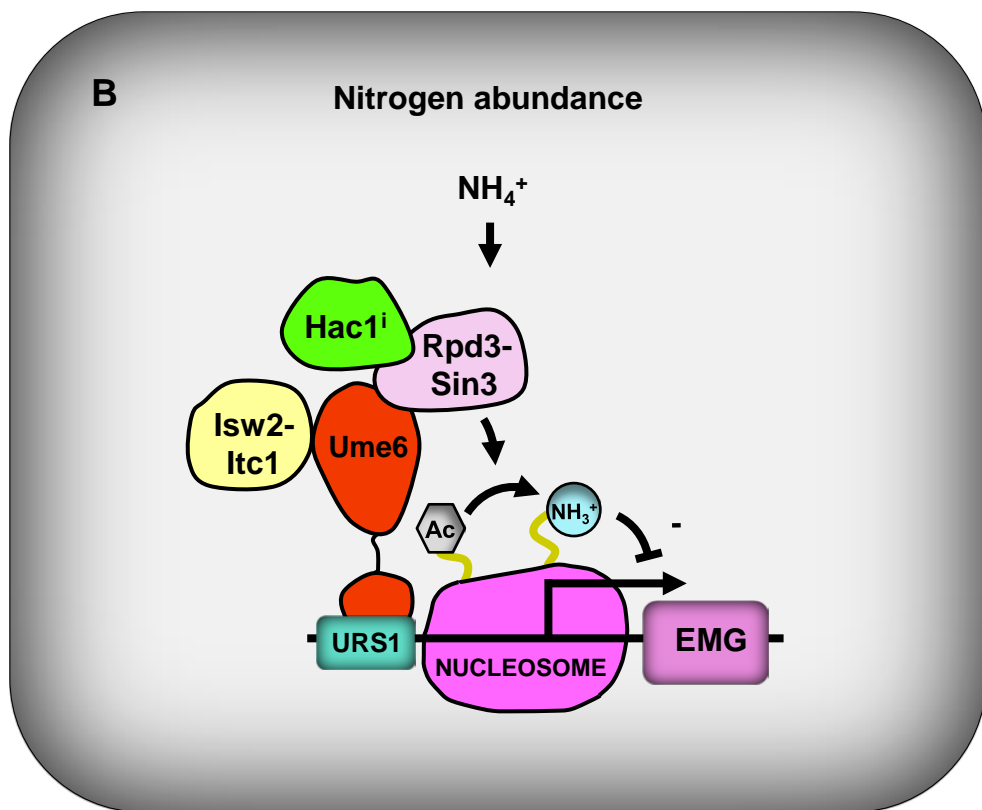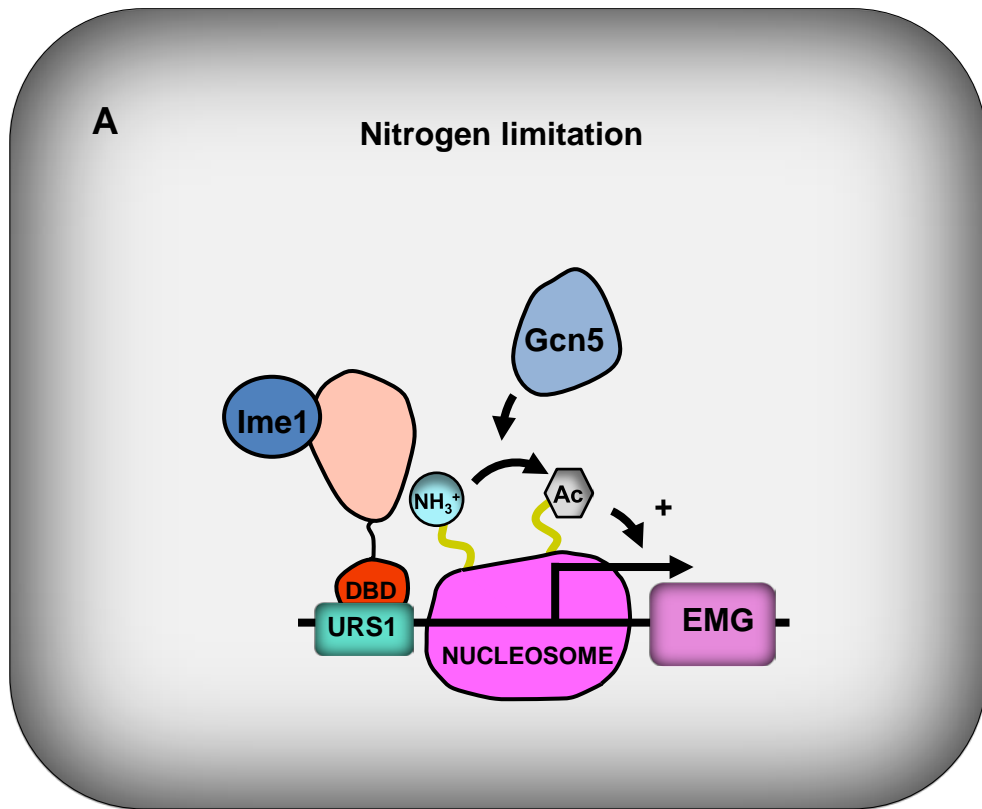
Figure 1.3 Interplay of transcriptional regulators, histone-modifying enzymes and chromatin remodelling complexes in regulation of early meiotic genes. **A -** Under nitrogen starvation, Ime1p associates with Ume6p and Gcn5p acetylates histone to induce early meiotic genes (EMGs). **B -** In presence of nitrogen Ume6p negatively regulates transcription of EMGs by recruitment of Sin3p-Rpd3p histone deacetylase (HDAC) which lead to histone deacetylation.

Rpd3p deacetylates histone tails associated with nucleosomes around the promoter region by removing acetyl group from N-terminal lysine residues of H2A, H2B, H3 and H4 and leads to repression (Kadosh and Struhl, 1998; Rundlett et al., 1998; Suka et al., 2001). *S. cerevisiae* forms Rpd3p large and small complexes known as Rpd3L and Rpd3S (Carrozza et al., 2005). The large complex Rpd3L typically contains Rpd3p, Ume1p, Sds3p, Sap30p and Pho23p subunits. Rpd3S complex in addition to Rpd3p, Ume1p and Sin3p, also contains Eaf3p and Rco1p. Both these complexes perform different functions. Rpd3L localizes primarily to the promoter regions and represses transcription. Set2p methyltransferase is recruited by RNA polymerase II to methylate transcribed regions (Joshi and Struhl, 2005). Eaf3p, subunit of Rpd3S complex has a chromodomain motif to recognise methyl-lysine modifications and recruits Rpd3S to the transcribed regions to suppress intragenic transcription initiation (Carrozza et al., 2005; Keogh et al., 2005). The *RPD3-SIN3* histone deacetylase (HDAC) complex is involved in regulation of a wide range of genes in meiosis, metabolism, osmotic stress, telomere boundary regulation, anaerobic growth (De Nadal et al., 2004; Ehrentraut et al., 2010; Kadosh and Struhl, 1997; Rundlett et al., 1998; Vidal and Gaber, 1991). Ume6p also recruits Isw2p a protein of the ATP-dependent chromatin remodelling complex Isw2p-Itc1p which is required for repression on early meiotic genes during mitotic growth of yeast possibly by maintaining repressed chromatin loci (Goldmark et al., 2000).

ISW2-ITC1 comprises a heterodimer of the Itc1p and Isw2p proteins and is a representative member of the ISWI subfamily of the SWI2/SNF2 family of chromatin remodeling proteins (Fitzgerald et al., 2004; Tsukiyama et al., 1999); both Itc1p and Isw2p are required for the chromatin remodeling activity of the holocomplex (Gelbart et al., 2001). In addition, two small histone fold containing proteins, Dpb4p and Dls1p, are present in at least a fraction of Isw2 complexes purified from yeast (McConnell et al., 2004). Isw2 has been demonstrated to affect *in vivo* repression of transcription of several genes (Fazzio et al., 2001; Goldmark et al., 2000; Kent et al., 2001; Sherriff et al., 2007) and, together with Ino80, to promote replication fork progression (Vincent et al., 2008). Isw1p functions with the Chd1p chromatin remodeler at few other genes (Alén et al., 2002; Xella et al., 2006). It has been suggested that Isw2 accomplishes these activities by modifying the spacing of sequential mononucleosomes along short, contiguous stretches of chromatin through

nucleosome sliding (Kagalwala et al., 2004; Tsukiyama et al., 1999). Interestingly, Isw2 complex is able to accomplish this sliding of nucleosomes without disrupting the integrity of the association of the DNA and the octamer (Fazzio and Tsukiyama, 2003; Kassabov et al., 2002). The Isw2 complex interacts efficiently with both naked DNA and nucleosomal arrays in an ATP-independent manner and both units are required for nucleosome stimulated ATPase activity and chromatin remodeling activity (spacing) (Gelbart et al., 2001). Isw2p-Itc1p spaces nucleosomes every 200 bp and the spacing is the function of its association with linker DNA, which is mediated by Itc1p. Extensive binding of Itc1p with the linker DNA is also suggested to prevent the nucleosomes from moving too close to each other and hence the length of linker DNA interaction maintains the spacing of nucleosomes. Isw2p-mediated repression by creating nuclease inaccessible chromatin structure that includes TATA box is likely to target the binding of TATA box binding protein (TBP). Isw2p mediated chromatin remodeling and Sin3p/Rpd3p histone deacetylase may cooperate to inhibit TBP binding at some target promoters including *HOP1* (Shimizu et al., 2003).

Ume6p is phosphorylated by Rim11p and possibly by Mck1p and interacts with Ime1p and transforms into an activator to induce meiosis (Bowdish et al., 1995; Mallory et al., 2007; Rubin-Bejerano et al., 1996; Washburn and Esposito, 2001). *IME2* is activated in a two step process where Sin3p-Rpd3p is inactivated and may be dissociated from Ume6p and then associated with Ime1p leading to transcriptional activation of *IME2* (Bowdish et al., 1995; Rubin-Bejerano et al., 1996). TATA box of *IME2* gene is occupied in the repressed conditions and induction of meiosis recruits chromatin structure remodelling complex (RSC) to remodel nucleosomes (Inai et al., 2007). Then association of SAGA complex containing Gcn5p histone acetyl transferase to *IME2* leads to its transcriptional activation (Burgess et al., 1999). Once the Ume6p mediated repression is relieved on URS1, early meiotic genes including *IME2* are expressed. Ime2p is a meiosis specific serine/threonine protein kinase and is functionally related to Cdc28p, the cyclin dependent kinase (Chu et al., 1998). Ime2p contains a TXY motif in its activation loop that is similar to activation loops of mitogen-activated protein kinases (MAPKs) (Schindler et al., 2003). *IME2* transcription which, begins shortly after induction of meiosis rises around the time of chromosomal divisions. The biphasic expression and accumulation of *IME2* requires Ime1p in the first phase (Mitchell et al., 1990) and Ndt80p in the second phase (Chu

et al., 1998). Ime2p firstly regulates EMGs expression through Ime1p and controls meiotic S phase by functionally replacing some, but not all Cdc28p mitotic S-phase promoting roles (Benjamin et al., 2003; Guttmann-Raviv et al., 2001; Honigberg, 2004). During early phase of sporulation, Ime2p also phosphorylates replication protein A. Ime2p represses the transcription of *IME1* eventually in the later stages of meiosis (Guttmann-Raviv et al., 2002; Shefer-Vaida et al., 1995; Smith and Mitchell, 1989). Ime2p also phosphorylates Ime1p and targets it for degradation (Guttmann-Raviv et al., 2002). Negative feedback regulation of Ime1p ensures its narrow window of expression in relation to Ime2p for progression of meiotic program.

Meiotic DNA replication follows the expression of *IME1* and *IME2* (Honigberg and Purnapatre, 2003). Ime2p phosphorylates Sic1p, an inhibitor of Clb-Cdc28p kinase and degrades it to initiate meiotic DNA replication (Dirick et al., 1998; Stuart and Wittenberg, 1998). Ime2p plays a role in the progression of meiosis by positively regulating Ndt80p through direct phosphorylation and promotes meiotic division (Benjamin et al., 2003; Foiani et al., 1996; Sia and Mitchell, 1995; Sopko et al., 2002) Ime2p is an unstable protein kinase and inactivation of Ime2p is needed for the formation of normal asci (Sari et al., 2008). This is supported by the evidence that Ime2p negatively regulates Sum1p, a repressor protein that functions against Ndt80p (Pak and Segall, 2002). The promoter region of *NDT80* contains two URS1 sites besides two middle sporulation elements (MSEs). *NDT80* is positively regulated by Ime1p and Ime2p. Ndt80p, once activated, induces expression of its own and other genes involved in middle stages of meiosis through MSEs (Chu et al., 1998). Ime2p also ceases the EMG expression by negatively regulating Ime1p (Guttmann-Raviv et al., 2001). In late stages of meiosis, Ime2p has been proposed to regulate Cdh1p, a targeting subunit of the anaphase-promoting complex/cyclosome and may thus regulate chromosome segregation by modulating the activity of this ubiquitin ligase (Bolte et al., 2002). Ime2p is degraded shortly after meiosis II is completed (Benjamin et al., 2003). Ubiquitin-mediated destruction of Ime2p occurs in a Grr1p-dependent manner when glucose, which inhibits meiosis, is added to sporulating cells (Purnapatre et al., 2005). In addition, it has been proposed that glucose can inhibit the Ime2p activity through the Gpa2p heterotrimeric GTP-binding protein (Donzeau and Bandlow, 1999). Ime2p is phosphorylated at Thr and Tyr residues in a Cak1p-dependent fashion (Schindler et al., 2003) and Ime2p autophosphorylates its

activation loop (Schindler and Winter, 2006). Later Ime2p is hyperphoshorylated and accumulated in meiotic M phase and is subsequently degraded. *RIM4* is required for *IME1* and *IME2* dependent transcriptional activation pathways and acts upstream of *IME2* (Soushko and Mitchell, 2000). *RIM4*, a gene which encodes a putative RNA binding protein is required for high level expression of EMGs, meiotic division and recombination (Deng and Saunders, 2001).

1.2.2 Pseudohyphal growth

S. cerevisiae diploid cells can undergo a dimorphic switch under nitrogen limitation in presence of a fermentable carbon source like glucose. Pseudohyphal growth is characterized by features like elongated cell shape, unipolar budding, symmetric cell division, adhesion of cells to each other after the cell division is completed and invasion of solid growth media (Gimeno et al., 1992; Kron et al., 1994). There is symmetric cell division in pseudohyphal growth as opposed to asymmetric cell division in budding (Kron and Gow, 1995). The presence of fusel alcohols, which are end products of catabolism of less preferred amino acids also induce pseudohyphal growth (Chen and Fink, 2006; Dickinson, 1996). The ability to form pseudohyphae in response to nutrient starvation is advantageous to yeast as this facilitates foraging for scarce nutrients. Also formation of pseudohyphae under stress may allow the cells to deal with stress by choosing alternative developmental program (Zaragoza and Gancedo, 2000). The haploids form filamentous growth when carbon source is limiting and is referred as haploid invasive growth. Haploid cells invade agar medium and show altered budding pattern, though invasive growth is less vigorous and cells less elongated than diploid pseudohyphal growth (Gancedo, 2001; Gimeno et al., 1992; Kron and Gow, 1995).

1.2.2.1 Nutrient sensing and pseudohyphal growth:

Glucose sensing occurs through G-protein coupled receptor Gpr1p, which interacts with G protein α-subunit Gpa2p and transmits the nutritional signal via PKA and cAMP synthesis (Kraakman et al., 1999; Xue et al., 1998; Yun et al., 1997; Yun et al., 1998). This association is necessary for pseudohyphal growth (Lorenz et al., 2000b; Xue et al., 1998). Nitrogen starvation induces *GPR1* transcription but the primary function of Gpr1p is glucose sensing. Gpr1p binds to glucose with low affinity and may monitor glucose levels necessary for filamentous growth or may integrate glucose and nitrogen signals in the pseudohyphal pathway. Rgt2p and Snf3p have also been proposed to bind to glucose and relay glucose signal. Glycolytic pathway intermediates are also sensed by the cells (Kruckeberg et al., 1998; Ozcan and Johnston, 1999; Rolland et al., 2001). Glucose phosphorylating enzymes (Glk1p, Glk2p and Hxk2p) also respond to the presence of glucose and regulate a large

number of genes (Johnston, 1999; Rolland et al., 2001). Pseudohyphal growth can also be triggered by maltose or maltotriose through a signaling pathway independent of Gpr1p (Van de Velde and Thevelein, 2008).

Pseudohyphal differentiation mainly responds to nitrogen starvation and poor nitrogen sources like proline (Gimeno et al., 1992; Lorenz and Heitman, 1998b). Mep1p, Mep2p and Mep3p are the ammonium transporters that are important to the regulation of pseudohyphal and invasive growth. Mep2p is important as it senses nitrogen starvation to signal the formation of pseudohyphal growth through cAMP-PKA pathway and at least activates transcriptional profile consistent with activation of MAPK pathway (Lorenz and Heitman, 1998a; Rutherford et al., 2008; Van Nuland et al., 2006). The amino acid transporter Ssy1p of the SPS nutrient sensing system, which sense extracellular amino acids has been shown to regulate invasive growth (Forsberg and Ljungdahl, 2001; Klasson et al., 1999). Gap1p is an amino acid permease, which is tightly regulated depending on the nitrogen source in the medium. The presence of preferable nitrogen source or high concentration of amino acids represses Gap1p (Magasanik and Kaiser, 2002). Gap1p transports all common amino acids, many D-amino acids and nonmetabolizable amino acid analogs. Upon nitrogen limitation Gap1p expression is induced by two GATA transcription factors Gln3p and Gat1p (Stanbrough and Magasanik, 1996; Stanbrough et al., 1995). Gap1p is also implicated in activation of the PKA pathway on addition of amino acids to nitrogen starved cells (Donaton et al., 2003). Gpa2p-Gpr1p is involved in nitrogen sensing as *gpa2* and *gpr1* strains show pseudohyphal growth defect. These growth defects can be rescued by introduction of constitutive RAS allele or addition of external cAMP (Kübler et al., 1997; Lorenz and Heitman, 1997; Lorenz and Heitman, 1998a; Lorenz and Heitman, 1998b; Lorenz et al., 2000b; Tamaki et al., 2000). Internal amino acid is sensed by general control system for amino acid biosynthesis. Gcn4p is activated in response to depletion of any amino acid and induces a number of genes involved in amino acid biosynthesis (Jia et al., 2000; Natarajan et al., 2001). This intracellular nitrogen sensing mechanism involves association of uncharged tRNA and Gcn2p kinase leading to its activation. Gcn2p phosphorylates eIF2α in response to amino acid starvation and other stimuli, reducing global protein synthesis (Dever, 2002; Hinnebusch, 2005). However, *GCN4* mRNA is upregulated by Gcn2p through upstream open reading frame (Mueller and Hinnebusch, 1986) and Gcn4p

upregulates genes for biosynthesis of amino acids. tRNA that decodes for glutamine codon CUG was shown to regulate pseudohyphal growth in response to amino acid and nitrogen availability (Beeser and Cooper, 2000; Murray et al., 1998). Glutamine is the main source of nitrogen in yeast cells for biosynthetic reactions and tRNA seems the likely mechanism to sense intracellular nitrogen.

1.2.2.2 Pathways regulating pseudohyphal growth

There are several pathways that function to induce and regulate pseudohyphal growth response. The formation of pseudohyphal growth requires coordination of at least two pathways, a mating and filamentation mitogen activated protein kinase (MAPK) signalling cascade and cAMP dependent protein kinase A (PKA) pathway and these pathways may act in parallel and partially overlapping manner.

1.2.2.2.1 The MAP Kinase pathway

The mating and filamentation MAP kinase pathway controls the activity of the heterodimeric transcription factor complex Ste12p-Tec1p (Gavrias 1996, Rupp 1999), which activates expression of *FLO11* and regulates cell elongation and cell adhesion [**Figure 1.4** and (Chen and Thorner, 2010)]. The transcription factor Tec1p is required for filamentous growth which is stimulated by mitogen activated protein kinase (MAPK) cascade and together with Ste12p binds to filamentous and invasion response elements (FREs) to activate target genes (Madhani et al., 1997). The mating and filamentation MAPK cascade consists of the MAPK kinase Ste11p, the MAPK kinase Ste7p, the MAPK Kss1p and the scaffold Ste5p, which is regulated by Msb2p (Cullen et al., 2004; Madhani and Fink, 1998). Msb2p recruits general signaling proteins, such as Sho1p and isoprenylated, plasma-membrane-tethered Cdc42p and its p21-activated kinase, Ste20p, to the filamentation MAPK cascade (Cullen et al., 2004). Cdc42p interacts with Ste20 to displace the negative regulator Hsl7p (Fujita et al., 1999; Leberer et al., 1997; Peter et al., 1996). Ste20p also responds to low nitrogen through Sho1p to activate the MAPK cascade (O'Rourke and Herskowitz, 1998). Ste20p phosphorylates Ste11p and activates its protein kinase, which in turn phosphorylates Ste7p (Choi et al., 1994; Wu et al., 1995). Kss1p, is activated when phosphorylated by Ste7p to induce Tec1p-Ste12p. Kss1p in its unphosphoryated form is associated with Ste12p and the negative regulators

Dig1p and Dig2p to inhibit it from inducing genes involved in invasive growth (Bardwell et al., 1998). Activation of Kss1p decreases Tec1p sumoylation with concurrent increase in the transcriptional activity of Tec1p (Wang et al., 2009). Thus the MAPK pathway regulates the transcriptional activation of *FLO11* through Tec1p-Ste12p. *FLO11* is an important flocculin during invasive and filamentous growth as *FLO11* deletion leads to loss of invasive and filamentous growth (Lo and Dranginis, 1998) while increasing the *FLO11* expression increases this phenotype (Palecek et al., 2000). The transcription factor Flo8p is also required for pseudohyphal and invasive growth (Liu et al., 1996) by regulating expression of the flocculins *FLO1*, *9* and *11* (Kobayashi et al., 1999). Ste12p and Tec1p regulate the expression of *FLO11* from MAPK cascade downstream of Kss1p, while Flo8p regulates Flo11p downstream of PKA pathway (Madhani et al., 1999). Flo8p seems to regulate invasive and filamentous growth in a pathway independent from Ste12p but acts downstream of the cAMP-PKA pathway (Rupp et al., 1999).

1.2.2.2.1.1 Related MAPK pathways and their signalling specificity

S. cerevisiae contain at least five distinct MAPK pathways involved in pheromone response (PH), high osmolarity glycerol (HOG), cell wall integrity (CWI) and spore wall assembly besides filamentation and invasive growth (FG) pathway (Gustin et al., 1998). This section provides a brief overview of PH pathway, HOG pathway and its shared common components with FG pathway. Also discussed in this section is the signalling specificity maintained by MAPK signalling of FG pathway, PH pathway and HOG pathway.

The mating or PH pathway is activated when haploid yeast senses pheromones of opposite mating type in its vicinity. Activation of the pheromone receptor Ste2p in *MAT***a** and Ste3p in *MAT*α cells leads to dissociation of a coupled heterotrimeric guanine nucleotide-binding protein (G protein) Gpa1p-Ste4p-Ste18p to activated Gα subunit (Gpa1p) and Gβγ (Ste4p/18p) subunits. Ste4p/18p tethers the MAP kinase module Ste11p/Ste7p/Fus3p to the plasma membrane through its interaction with their scaffold protein Ste5p. MAPK Fus3p and Kss1p are phosphorylated by Ste7p, which in turn phosphorylate the transcriptional activator Ste12p. Ste12p initiates the transcription of pheromone response genes and transiently arrests cell cycle on G1 to induce cell fusion with the mating partner [(**Figure 1.4**) and reviewed in (Schwartz and Madhani, 2004)].

The HOG MAPK pathway is activated through sensor protein Sho1p and partly through Sln1p. Under high-salt conditions, interplay between membrane anchor protein Sho1p and osmosensor membrane proteins Msb2p and Hrk1p tethers the MAP kinase module Ste11p/Pbs2p/Hog1p to plasma membrane (**Figure 1.4**) (Maeda et al., 1995; Tatebayashi et al., 2007; Tatebayashi et al., 2006). Ste11p activates the Pbs2p MAPKK, which then activates the Hog1p MAPK (Posas and Saito, 1997). Signalling through Sln1p activates the redundant Ssk2p and Ssk22p MAPKKKs and ultimately Hog1p but does not involve the common MAPKKK Ste11p. Activated Hog1p initiates adaptive responses to high osmolarity, including temporary arrest of the cell-cycle progression, readjustment of the transcription and translation patterns, and glycerol synthesis [(**Figure 1.4**) and (Bilsland-Marchesan et al., 2000; Escote et al., 2004; Hohmann, 2002; O'Rourke and Herskowitz, 2004; Teige et al., 2001)].

The common components of all the three pathways are Cdc42p, p21-activated kinase Ste20p, adaptor protein Ste50p and Ste11p. Cells employ compartmentalization, use of scaffold proteins in distinct macromolecular complexes and cross-inhibition to maintain specificity and avoid inappropriate activation of other pathways.

1.2.2.2.1.1.1 Crosstalk between FG and PH MAPK modules: FG MAPK pathway activates Ste11p, Ste7p and Kss1p to promote cell adhesion, cell elongation and reorganisation of cell polarity, through Kss1p mediated activation of Ste12p-Tec1p (**Figure 1.4**). Stimulation of the FG pathway through the Msb2p sensor activates Kss1p and does not activate Fus3p because Fus3p is sequestered by Ste5p binding and is only activated when recruited to the plasma membrane. Also nutritional starvation activates Ste11p and Ste7p by a mechanism that does not involve Ste5p scaffold. Activated Kss1p ensures that Tec1p is not degraded, and that Ste12p-Tec1p-dependent FG-specific gene expression is induced. Feedback phosphorylation of Ste7p by Kss1p specifies an invasive growth response through selective activation of Kss1p and filamentation-specific gene expression. This is because mating-specific gene expression is suppressed by the feedback phosphorylation status of Ste7p (Maleri et al., 2004). The kinase cascade of Ste20p, Ste11p, and Ste7p, and transcriptional activator Ste12p, also function in pheromone

pathway. Thus, the pheromone pathway and the FG pathway share a common MAPKKK (Ste11p) and MAPKK (Ste7p). However, Ste7p activates Fus3p in response to pheromones and it has been shown that Fus3p inhibits filamentous growth through degradation of Tec1p, which is a cofactor for Ste12p in the expression of filamentation genes. Fus3p phosphorylates threonine 273 in Tec1p, which leads to ubiquitination and degradation through an SCF ubiquitin protein ligase (Bao et al., 2004; Chou et al., 2004). Tec1p is not a substrate for Kss1p, so Tec1p remains stable during filamentous growth (Chou et al., 2004). The scaffold protein Ste5p insulates the mating pathway from the filamentation pathway, as shown by analysis of a point mutation in Ste5p that confers increased activation of Kss1p and reduced Fus3p-dependent degradation of Tec1p (Schwartz and Madhani, 2006). Ste7p and Fus3p can bind through docking interaction and do not need tethering by Ste5p scaffold protein for Fus3p activation. However Ste5p is important as it was shown that minimal scaffold (ms) region in Ste5p selectively promotes Ste7p to Fus3p signalling (Good et al., 2009). This is further supported by the data that constitutively active Ste7p mutant poorly activated Fus3p (Maleri et al., 2004). Pheromones also activate Kss1p (**Figure 1.4**), but the activation is gradual and transient as compared to Fus3p (Hao et al., 2008). However Fus3p and Kss1p can phosphorylate Dig1p/Dig2p, but Fus3p mediated degradation of Tec1p prevents formation of Tec1p/Ste12p heterodimer for FG-specific gene expression. Instead Fus3p phosphorylates Ste12p, which homodimerizes and binds to pheromone response element (PRE) of pheromone response genes (Olson et al., 2000; Yuan and Fields, 1991).

1.2.2.2.1.1.2 Crosstalk between FG and HOG MAPK modules: The HOG MAPK module uses Ste11p, Pbs2p and Hog1p while FG MAPK module uses Ste11p, Ste7p and Kss1p, the common component being the MAPKKK Ste11p. The HOG and the FG pathways also share components like Sho1p and Msb2p upstream of Ste11p. (Cullen et al., 2004; Pitoniak et al., 2009; Tatebayashi et al., 2007). In the HOG pathway, the Msb2p or Hkr1p and Sho1p recruit the Pbs2p MAPKK to the plasma membrane (Reiser et al., 2000). Ste50p interacts with Sho1p to bring Ste11p into close proximity with Pbs2p, thereby activating Pbs2p (Tatebayashi et al., 2006). Finally, Pbs2p activates the Hog1p MAPK, which is tightly bound to Pbs2p by

multiple docking interactions (Murakami et al., 2008). Pbs2p cannot phosphorylate either Fus3p or Kss1p, because their docking sites are incompatible. In FG pathway Msb2p and Sho1p activate Kss1p through Ste11p without the need for any known scaffold protein (Good et al., 2009). Osmostress can activate the Kss1p MAPK very weakly and transiently (Shock et al., 2009; Wang et al., 2009), while glycosylation defects that activate Kss1p do not activate Hog1p (Yang et al., 2009). In the absence of Pbs2p or Hog1p, however, osmostress robustly activates Kss1p, and induces FG-like polarized cell growth (O'Rourke and Herskowitz, 1998). Conversely, activation of Hog1p, either by osmostress or by overexpression of Pbs2p, inhibits FG responses (Pitoniak et al., 2009). Using an ATP analog-sensitive Hog1p mutant, it was directly shown that the cross-talk barrier requires Hog1p kinase activity (Westfall and Thorner, 2006). But it is yet unclear how Hog1p prevents the cross talk between these pathways. In the absence of Ste7p or Kss1p/Fus3p, glycosylation defects activate Hog1p, indicating that the FG pathway also cross-inhibit the HOG pathway (Yang et al., 2009). Thus, a reciprocal inhibitory loop exists between the HOG and FG MAPK modules that allow stable activation of only one or the other pathway under various stress conditions. In wild-type cells both Ste7p and Kss1p are phosphorylated in response to osmostress, but signalling specificity is maintained and FG pathway genes are not transcribed under these conditions (Davenport et al., 1999; O'Rourke and Herskowitz, 2004; Westfall and Thorner, 2006). This signalling specificity may be achieved through HOG signalling by preventing DNA binding of Tec1p and thereby interrupting FG pathway signalling (Shock et al., 2009). Another group reported that specificity may be maintained in response to osmostress when Hog1p phosphorylates Ste50p and that this phosphorylation of Ste50p limits the duration of Kss1p activation to prevent FG pathway activation (Hao et al., 2008). Kss1p inhibits activation of Hog1p MAPK indirectly through the Ptp2 protein phosphatase (Saito and Tatebayashi, 2004). The mechanistic detail of cross-pathway inhibition between the HOG and the FG pathways is still unclear. It will be important to obtain a more detailed understanding of how the HOG and the FG pathways are activated, respectively, by osmostress and nutritional conditions.

1.2.2.2.1.1.3 Crosstalk between PH and HOG modules: Both modules are activated by the membrane-bound Ste20p kinase that phosphorylates and activates Ste11p. The pheromone signalling activates Fus3p through Ste7p which is

dependent on Ste5p scaffold protein. Ste7p cannot activate Hog1p, as the docking sites in Ste7p have no affinity to Hog1p (Remenyi et al., 2005). HOG pathway activates Hog1p with Sho1p, Pbs2p and Ste5p co-scaffolds. When Ste7p was covalently attached to Ste11p, only pheromone pathway was activated while fusion of Pbs2p to Ste11p only activated HOG pathway (Harris et al., 2001). This indicated that robust protein-protein complexes can specify which MAPK pathway is activated. Activation of the HOG pathway triggers the activity of phosphatases, which then feedback to inhibit other MAPK pathways; for example, by dephosphorylating Fus3p and Kss1p (Davenport et al., 1999; Hall et al., 1996). Such phosphatase activity has, however, not been demonstrated in wild-type cells. Fus3p activates Fus1p, which binds and inhibits Sho1p arm of HOG pathway (Nelson et al., 2004). Hog1p also negatively regulates Fus3p possibly by activating Msg5p phosphatase (Hall et al., 1996). Thus, these two MAPK modules are securely insulated from each other by specific scaffolds, docking interactions, cross-pathway inhibition and possibly by phosphatases.

1.2.2.2.2 The PKA pathway is activated by the D-glucose sensor G-protein coupled receptor Gpr1p (Lorenz et al., 2000b; Tamaki et al., 2000) and the high affinity ammonium permease Mep2p [**Figure 1.4** (Boeckstaens et al., 2007; Lorenz and Heitman, 1998b; Rutherford et al., 2008)]. Protein kinase A (PKA) is activated by heteromeric G-protein α subunit Gpa2p activated adenylate cyclase (Kübler et al., 1997; Lorenz and Heitman, 1997). Ras2p, a GTP binding protein plays an important role in pseudohyphal growth as expression of constitutively active *RAS*^{Val19} decreased GTPase activity and induced pseudohyphal growth in diploid yeast (Gimeno et al., 1992). The *ras2/ras2* diploid was still able to induce pseudohyphal growth with round cells in response to nitrogen starvation (Kübler et al., 1997; Mösch et al., 1999). A downstream target of Ras2p is adenylate cyclase Cyr1p (Thevelein, 1991; Thevelein, 1992). PKA, which is activated consists of three catalytic subunits in S. *cerevisiae*, Tpk1p, Tpk2p and Tpk3. Tpk2p directly interacts with Sfl1p and inhibits, the transcriptional repressor of *FLO11* (Robertson and Fink, 1998). Tpk2p phosphorylates Flo8p to stimulate its binding to the *FLO11* promoter and activation of *FLO11* (Pan and Heitman, 1999; Pan and Heitman, 2002). *TPK1* and *TPK3* deletion leads to enhanced pseudohyphal growth (Pan and Heitman, 1999; Robertson and Fink, 1998), suggesting that *TPK1* and *TPK3* are inhibitors of pseudohyphal growth,

but the substrates of *TPK1* and *TPK3* are yet unidentified. Bcy1p forms a negative regulatory subunit of PKA, which dissociates on cAMP stimulation. Mutations in *BCY1,* that forms a complex with Tpk1-3p, activate PKA and enhance filamentous growth at both low and high nitrogen concentrations (Pan and Heitman, 1999). Flo8p and Sfl1p act antagonistically to regulate the expression of *FLO11* in response to cAMP stimulus to induce pseudohyphal growth depending on nutritional signals (Lorenz et al., 2000b; Rupp et al., 1999). The importance of cAMP-PKA pathway in pseudohyphal growth comes from the observation, that external stimulus of cAMP induces pseudohyphal growth while overexpression of phosphodiesterase Pde2p blocks pseudohyphal growth (Ward et al., 1995).
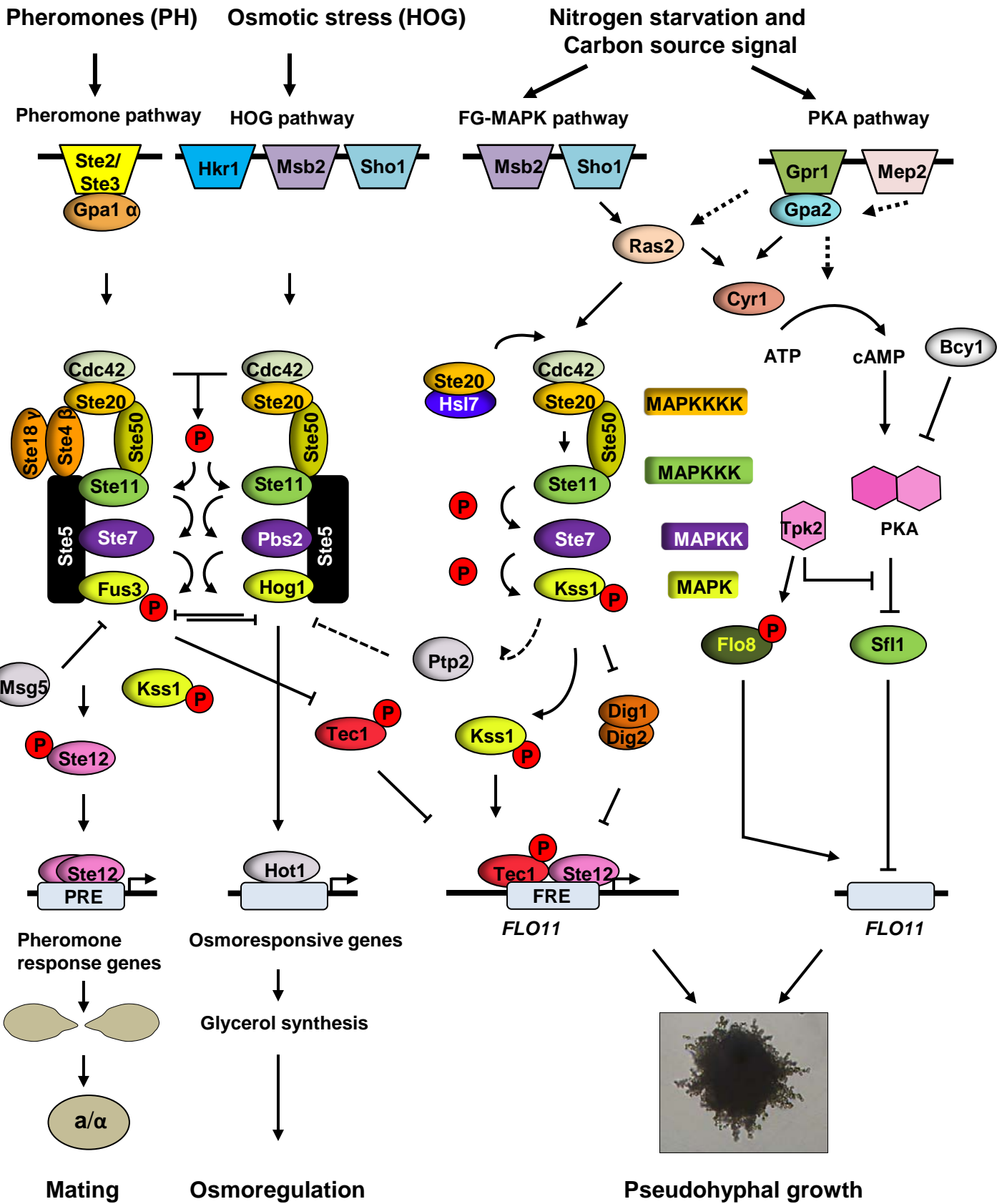
Figure 1.4 MAPK and PKA signalling cascade in pseudohyphal growth. This model provides an interpretation of MAPK and PKA pathways involved in pseudohyphal growth (FG) based on the existing data. Both the pathways control expression of *FLO11* and large collection of other genes required for pseudohyphal growth. MAPK modules of PH pathway, HOG pathway and FG pathway are also shown. Though these MAPK share common components, they maintain signalling specificity (see text for details). Dotted lines indicate that the relationship is unclear.

1.2.2.2.3 Other pathways involved in filamentous differentiation

Stress-induced signaling also plays an important role in induction of pseudohyphal growth. In addition to nitrogen and carbon starvation, oxygen limitation may also affect dimorphic switching in both haploids and diploids (Wright et al., 1993). Hap2-3-4-5p complex responds to hypoxic conditions and regulates oxygen regulated genes. *FLO11* (also known as *MUC1)* expression has been shown to increase under hypoxic conditions (ter Linde et al., 1999), suggesting that pseudohyphal growth may be induced in absence of oxygen. Nutrient responsive TOR signalling has also been shown to promote pseudohyphal growth. Sublethal concentration of rapamycin inhibits pseudohyphal growth in response to nitrogen limitation (Cutler et al., 2001). Mitochondrial retrograde (RTG) signalling pathway is also required for pseudohyphal growth through MAPK pathway as deletion of RTG signalling cascade components showed defect in MAPK activation (Chavel et al., 2010).

Environmental stress like heat stress also induces pseudohyphal growth (Zitomer and Lowry, 1992). Osmotic stress transduced via the Sho1p receptor may also enhance pseudohyphal growth (O'Rourke and Herskowitz, 1998). Additionally, various alcohols also induce pseudohyphal differentiation, like ethanol enhances pseudohyphal growth in diploid strains and other fusel alcohols including 1- butanol, isoamyl alcohol and *n*-amyl alcohol stimulate filamentous growth in haploids growing in glucose containing liquid medium (Lorenz et al., 2000a). The metabolic intermediate responsible for generating a filamentous growth signal or the induction of filamentous growth may suggest that the alcohols serve as signals to switch to alternate developmental pathway. Skn7p, a transcription factor that mediates oxidative stress responses downstream of PKA, is required for filament formation in response to nitrogen starvation (Lorenz et al., 2000b). In addition, the stress-responsive transcriptional repressor Xbp1p represses *CLB2* expression to induce cell elongation and filament formation in response to nitrogen starvation (Miled et al., 2001). Ras2p activity also decreases the activity of the stress responsive transcription factors Msn2p and Msn4p. This suppressed stress response has been suggested to be responsible for inducing invasive growth (Stanhill et al., 1999). Mutations in *BIR1*, a gene homologous to inhibitor of apoptosis (IAP) proteins in vertebrates, also enhance pseudohyphal growth but block sporulation during carbon source deprivation (Uren et al., 1999). Not surprisingly, genes linking nutrient

regulation to cell growth and division also affect pseudohyphal growth. The abundance and activity of the G1 cyclin Cln3p has multiple connections to cell-size control and nutrient sensing during vegetative growth as Cln3p accumulates when cells have sufficient nutrients to continue growth. Deletion of *CLN3* confers enhanced pseudohyphal growth (Loeb et al., 1999), suggesting that Cln3p abundance may carry part of the nitrogen starvation signal. Overexpression of *WHI2*, a gene required for cell cycle arrest upon carbon source depletion, stimulates filamentous growth (Radcliffe et al., 1997). However, *WHI2* is not required for pseudohyphal growth and is partially blocked by mutations in the STE MAPK pathway. Deletion of the Whi3p RNA-binding protein abrogates pseudohyphal growth, leading to small round cells on nitrogen starvation media (Mösch and Fink, 1997). Mutations in mannose utilization and protein glycosylation pathways activate MAPK signalling pathways used in invasive and filamentous growth.

The unfolded protein response pathway transcription factor Hac1[i]p plays an interesting role in pseudohyphal differentiation. Ire1p is activated in response to build up of unfolded proteins in the ER by dissociation of Ire1p from Kar2/BiP and oligomerization of lumenal domains of Ire1p (Bertolotti et al., 2000; Korennykh et al., 2009; Shamu and Walter, 1996). This is followed by trans autophosphorylation activating the endoribonuclease activity of Ire1p (Bertolotti et al., 2000), which splices constitutively expressed Hac1 mRNA. Ire1p cleaves *HAC1* mRNA 5' and 3' exon-intron junctions in an unconventional non spliceosome fashion (Sidrauski and Walter, 1997). The 252 nucleotide intron with splice sites is shown in **Figure 1.5 A**. The exons are ligated by tRNA ligase, Rlg1p thus producing spliced *HAC1[i]* mRNA (Sidrauski et al., 1996). Induced *HAC1[i]* mRNA is translated into Hac1[i]p, which is translocated to the nucleus and induces expression of many chaperone genes, components of ERAD and phospholipid biosynthesis genes (Schröder and Kaufman, 2005). High nitrogen concentrations stimulated *HAC1* mRNA splicing, which ceased during nitrogen starvation (**Figure 1.5 B**). Therefore, nitrogen starvation may at least partially stimulate filamentous growth by slowing protein translation rates, inactivating the unfolded protein response, and inhibiting *HAC1* splicing (Schröder et al., 2000). Other yeast developmental responses, such as entering the sporulation pathway, also respond to environmental stresses. In general, sporulation occurs under conditi-
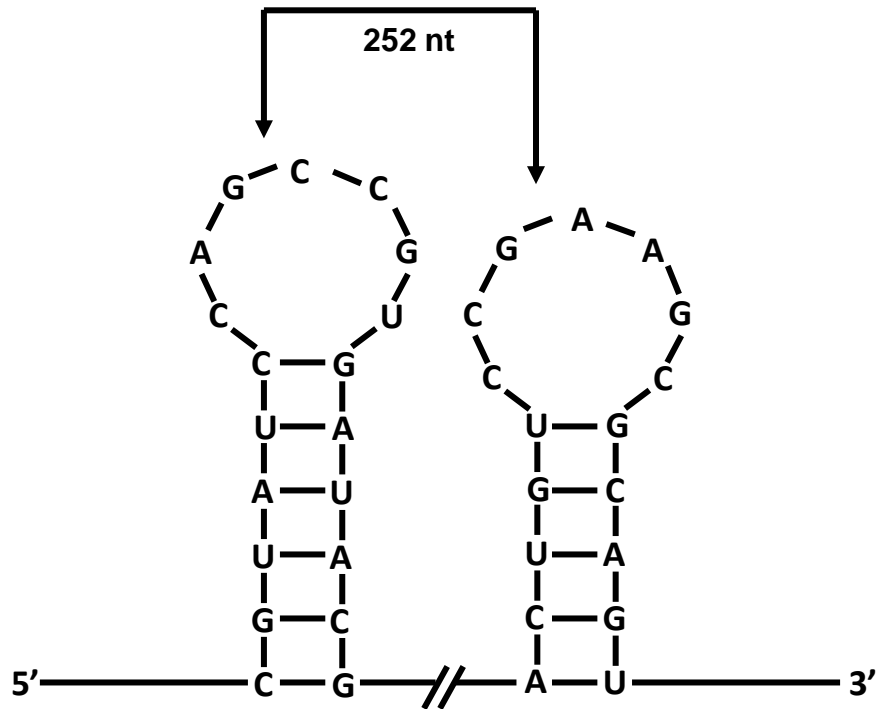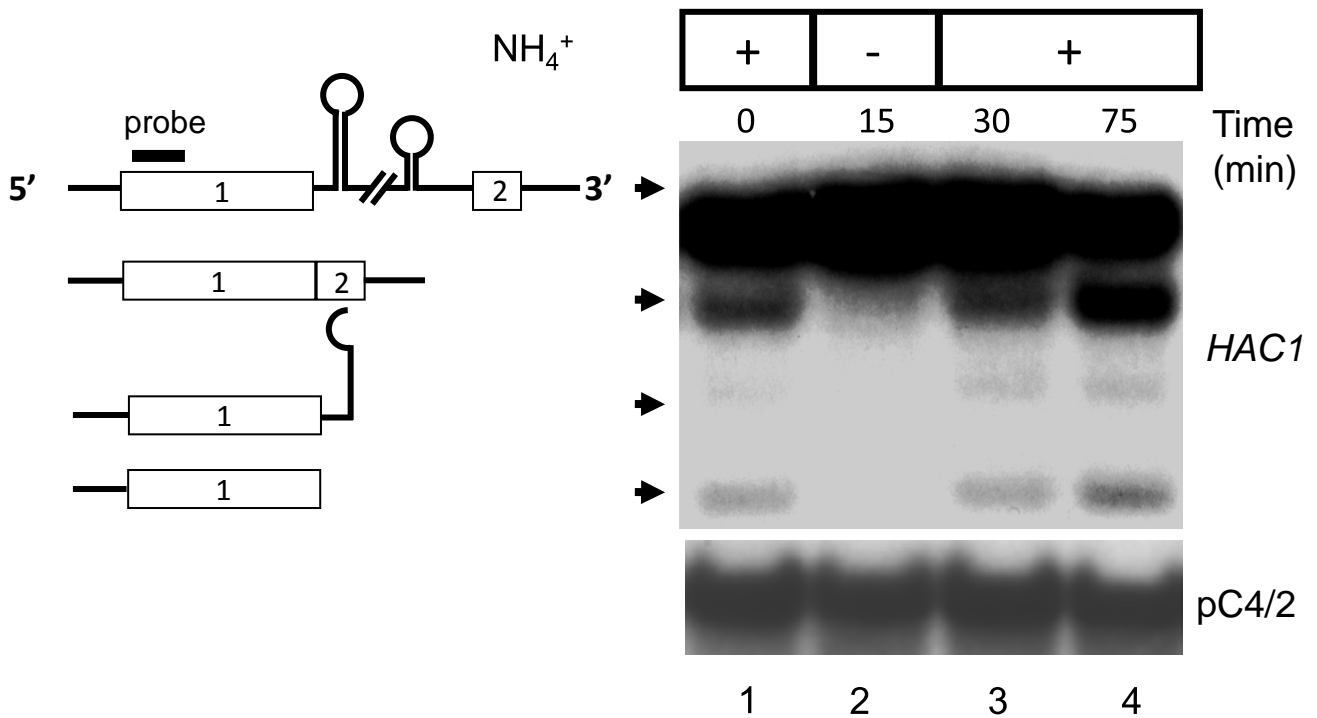
Figure 1.5 *HAC1* mRNA splicing in *S. cerevisiae*. A. Secondary structure of *HAC1* mRNA 3' UTR. Arrows indicate cleavage site. **B.** *HAC1* mRNA splicing products as detected by Northern analysis with a probe binding to the 5' region. WT strain grown to mid-log phase on acetate (*lane 1*) after nitrogen starvation (*lane 2*), and 15 and 60 min after addition of ammonium sulphate to cells starved for nitrogen for 15 min (*lane 3,4*) (Schroeder *et al* 2000).

-ons of nitrogen and carbon starvation while pseudohyphal differentiation is induced in nitrogen-poor but carbon rich environments. This switch may be mediated by Gpa2, which, when overexpressed, reduces sporulation but enhances filamentous growth (Donzeau and Bandlow, 1999; Lorenz and Heitman, 1997). Gpa2p appears to direct cells toward pseudohyphal growth rather than sporulation by directly interacting with the Ime2p kinase (Donzeau and Bandlow, 1999). In turn, overexpression of Ime2p inhibits pseudohyphal growth but enhances sporulation in the presence of glucose and nitrogen while *RIM1*, *8*, *9* and *13* mutations reduce *IME2* activity and switch cells from meiotic division to filamentous growth (Su and Mitchell, 1993a; Su and Mitchell, 1993b).

1.2.2.2.4 Other proteins involved in regulation of pseudohyphal growth

There are a number of other genes involved in the regulation of pseudohyphal growth whose precise role is not very clear. *PHD1* gene is induced in low nitrogen conditions (Erdman et al., 1998) and when overexpressed in nutrient rich condition induces vigorous pseudohyphal growth (Gimeno and Fink, 1994). *PHD1* transcription is induced by mating pheromones and nitrogen starvation and deletion of *PHD1* with deletion of *STE12* completely suppresses pseudohyphal growth (Gimeno and Fink, 1994; Lo et al., 1997). Sok2p is also involved in negatively regulating pseudohyphal growth as *sok2/sok2* diploids show increased pseudohyphae. Sok2p seems to act downstream of PKA subunits (Ward et al., 1995) but also in a separate, PKA independent pathway (Pan and Heitman, 2000). The forkhead transcription factor Fkh1p and Fkh2p also regulate pseudohyphal growth and invasive growth as deletion of both transcription factors induces filamentous growth (Hollenhorst et al., 2000). Fkh1p and Fkh2p regulate transcription of *CLB2* and other genes involved in mitosis, showing the link between cell cycle and pseudohyphal growth (Zhu et al., 2000). Interestingly, overexpression of the Yak1 kinase, an antagonist of the cAMP-PKA pathway, enhances pseudohyphal growth in response to nitrogen starvation (Zhang et al., 2001). In the absence of glucose, Yak1 localizes to the nucleus where it phosphorylates Pop2, a transcriptional regulator of glucose-repressed genes (Moriya et al., 2001). Thus Yak1 may be a key link between glucose sensing and invasive or filamentous growth. The RNA polymerase II complex also regulates invasive and filamentous growth, perhaps by altering expression of effectors and

repressors of these processes. Overexpression of the RNA polymerase subunit *RPB7* causes cell elongation and filament formation (Khazak et al., 1995). Also, mutations in other components of the RNA polymerase II complex (Ssn3p, Ssn8p, Srb8p, Cse2p and Med1p) constitutively activate invasive growth in haploids (Palecek et al., 2000).

1.3 The N-end Rule: Protein destabilisation using the N-end rule

Proteins function as important structural and functional entities in the cell to regulate a vast number of pathways. Proteins are in a dynamic state in the cell being continuously synthesized and degraded. Proteins are degraded to modulate levels of certain regulatory proteins or to get rid of damaged proteins. These proteins are conjugated to ubiquitin by the function of three enzymes: E1 ubiquitin activating enzymes, E2 ubiquitin conjugation enzymes and E3 ubiquitin ligases. The ubiquitinated protein is then degraded by the 26S proteosome. Methionine is by default the first amino acid incorporated during translation and this can be replaced with other destabilising amino acid residues to derive proteins of different half-life. Thus the N-terminal amino acid residue can determine the stability of the protein and this pathway is called N-end rule (Varshavsky, 1997). The N-end rule has been found in organisms ranging from *E. coli, S. cerevisiae, A. thaliana* to mammalian cells (Tasaki and Kwon, 2007). Artificially engineered chimeric ubiquitin-β-galactosidase protein encoded by Ub-*lacZ* is an artificial N-end rule substrate. β-Galactosidase encoded by *lacZ* is routinely used to monitor transcriptional activity in S. *cerevisiae* and has a half-life of >30 h (Bachmair and Varshavsky, 1989). The chimera of ubiquitin and β-galactosidase encodes a protein in yeast in which the nascent protein is deubiquitinated exposing the N-terminus (Bachmair et al., 1986). The ubiquitin moiety is cleaved by ubiquitin-specific proteases (Ubp) like *UBP1/2/3* and *YUH1* found in yeast (Bachmair et al., 1986; Baker et al., 1992; Tobias et al., 1991; Tobias and Varshavsky, 1991). The metabolic instability of engineered N-end rule substrates is due to the degradation signals called degrons, which is recognised by N-recognins. In eukaryotes, the N-degron consists of three determinants: a destabilizing N-terminal amino acid of the protein substrate, the internal lysine residue which forms the anchor for ubiquitin chain and the conformationally flexible region in the vicinity of the other determinants required for ubiquitylation and/or degradation (Hu et al., 2006). The N-end rule follows a hierarchic structure where asparagine (Asn) and glutamine (Gln) are tertiary destabilizing residues. They function by enzymatic deamidation to form secondary destabilizing residues aspartate (Asp) and glutamate (Glu) (Baker and Varshavsky, 1995; Kwon et al., 2000). These secondary destabilising residues are then conjugated to arginine (Arg) by *ATE1* encoded arginyl-tRNA protein transferase to derive the protein substrate with Arg for degradation. Phenylalanine, leucine, tryptophan, tyrosine, isoleucine, lysine and histidine besides arginine form

other primary destabilizing residues (Balzi et al., 1990; Davydov and Varshavsky, 2000; Hu et al., 2005; Kwon et al., 2002; Kwon et al., 1999; Lee et al., 2005b). N-recognins are a class of E3 ubiquitin ligases that tag the N-end rule substrates with ubiquitin via covalent bonding (Hu et al., 2006) and allow degradation by 26S proteosome. In yeast *UBR1* encodes the sole E3 ubiquitin ligase responsible for ubiquitylation of proteins with destabilising N-terminal residues (Alén et al., 2002; Xie and Varshavsky, 1999). The 225 kDa N-recognin Ubr1p consists of at least two binding sites identifying N-terminal residues. Type 1 residues are basic amino acid residues like Arg, Lys and His and type 2 residues are bulky hydrophobic residues like Phe, Leu, Trp, Tyr and Ile (Varshavsky, 1997). Therefore replacing default N-terminal amino acid residue, methionine with destabilising residues can change half-life of the protein. (**Table 1.1**) shows half-life of β-galactosidase destabilised with the amino acid residues as indicated.

The N-end rule functions naturally in a number of pathways which include the regulation of import of short peptides through ubiquitination and degradation of *CUP9*, a transcriptional repressor of *PTR2* peptide transporter (Alén et al., 2002), regulation of signal transduction and cell differentiation in response to mating pheromones through degradation of *GPA1* (Madura and Varshavsky, 1994), the fidelity of the chromosome segregation by degradation of the SCC1 cohesin subunit (Alén et al., 2002; Rao et al., 2001; Turner et al., 2000), regulation of apoptosis by degradation of caspase cleaved inhibitor *DIAP1* of apoptosis (Ditzel et al., 2003; Varshavsky, 2003), the regulation of meiosis (Kwon et al., 2003), leaf senescence and seed germination in plants (Yoshida et al., 2002), control of shoot and leaf development (Graciet et al., 2009) and neurogenesis and cardiovascular development in mammals (An et al., 2006; Johnson et al., 1990; Kwon et al., 2002; Lee et al., 2005b). In order to monitor transcriptional activity mediated through URS1, the URS1-*CYC1*-Ub-*lacZ* reporters were constructed in the current study exploiting N-end rule pathway.

Table 1.1 Destabilisation of β-galactosidase proteins by N-end rule in S. *cerevisiae*.

X amino acid residue	Half-life of X- β-gal
Arg	~2 min
Lys, Phe, Leu, Trp, Asp, Asn and His	~3 min
Tyr and Gln	~10 min
Ile and Glu	~30 min
Pro*	>5h
Met, Cys, Ala, Ser, Gly, Val and Thr	>30h

Table 1.1 Varying half lives of X-β-gal proteins exposing different amino acids at the N-terminal end in S. *cerevisiae* measured at 30°C. Reproduced from (Bachmair and Varshavsky, 1989; Balzi et al., 1990; Gonda et al., 1989). *Ub-Pro-β-gal is deubiquitinated 20 times slower than the other Ub-X-β-gal proteins and is a long lived protein in yeast.

1.4 Unfolded protein response pathway and its role in nutrient sensing and developmental programs

The unfolded protein response (UPR) pathway is induced in response to accumulation of unfolded proteins in the endoplasmic reticulum (ER). The cells respond to this ER stress through a signal transduction pathway that transduces the signal of unfolded or misfolded proteins from the ER lumen to the nucleus (Schröder and Kaufman, 2005). ER expansion and upregulation of chaperone gene expression are the main events occurring in this pathway, which leads to decrease in load of unfolded proteins in ER (**Figure 1.6**). The following sections discuss UPR pathway in yeast and mammals and its role in nutrient sensing and developmental programs.

1.4.1 UPR pathway in yeast:

In budding yeast *S. cerevisiae,* Ire1p (<u>I</u>nositol <u>re</u>quiring) in unstressed conditions is bound to BiP/GRP78/KAR2 chaperones in a monomeric form (Bertolotti et al., 2000; Harding et al., 2000; Urano et al., 2000a; Urano et al., 2000b). On an increase of unfolded proteins in the ER, BiP/GRP78/KAR2 bind the unfolded polypeptides, rendering Ire1p relatively free. Ire1p now oligomerizes and undergoes autophosphorylation through its serine threonine kinase domain, activating its RNAse domain. Ire1p was shown to be forming a higher order oligomer to actuate response to counter the buildup of unfolded proteins in the ER (Korennykh et al., 2009). Activated Ire1p splices at the 5' and 3' exon-intron junctions of *HAC1* messenger RNA (**Figure 1.5 A**). The exons are ligated by transfer RNA ligase (Rlg1p) (Sidrauski et al., 1996). *HAC1* mRNA encodes Hac1^{i}p, basic leucine zipper transcription factor (bZIP) (Cox and Walter, 1996; Kawahara et al., 1997; Sidrauski et al., 1996). Thus Hac1^{i}p ("i" for induced) then activates genes by binding to the consensus sequence Unfolded Protein Response Element (UPRE; CAGCGTG) present in the promoters of responsive genes like chaperone genes and activate their transcription (Mori et al., 1996; Mori et al., 1998; Mori et al., 1992). The expressed chaperones would necessarily help to deal with ER unfolded protein stress. Unspliced *HAC1^u* mRNA is poorly translated and is unable to activate transcription as efficiently as Hac1^{i}p synthesized from spliced *HAC1^i* mRNA (Chapman and Walter, 1997; Cox et al., 1997; Welihinda et al., 2000). The transcriptional activation through UPRE is dependent on a functional SAGA histone

acetyltransferase (Welihinda et al., 1997) and Hac1^{i}p *in vitro* interacts with Gcn5p the catalytic subunit of SAGA (Welihinda et al., 2000).

1.4.2 Mammalian UPR pathway:

In higher eukaryotes, there are two orthologs of yeast Ire1p, IRE1-α and IRE1-β. Activated Ire1p splices *XBP1* mRNA encoding the bZIP transcription factor X-box binding protein (Xbp-1) in metazoans which activates UPR-target genes (Yoshida et al., 2001). Unspliced *XBP1*-mRNA (*XBP1^u*) encodes a short lived protein responsible for repression of these UPR target genes (Yoshida et al., 2006). The splicing of *XBP1* mRNA by Ire1p excises an intron resulting in a frameshift in the *XBP1* transcript (*XBP1^s*) resulting into Xbp1^s similar to Hac1^{i}p in yeast (**Figure 1.6**). *IRE1* is also involved in activation of cell death pathways in response to prolonged ER stress by its interaction with tumor necrosis associated factor (TRAF2) to modulate the activity of c-JUN N-terminal kinase (JNK) pathway via the apoptosis signaling-regulated kinase 1 (ASK-1), which controls apoptosis through caspase-12 activation (Hetz et al., 2006; Nishitoh et al., 2002; Urano et al., 2000b; Yoneda et al., 2001). The non-specific Ire1p RNAse activity has also been suggested to reduce global reduction of protein into ER by degradation of mRNA localized to ER membrane (Hollien et al., 2009). The Ire1p mediated mRNA splicing of *HAC1*/XBP1 is conserved from yeast to mammals while higher eukaryotes have evolved additional sensors of ER stress in protein kinase activity of PKR-like endoplasmic reticulum kinase/pancreatic eIF2ɑ-kinase (PERK) and activating transcription factor 6 (ATF6) (**Figure 1.6**). The UPR regulates translation through attenuation of general transcription by increasing the protein kinase activity of PERK, which in turn phosphorylates the eIF2α translation initiation factor inhibiting general translation (Harding et al., 1999). Under conditions of ER stress, BiP dissociates from lumenal domain of PERK triggering oligodimerization, autophosphorylation and leading to activation of its cytosolic kinase domain (Bertolotti et al., 2000; Harding et al., 2000; Liu et al., 2003; Ma et al., 2002; Ron and Walter, 2007; Urano et al., 2000a; Urano et al., 2000b). PERK phosphorylation of eIF2α not only decreases the protein folding load of ER, but also activates NFκB signaling and potentially promoting cell survival and an inflammatory response (Deng et al., 2004; Jiang et al., 2003). eIF2α phosphorylation selectively increases translation of activating

transcriptions factor 4 (ATF 4) mRNA through upstream open reading frames (uORFs) present in the ATF4 transcript (Lu et al., 2004; Vattem and Wek, 2004). ATF4 localizes to the nucleus and activates transcription of genes encoding amino acid transporters, redox enzymes that promote protein folding in the ER lumen and a proapoptotic transcription factor called CCAAT enhancer- binding homologous protein (CHOP) (Jiang et al., 2004; Schröder and Kaufman, 2005). ATF4 also increases transcription of *XBP1* mRNA and augments the UPR response (Yoshida et al., 2000). Dephosphoryaltion of eIF2α by the association of protein phosphatase I (PPI) to constitutively expressed repressor of eIF2α phosphorylation (CReP) and stress inducible ATF4 target, growth arrest and DNA damage inducible gene 34 (GADD34) relieves PERK dependent translation attenuation (Brush et al., 2003; Ma and Hendershot, 2003). The third sensor of ER stress, activating transcription factor (ATF6) is also regulated by its interaction with BiP and release of BiP allows ATF6 packaging into COPII vesicles to be translocated to Golgi under ER stress (Chen et al., 2002). In Golgi, ATF6 is sequentially cleaved by site-1-protease (S1P) and site-2-protease (S2P) to release a 50 kDa cytosolic domain (Haze et al., 1999). This portion of ATF6 may then heterodimerize with XBP1 and localize to the nucleus to activate genes encoding ER chaperones (Yoshida et al., 2000). The ER associated protein degradation (ERAD) pathway is also activated to degrade unfolded/misfolded proteins (Casagrande et al., 2000; Friedlander et al., 2000; Travers et al., 2000). Thus, upregulation of chaperones synergizes with translational control and protein degradation machinery in protecting cells against unfolded and misfolded proteins.
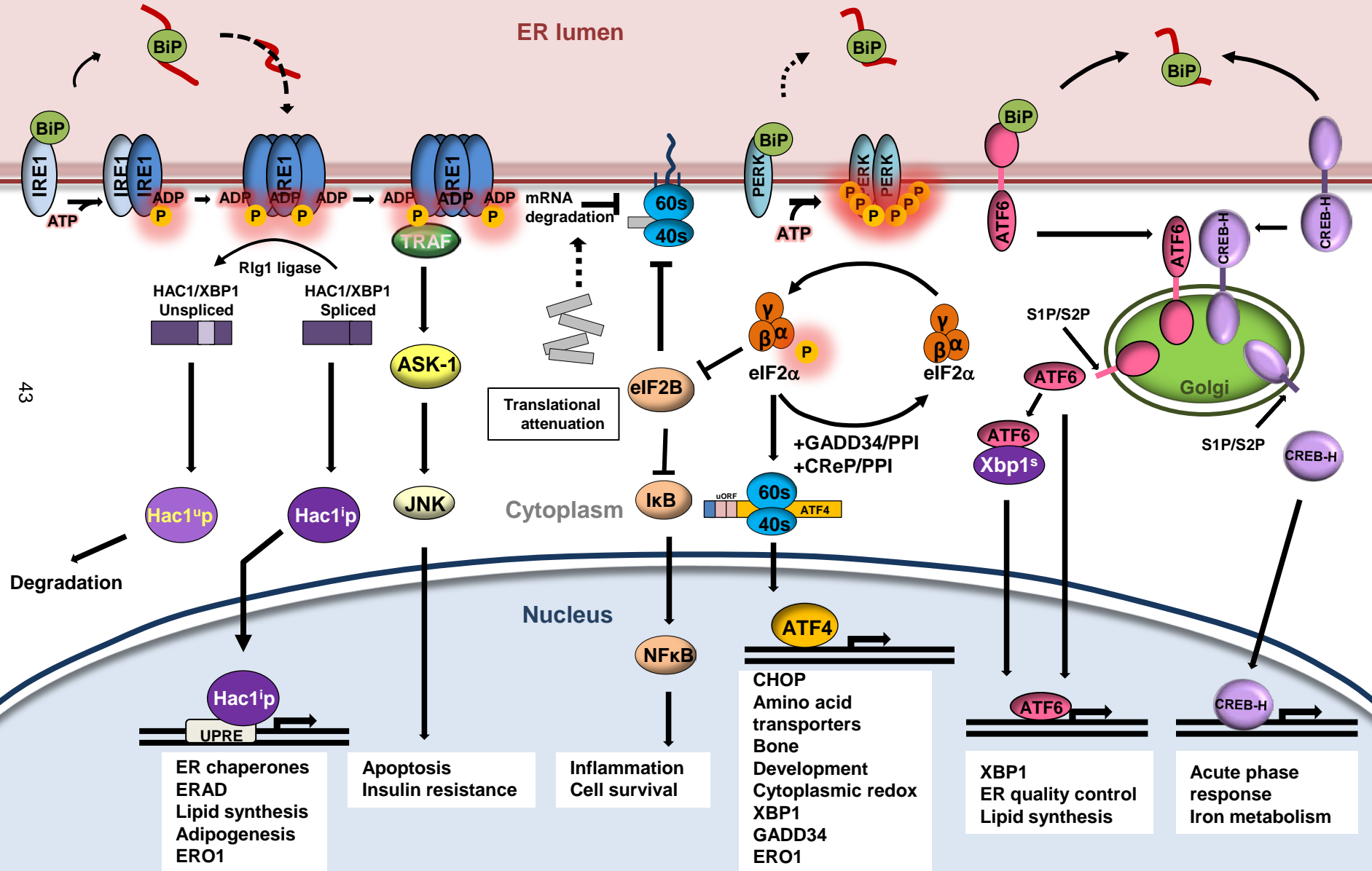
Figure 1.6 Unfolded protein response pathway in yeast and mammalian cells.
Three sensors of unfolded protein in ER, IRE1, PERK and ATF6 initiate signalling cascade that restores ER homeostasis and if needed be undergoes apoptosis. UPR also regulates metabolic pathways, cell differentiation and inflammation and cell survival. UPR in yeast is triggered in presence of unfolded proteins by activation of Ire1p, whose ribonuclease activity splices *HAC1* mRNA to synthesize Hac1^{i}p. The newly synthesized Hac1^{i}p induces transcription of genes containing UPRE (chaperones and foldases), components of ER-associated degradation (ERAD) pathway and proteins involved in phospholipid biosynthesis for ER expansion. *XBP1* mRNA is spliced by mammalian homologues of yeast *IRE1, IRE1-α* and *IRE1-β.* This splicing causes frameshift in *XBP1* transcript, which is translated into Xbp1 activating UPR target genes like yeast. When ER stress is prolonged, IRE1 activates cell death pathways in association with tumor necrosis associated factor 2 (TRAF2) to modulate the activity of the c-Jun N-terminal kinase (JNK) pathway via the apoptosis signaling-regulating kinase (ASK1), which controls apoptosis. In higher eukaryotes PERK and ATF6 form additional branch of UPR. Under ER stress, PERK is dissociated from BiP, triggering PERK dimerization, autophosphorylation and activation of cytosolic kinase domain. Activated PERK phosphorylates translation initiation factor eIF2α, which attenuates global protein translation reducing protein load of ER. ATF4, however is exempted from this embargo due to selective transcription through conserved upstream ORFs (uORFs) in *ATF4* mRNA. The ATF4 localizes to the nucleus and upregulates genes encoding amino acid transporters, promote protein folding proteins (e.g., ERO1), and a proapoptotic transcription factor called the CCAAT enhancer-binding homologous protein (CHOP), transcription of XBP1 mRNA. High eIF2α phosphorylation activates NF-κB signalling, which promotes cell survival and inflammatory response. Activating transcription factor 6 (ATF6) is also regulated by interaction with BiP in the ER lumen. ATF6 dissociates from BiP, permitting ATF6 to pack into COPII vesicles for trafficking to the Golgi. ATF6 is sequentially cleaved by the site-1-protease (S1P) and site-2-protease (S2P) in Golgi, with release of the 50 kDa cytosolic domain of ATF6. This portion of ATF6 may then heterodimerize with XBP1 before trafficking to the nucleus to activate genes encoding ER chaperones. ATF6 shares homology with two tissue-specific proteins: CREB-H in hepatocytes and OASIS in astrocytes (not shown), which activate the stress-dependent transcription of genes with promoters containing inflammatory response elements and cAMP-responsive elements, respectively. Thus the UPR integrates all three pathways to restore ER homeostasis.

1.4.3 Role of UPR in nutrient sensing and differentiation of yeast

The UPR pathway when induced regulates the transcription of 381 open reading frames in yeast. Roughly 50% of ORFs were known to function in the secretory pathway, but still ~100 ORFs were known to be regulated by UPR but had other known functions unrelated to secretory pathway, indicating that they may be related to other cellular processes (Travers et al., 2000). One function of UPR is control of differentiation responses like meiosis and pseudohyphal growth in *S. cerevisiae.* Yeast responds characteristically to its nutrient niche and the differentiation responses are controlled by a combination of cell type and environmental cues. Under nitrogen starvation conditions diploid yeast undergoes pseudohyphal growth in presence of a fermentable carbon source (Gimeno et al., 1992), while sporulation occurs in the presence of a non-fermentable carbon source (Kupiec et al., 1997). UPR pathway senses the nitrogen availability and regulates the differentiation of yeast. The splicing of *HAC1* mRNA is seen in nitrogen-rich conditions, but the splicing is inhibited under nitrogen starvation (**Figure 1.5 B**). In nitrogen-rich conditions the UPR pathway represses both the pseudohyphal growth and meiosis (Schröder et al., 2000). Overexpression of Hac1[i]p decreased activation of early meiotic genes (EMGs) under nitrogen starvation, while deletion of *HAC1* increased mRNA levels of EMGs under nitrogen-rich conditions, but Ime1p levels were not affected. The negative regulation of EMGs' transcription through Hac1[i]p requires Ume6p. Ume6p recruits the *ISW2* chromatin remodeling complex (Goldmark et al., 2000) and the Rpd3-Sin3 HDAC (Schröder et al., 2004) to Upstream Repressing Sequence 1 (URS1). URS1 can be found in promoters of meiosis-specific genes like *SPO13*, *HOP11* and *IME2* and non-meiotic genes like *CAR1* (Gailus-Durner et al., 1996). Overexpression of Hac1[i]p also repressed pseudohyphal growth and deletion of *HAC1* or *IRE1* derepressed pseudohyphal growth. UPR inducing drugs like tunicamycin and 2-deoxyglucose repressed pseudohyphal growth in wild-type but not in *ire1Δ* and *hac1Δ* (Schröder et al., 2000). These data show that Hac1[i]p is synthesized in response to nitrogen-rich environment and negatively regulates nitrogen starvation responses. Schroder et al, 2000 suggested a model of UPR-signaling pathway sensing the nutritional state of the cell and regulating the nitrogen starvation induced differentiation responses (**Figure 1.7**). The splicing of *HAC1* mRNA in response to extracellular nitrogen may be due to increased protein synthesis leading to high levels of newly synthesized unfolded

polypeptides in nitrogen-rich conditions compared to nitrogen-starved conditions and this activates the UPR by splicing of *HAC1* mRNA. On the contrary, nitrogen starved conditions have lower rates of protein synthesis decreasing the ER load, leading to Ire1p inactivation and shutting off the Hac1^{i}p synthesis. Thus UPR plays a role in nutrient sensing and controlling differentiation events in yeast.

1.4.4 Basal UPR pathway in yeast:

Healthy cells under nutrient rich conditions also experience basal UPR activity in presence of unfolded proteins in ER. Synthetic lethalities in yeast between UPR and ERAD (Travers et al., 2000) or chaperone machinery (Tyson and Stirling, 2000), and increase in UPR signaling have been reported with defective ERAD in yeast (Cox and Walter, 1996) and mammalian cells (Hori et al., 2004; Lee et al., 2003). *HAC1* mRNA splicing varies dynamically in response to nitrogen availability and presence of different carbon sources. *HAC1* mRNA splicing is induced under nitrogen-rich conditions, while spliced *HAC1* ceases as nitrogen becomes limiting. The level of *HAC1* mRNA splicing is induced tenfold in non-fermentable carbon source compared to fermentable carbon sources. These data indicate that the UPR senses the changes to its nutritional environment and controls nutritional and differentiation programs, besides the basal UPR that serves to aid protein folding in healthy cells (Schröder et al., 2000). The repression of metabolic genes *ACS1* encoding acetyl coenzyme A synthethase, *CAR1* encoding arginase, and *INO1* in Ume6p and RPD3-SIN3 HDAC-dependent manner further highlights the role of UPR in healthy cells to its metabolic regulation (Schröder et al., 2004).
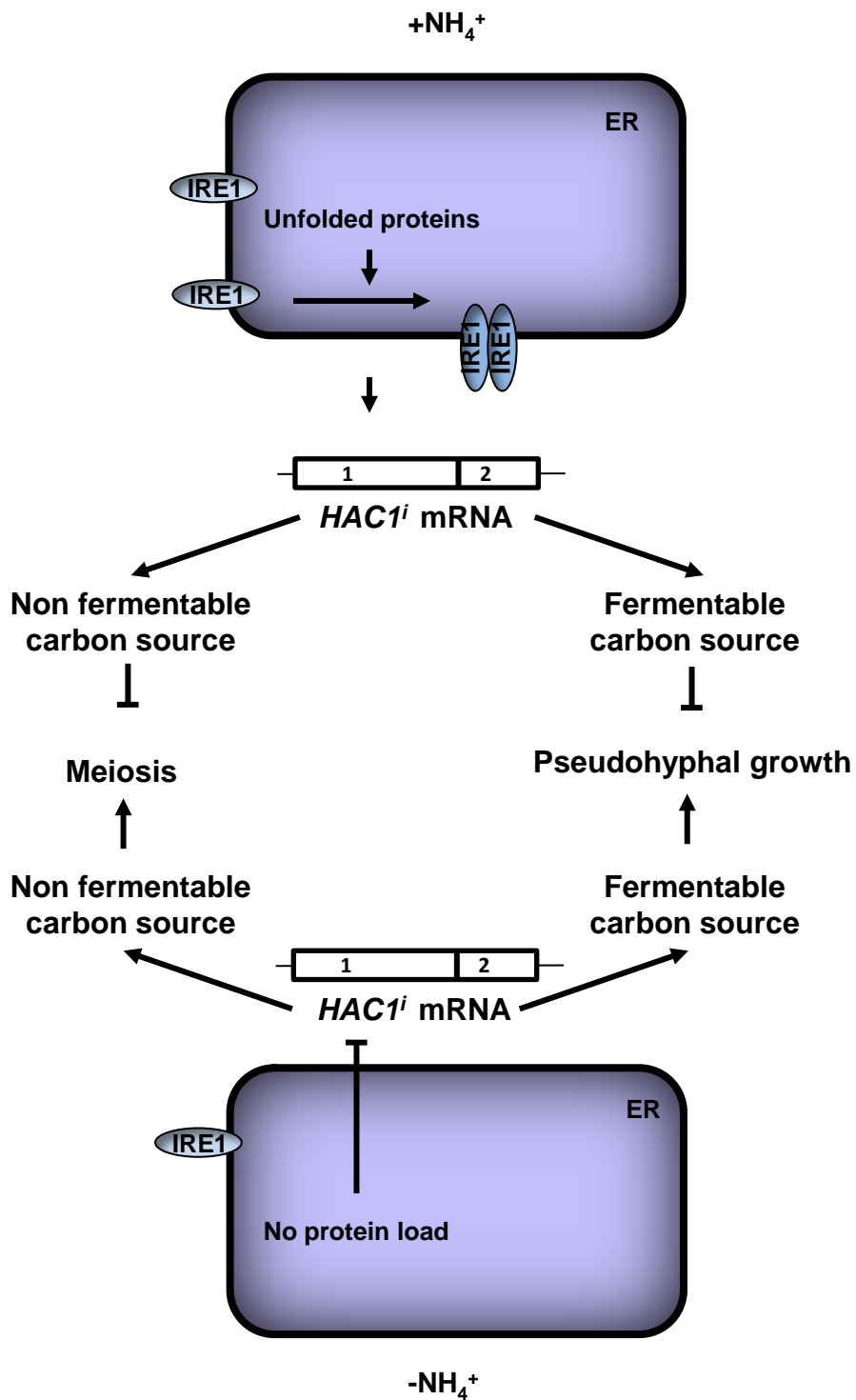
Figure 1.7 UPR as a nutrient sensor regulating differentiation events in yeast. In nitrogen rich environment, *HAC1* mRNA is spliced due to high protein synthesis, which represses pseudohyphal growth and meiosis. When nitrogen is limiting the Hac1[i] p synthesis is shut off and depending on the carbon source cells undergo meiosis or pseudohyphal growth.

1.4.5 Role of UPR in nutrient sensing and differentiation in higher eukaryotes:

In higher eukaryotes changes in glucose levels are responded by UPR. Decreased glucose levels induce the ER chaperone machinery indicating that UPR responds to nutritional state of the cell. Here this section provides an overview of UPR and its role in nutrient sensing and differentiation.

1.4.5.1 Glucose regulated events in pancreatic β-cells and plasma B-cells:

Hypoglcemia induced ER stress and UPR in liver cells and abrogation of PERK pathway in mice leads to hypoglycemia due to reduced levels of glycogen and phosphoenol pyruvate carboxykinase, a rate limiting step in gluconeogenesis (Gonzales et al., 2008; Scheuner et al., 2001). Decreased glucose levels induce eIF2α phosphorylation by PERK and limit translation to decrease proinsulin production in β-cells (Scheuner et al., 2001). A nearly fivefold increase in total protein synthesis, ~50% of which is proinsulin production, challenges the folding capacity of ER in glucose stimulated β-cells. UPR responds by adjusting organelle mass and induces chaperones and foldases to maintain favorable environment for proper folding of proinsulin in cases of hyperglycemia, insulin resistance or high fat diet (Scheuner and Kaufman, 2008). As glucose levels rise, the ADP/ATP ratio increases, inactivating PERK signaling and inducing proinsulin production (Scheuner et al., 2001). The role of protein phosphatase 1 (PP1) has been proposed, where in the presence of glucose, eIF2α is dephosphorylated to allow proinsulin production (Vander Mierde et al., 2007). eIF2α phosphorylation is also required for maintenance and function of differentiated β-cells (Back et al., 2009). In this way glucose sensing by β-cells to control proinsulin production may have evolved ER signaling to support this specialized cell type. Decreased or increased glucose levels trigger ER stress in isolated pancreatic islets and insulinoma cells (Elouil et al., 2007; Greenman et al., 2007). High glucose and high fatty acid supply induce ER stress in β-cells and play a part in development of type 2 diabetes. Sustained ER stress reduces insulin expression and increases apoptosis (Kaneto et al., 2006; Laybutt et al., 2007). It has been proposed that ER stress suppresses insulin biosynthesis at the transcriptional level by JNK activation (Kaneto et al., 2006). UPR related events are seen in β-cells of type 2 diabetes and CHOP mediated apoptosis is a fundamental contributing factor to β-cell failure in the

disease (Laybutt et al., 2007; Scheuner and Kaufman, 2008). Further β-cell dysfunction has also been related to ER stress in animal models with defective disulphide bridge formation in proinsulin (Herbach et al., 2007). The mice with impaired disulfide bond formation in proinsulin induce diabetes, while similar mutation in human insulin gene induces permanent neonatal diabetes (Huang et al., 2007; Stoy et al., 2007). So the involvement of glucose in controlling proinsulin translation by UPR is also evident in pancreatic β-cells.

Differentiation of B-cells: The role of UPR in differentiation in mammalian system is reported in the terminal differentiation of B-cells to antibody secreting plasma cells. UPR is activated on antigenic stimulation of B lymphocytes to terminally differentiate into plasma cells producing high rate of antibodies to deal with antigen. IRE1 mediated XBP1 splicing is required to drive the differentiation and activation of UPR is needed to expand the ER and meet the demand of high secretory activity of B-cells (Calfon et al., 2002; Iwakoshi et al., 2003; Lee et al., 2005a; Reimold et al., 2001; Zhang et al., 2005). This is consistent with the requirement for XBP1 in pancreatic acinar cell development (Lee et al., 2005a). A key role of Xbp1 is in ER expansion through induction of phospholipid biosynthesis and membrane proliferation for plasma cell differentiation (Shaffer et al., 2004; Sriburi et al., 2004). Terminal differentiation of B-cells requires repression of c-*myc* transcription (Lin et al., 2000) through recruitment of mammalian Rpd3p orthologs to the c-*myc* promoter by Blimp-1 (Yu et al., 2000). These data together with the observation that the UPR controls HDACs in yeast suggests that UPR signaling is not only important to drive but also important to maintain differentiation in mammals.

1.4.5.2 UPR and Insulin signaling:

Under nutrient excess, insulin levels rise and activate downstream signaling pathways. Insulin stimulates glucose uptake, nutrient storage and protein synthesis after binding to the insulin receptor (IR) to promote differentiation and growth (Draznin, 2006; Nandi et al., 2004; Saltiel and Kahn, 2001; Saltiel and Pessin, 2002; Shulman, 1999; Taniguchi et al., 2006). Binding of insulin to the IR induces a conformational change in the IR and activates tyrosine autophosphorylation of the IR, IR substrate (IRS) 1, 2, 3, and 4, and of several SRC homology 2 (SH-2) domain containing (SHC) proteins.

Tyrosine-phosphorylated IRS and SHC proteins are anchoring points for proteins containing SH-2 domains, including recruitment of both SH-2 domains in the regulatory subunits of phosphatidylinositol (PI) 3-kinase (PI3K). p85 is the regulatory subunit of PI3K and this interaction relieves the basal repression of catalytic subunit of PI3K (p110). Activated PI3K catalyzes the formation of PI-3,4-bisphosphate and PI-3,4,5-trisphosphate and recruitment of phosphoinositide-dependent kinases (PDK) 1 and 2 and several protein kinase B (PKB/AKT) isoforms to the plasma membrane. PDKs when co-localized at the plasma membrane phosphorylate and activate PKB1, -2, and -3. Activated PKB controls many cellular events, including glucose transport, protein and glycogen synthesis, cell proliferation and survival by phosphorylation of numerous substrates. The importance of PI3K in mediating the metabolic actions of insulin is supported by studies where genetic or pharmacological inhibition of PI3K completely abolishes insulin stimulation of glucose transport, lipogenesis and glycogen synthesis (Cheatham et al., 1994; Sharma et al., 1998). More evidence comes from the fact that alterations in insulin stimulation of PI3K activity have been observed in mouse models of obesity, as well as in humans with type 2 diabetes (Bandyopadhyay et al., 2005; Cusi et al., 2000; Heydrick et al., 1995).

Recent results show that p85α and p85β, the regulatory subunits of PI3K interact with XBP1 and increase its nuclear translocation in response to insulin, thereby activating UPR (Park et al., 2010; Winnay et al., 2010). The results also show that p85α deficient cultured cells or hepatocytes result in reduced nuclear accumulation of XBP1 after ER stress and considerably attenuate UPR by reduction in IRE1α and ATF6 pathway activation and a concomitant reduction in the expression of UPR targets at the mRNA and protein levels. However translocation of XBP1 to nucleus can resolve ER stress with limited activation of PERK arm of UPR. But obese mice with refeeding and metabolic overload led to severe PERK phosphorylation. So the intact response of p85 to insulin receptor signaling is necessary for activation of UPR to deal with metabolic overload. This is especially important because when insulin levels rise in response to excess of nutrient availability the activation of insulin receptor signaling increases protein synthesis, nutrient storage and promotes differentiation and growth (Nandi et al., 2004; Saltiel and Pessin, 2002; Taniguchi et al., 2006). This metabolic overloading causes ER stress and activation of the PERK arm of UPR downregulates the protein load by reducing global translation (Harding

et al., 2000; Harding et al., 1999) and increased IRE1 kinase activity blocks insulin receptor signaling. So a model was proposed where decrease in p85α leads to a reduced nuclear translocation of XBP-1 and therefore reduce cellular response to ER stress and a decrease in ATF6α pathway activation. Conversely, active insulin receptor signaling increased the efficiency of XBP-1s by promoting its association with p85, leading to faster and higher upregulation of the chaperones, without chronic activation of UPR (Park et al., 2010; Winnay et al., 2010). This highlights the critical role of PI3K regulatory subunits in modulating the UPR.

Mice with genetic or diet-induced obesity show a considerable elevation in ER stress, with elevated phosphorylation of PERK and IRE1α and enhanced splicing of XBP-1 (Özcan et al., 2004). Conversely, the increase in insulin sensitivity associated with weight loss is associated with a substantial reduction in markers of UPR activation (Gregor et al., 2009). Enhancement of protein folding led to improvements in obesity-associated insulin resistance and glucose metabolism (Ozawa et al., 2005; Özcan et al., 2006). So UPR may decrease insulin sensitivity in obese state through IRE1α-dependent activation of c-Jun N-terminal kinase (JNK), which leads to phosphorylation of insulin receptor substrate-1 (IRS-1) on inhibitory serine residues (Audhya et al., 2004; Herschkovitz et al., 2007; Tanti et al., 2004). When subjected to a high-fat diet, XBP-1–heterozygous mice gain more weight and become more insulin resistant than control mice (Özcan et al., 2004). These mice also show an increase in ER stress in adipose tissue, with enhanced PERK and IRE1α phosphorylation and activation of JNK. Likewise, XBP-1-deficient fibroblasts show enhanced PERK phosphorylation, hyperactivation of JNK and increased serine phosphorylation of IRS-1 (Özcan et al., 2004). The ER stress response has been strongly implicated in the pathophysiology of diabetes, affecting both insulin sensitivity in liver and fat, and the survival of pancreatic β-cells (Calfon et al., 2002; Eizirik et al., 2008; Fonseca et al., 2007; Nakatani et al., 2005). Adipose tissues from obese, insulin-resistant mice and humans show a persistent low level of inflammation in addition to activation of ER stress pathways, including induction of the UPR. Therefore inflammation is a common feature of obesity and type 2 diabetes (Hotamisligil, 2006; Özcan et al., 2004; Shoelson et al., 2006; Wellen and Hotamisligil, 2005). In obese mice, there is a ~50% reduction in p85α expression in

liver (Kerouz et al., 1997). In response to excess nutrients IRE1-XBP1-p85α pathway manage ER homeostasis and modulate insulin sensitivity but failure of this pathway in obesity leads to activation of UPR promoting proinflammatory and proapoptotic state (Park et al., 2010; Winnay et al., 2010). This link between the regulatory subunit of PI3K regulated by insulin and the cellular response to ER stress establishes a role of UPR in nutrient sensing mechanism in higher eukaryotes and its regulation of cellular processes. The crosstalk between the PI3K system and the UPR might have evolved to ensure the utilization of nutrients at the highest level of their availability in cell types requiring increased protein load without needing to activate other arms of UPR that would otherwise block protein synthesis.

1.5 Aims and Objectives

Aims:

A) Study of regulation of EMGs under nutrient-rich conditions

- To investigate whether Hac1[i]p mediates repression on EMGs through URS1 in a nitrogen-rich environment
- To study the role of histone and chromatin modifying complexes in regulation of URS1-controlled genes under nutrient rich conditions

S. cerevisiae responds to their nutritional environment and decide their cell fate. The yeast responds to nitrogen starvation by differentiating to form a spore or pseudohyphal growth depending on the type of carbon source. Nitrogen-rich conditions repress these differentiation events. The unfolded protein response pathway is known to contribute to control of these nitrogen starvation responses. Under nitrogen-rich conditions Hac1[i]p is synthesized but when extracellular levels of nitrogen drop, Hac1[i]p synthesis ceases. Pseudohyphal growth is repressed by activation of UPR or by overexpression of Hac1[i]p. The *hac1Δ/hac1Δ* strains show derepression of pseudohyphal growth. Negative regulation of early meiotic genes is shown by increased levels of mRNA levels in the absence of Hac1[i]p and repression in the presence of Hac1[i]p under nitrogen starved conditions. Therefore, Hac1[i]p inhibits meiosis under nitrogen starved conditions. Hac1[i]p-mediated negative regulation also requires the function of *RPD3-SIN3* HDAC under these conditions, while the *ISW2-ITC1* chromatin remodelling complex was dispensable for this repression. However, the URS1-mediated repression in the presence of extracellular nitrogen has not been demonstrated. Therefore, demonstration of Hac1[i]p-mediated negative regulation of early meiotic genes through URS1 under nitrogen-rich conditions would further strengthen the case for involvement of the UPR sensing nitrogen. This will provide direct evidence of control of differentiation responses by UPR. UAS-less URS1-*CYC1-lacZ* reporters have been used to demonstrate negative regulation by Hac1[i]p at URS1 under nitrogen-starved conditions. But under nitrogen-rich conditions, β-galactosidase expression from these reporters is barely detectable. Therefore, these reporters did not yield conclusive data and could not be used here. Therefore, to test whether Hac1[i]p

negatively regulates the transcription of early meiotic genes through URS1 under nitrogen-rich conditions, I constructed URS1-*CYC1*-Ub-X-*lacZ* reporters. Destabilised β-galactosidase expressed from these reporters would have robust mitotic expression and different half lives as a result of the N-end rule. URS1-*CYC1*-Ub-X-*lacZ* reporters have been tested in different deletion strains of genetic elements to validate these reporters. Further, functional URS1-*CYC1*-Ub-X-*lacZ* reporters could be used in genetic screens. Hac1[i]p upregulates ER chaperone expression through UPRE elements by histone acetylation of promoters by the SAGA histone acetyltransferase (Welihinda et al., 1997; Welihinda et al., 2000). Hac1[i]p also negatively represses EMGs via URS1 and requires the function of the *RPD3-SIN3* HDAC. The URS1-*CYC1*-Ub-X-*lacZ* reporters will be handy in studying the structural features of Hac1[i]p which is involved in transcriptional activation and repression. These functional reporters can be used to investigate transcription factors, histone deacetylases and chromatin remodelling factors involved in the regulation of EMGs through URS1 under nitrogen-rich conditions.

B) Role of non-fermentable carbon sources in pseudohyphal growth

- To investigate the effects and role of non-fermentable carbon sources on pseudohyphal growth

Nitrogen starvation in the presence of a fermentable carbon source initiates pseudohyphal growth differentiation in *S. cerevisiae*. The UPR pathway also repressed pseudohyphal growth under nitrogen-rich conditions as *ire1Δ/ire1Δ* and *hac1Δ/hac1Δ* diploids also showed increased pseudohyphal growth and expression of Hac1[i]p repressed pseudohyphal growth. Thus cells compromised in UPR pathway under sporulation inducing conditions (limiting nitrogen and acetate), responded inappropriately by switching to pseudohyphal growth. Splicing of *HAC1* mRNA was higher in the presence of acetate as compared to other carbon sources (Schröder et al., 2000). These observations suggest that at least when UPR is defective, cells exhibit pseudohyphal growth on a non-fermentable carbon source. Therefore, it would be interesting to test whether **a**/α diploid cells also induce pseudohyphal growth on non-fermentable carbon source. If this is the case, genetic elements involved in this

phenomenon can be investigated. Thus this study will provide us an insight into effect of non-fermentable carbon sources on pseudohyphal growth.

Chapter 2

Materials and Methods

2.1 Chemicals, media, reagents and commercial kits

Table 2.1 List of Chemicals

Sr. No	Chemical	Company , Catalogue No.
1.	Acetic acid	Fisher Scientific, # A/0360/PBH
2.	Agar	Fisher Scientific, # 9002-18-0
3.	Agarose molecular grade	Bioline, # BIO-41025
4.	Albumin	Sigma-Aldrich, # A2153-50G
5.	Ammonium persulphate	Fisher Scientific, # BP179-25
6.	Calcium chloride	Sigma-Aldrich, # C1016-100G
7.	Clelands reagent	Calbiochem, # 233155
8.	Dimethyl sulfoxide	Sigma-Aldrich, # D5879
9.	Disodium hydrogen orthophosphate dodecahydrate	Fisher Scientific, # 10039-32-4
10.	Disodium hydrogen phosphate	Sigma-Aldrich, # S3264-250G
11.	Ethanol	Fisher Scientific , # E/0500/17
12.	Ethylenediaminetetraacetic acid (EDTA)	Fisher Scientific, # BPE119-500
13.	Ficoll 400	Fluka, # 46327
14.	D-Glucose	Fisher Scientific, # 50-99-7
15.	Glycerol	Fisher Scientific, # 56-81-5
16.	Hydrochloric acid	Fisher Scientific , # H/1100/PB17
17.	Iso-amyl alcohol	BDH, # 272124U

18.	Isopropyl β-D-thio-galactopyranoside (dioxane free)	Melford, # MB 1008
19.	Lithium Acetate	Fisher Scientific , # L/2050/50
20.	Magnesium chloride	BDH, # 2909647
21.	Magnesium sulphate	Fisher Scientific, # M/1050/53
22.	2-Nitrophenyl-β-D-galactopyranoside	BDH, # 400312X
23.	Phenol:CHCl$_3$:isoamylalcohol (25:24:1;v/v/v)	Fisher Scientific, # BPE1752P-400
24.	Polyethylene glycol 4000	Sigma-Aldrich, # P 3640
25.	Potassium acetate	Fisher Scientific, # P3760153
26.	Poatassium chloride	Fisher Scientific, # P/4240/53
27.	Potassium dihydrogen phosphate	Fisher Scientific, # 7778-77-0
28.	Potassium phthalate monobasic	Sigma-Aldrich, # P6758 -500 G
29.	Protease inhibitor cocktail • Complete • Mini	Roche Applied Science, # 11836153001 # 11836153001
30.	Sheared salmon sperm DNA (8.31 mg/ml or 6.89 mg/ml)	Sigma, # D-1626
31.	Sodium chloride	Fisher Scientific, # 7647-14-5
32.	Sodium dodecyl sulfate	Promega, # H5114

33.	Sodium hyroxide	Anal-R Normapur, # 28244.262
34.	Tris (hydroxymethyl) methylamine	Fisher Scientific, # T/3710/60
35.	Tween 20	Fisher Scientific, # BPE 337-500

Table 2.2 Media reagents

Sr. No.	Chemical	Company, Cat. No.
1.	LB broth	Formedium, # LBXO102
2.	LB agar	Formedium, # LBXO202
3.	YNB agar	Formedium, # CCMO210
4.	YNB broth	Formedium, # CCMO110
5.	YNB w/o a.a.	Formedium, # CYNO405
6.	YNB w/o a.a. w/o ammonium sulphate	Formedium, # CYNO501
7.	Difco YNB w/o a.a.	BD, # 291940
8.	Difco agar noble	BD, # 214220
9.	Bacto-peptone	BD, # 211677
10.	Bacto-yeast extract	BD, # 212750
11.	Agar	Fisher Scientific, # 9002-18-0

Table 2.3 List of Reagents/Enzymes/Antibiotics

Sr.No	Enzymes/Antibiotics	Company, Cat. No.
1.	1 U/µl β-galactosidase	Promega, # E2000
2.	5 Weiss U/µl T4 DNA ligase	Fermentas, # EL0011
3.	*Pfu* DNA polymerase	Fermentas, # EP0501
4.	RNase A, 10-20 mg/ml, DNase-free	Fermentas, # EN0531
5.	1 U/µl Calf intestine alkaline phosphatase	New England BioLabs, # M0290L
6.	Glusulase	Perkin Elmer, # NEE154
7.	Turbo *Nar*I	Promega, # R7261
8.	PspOMI	New England BioLabs , # R0653
9.	*Bam*HI	Fermentas, # ER0051
10.	*Bau*I	Fermentas, # ER1841
11.	*Eco*32I (*Eco*RV)	Fermentas, # ER0301
12.	*Eco*RI	Fermentas, # ER0271
13.	Ampicillin 100 µg/ml	Melford, # A0104
14.	Tetracycline 12.5 µg/ml	Fluka Biochemika, # 87130
15.	Hygromycin B	Duchefa Biochemie, # 31282-04-9

16.	Tunicamycin(*Streptomyces lysosuperficus*)	Calbiochem, # 654380
17.	G-418	Melford, # G0175
18.	Kanamycin	Gibco, # 11815-024

Table 2.4 List of Commercial kits

Sr.No	Kit	Company, Cat. No.
1.	Reagent A (Bio-Rad *DC* Protein Assay)	BioRad, # 500-0113
2.	Reagent B (Bio-Rad *DC* Protein Assay)	BioRad, # 500-0114
3.	Bovine serum albumin (BSA) standard	Sigma-Aldrich, # A2153-50G
4.	5 x Reporter lysis buffer	Promega, # E3971
5.	Wizard SV Gel and PCR clean up system	Promega, # A9282
6.	Qiagen Miniprep Kit	Sigma-Aldrich, # 27104
7.	GeneElute^{TM} HP Plasmid Midiprep kit	Sigma-Aldrich, # NA0200
8.	Genelute^{TM} Gel extraction kit	Sigma-Aldrich, # NA1111
9.	GeneElute^{TM} HP Plasmid Maxiprep kit	Sigma-Aldrich, # NA0310
10.	Gene Ruler^{TM} 1Kb DNA ladder	Fermentas Life Sciences, # SM0311

| 11. | 2 mM dNTPs | Fermentas Life Sciences, # R0181 |
| 12. | QIAprep Spin Miniprep kit | Qiagen, # 27104 |

Table 2.5 List of amino acids and media supplements

Sr.No	Enzyme/Antibiotic	Company, Cat. No.
1.	Adenine sulphate	Fluka, # 01880
2.	Inositol	Formedium, # DOCO200
3.	L-Lysine	Formedium, # DOCO161
4.	L- Methionine	Formedium, # DOCO168
5.	L-Valine	Formedium, # DOCO1197
6.	L-Threonine	Formedium, # DOCO185
7.	Isoleucine	Formedium, # DOCO152
8.	L-Aspartic acid	Formedium, # DOCO121
9.	L-Tyrosine	Formedium, # DOCO192
10.	L-Arginine	Formedium, # DOCO108
11.	L-Glutamic acid	Calbiochem , # 3510
12.	L-Histidine	Formedium, # DOCO148
13.	Uracil	Formedium, # DOCO300

14.	L-Phenylalanine	Formedium, # DOCO173
15.	L-Tryptophan	Formedium, # DOCO188
16.	L-Leucine	Formedium, # DOCO157
17.	L-Serine	Formedium, # DOCO181

2.2 List of primers and oligonucleotides

Table 2.6. List of primers and oligonucleotides. Oligonucleotides were synthesized by Eurogentec Ltd. Lyophiized primers were resuspended in sterile water to a final concentration of 100 µM and stored at -20°C.

Sr.No.	Primer	Sequence
1.	A1	GCATTAATGAATCGGCCAAC
2.	A2	ACTAAATTAATAATGCAGATTTTCGTCAAGACTTTGACCGG
3.	B1	ATAGCAGAATGGGCAGACATTAC
4.	B2	TGACGAAAATCTGCATTATTAATTTAGTGTGTGTATTTGTGTTTGCG
5.	I-β-gal	CCGGATCCGTGTATACCACCTCTTAGCCTTAGCACGAGATGTAAGG
6.	Q-β-gal	CCGGATCCGTGCTGACCACCTCTTAGCCTTAGCACGAGATGTAAGG

2.3 List of plasmids

Table 2.7. List of plasmids
Plasmids were maintained in *E.coli* (DH5α or XL10-GOLD) strains with ampicillin as selection marker. XL10-GOLD *E.coli* cells were selected by antibiotic tetracycline encoded by F´ episome. Plasmids in *S. cerevisiae* were selected by metabolic marker as indicated below. **Note: x** is the N-terminal amino acid of β-galactosidase.

Sr.No.	Plasmids	Description	Source
1.	pLGΔ312S	*CYC1-lacZ*-URA3-2µ	(Guarente and Mason, 1983)
2.	pLGΔ312S-IME2, pLGΔ312S-INO1	URS1(IME2)-*CYC1-lacZ*-URA3-2µ, URS1(INO1)-*CYC1-lacZ*-URA3-2µ	(Kadosh and Struhl, 1997)
3.	pUB23-M, pUB23-K, pUB23-L and pUB23-R	*GAL1, 10*-Ub-**x**-*lacZ*-URA3-2µ	(Bachmair and Varshavsky, 1989)
4.	pVP-IME2-M-β-gal, pVP-IME2-K-β-gal, pVP-IME2-L-β-gal, pVP-IME2-R-β-gal, pVP-IME2-I-β-gal and pVP-IME2-Q-β-gal	URS1(*IME2*)-*CYC1*-Ub-**x**-*lacZ*-*URA3*-2µ	This study
5.	pVP-INO1-M-β-gal, pVP-INO1-K-β-gal, pVP-INO1-L-β-gal,	URS1(*INO1*)-*CYC1*-Ub-**x**-*lacZ*-*URA3*-2µ	This study

	pVP-INO1-R-β-gal, pVP-INO1-I-β-gal and pVP-INO1-Q-β-gal		
6.	pVP-M-β-gal, pVP-K-β-gal, pVP-L-β-gal, pVP-R-β-gal, pVP-I-β-gal and pVP-Q-β-gal	*CYC1*-Ub-**x**-*lacZ-URA3*-2μ	This study
7.	pRS314-*HAC1^i*	HA-*HAC1^i*-TRP1-CEN	(Schröder et al., 2004)
8.	p2UG	GRE$_3$-*CYC1*-URA3-2μ	(Schena et al., 1991)
9.	pG-N795	GPD-N795-TRP1-2μ	(Schena et al., 1991)
10.	p2UG-HA-*HAC1^i*	GRE$_3$-*CYC1*-HA-*HAC1^i*-URA3-2μ	(Schröder et al., 2004)

2.4 List of strains:

Table 2.8 List of strains

Sr.No.	Organism	Name	Genotype	Source
1.	*S.cerevisiae*	MSY134-36	SK-1 MAT**a** *arg6 rme1Δ5*::*LEU2 ura3 leu2*::*hisG trp1*::*hisG lys2* ho::*LYS2*	(Schröder et al., 2004)
2.	*S.cerevisiae*	MSY136-40	SK-1 MATα *arg6 rme1Δ5*::*LEU2 ura3 leu2*::*hisG trp1*::*hisG lys2* ho::*LYS2*	(Schröder et al., 2004)
3.	*S.cerevisiae*	MSY 184-55	SK-1 MAT**a** *arg6 rme1Δ5*::*LEU2 ume6-5*::*LEU2 ura3 leu2 trp1 lys2* ho::*LYS2*	(Schröder et al., 2004)
4.	*S.cerevisiae*	MSY 289-02	SK-1 MAT**a** *arg6 rme1Δ5*::*LEU2 ura3 leu2*::*hisG trp1*::*hisG lys2* ho::*LYS2 rpd3Δ*::*hphMX4*	Schröder Lab Strain Collection
5.	*S.cerevisiae*	MSY 283-06	SK-1 MAT**a** *arg6 rme1Δ5*::*LEU2 ura3 leu2*::*hisG trp1*::*hisG lys2* ho::*LYS2 isw2 Δ::kanMX2*	Schröder Lab Strain Collection
6.	*S.cerevisiae*	RCY 20-05	SK-1 MAT**a** *arg6 rme1Δ5*::*LEU2 sin3Δ* ::*LEU2 ura3 leu2*::*hisG trp1*::*hisG lys2* ho::*LYS2*	Schröder Lab Strain Collection
7.	*S.cerevisiae*	MSY 301-03	SK-1 MAT**a** *arg6 rme1Δ5*::*LEU2 ura3 leu2*::*hisG trp1*::*hisG lys2*	Schröder Lab Strain

			ho::*LYS2 itc1Δ::natMX4*,	Collection
8.	*S.cerevisiae*	MSY 138-17	SK-1 MATα *his3ΔSK rme1Δ5*::*LEU2 ura3 leu2*::*hisG trp1*::*hisG lys2* ho::*LYS2*	(Schröder et al., 2004)
9.	*S.cerevisiae*	MSY 296-01	SK-1 MATα *his3ΔSK rme1Δ5*::*LEU2 ura3 leu2*::*hisG trp1*::*hisG lys2* ho::*LYS2 hac1Δ::kanMX2*	Schröder Lab Strain Collection
10.	*S.cerevisiae*	AMP 109	SK-1 MAT **a**/α *ura3/ura3 leu2::hisG/leu2::hisG trp1::hisG/trp1::hisG lys2/lys2 ho::LYS2/ho::LYS2*	(Vidan and Mitchell, 1997)
11.	*S.cerevisiae*	AMP 1618	SK-1 MATα *met4* rme1D5::*LEU2 IME2-20-lacZ*::*LEU2 ura3 leu2*::*hisG trp1*::*hisG lys2* ho::*LYS2*	(Vidan and Mitchell, 1997)
12.	*S.cerevisiae*	AMP 1619	SK-1 MATa *arg6* rme1D5::*LEU2 IME2-20-lacZ*::*LEU2 ura3 leu2*::*hisG trp1*::*hisG lys2* ho::*LYS2*	(Vidan and Mitchell, 1997)
13.	*S.cerevisiae*	MSY 33-12	SK-1 MAT**a** *his3ΔSK leu2 ura3 trp1 lys2* ho::*LYS2*	Schröder Lab Strain Collection
14.	*S.cerevisiae*	MSY160-88	SK-1 MATα *met4 ura3 leu2 trp1 lys2* ho::*LYS2 arg6*	Schröder Lab Strain Collection

15. *S.cerevisiae*	MSY 33-12 x MSY 160-88	SK-1 MAT**a**/α *ura3/ura3 leu2/leu2 trp1/trp1 lys2/ lys2* ho::*LYS2/*ho::*LYS2*	This study
16. *S.cerevisiae*	MSY 673-01	SK-1 MATα *his3ΔSK leu2 ura3 trp1 lys2* ho::*LYS2 rtg2Δ::kanMX2*	This study
17. *S.cerevisiae*	MSY 669-01	SK-1 MAT**a** *met4 ura3 leu2 trp1 lys2* ho::*LYS2 rtg2Δ::kanMX2*	This study
18. *S.cerevisiae*	MSY 673-01 x MSY 669-01	SK-1 MAT**a**/α *ura3/ura3 leu2/leu2 trp1/trp1 lys2/ lys2* ho::*LYS2*/ho::*LYS2 rtg2Δ::kanMX2/ rtg2Δ::kanMX2*	This study
19. *S.cerevisiae*	MSY 676-01	SK-1 MATα *his3ΔSK leu2 ura3 trp1 lys2* ho::*LYS2 rtg3Δ::kanMX2*	This study
20. *S.cerevisiae*	MSY 678-02	SK-1 MAT**a** *met4 ura3 leu2 trp1 lys2* ho::*LYS2 rtg3Δ::kanMX2*	This study
21. *S.cerevisiae*	MSY 676-01 x MSY 678-02	SK-1 MAT**a**/α *leu2/ leu2 ura3/ ura3 trp1/ trp1 lys2/ lys2* ho::*LYS2/* ho::*LYS2 rtg3Δ::kanMX2/ rtg3Δ::kanMX2*	This study
22. *S.cerevisiae*	MSY 38-03	SK-1 MATa *arg6 his3ΔSK leu2 ura3 trp1 lys2* ho::*LYS2*	Schröder Lab Strain Collection
23. *S.cerevisiae*	MSY 160-88	SK-1 MATα *arg6 met4 ura3 leu2 trp1 lys2* ho::*LYS2*	Schröder Lab Strain Collection
24. *S.cerevisiae*	MSY 38-03 x	SK-1 MAT**a/**α *arg6/arg6 ura3/ ura3 leu2/ leu2 trp1/ trp1 lys2/ lys2*	This study

		MSY 160-88	ho::*LYS2*/ho::*LYS2*	
25.	*S.cerevisiae*	MSY 659-01	SK-1 MATα *arg6 his3ΔSK leu2 ura3 trp1 lys2* ho::*LYS2*rtg1Δ*::kanMX2*	This study
26.	*S.cerevisiae*	MSY 656-01	SK-1 MATa *arg6 met4 ura3 leu2 trp1 lys2* ho::*LYS2* rtg1Δ*::kanMX2*	This study
27.	*S.cerevisiae*	MSY 659-01 x MSY 656-01	SK-1 MAT**a**/α *arg6/ arg6 ura3/ ura3 leu2/ leu2 trp1/ trp1 lys2/ lys2* ho::*LYS2*/ho::*LYS2* rtg1Δ*::kanMX2*/ rtg1Δ*::kanMX2*	This study
28.	*E.coli*	DH5α	F⁻ φ80*lac*ZΔM15 Δ(*lac*ZYA-*arg*F)$_{U169}$ *rec*A1 *end*A1 *hsd*R17(r$_k$⁻, m$_k$⁺) *pho*A *sup*E44 *thi*-1 *gyr*A96 *rel*A1 λ⁻	Schröder Lab Strain Collection
29.	*E.coli*	XL10-Gold	Tet^r Δ(*mcr*A)183 Δ(*mcr*CB-*hsd*SMR-*mrr*)173 *end*A1 *sup*E44 *thi*-1 *rec*A1 *gyr*A96 *rel*A1 *lac* Hte [F' *pro*AB *lac*I^{q}Z ΔM15 Tn*10* (Tet^r) Amy Cam^r]	Stratagene
30.	*E.coli*	SCS110	*rpsL* (Str^r) *thr leu endA thi-1 lacY galK galT ara tonA tsx dam dcm supE44* Δ(lac-proAB) [F´ *traD36 proAB lac*I^{q}ZΔM15]	Schröder Lab Strain Collection

2.5 Stock solution

Note: Solutions were preferably made in high-purity H_2O (conductivity = 18 $\mu^{-1}m^{-1}$) and autoclaved. If this was not possible, solutions were are prepared in autoclaved high-purity H_2O and then filter sterilized by filtration over a 0.22 μm filter.

Table 2.9 Stock solutions

Sr. No.	Solution	Quantity	Composition	Recipe
1.	**10 g/l bromophenol blue**	10 ml	10g/l bromophenol blue	Dissolved 100 mg bromophenol in ~9 ml H_2O. Added H_2O to 10 ml.
2.	**2 x assay buffer**	400 ml	200 mM $Na_xH_{3-x}PO_4$ (pH 7.3) 2 mM $MgCl_2$ 100 mM α-mercaptoethanol 1.33 mg/ml 2-nitrophenyl-β-D-galactopyranoside	177 ml 0.4 M Na_2HPO_4 23 ml 0.4 M NaH_2PO_4 0.8 ml 1 M $MgCl_2$ 2.8 ml β-mercaptoethanol 532 mg 2-nitrophenyl-β-D-galactopyranoside. Added H_2O to 400 ml and mixed. Stored in 50 ml aliquots at -20°C.
3.	**Na_2CO_3, 1 M**	500 ml	1 M Na_2CO_3	Dissolved 53.0 g Na_2CO_3 in ~400 ml H_2O. Added H_2O to 500 ml
4.	**Tris·HCl (pH 6.8), 1 M**	1 l	Tris·HCl (pH 6.8), 1 M	Dissolved 121.14 g Tris in ~800 ml H_2O. Adjusted pH to 6.8 with conc. HCl (~42 ml). Added H_2O to 1 l. Autoclaved

5.	**Tris·HCl (pH 7.5), 1 M**	1 l	Tris·HCl (pH 7.5), 1 M	Dissolved 121.14 g Tris in ~800 ml H_2O. Adjusted pH to 7.5 with conc. HCl (~42 ml). Added H_2O to 1 l. Autoclaved.
6.	**Tris·HCl (pH 8.0), 1 M**	1 l	Tris·HCl (pH 8.0), 1 M	Dissolved 121.14 g Tris in ~800 ml H_2O. Adjusted pH to 8.0 with conc. HCl (~42 ml). Added H_2O to 1 l. Autoclaved.
7.	**1 x Tris·Acetate· EDTA (1xTAE)**	1 l	40 mM Tris·HOAc 2 mM M EDTA pH ~8.5	Dissolved 4.84 g Tris in ~800 ml H_2O and added 1.41 ml acetic acid and 0.74 g$Na_2EDTA·2H_2O$.Added H_2O to 1 l and adjusted the pH to ~8.5
8.	**10% (w/v) SDS**	500 ml	10% (w/v) SDS	Dissolved 50 g SDS in ~450 ml H_2O. Added H_2O to 500 ml. Did NOT autoclave
9.	**70% (v/v) EtOH**	50 ml	70% (v/v) EtOH	Mixed 35 ml EtOH and 15 ml H_2O and stored at -20°C.
10.	**EDTA, 0.5 M**	500 ml	EDTA, 0.5 M	Dissolved 93.1 g $Na_2EDTA·2H_2O$ in ~350 ml H_2O. Adjusted pH to 8.0 with 10 M NaOH (~25 ml). Added H_2O to 500 ml. Autoclave

11.	**1 M LiOAc**	250 ml	1 M LiOAc	25.50 g LiOAc·2H$_2$O Dissolved in ~200 ml H$_2$O. Added H$_2$O to 250 ml. Filter sterilized,
12.	**5 M KOAc, pH 4.8**	500 ml	5 M KOAc, pH 4.8	147.5 ml HOAc, add H$_2$O to ~450 ml, adjusted pH to 4.8 w/ KOH pellets while cooling in an ice/H$_2$O bath. Added H$_2$O to 500 ml and autoclaved.
13.	**10 x TE (pH 8.0)**	4 l	100 mM Tris·HCl (pH 8.0) 10 mM EDTA	400 ml 1 M Tris·HCl (pH 8.0) 80 ml 0.5 M EDTA Added H$_2$O to 4 l. Autoclaved
14.	**MgCl$_2$, 1 M**	100 ml		Dissolved 20.33 g MgCl$_2$·6 H$_2$O in ~80 ml H$_2$O. Added H$_2$O to 100 ml. Autoclaved.
15.	**5 M KOAc, pH 4.8**	500 ml	5 M KOAc, pH 4.8	147.5 ml HOAc, added H$_2$O to ~450 ml, adjusted pH to 4.8 w/ KOH pellets while cooling in an ice/H$_2$O bath. Added H$_2$O to 500 ml and autoclaved.
16.	**NaOH, 10 M**	500 ml	10M NaOH	Dissolved 200 g NaOH in ~350 ml H$_2$O. *Solution gets very hot!* Stored in a polyethylene bottle

17.	10 x SDS-PAGE buffer	1 l	1.92 M glycine 0.248 M Tris 10 g/l SDS	144.13 g glycine 30.03 g Tris 10.00 g SDS Add H_2O to ~ 900 ml, stir until completely dissolved, then add H_2O to 1 l.
18.	6 x SDS-PAGE sample buffer	10 ml	350 mM Tris·HCl, pH 6.8 30% (v/v) glycerol 10% (w/v) SDS 0.5 g/l bromophenol blue 2% (v/v) β-mercaptoethanol	3.50 ml 1 M Tris·HCl 3.78 g glycerol 1.00 g SDS 500 µl 10 g/l bromophenol blue 200 µl β-mercaptoethanol Add H_2O to ~ 9 ml, dissolve over-night if necessary. Add H_2O to 10 ml.
19.	30% (v/v) glycerol	500 ml	30% (v/v) glycerol	189 g glycerol. Added H_2O to ~400 ml, mixed well by stirring. Added H_2O to 500 ml and autoclaved.
20.	50 mg/ml ampicillin	10 ml	50g/ml ampicillin	Dissolved 500 mg ampicillin in 10 ml sterile H_2O.Filter sterilized. Mixed and aliquoted in smaller volumes.
21.	12.5 mg/ml Tetracycline	10 ml	12.5 mg/ml Tetracycline	Dissolved 125 mg tetracycline in sterile 10 ml of 70% ethanol. Mixed and aliquoted in smaller volumes.

2.6 Yeast and bacteriological media

Table 2.10 Liquid media for *Escherichia coli*

Medium	Composition	Quantity	Recipe
LB broth, Lennox	10 g/l tryptone 5 g/l yeast extract 5 g/l NaCl	1 l	20 g LB broth, Lennox formulation Added H_2O to ~900 ml, stirred until all solid haddissolved, added H_2O to 1 l, dispensed into bottles and autoclaved.
1 x TSS	10 g/l tryptone 50 g/l yeast extract 5 g/l NaCl 100 g/l polyethylene glycol 3350 5% (v/v) DMSO 50 mM $MgCl_2$	1 l	Added 10 g tryptone, 50 g yeast extract, 5 g Nacl, 100g polyethylene glycol 3350, 50 ml DMSO, 50 ml of 1M $MgCl_2$ to 900 ml H_2O. Adjusted the pH to 6.5 with HCl. Filter sterilized and stored protected from light at 4°C

Table 2.11 Solidified media for *Escherichia coli*

Medium	Composition	Quantity	Recipe
LB agar, Lennox	10 g/l tryptone 5 g/l yeast extract 5 g/l NaCl 15 g/l agar	1 l	35 g LB agar, Lennox formulation Added 1 l H$_2$O, mixed until suspension is homogenous, and autoclaved. Poured the plates. Stored at 4°C after plates solidified.
LB agar, Lennox + 100 µg/ml ampicillin	10 g/l tryptone 5 g/l yeast extract 5 g/l NaCl 15 g/l agar 100 µg/ml ampicillin	1 l	35 g LB agar, Lennox formulation Added 1 l H$_2$O, stir until mixture was homogenous and autoclaved. Allowed to cool down to ~55°C, added 2 ml 50 mg/ml ampicillin, mixed, and poured plates. Stored at 4°C for 2 weeks after plates had solidified.
LB agar, Lennox + 100 µg/ml ampicillin + 12.5 µg/ml tetracycline	10 g/l tryptone 5 g/l yeast extract 5 g/l NaCl 15 g/l agar 100 µg/ml ampicillin 12.5 µg/ml tetracycline	1 l	35 g LB agar, Lennox formulation. Added 1 l H$_2$O, stirred until mixture was homogenous and autoclaved. Allowed to cool down to ~55°C, added 2 ml 50 mg/ml ampicillin, 12.5 µl of 12.5 mg/ml tetracycline, mixed, and poured plates. Stored at 4°C for

LB agar, Lennox + 100 µM IPTG + 20 µg/ml X-Gal	10 g/l tryptone	1 l	35 g LB agar, Lennox formulation
	5 g/l yeast extract		Added 1 l H$_2$O, stir until mixture was homogenous and autoclaved. Allowed to cool down to ~55°C, added 0.5 ml 40 mg/ml X-gal, 1 ml 100 mM IPTG, mixed, and poured plates. Stored at 4°C in the dark after plates had solidified.
	5 g/l NaCl		
	15 g/l agar		
	100 µM IPTG		

Table 2.12 Liquid media for *Saccharomyces cerevisiae*

Medium	Composition	Quantity	Recipe
C-SPO medium	2% (w/v) KOAc	600 ml	12 g KOAc
	30 mg/l L-Tyr		18 mg L-Tyr
	20 mg/l adenine sulfate		10 ml 1.2 g/l adenine sulfate
	20 mg/l uracil		5 ml 2.4 g/l uracil
	20 mg/l L-His·HCl		5 ml 2.4 g/l L-His·HCl[1,2]
	20 mg/l L-Arg·HCl		5 ml 2.4 g/l L-Arg·HCl
	20 mg/l L-Met		5 ml 2.4 g/l L-Met
	40 mg/l L-Trp		10 ml 2.4 g/l L-Trp[1,2]
	30 mg/l L-Lys·HCl		5 ml 3.6 g/l L-Lys·HCl
	100 mg/l L-Leu[3]		10 ml 3.6 g/l L-Leu
	50 mg/l L-Phe		10 ml 3.0 g/l L-Phe
	5 mg/l *myo*-inositol		500 µl 10 g/l *myo*-inositol
			Added H_2O to 580 ml, stirred until all solid dissolved, dispensed into bottles and auto-claved. After the medium cooled down to ~55°C added:
	210 mg/l L-Thr		5.25 ml 24 g/l L-Thr[2]

All stock solutions were sterilized by autoclaving unless otherwise indicated (note 2).

1) Stored stock solution at 4°C. Filter sterilized.

2) 100 mg/l L-Leu is specially for SK-1 strains. The usual concentration is 30 mg/l L-Leu.

3) C-SPO dropout medium was made excluding the concerned amino acid stocks.

PSP2 medium	0.67% (w/v) yeast nitrogen base w/o amino acids	600 ml	4 g yeast nitrogen base w/o amino acids
	0.10% (w/v) bacto-yeast extract		0.6 g bacto-yeast extract
	1% (w/v) KOAc		6 g KOAc
	30 mg/l L-Tyr		18 mg L-Tyr
	50 mM K-phthalate (pH 5.0)		Dissolve d 6.13 g K-phthalate in ~400 ml H_2O, adjusted pH to 5.0 with KOH pellets
	20 mg/l uracil		5 ml 2.4 g/l uracil
	20 mg/l L-Arg·HCl		5 ml 2.4 g/l L-Arg·HCl
	20 mg/l L-His·HCl		5 ml 2.4 g/l L-His·HCl[1,2]
	20 mg/l L-Met		5 ml 2.4 g/l L-Met
	20 mg/l L-Trp		5 ml 2.4 g/l L-Trp[1,2]
	30 mg/l L-Ile		5 ml 3.6 g/l L-Ile
	30 mg/l L-Lys·HCl		5 ml 3.6 g/l L-Lys·HCl
	150 mgl/ L-Val		5 ml 18 g/l L-Val
	375 mg/l L-Ser		5 ml 45 g/l L-Ser
	20 mg/l adenine sulfate		10 ml 1.2 g/l adenine sulfate
	50 mg/l L-Phe		10 ml 3.0 g/l L-Phe
	100 mg/l L-Glu		10 ml 6.0 g/l L-Glu
	100 mg/l L-Leu[3]		16.7 ml 3.6 g/l L-Leu
			Added H_2O to 580 ml, stirred until all solid had dissolved, dispensed into bottles and autoclaved. After the medium did cool down to ~55°C added:
	100 mg/l L-Asp		15 ml 4.0 g/l L-Asp[2]
	200 mg/l L-Thr		5 ml 24 g/l L-Thr[2]

SD medium	0.67% (w/v) yeast nitrogen base w/o amino acids	600 ml	4 g yeast nitrogen base w/o amino acids
	2% (w/v) D-glucose		12 g D-glucose
	30 mg/l L-Tyr		18 mg L-Tyr
	20 mg/l uracil		5 ml 2.4 g/l uracil
	20 mg/l L-Arg·HCl		5 ml 2.4 g/l L-Arg·HCl
	20 mg/l L-His·HCl		5 ml 2.4 g/l L-His·HCl[1,2]
	20 mg/l L-Met		5 ml 2.4 g/l L-Met
	20 mg/l L-Trp		5 ml 2.4 g/l L-Trp[1,2]
	30 mg/l L-Ile		5 ml 3.6 g/l L-Ile
	30 mg/l L-Lys·HCl		5 ml 3.6 g/l L-Lys·HCl
	150 mg/l L-Val		5 ml 18 g/l L-Val
	375 mg/l L-Ser		5 ml 45 g/l L-Ser
	20 mg/l adenine sulfate		10 ml 1.2 g/l adenine sulfate
	50 mg/l L-Phe		10 ml 3.0 g/l L-Phe
	100 mg/l L-Glu		10 ml 6.0 g/l L-Glu
	100 mg/l L-Leu[3]		16.7 ml 3.6 g/l L-Leu
			Added H_2O to 580 ml, stirred until all solid had dissolved, dispensed into bottles and autoclaved. After the medium did cool down to ~55°C added:
	100 mg/l L-Asp		15 ml 4.0 g/l L-Asp[2]
	200 mg/l L-Thr		5 ml 24 g/l L-Thr[2]

YPAc broth	1% (w/v) bacto-yeast extract	1. Dissolved 10 g bacto-yeast extract, 20 g bacto-peptone, and 20 g KOAc in ~800 ml H_2O.
	2% (w/v) bacto-peptone	2. Added H_2O to 1 l and mixed. Dispensed into bottles.
	2% (w/v) KOAc	3. Autoclaved.
YPD broth	1% (w/v) bacto-yeast extract 1 l	1. Dissolved 50 g YPD broth powder in ~800 ml H_2O.
	2% (w/v) bacto-peptone	2. Added H_2O to 1 l and mix.
	2% (w/v) D-glucose	3. Dispensed into bottles.
		4. Autoclaved.

Table 2.13 Solidified media for *Saccharomyces cerevisiae*

Medium	Composition	Quantity	Recipe
PSP2 agar	0.67% (w/v) yeast nitrogen base w/o amino acids	600 ml	4 g yeast nitrogen base w/o amino acids
	0.10% (w/v) bacto-yeast extract		0.6 g bacto-yeast extract
	1% (w/v) KOAc		6 g KOAc
	2% (w/v) agar		12 g agar
	30 mg/l L-Tyr		18 mg L-Tyr
	20 mg/l uracil		5 ml 2.4 g/l uracil
	20 mg/l L-Arg·HCl		5 ml 2.4 g/l L-Arg·HCl
	20 mg/l L-His·HCl		5 ml 2.4 g/l L-His·HCl[1,2]
	20 mg/l L-Met		5 ml 2.4 g/l L-Met
	20 mg/l L-Trp		5 ml 2.4 g/l L-Trp[1,2]
	30 mg/l L-Ile		5 ml 3.6 g/l L-Ile
	30 mg/l L-Lys·HCl		5 ml 3.6 g/l L-Lys·HCl
	150 mgl/ L-Val		5 ml 18 g/l L-Val
	375 mg/l L-Ser		5 ml 45 g/l L-Ser
	20 mg/l adenine sulfate		10 ml 1.2 g/l adenine sulfate
	50 mg/l L-Phe		10 ml 3.0 g/l L-Phe
	100 mg/l L-Glu		10 ml 6.0 g/l L-Glu
	100 mg/l L-Leu[3]		16.7 ml 3.6 g/l L-Leu
	50 mM K-phthalate (pH 5.0)		Dissolved 6.13 g K-phthalate in ~400 ml H_2O, adjusted pH to 5.0 with KOH pellets, and added H_2O to 488 ml. Mixed all components by stirring until the suspension is homogenous and autoclaved. After the medium did cool down to ~55°C added:

	100 mg/l L-Asp	15 ml 4.0 g/l L-Asp[2]
	200 mg/l L-Thr	5 ml 24 g/l L-Thr[2]
		Poured ~25 ml into one 90 mm petri dish.
SD agar	0.67% (w/v) yeast nitrogen base w/o amino acids	600 ml	4 g yeast nitrogen base w/o amino acids
	2% (w/v) D-glucose	12 g D-glucose
	2% (w/v) agar	12 g agar
	30 mg/l L-Tyr	18 mg L-Tyr
	20 mg/l uracil	5 ml 2.4 g/l uracil
	20 mg/l L-Arg·HCl	5 ml 2.4 g/l L-Arg·HCl
	20 mg/l L-His·HCl	5 ml 2.4 g/l L-His·HCl[1,2]
	20 mg/l L-Met	5 ml 2.4 g/l L-Met
	20 mg/l L-Trp	5 ml 2.4 g/l L-Trp[1,2]
	30 mg/l L-Ile	5 ml 3.6 g/l L-Ile
	30 mg/l L-Lys·HCl	5 ml 3.6 g/l L-Lys·HCl
	150 mgl/ L-Val	5 ml 18 g/l L-Val
	375 mg/l L-Ser	5 ml 45 g/l L-Ser
	20 mg/l adenine sulfate	10 ml 1.2 g/l adenine sulfate
	50 mg/l L-Phe	10 ml 3.0 g/l L-Phe
	100 mg/l L-Glu	10 ml 6.0 g/l L-Glu
	100 mg/l L-Leu[3]	16.7 ml 3.6 g/l L-Leu
		Added 488 ml H_2O in a 1 l Erlenmeyer flask, stirred until the suspension is homogenous, and autoclaved. After the medium did cool down to ~55°C added:
	100 mg/l L-Asp	15 ml 4.0 g/l L-Asp[2]
	200 mg/l L-Thr	5 ml 24 g/l L-Thr[2]
		Poured ~25 ml into one 90 mm

			petri dish.
SLA agar	0.17% (w/v) yeast nitrogen base w/o amino acids and w/o ammonium sulphate	600 ml	1.02 g yeast nitrogen base w/o amino acids w/o and ammonium sulphate
	2%(w/v)D-glucose/ Potassium acetate/ L-Lactate/ Pyruvate/Glycerol/Ethanol		12 g D-glucose/Potassium acetate/L-Lactate/ Pyruvate/Glycerol/Ethanol
	2% (w/v) agar		12 g agar
	5 mg/l uracil		1.25 ml 2.4 g/l uracil
	5 mg/l L-Trp		1.25 ml 2.4 g/l L-Trp
	5 mg/l L-Lys·HCl		0.83 ml 3.6 g/l L-Lys·HCl
	5 mg/l L-Leu		0.83 ml 3.6 g/l L-Leu
	50 µM Ammonium Sulfate		0.03 ml of 1 M $(NH4)_2SO_4$
			Added H_2O to make 600 ml in a 1 l Erlenmeyer flask, stirred until the suspension is homogenous, and autoclaved. Pour ~25 ml of media into each petri dish and allow to set.

YPAc agar	1% (w/v) bacto-yeast extract 1 l	1. Added 1 l H_2O to 10 g bacto-yeast extract, 20 g bacto-peptone, 20 g KOAc, and 20 g agar in a 2 l Erlenmeyer flask.
	2% (w/v) bacto-peptone	
	2% (w/v) KOAc	
	2% (w/v) agar	
		2. Stirred until suspension is homogenous.
		3. Autoclaved.
		4. Allowed solution to cool to ~55°C.
		5. Poured ~25 ml into one 90 mm Petri dish.
YPD agar	1% (w/v) bacto-yeast extract 1 l	1. Added 1 l H_2O to 65 g YPD agar powder in a 2 l Erlenmeyer flask.
	2% (w/v) bacto-peptone	
	2% (w/v) D-glucose	
	1.5% (w/v) agar	
		2. Stirred until suspension is homogenous.
		3. Autoclaved.
		4. Allowed solution to cool to ~55°C.
		5. Poured ~25 ml into one 90 mm Petri dish.
YPD + 1 mg/ml hygromycin B agar	1% (w/v) bacto-yeast extract 1 l	1. Added 1 l H_2O to 65 g YPD agar powder in a 2 l Erlenmeyer flask.
	2% (w/v) bacto-peptone	
	2% (w/v) D-glucose	
	1.5% (w/v) agar	
	600 µg/ml hygromycin B	2. Stirred until suspension is homogenous.
		3. Autoclaved.
		4. Allowed solution to cool to ~55°C.
		5. Added 20 ml 50 mg/ml

		hygromycin B (filter sterilized) and mixed.
		6. Poured ~25 ml into one 90 mm Petri dish.
YPD + 50 µg/ml X-Gal agar	1% (w/v) bacto-yeast extract 1 l 2% (w/v) bacto-peptone 2% (w/v) D-glucose 1.5% (w/v) agar 50 µg/ml X-Gal 0.1 M $Na_xH_{3-x}PO_4$ (pH 7.0)	1. Added 900 ml H_2O to 65 g YPD agar powder in a 2 l Erlenmeyer flask. 2. Stirred until suspension is homogenous. 3. Autoclaved. 4. Allowed solution to cool to ~80°C. 5. Added 100 ml 1 M $Na_xH_{3-x}PO_4$ (pH 7.0), 1.25 ml 40 mg/ml X-Gal, and mixed. 6. Poured ~25 ml into one 90 mm Petri dish.

2.7 Protocols

2.7.1 Microbiology

2.7.1.1 *S. cerevisiae* cell culture

Protocol: A pair of forceps was dipped in ethanol and passed briefly through Bunsen burner. A single isolated *S. cerevisiae* colony was picked up with tip of the toothpick using forceps from an appropriate agar plate and was aseptically inoculated to 14ml sterile tube containing 2-4 ml appropriate medium. The tubes were then incubated in incubator shaker at 30ºC until saturation (generally 2-3 days). The tubes were removed from the incubator and vortexed to resuspend cells. 50 µl cell suspension and 450 µl of medium used to grow the overnight cultures were added to semi-micro cuvette and mixed. This is 1:10 dilution of original grown culture. Using 500 µl of medium as blank for spectrophotometer, the absorbance at A_{600} of 1:10 diluted culture was determined. A_{600} readings are linear up to A_{600} ~0.6. If A_{600} was more 0.6, sample was diluted 10-fold or higher. Appropriate medium was added to sterile Erlenmeyer flasks with at least twice as big size as the intended culture volume working under aseptic conditions. *S. cerevisiae* cultures grown in medium supplemented with acetate as carbon source were grown in Erlenmeyer flasks with baffles for better aeration and agitation. The amount of inoculum to be added was calculated as the amount required to yield A_{600} ~0.01. From 14ml culture tubes with yeast culture, the calculated culture was added to flasks. The flasks were placed into a shaker incubator with shaking at 225 – 250 rpm at 30ºC overnight. The growth of the culture was monitored at regular intervals once visible growth was seen after 12-24 h by removing 500 µl and pipeting into a disposable semi-micro cuvette and determining the A_{600} of the sample. Cultures grown in YPD were monitored at intervals of 1.5-2 h and PSP2, SD or YPAc grown cultures were monitored every 2-4 h. When the yeast culture achieved A_{600} between 0.3 – 0.6, this was considered as exponential growth phase.

Reference: (Treco and Winston, 1997)

2.7.1.2 Yeast Culture Sample Collection

Protocol: Yeast culture to be sampled was transferred into an ice-cold 15 or 50 ml centrifuge tube. Approximately ~20 ml of culture volume was collected for β-galactosidase reporter assays. The sample volume for yeast strains expressing URS1-*CYC1*-Ub-x-*lacZ* reporters with 'x' as Arg or Leu was ~50 ml. The tubes were centrifuged at 3000 rpm, 4°C for 2 min to sediment the cells. The supernatant was discarded and the cells were frozen in liquid nitrogen and stored in a -20°C or -80°C freezer for longer periods.

Reference: (Treco and Winston, 1997)

2.7.1.3 Frozen Yeast Stock Cultures
Reagents:

- Freshly grown yeast culture in YPD broth or SD medium. Yeast nitrogen base without amino acids from Formedium has been specifically used to make the SD medium for the purposes of making frozen stocks.

Protocol: The cryotubes were labelled with strain name and date using an ethanol resistant pen or the labelling system. 1 ml 30% (v/v) glycerol was dispensed into each cryotube. The cells grown were resuspended by briefly vortexing and pipetted 1 ml cell suspension into the appropriate cryotube. The frozen stocks were made in duplicates for each strain or clone. The cryotubes were closed tightly and mixed by inverting and placing the tube into an ethanol/dry ice bath or into liquid nitrogen. Once the culture is frozen, the cryotubes were placed into a cryobox in a -70°C freezer.

Reference: (Treco and Lundblad, 1993)

2.7.1.4 *E. coli* cell culture

Protocol: A pair of forceps was dipped in ethanol and passed briefly through Bunsen burner. A single *E. coli* colony from an appropriate agar plate was picked up using forceps and toothpick. Toothpick was aseptically added to 14ml sterile tube containing 2-3 ml LB medium supplemented with appropriate antibiotics to inoculate

the culture. The tubes were then incubated in incubator shaker at 37ºC overnight or 16 h. These cultures were used for plasmid minipreparation or for inoculating larger volumes of culture for maxipreparation. The overnight grown culture was diluted 1:100 into the new medium (For poorly replicated plasmids inoculum was washed three times with 1 ml H_2O). Appropriate medium was added to sterile Erlenmeyer flasks under aseptic conditions. The final flasks for growth were at least twice as big size as the intended culture volume. The flasks were placed into a shaker incubator with shaking at 225 – 250 rpm at 37ºC overnight. The growth of the culture was monitored by removing 500 µl every 30 mins (LB broth cultures) and pipeting into a disposable semi-micro cuvette and determining the A_{600} of the sample.

Appropriate antibiotics added to LB broth as follows:

Antibiotic	Stock solution	Working concentration	Dilution
ampicillin	100 mg/ml in H_2O	100 µg/ml	1:1000
tetracycline	12.5 mg/ml in	12.5 µg/ml	1:1000

Reference: (Elbing and Brent, 2002)

2.7.1.5 Frozen *E. coli* Stock Cultures

Protocol: A single colony was picked up to inoculate 3 ml LB broth containing appropriate antibiotics and incubated at the 37ºC temperature overnight with shaking at 220 rpm until it reaches an $A_{600\ nm}$ of ~0.5. The cryotubes were labelled with strain name and the day's date using an ethanol resistant pen or using the labelling system. 0.5 ml 30% (v/v) glycerol was dispensed into each cryotube. The cells were resuspended by briefly vortexing and 1.375 ml of cell suspension was pipetted into the appropriate cryotube. The frozen stocks were made in duplicate for each strain or clone. The cryotube was closed tightly, mixed by inverting and placed into an ehanol/dry ice bath or into liquid nitrogen. Once the culture was frozen the cryotubes were placed into a cryobox in -70°C freezer.

Reference: (Elbing and Brent, 2002)

2.7.2 Yeast genetics

2.7.2.1 Mating of Yeast Strains

Protocol: Two haploid strains of opposite mating type were cross streaked on a YPD plate. Each parental strain was streaked as controls as shown in Fig 2.1. The plates were incubated overnight at 30°C. The master plate with controls and mated strains was replica plated to a selective plate that selects for growth of the diploid strain. The plate was then incubated at 30°C until patches are grown (2-3 days). Patches for single colonies were streaked on a selective plate that selects for growth of the diploid strain and against growth of the two haploid strains. Around 6-8 isolated colonies were tested for growth on non-fermentable carbon sources by streaking a small fraction of the colony on YPAc plate. The YPAc plates were incubated for 1 - 3 days at 30°C and scored streaks for growth. The colonies showing strong growth on the YPAc plate were selected for further processing.
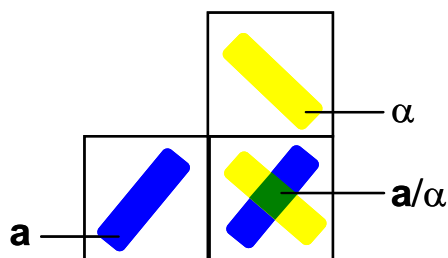
Figure 2.1. Mating of haploid yeast strains by crossing of patches on a YPD

Reference: (Treco and Winston, 1997)

2.7.2.2 Random Spore Isolation

Protocol

Spore dissection: 1 ml YPD broth was inoculated with cells from one isolated colony of a diploid a/α yeast strain and incubated with shaking (~250 rpm) at 30°C until cells have grown to saturation (1-2 d). 4 ml YPAc broth was inoculated with 40 µl of the saturated YPD culture and grown with shaking (~250 rpm) at 30°C until cells had grown to saturation (~2 d). The cells were collected by centrifugation for 2 min at 3000 rpm and RT and the supernatant was discarded. The pellet was washed by

addition of 4 ml H_2O and resuspending cells by vortexing, and collect cells by centrifugation as earlier. These cells were resuspended in 4 ml C-SPO medium by vortexing and incubated with shaking (~250 rpm) at 30°C for 3 – 5 d to sporulate the yeast cells. The cells were collected by centrifugation as earlier and resuspended in 1 ml H_2O by vortexing, and transferred to a 1.5 ml microcentrifuge tube. The cells were collected by centrifugation for 10 – 15 s at 12,000 g and supernatant was aspirated. The pellet were resuspended in 90 µl H_2O. 10 µl glusulase was added to this tube and mixed well and incubate for 30 min at 30°C. The cell wall digestion was terminated by addition of 1 ml H_2O. The tube was centrifuged for 10 – 15 s to collect cells and supernatant was discarded. Cells were washed once with 1 ml H_2O and resuspended in 0.1 ml H_2O by vortexing the cell suspension at maximum speed for 2 min. Cell suspension was completely pipetted out, 1 ml H_2O was added, vortexed at maximum speed for 10 s, and pipetted out the H_2O. This step was repeated twice. 0.01% (v/v) NP-40 was added and vortexed at maximum speed for 10 s. Cell suspension was sonicated in an ice/H_2O bath for 10 s at 150 W and incubated for 1 min on ice to dissipate heat. This step was repeated five times. 10 µl cell suspension was counted in a haemocytometer to ascertain number of cells per ml. Based on the cell count 10, 100, 1,000, and 10,000 cells were plated onto five agar plates each (YPD agar plates or selective plates). The plates were incubated at 30°C until colonies are grown (2-3 d). Only well separated colonies on the plate were processed further.

Determination of spore genotype

The plates with well separated colonies were replica plated on YPAc agar plate to screen for growth on non-fermentable carbon sources and on selective plates to screen for particular genotypes. The plates were then incubated at 30°C until colonies were grown. If desired, regrow master plate by incubating at 30°C. The colonies that didn't grow on acetate were discarded. 3-4 times (in multiples of 48) more colonies were streaked for single colonies on YPD agar plates than genotypes that were generated by sporulation of the diploid strain. The plates were then incubated at 30°C until colonies are grown (~2 days). Individual patches were made on a YPD agar plate. Parental haploid strains that were used to construct the diploid strain were patched as controls. The plates were then incubated at 30°C until patches were grown (~2 days). These patches were replica plated to YPAc agar

plates and selective plates to determine genotypes based on growth assays for metabolic and drug resistance markers. Mating type was tested by colony PCR analysis. Growth was monitored regularly and growth was recorded.

Reference: (Spencer and Spencer, 1996)

2.7.3 Cell Biology

2.7.3.1 Pseudohyphal growth assays

Protocol: Desired freshly grown diploid cells grown on appropriate plates were taken with a inoculating loop working aseptically. This loop full of yeast cells was streaked onto synthetic low ammonium (SLA) medium plates to obtain single colonies. SLA plates contained 2% of indicated carbon source. The streaking was done taking care not to scratch the agar surface. The plates were then incubated at 30°C and pseudohyphal growth was observed regularly after ~2d. At least ten colonies were photographed for each plate with an inverted microscope at magnification of 40-100x.

Reference: (Schröder et al., 2000)

2.7.3.2 Construction of Petit mutants

Protocol: 2 ml YPD broth was supplemented with 10 µg/ml of ethidium bromide working aseptically. A single colony of desired yeast strain to construct petit mutant was inoculated in the tube from previous step and incubated o/n at 30°C in incubator shaker. The culture from this tube was streaked to get isolated colonies YPD plates. YPD plates were incubated 30°C until the colonies form. The YPD plate with isolated colonies was replica plated on YPAc plate. The colonies unable to grow on YPAc plate were chosen and streaked for single colonies. These colonies were tested once again on YPAc plate and used for further experiments.

Reference: (Fox et al., 1991)

2.7.3.3 Induction of Expression from Glucocorticoid Response Elements (GRE) in *S. cerevisiae*

Reagents

- Exponentially growing yeast culture transformed with an empty GRE expression vector or an GRE expression vector controlling expression of your desired protein and a vector expressing the rat glucocorticoid receptor
- 100 mM deoxycorticosterone (DOC) in EtOH, filter sterilised, stored at -20°C

Protocol: Exponentially growing untreated culture was taken as 0 h sample working aseptically close to the flame of a Bunsen burner. Approximately ~10 ml culture was removed for β-galactosidase assays. The cells were collected by centrifugation at 3000 rpm, 4°C for 2 min and placed tubes on ice. The supernatant was decanted and the tubes containing pellet was frozen in liquid nitrogen and stored at -20°C or -80°C. The remaining exponentially growing yeast culture was split into the desired number of cultures in Erlenmeyer flasks working close to the flame of a Bunsen burner. The expression was induced by adding 1 – 100 μM DOC depending on the experiment. The flasks were returned into the shaker and the cultures were incubated at 30°C, 225-250 rpm for 0.25 – 4 h (as desired). Samples were collected as described in protocol **2.7.1.2**.

Reference: (Schena et al., 1991)

2.7.4 Protein Biochemistry

2.7.4.1 Protein Extraction for β-Galactosidase Assays

Reagents:

- 10-20 ml yeast culture samples were washed and stored in 2ml screw cap tubes. Samples were stored at -20°C.
- 5 x Reporter Lysis Buffer was stored at RT
- Roche Complete Protease Inhibitor (RPI) tablets

- 1 x RLB + RPI, ice-cold, made fresh. To make fresh added 4 Vol. H_2O to 1 Vol. 5 x RLB, mixed and placed on ice. One Roche Complete Protease Inhibitor tablet was added to 50 ml of 1 x RLB

- Glass beads, $\varnothing$ = 0.5 mm

Protocol: The yeast culture samples were thawed at RT and placed on ice. 400 µl ice-cold 1 x RLB + RPI were added to a 2.0 ml flat bottom microcentrifuge tube containing the cell pellet and the cells were resuspended by vortexing. To this ~150 mg glass beads were added and the cells and glass beads were vortexed briefly at maximum speed and placed on ice. The tubes were then placed into the Precellys 24 Instrument and cells homogenized with two 30 second cycles of 6, 500 rpm at 4°C. Then the glass beads and cell debris were sedimented for 2 min at 12000 g, 4°C and the supernatant transferred into a labelled fresh tube. The tubes containing the cell lysates were centrifuged once again for 2 min at 12000g, 4°C. Finally the samples were stored on ice or in a fridge while performing β-galactosidase assays and protein assays.

2.7.4.2 β-Galactosidase Assay

Reagents:

- Protein samples
- 5 x Reporter Lysis Buffer, stored at RT
- 1 x RLB + RPI, ice cold. Made fresh by adding 4 Vol. H_2O to 1 Vol. 5 x RLB, mixed and placed on ice. One Roche Complete Protease Inhibitor tablet was added to 50ml of 1 x RLB.
- Roche Complete Protease Inhibitor (RPI) tablets
- 2 x assay buffer
- 1 U/µl β-galactosidase
- 1 M Na_2CO_3

Protocol:

β-galactosidase standard: 1 µl 1 U/µl β-galactosidase was added to 99 µl ice-cold 1 x RLB+RPI in a tube. The contents of the tube were mixed and tube was stored on ice. 10 µl of this 1:100 dilution (10 mU/ µl β-galactosidase) was added to 990 µl ice-cold 1 x RLB in a new tube and mixed. The tube was then placed on ice. The standards were pipetted into the wells of a 96 well microtiter plate as outlined in the following table. Each standard concentration was prepared in duplicates. 1 x RLB + RPI was used to make these dilutions.

β-galactosidase standard [mU/50 µl]	Volume of 0.1 mU/µl β-galactosidase solution (step 2)	Volume of 1 x RLB
0.0	0 µl	50 µl
1.0	10 µl	40 µl
2.0	20 µl	30 µl
3.0	30 µl	20 µl
4.0	40 µl	10 µl
5.0	50 l	0µl

The protein samples were diluted into the linear range of the β-galactosidase standard using 1 x RLB + RPI. Dilutions up to 50-fold were directly prepared in the wells of the microtiter plate, higher dilutions were prepared in 1.5 ml microcentrifuge tubes and 50 µl of the dilution was added to a well of the microtiter plate. β-galactosidase activity was determined in all samples at least in duplicate. 50 µl of 2 x assay buffer was added to each well. The plate was covered with parafilm and incubated at 37°C for 30 min. The reaction was stopped by adding 150 µl 1 M Na_2CO_3. Air bubbles were removed before reading the absorbance of the samples at 405 – 420 nm in a microtiter plate reader. A wavelength of 340 nm was used as a reference wavelength.

Reference: (Miller, 1972; Rosenthal, 1987)

2.7.4.3 Protein Assay for β-galactosidase assay

Reagents:

- Protein samples were kept on ice.
- Reagent A (Bio-Rad *DC* Protein Assay)
- Reagent B (Bio-Rad *DC* Protein Assay)
- Bovine serum albumin (BSA) standard

Protocol: The protein samples were diluted 1:5 or 1:2 in H_2O. 5 µl sample, standard including the blank, and buffer control were pipetted into a clean, dry microtiter plate. For all samples, blanks, buffer controls, and standards at least two replicates were prepared. The buffer control was 1 x RLB + RPI diluted 1:5 or 1:2 in H_2O. 25 µl reagent A and 200 µl reagent B were added into each well using a multichannel pipette and incubated at RT for 15 min with gentle shaking at 50 rpm on an orbital shaker and the absorbance was read at 750 nm in a microplate reader.

Reference: (Lowry et al., 1951)

2.7.5 Molecular Biology

2.7.5.1 Polymerase Chain Reaction (PCR)
Reagents:
- DNA template: 5ng/µl plasmid DNA
- 10 x Pfu DNA polymerase buffer w/o $MgCl_2$
- 2 mM dNTPs
- 25 mM $MgCl_2$
- *Pfu* DNA polymerase (2.5 U/µl)
- Primers (100 µM)

Protocol: For a 10 µl analytical (PCR) mix the following:

      1.0   µl   10 x *Pfu* DNA polymerase buffer w/o $MgCl_2$

      1.0   µl   2 mM dNTPs

x	µl	25 mM MgCl$_2$ (0.5 – 6.0 mM)
0.1	µl	primer 1
0.1	µl	primer 2
0.2	µl	*Pfu* DNA polymerase
1.0	µl	Template
6.6 - x	µl	H$_2$O
10	µl	Total

Remarks: For 'N' reactions, (N+2)10 µl was prepared, premix, mixed, and suspended into individual tubes. For preparative PCRs, 1 µl 5 U/µl *Pfu* DNA polymerase was used in 100 µl final volume.

Reference: (Kramer and Coen, 2001)

2.7.5.2 DNA agarose gel electrophoresis
Reagents:

- DNA molecular weight marker/DNA mass standard

- 10 x DNA sample loading buffer: 20% (w/v) Ficoll 400
                                        0.1 M NA$_2$EDTA, pH 8.0
                                        1% (w/v) SDS
                                        0.25% bromophenol blue
                                        0.25% xylene cyanol

Protocol: An adequate volume of 1 x TAE was prepared to fill the electrophoresis tank and to prepare the gel. The desired amount of electrophoresis-grade agarose was added into an Erlenmeyer flask and appropriate volume of 1 x TAE was added for pouring the gel. The agarose was melted in a microwave oven at the highest power setting for 1 – 5 min, swirling every ~30 to 60 s to ensure even mixing and to avoid boiling over of the agarose solution. The agarose solution was then cooled down to 55°C. Ethidium bromide was added to the concentration of 0.5 µg/ml to agarose solution and the contents were mixed by swirling. The gel casting platform

was sealed either using a tape or placing in the slot in the electrophoresis tank designed to cast gels. The melted agarose was poured into the casting platform and the gel comb was inserted making sure that no bubbles are trapped underneath the combs and all bubbles on the surface of the agarose are removed before the gel sets. After the gel had solidified the casting platform was removed to open the sealed ends and the gel comb was removed taking care not to tear the sample wells. The gel casting platform containing the set gel was placed into the electrophoresis tank. 1 x TAE was added to cover the gel to a depth of about 1 mm (or just until the tops of the wells are submerged). The DNA samples were prepared in a 1.5 ml microcentrifuge tube as follows:

x   µl DNA sample

(0.9·z – x) µl H_2O

_____

(0.1·z)   µl 10 x DNA sample loading buffer

z   µl total (z ≤ well volume)

Using a pipette the samples were loaded into the wells. An appropriate DNA molecular weight marker was also included in the gel run. The leads were attached to the power supply unit and the other end placed on top of the electrophoresis tank so that the DNA will migrate into the gel toward the anode or positive lead. The voltage was set to the desired level, typically 1 to 5 V/cm of gel, to begin electrophoresis. The progress of the separation was monitored by the migration of the dyes in the loading buffer. The electrophoresis was continued until the dye front reached 70 % of the gel length or to achieve desired resolution of bands. The power supply was turned off and visualized the DNA by placing the gel onto a UV light source (λ = 254nm).

Reference: (Voytas, 2000)

2.7.5.3 Restriction Endonuclease Digestion

Protocol: The reaction mixture was prepared as per the table below in a 1.5 ml microcentrifuge tube:

0.9 z – x -y	µl	H$_2$O
x	µl	DNA solution,
0.1 z	µl	10 x restriction endonuclease buffer
y	µl	restriction endonuclease in 50% (v/v) glycerol
z	**µl**	**Total**

Remarks:

- For digests with several restriction endonucleases: $y = \Sigma y_i$.
- The maximum for y is 0.1 z ($y_{max} = 0.1\ z$)
- z is usually defined by the size of the wells of the agarose gel. Otherwise, z = 20 µl or z = 100 µl.

The tubes were mixed well by flipping (not vortexing) and briefly centrifuged in a microcentrifuge to collect all liquid at the bottom of the tube. The tubes were then incubated at the desired temperature for the desired time.

Reference: (Bloch and Grossmann, 1995)

2.7.5.4 Dephosphorylation of DNA 5' termini with calf intestinal alkaline phosphatase (CIAP)

Protocol: The amount of DNA ends [in picomoles] that had to be dephosphorylated was calculated. Calf intestine alkaline protease (CIAP) was diluted for immediate use in 1 x CIAP reaction buffer to a final concentration of 0.01 U/µl. Each picomole of DNA ends will require 0.01 U CIAP.

The reaction mixture was made in a 1.5 ml microcentrifuge tube as follows:

X	µl	DNA (up to 10 picomoles)
5	µl	10 x CIAP reaction buffer
X	µl	0.01 U/µl CIAP
45 – 2 x	µl	H$_2$O
50	**µl**	**Total**

The tubes were mixed well by flipping (not vortexing) and briefly centrifuged in a microcentrifuge to collect all liquid at the bottom of the tube. The tubes were then

incubated at 37°C for 30 min and an additional x µl 0.01 U/µl CIAP was added and incubated further for 30 min at 37°C. 300 µl 10 mM Tris·HCl (pH 7.5), 200 mM NaCl, 1 mM EDTA, 0.5% (w/v) SDS was added to stop the reaction. The preparation was subjected to phenol: $CHCl_3$ extraction and purified the DNA using a spin column.

Reference: (Tabor, 1987)

2.7.5.5 DNA Ligation with T4 DNA ligase

Protocol:

Ligation of 5' and 3' overhanging ends

The ligations were set-up on the basis of guidelines as below: Use 50 ng vector DNA and an 1:1 – 1:3 molar ratio of vector to insert DNA. The following mix was added into a 1.5 ml microcentrifuge tube:

X	µl	vector DNA (50 ng)
Y	µl	insert DNA (1:1 – 1:3 molar ratio vector:insert)
1	µl	10 x T4 DNA ligase buffer
0.2	µl	5 Weiss-U/µl T4 DNA ligase
8.8 – x - y	µl	H_2O
10	**µl**	**Total**

The tubes were mixed well by flipping (not vortexing) the tube and briefly centrifuged in a microcentrifuge to collect all liquid at the bottom of the tube. The tubes were then incubated at 16°C for ≥ 16 h and stored at 4°C. The ligation mixture was transformed into *E. coli* by chemical transformation or after purification by electroporation.

Reference: (Cherepanov and de Vries, 2001; Rossi et al., 1997)

2.7.5.6   Plasmid DNA miniprep from *E. Coli*

Protocol: 1.5 ml of a saturated overnight *E. coli* culture was transferred into a 1.5 ml microcentrifuge tube. The remainder of the culture was stored at 4°C. The cells were collected by centrifugation for 1 min at 14,000 g, RT and the supernatant aspirated.

The tubes were centrifuged again for 1 min at 14,000 g, RT and supernatant was aspirated. 100 µl 50 mM D-Glc, 25 mM Tris·HCl (pH 8.0), 10 mM EDTA was added and the cells were resuspended by vortexing or pipetting up and down. The tubes were incubated for 5 min at RT. Then added 200 µl 0.2 N NaOH, 1% (w/v) SDS and mixed by inverting tubes 4-6 times and incubated on ice for 5 min. 150 µl ice-cold 5 M KOAc (pH 4.8) was added and mixed by inverting tubes 4 - 6 times and incubated for 5 min on ice. This was followed by centrifugation for 3 min at 14,000 g, 4°C and transferred the supernatant into a new microcentrifuge tube. 0.8 ml ethanol were added and mixed by inverting the tubes 2-3 times. The tubes were then incubated at RT for 2 min or stored at - 20°C. The tubes were then centrifuged for 1 min at 14,000 g, RT and the supernatant was discarded. 1 ml 70% ethanol, was added to the tubes and centrifuged for 1 min at 14,000 g, RT. The supernatant was discarded by aspiration or inverting the tube and centrifuged again briefly to collect the remaining liquid at the bottom. The residual 70% ethanol was pipetted out and the pellets were dried in air for 5 min at RT. The pellets were resuspended in 30 µl 1 x TE (pH 8.0), 0.3 mg/ml RNase A and incubated at 4°C until pellets are dissolved (~0.5 - 1 h).

Reference: (Sambrook, 1989)

2.7.5.7 Plasmid Midiprep: GenElute™ High Performance (HP) Plasmid Midiprep Kit (Sigma-Aldrich)

Protocol:

The kit was stored at room temperature. Once the RNase A solution was added to the resuspension solution it was stored at 2 to 8°C. The neutralization solution was also stored at 2 to 8 °C. The reagents were mixed thoroughly and examined for precipitation. If any reagent formed a precipitate upon storage, it was warmed at 55-65°C until the precipitate dissolved and was cooled down to room temperature before use. The resuspension solution was prepared by adding 750 µl RNase A provided in the kit and stored at 4°C. Wash solution 2 was diluted with 120 ml of 95-100% ethanol prior to initial use. A single colony was inoculated in 2 ml LB broth with appropriate antibiotics and incubated overnight at 37°C to prepare the preculture. 50 ml of LB broth containing appropriate antibiotic was inoculated from the preculture at a dilution of 1:200 to 1:500 and incubated overnight at 37°C. The cells from 50 ml

overnight grown culture were harvested by centrifugation at 5,000 x g for 10 min and the supernatant was discarded. All steps were carried out at room temperature. The cells were resuspended in 4 ml of resuspension solution by pipetting up and down, or vortexing to make sure that the cells are resuspended. The resuspended cells were lysed by adding 4 ml of the lysis solution and immediately mixing the contents by gently inverting 6 to 8 times and letting the mixture sit for 3 to 5 min until it became clear and viscous. The lysis was not prolonged more than 5 min. A filter syringe was prepared by removing the plunger and placing the barrel in a rack to keep the syringe barrel upright. The lysed cells were neutralized by adding 4 ml of chilled neutralization solution and gently inverted 4 to 6 times. A white aggregate (cell debris, proteins, lipids, SDS, and chromosomal DNA) was formed to which 3 ml of binding solution was added and inverted 1 to 2 times. The lysate was immediately poured into the barrel of the filter syringe and sit for 5 min. Meanwhile a binding column was placed into a collection tube provided and 4 ml of column preparation solution was added to the column and spun in a swinging bucket rotor at 3,000 x g for 2 min. The eluate was discarded. The content of the filter syringe barrel was emptied into the binding column by gently inserting the plunger to expel half of the cleared lysate into the column. The plunger was pulled back slightly to stop the flow of the remaining lysate. The column assembly was spun in a swinging bucket rotor at 3,000 x g for 2 min and the eluate discarded. The rest of the cleared lysate was added to the column and spun at 3,000 x g for 2 min. 4 ml of wash solution 1 was added to the column and spun in a swinging bucket rotor at 3,000 x g for 2 min. The eluate was discarded. 4 ml of wash solution 2 was added to the column and spun in a swinging bucket rotor at 3,000 x g for 5 min. The binding column was transferred to a new collection tube and 1 ml of elution solution was added to the column and was kept at RT for 5 min. The column assembly was centrifuged in a swinging bucket rotor at 3,000 x g for 5 min to recover the plasmid. The plasmid DNA present in the eluate was concentrated by ethanol precipitation. The plasmid solution was transferred to tubes that can withstand 15,000 x g. 0.1 volume of 3.0 M sodium acetate, pH 5.2, and 2.5 volume of 95-100 % ethanol was added to the plasmid solution and mixed well by inversion and incubated at -70°C for ≥ 30min. The tubes were centrifuged at ≥15,000 x g at 4°C for 30 min and the supernatant was decanted, being careful not to disturb the pellet. The pellet was rinsed with 1.5 ml of 70% ethanol and centrifuged as before for 10 min. The supernatant was carefully

decanted and the pellet was dried until the residual ethanol evaporated. The DNA pellet was resuspended in 100 µl of 1 x TE (pH 8.0) and stored in refrigerator.

Reference: (Birnboim and Doly, 1979; Vogelstein and Gillespie, 1979)

2.5.7.8 Promega Wizard® SV Gel and PCR Clean-Up System
Protocol:

For DNA extraction from agarose gels: The membrane wash solution was prepared by adding the suggested volume of 95% ethanol to the membrane wash solution prior to beginning the procedure. For DNA extraction from agarose gels the gel slice containing the DNA was weighted and mixed in the membrane binding solution at a ratio of 10µl of solution per 10 mg of agarose gel slice. The mixture was vortexed and incubated at 65°C for 10 min or until the gel slice is completely dissolved. The tube was vortexed every few min to increase the rate of melting the agarose gel. The tubes were centrifuged briefly at room temperature to ensure the contents are at the bottom of the tube.

For cleaning plasmid preparation and PCR amplification products: The plasmid preparation or amplified PCR product was added to an equal volume of membrane binding solution

DNA Purification: One SV minicolumn was placed in one collection tube for each purification reaction. The mixture of membrane binding solution with gel slice/plasmid solution/PCR product (prepared as described above) was added to the SV minicolumn assembly and incubated for 2 min at room temperature. The SV minicolumn assembly was centrifuged at 16,000 × g for 2 min. The SV minicolumn was removed from the spin column assembly and the liquid was in the collection tube was discarded. The SV minicolumn was replaced onto the collection tube. The column was washed by adding 700µl of membrane wash solution, previously diluted with 95% ethanol, to the SV minicolumn and centrifuging the SV minicolumn assembly for 1 min at 16,000 × g (14,000rpm). The collection tube was emptied as before and placed the SV minicolumn back in the collection tube. The wash step was repeated with 500µl of membrane wash solution and the SV minicolumn assembly was centrifuged for 5 min at 16,000 × g. The SV minicolumn assembly was removed

from the centrifuge, being careful not to wet the bottom of the column with the flowthrough. The collection tube was emptied and the column assembly was recentrifuged for 1 min to allow evaporation of any residual ethanol. The SV minicolumn was carefully transferred to a clean 1.5 ml microcentrifuge tube. 50μl of nuclease-free water was added directly to the center of the column without touching the membrane with the pipette tip and incubated at room temperature for 2 min. The elution volume depended on the downstream application. The tube containing the column assembly was centrifuged for 1 min at 16,000 × g and the SV minicolumn was discarded. The microcentrifuge tube containing the eluted DNA was stored at 4°C or -20°C.

2.7.5.9 Phenol/CHCl$_3$ Extraction of DNA

Protocol:

All steps were performed in a fume hood. 1 Vol. Phenol/CHCl$_3$/isoamylalcohol (25/24/1 v/v/v), saturated with 1 M Tris·HCl (pH 8.0) was added to the DNA sample. The mixture was briefly vortexed to homogenize the aqueous and phenolic phases and then centrifuged at 12,000 g, RT for 1 min to separate both phases. The upper aqueous phase was transferred into a new 1.5 ml microcentrifuge tube. A white protein precipitate may form between the two phases, depending on the amount of protein in the sample. Care was taken as to not transfer any protein precipitate into the new 1.5 ml microcentrifuge tube. Repeated the above two steps at least once or until a protein precipitate between the aqueous and phenolic phase was no longer present. Then pooled both phenolic phases in a 1.5 ml microcentrifuge tube and extracted the pooled phenolic phase with ¼ Vol. 1 x TE (pH 8.0) as described earlier and pooled both the aqueous phases. Added 1 Vol. CHCl$_3$/isoamylalcohol (24/1 v/v) to the pooled aqueous phase and repeat it at least once. *Remark: One CHCl$_3$/isoamylalcohol (24/1 v/v) extraction is not sufficient to remove all traces of phenol. Four extractions are, but the minimal number of extractions requires to complete remove the phenol, is somewhere between two and four.* Vortexed briefly to mix the aqueous and organic phase. Centrifuged at 12,000 g, RT for 1 min to separate both phases. The upper, aqueous phase was transferred into a new 1.5 ml microcentrifuge tube and processed as desired or stored at 4ºC.

Reference: (Sambrook, 1989)

2.7.5.10 Transformation of Yeast with LiOAc/PEG

Protocol: The cells were grown by inoculating 2 ml YPD broth with a single colony and incubated until saturation ($A_{600} > 3.0$) at 30°C. This was the preculture. For each transformation 5 ml YPD broth was inoculated with an $A_{600nm} = 0.01$ using the preculture and incubated at 30°C with shaking at 250 rpm. The absorbance was measured regularly until $A_{600nm} = 0.8-1.2$ was reached. The culture was transferred to a 50 ml tube and the cells were collected by centrifugation for 2 min at 3000 rpm, 4°C. The supernatant was decanted and the cells were placed on ice. While the cells were centrifuging the sheared salmon sperm DNA was thawed in a 37°C water bath, then placed on ice. The cell pellet was resuspended in 5-10 ml one-step buffer by vortexing. The cells were centrifuged for 2 min at 3000 rpm, 4°C, the supernatant was decanted and placed on ice. The residual liquid was aspirated and 88 μl of one-step buffer was added to a cell pellet obtained from 5 ml of YPD broth. The cell pellet was resuspended by vortexing to remove any cell clumps and placed on ice. The salmon sperm DNA was denatured by boiling (100°C) for 5 min in a heat block and placing on ice. The transforming DNA was dispensed into 1.5 ml microcentrifuge tubes and placed on ice. 12 μl 8.31 mg/ml (14.5 μl 6.89 mg/ml) sheared salmon sperm DNA was also added to each tube containing the transforming DNA using a large orifice pipette tip. 88 μl cell suspension from earlier step was added to tubes containing transforming DNA and 100 μgm sheared salmon sperm DNA using large orifice pipette tips. The tubes were vortexed for 15 s at maximum speed and incubated the cells in a 42°C water bath for 30 min without mixing. The tubes were placed on ice. The cells were collected by centrifugation in a microcentrifuge for 10 s at RT and placed on ice. The supernatant was pipetted out completely and the pellet was resuspended in 200 μl H_2O by pipetting up and down until no cell clumps remained. The whole content of a tube was plated onto an appropriate plate. The plates were incubated at 30°C in an incubator until colonies formed (usually 3-14 days). The colonies that appeared on the plate after the incubation period were streaked for single colonies. These were then tested for their growth on non-fermentable carbon source by streaking the colonies on PSP2/YPAc plate. The colonies that were able to grow on non-fermentable carbon source were preserved as frozen stocks.

Transformation controls:

Each time yeast cells are transformed included the following controls:

- **Negative control:** 100 µl cells were transformed with 5 µl 1 x TE (pH 8.0) to test for sterility of the reagents and procedure.

- **Positive control:** One transformation with 100 ng of an autonomously replicating yeast plasmid was used for positive control to determine the transformation efficiency (colonies/µg transforming DNA).

Reference: (Chen et al., 1992)

2.7.5.11 Preparation of electrocompetent *E. Coli*

Protocol: 500 ml LB broth was inoculated with 5 ml of a fresh overnight *E. coli* culture. The cells were grown at 37ºC with shaking at ~250 rpm until an A_{600nm} of 0.5 was reached. The cells were transferred to an ice-cold 500 ml centrifuge bottle and chilled on ice for 15 min. The cells were collected by centrifugation at 4000 *g*, 4ºC for 15 min and the supernatant was decanted. The cells were washed by adding 500 ml ice-cold water, resuspended by vortexing and centrifuged at 4000 *g*, 4ºC for 15 min. The supernatant was decanted and the cells were washed twice as described in the earlier step. The cells were now resuspended in 8 ml ice-cold 10% (v/v) glycerol and transferred to a preweighted, ice-cold 40 ml centrifuge tube and centrifuged for 10 min at 4ºC at 3000 *g*. The supernatant was decanted and the tube was weighed. The weight of the pellet was calculated and resuspended by vortexing in one cell volume ice-cold 10% (v/v) glycerol. The cells were aliquoted into 40 µl aliquots into ice-cold 1.5 ml microcentrifuge tubes and frozen in a dry ice/ethanol bath or in liquid nitrogen and store at -70ºC indefinitely.

Reference: (Seidman et al., 1997a)

2.7.5.12 Electroporation of electrocompetent *E. Coli*
Reagents:
- Electrocompetent *E. coli* cells
- Control plasmid pUC18 (10 pg/µl)

- Plasmid DNA for transformation
- Ligation reactions: Clean-up on a PCR purification column.
- Elute with 20 µl elution buffer. Use 5 µl eluate for electroporation.
- 2 M D-glucose, filter sterilized
- 1 N HCl
- LB plates with appropriate antibiotics (ampicillin 100µgm/ml and tetracycline 12.5 µgm/ml)
- LB broth
- LB broth + 20 mM D-glucose

Protocol: The pulse controller was set to 200 Ω. For each electroporation 1 ml LB + 20 mM D-Glc was prepared in a 1.5 ml microcentrifuge tube. The electrocompetent cells were thawed by taking out the tubes from - 80ºC freezer and immediately placed on ice. The DNA (up to 5 µl) was added to the tube containing electrocompetent cells and the mix was placed on ice. The cell suspension was then pipetted into an ice cold electroporation cuvette to the bottom of the cuvette and gently tapped to remove any foam or air bubbles in the cell suspension. The outside of the cuvette was wiped dry, and placed into a chilled safety chamber slide. The cuvette was then pulsed at 25µF, 2.5 kV. The time constant was kept above 5.0 ms. 1 ml LB + 20 mM D-glucose was added immediately to the cuvette using a 1000 µl pipette and the cells were transferred into a 14 ml culture tube. These tubes were then incubated in a 37ºC shaker for 1 h with shaking (~220 rpm). The cells were plated at different aliquots of 5, 10, and 200 µl onto LB-agar plates containing appropriate antibiotics. The remaining cell suspension was centrifuged for 1 min at 15,000 g at RT to collect cells. The supernatant was aspirated and the cell pellet resuspended in 100 – 200 µl H$_2$O and plated onto LB-agar plates containing appropriate antibiotics. The plates were then incubated in a 37ºC incubator for 16 h. The plates were then observed for appearance of colonies which were then stored in the refrigerator until the colonies were used as inoculum for plasmid minipreparation. The following controls were used with each batch of electroporation. Negative controls were included with 5 µl of 1 x TE (pH 8.0) to determine any possible contamination. In the positive controls 10 pg of pUC18 plasmid was used to determine the efficiency of transformation. The ligation mixtures for transformation were subjected to purification by PCR-clean up column.

Reference: (Seidman et al., 1997a)

2.7.5.13 Preparation of chemically competent *E. coli* cells

Protocol: LB broth 4 ml was inoculated with one colony *E. coli* cells from a fresh LB agar plate and grown overnight at 37°C with shaking at 225 rpm. The overnight culture was diluted 1:100 into LB broth and incubated at 37°C with shaking at 225 rpm. After ~1 h, the absorbance $A_{600\ nm}$ of the culture was measured and then monitored every 15 - 30 min. The culture was transferred to a weighed centrifuge tube when the 0.3 – 0.4 $A_{600\ nm}$ was reached and precooled on ice. The tube was then centrifuged for 10 min at 1000 g and 4°C to collect the cells and the supernatant was decanted. The centrifuge tube was weighed and the cell pellet was resuspended by gently shaking in 1/10 of the original culture volume ice-cold 1 x TSS. The cells were aliquoted in ice-cold 1.5 ml microcentrifuge tubes as aliquots of 100 – 500 µl and frozen in liquid nitrogen or a dry ice/ethanol bath. The cells were stored at -70°C indefinitely.

Reference: (Seidman et al., 1997b)

2.7.5.14 Chemical Transformation of *E. Coli*

Protocol: The competent cells were thawed by taking them out of the -80ºC freezer and immediately putting them on ice. Upto 5 µl of DNA solution was added to microcentrifuge tubes and placed on ice. The thawed competent cells were mixed carefully by inverting the tube once or twice and 100 µl of competent cells were added to tubes containing DNA. The tubes were gently flipped to mix the contents and incubated on ice for 30 min. At the end of the incubation period the tubes were placed into a 1.5 ml microcentrifuge tube swimmer and placed into a 42ºC waterbath for exactly 90 sec without moving the tubes. The microcentrifuge tubes with the swimmer was taken out of the waterbath and placed immediately on ice for 5 min. 900 µl LB broth + 20 mM D-glucose was added to each tube and transferred to 14 ml culture tubes, and incubated at 37ºC with shaking (~220 rpm) for 1 h. 200 µl cell suspension was plated onto LB-agar plates containing appropriate antibiotics. The remaining cell suspension was centrifuged for 1 min at 15,000 g at RT to collect cells

and the supernatant was discarded. The cells pelleted were resuspended in 100 –
200 μl H$_2$O and plated onto LB-agar plates containing appropriate antibiotics. The
plates were incubated in a 37°C incubator for 16 h and colonies counted. The plates
were stored in the refrigerator until the colonies were used as an inoculum for
plasmid minipreparation. The controls were used with each batch of electroporation.
Negative controls were included with 5 μl of 1 x TE (pH 8.0) to determine any
possible contamination. In the positive controls 100 pg of pUC18 plasmid was used
to determine the efficiency of transformation.

Reference: (Seidman et al., 1997b)

2.7.5.15 Gap-repair technique for recombinational cloning in yeast

Reagents

- Vector DNA (~1 ug/transformation)
- Insert DNA (~200 ng/transformation)
- Yeast culture for transformation
- E. coli XL10 GOLD competent cells
- SD medium lacking uracil made with yeast nitrogen base from Becton Dickinson
- SD agar plates lacking uracil
- QIAprep Spin Miniprep kit

Protocol: A WT *S. cerevisiae* strain (*ura3*) was transformed with ~1 μg of vector
DNA and ~200 ng of insert DNA by LiOAc transformation as described in **2.7.5.10**.
The cells were plated onto selective SD plate lacking uracil and incubated at 30°C
until the colonies formed. Single colonies were picked up and inoculated in 2-4 ml
synthetic dextrose (SD) medium lacking uracil made with yeast nitrogen base from
Becton Dickinson. The tubes were then incubated in shaker incubator at 30°C for ~2
days or until saturation. The cells were harvested by centrifugation at 5000g, 5 min
and the supernatant discarded. The cells were resuspended in 250 ul Buffer P1
(containing 0.1 mg/ml RNAse A) and transferred to a 2 ml flat bottom tube. Glass
beads (~150 mg) were added to this tube and the cells were lysed using Precellys 24

instrument (two 30 second cycles of 6, 500 rpm at 4°C by using cycles for 30 s each). The tube was centrifuged at 5000 g, 5 min at 4ºC and supernatant was transferred to a fresh 1.5 ml tube. 250 µl lysis buffer P2 was added to the cell lysate, inverted gently 4-6 times and incubated on ice for 5 min. 350 µl neutralization buffer N3 was added to the tube and gently inverted 4-6 times to neutralize. The lysate was centrifuged for 10 min at 10,000 g at 4°C. QIAprep spin column was placed in a 2ml collection tube and cleared lysate form earlier step was applied to it. The whole assembly was centrifuged for 30-60s 10,000 g at 4°C and follow through was discarded. QIAprep spin column was washed by adding 0.75 ml of Buffer PE and centrifuging 30-60s (10,000 g). The follow-through was discarded and QIAprep spin column assembly was centrifuged again for 1 min to get rid of any residual wash buffer. QIAprep spin column was transferred to a fresh collection tube and 25 µl of 1XTE was applied to the center. The column was left to stand for 2 min at RT and then centrifuged for 1 min. The eluate was used to transform *E. coli* XL10 GOLD cells as described in **2.7.5.14**. The plasmids extracted from the clones were subjected to restriction digestion analysis and fragments of interest were checked by sequencing.

Reference: (Ma et al., 1987)

2.7.5.16 Site directed mutagenesis

Reagents:

- QuikChange II XL Site-Directed Mutagenesis kit (Stratagene 200521)
- Plasmid DNA isolated from *dam*⁺ strains
- Oligonucleotides: I-β-gal and Q-β-gal (**Table 3.1**)

Protocol: Two complimentary oligonucleotides I-β-gal and Q-β-gal containing the silent restriction site *Bau*I flanked by unmodified nucleotide sequence were synthesized. Oligonucleotides also contained mutation that introduces isoleucine or glutamine amino acid as the first amino acid of β-galactosidase. Control and sample reactions were prepared as indicated below:

5 µl of 10× reaction buffer

2 µl (10 ng) of pWhitescript 4.5-kb control plasmid (5ng/µl) or dsDNA template

1.25 µl (125 ng) of oligonucleotide primer #1 (100 ng/µl)

1.25 µl (125 ng) of oligonucleotide primer #2 (100 ng/µl)

1 µl of dNTP mix

3 µl of QuikSolution reagent

36.5 µl of double-distilled water (ddH2O) to a final volume of 50 µl

Then 1 µl of *PfuUltra* HF DNA polymerase (2.5 U/µl) was added to each reaction. The thermal cycler was used for mutant strand synthesis. A 5 min extension time at 95°C followed by 18 cycles of 95°C for 50 sec, 60°C for 50 sec and 68°C for 1 min/kb of plasmid length followed by 68°C for 7 min was used. Following temperature cycling, the reaction tubes were placed on ice for 2 min to cool the reactions to 37°C. The reaction mixtures were digested with 1ul of *Dpn*I (10 U/µl) for 1 h at 37°C to remove non mutated parental DNA. 2µl of *Dpn*I digested DNA was transformed in *E.coli* as per protocol 2.7.5.14. Mutated plasmids should now have a *Bau*I site introduced with the oligonucleotides. These plasmids were selected based on digestion with *Bau*I restriction enzyme and confirmed by sequencing.

Reference: (Cormack, 1997)

2.7.5.17 DNA sequencing

Protocol

Plasmid DNA samples (at least 125 ng per reaction) were provided after checking on the agarose gel with Restriction digestion analysis. The primers covering overlapping regions were provided at the concentration of 3.2pmol/µl.DNA sequencing was carried out by DNA Sequencing Facility at Durham University. The DNA sequencing was undertaken using an Applied Biosystems 3730 DNA Analyser. The sequence data that was generated was analyzed using BioEdit software.

2.7.5.18 Immunoprecipitation

Reagents:

- Lysis buffer,   50 mM $Na_xH_{3-x}PO_4$ (pH 7.3)
  ice-cold: 150 mM NaCl
  10% (v/v) glycerol
  1 mM EDTA
  1 mM Na_3VO_4
  10 mM NaF
  0.25% (v/v) NP-40

  add fresh: 7 mM β-mercaptoethanol
  1 µg/ml pepstatin
  1 tablet complete mini protease inhibitors/10 ml

- 6 x SDS-PAGE   350 mM Tris-HCl (pH 6.8)
  sample buffer: 30% (v/v) glycerol
  10% (w/v) SDS
  0.2 g/l bromophenol blue
  0.6% (v/v) β-mercaptoethanol

- Protein A sepharose, 50% (w/v) slurry in PBS + 0.01% (w/v) NaN_3
- Protein G PLUS agarose, 25% (w/v) slurry

Protocol

Note: All steps in this protocol are performed on ice or at 4°C, if not indicated otherwise.

Yeast culture samples were thawed at RT and placed on ice. 5 ml ice-cold H_2O was added to each tube, cells were resuspended and centrifuge for 2 min at 3000 rpm, 4°C to sediment cells. The supernatant was decanted and 1 Vol. ice-cold lysis buffer was added. The cells were lysed by two passages through a French press and the solution was transferred into 1.5 ml microcentrifuge tubes and centrifuged at 10,000 g, 4°C for 10 min. Supernatant was transferred into new tubes and protein concentration was determined using Bio-Rad *DC* Protein Assay kit. Equal protein amounts were used in each immunoprecipitation with maximum volume not exceeding ~ 500 µl. 50 µg protein was saved for a Western blot with anti-PGK as a

loading control for the immunoprecipitation. The volume was adjusted to 500 µl with ice-cold lysis buffer in 1.5 ml screw-cap microcentrifuge tube. 20 µl 25% (w/v) protein A or G agarose were added using large orifice pipette tips to each immunoprecipitation and incubated for 1 h with over head rotation at 4°C. The tubes were centrifuge for 2 min at 12,000 g, 4°C to collect beads and the supernatant was transferred quantitatively into a new tube. Antibodies and competing peptides were added to respective tubes and incubated with over head rotation overnight at 4°C. 20 µl 50% (w/v/) protein A or G sepharose slurry was added to each immunoprecipitation and incubated for another 1 – 2 h at 4°C with overhead rotation. Immunoprecipitation reactions were transferred into 1.5 ml spin filter microcentrifuge tubes and centrifuged for 2 min at 12,000 g. The flow through was discarded and spin filter was placed into a new 1.5 ml centrifuge tube. The sepharose beads were washed 3 times with 500 µl ice-cold lysis buffer with 0.1% (v/v) NP-40 and once with 500 µl ice-cold lysis buffer without NP-40. Supernatant was separated from beads by centrifugation for 2 min at 12,000 g, 4°C. Tubes were centrifuged once more for 2 min at 12,000 g and 4°C and placed into a clean 1.5 ml microcentrifuge tube. 15 – 20 µl 6 x SDS-PAGE sample buffer was added and the samples boiled for 3 min in a heat block. After the samples cooled down, eluate was collected by centrifugation for 2 min at 12,000 g, RT and used for SDS-PAGE gels.

Reference: (Bonifacino et al., 1999)

2.7.5.19 SDS-PAGE gel electrophoresis

Protocol: The electrophoresis unit and criterion 4-15% Tris-HCl gradient precast gels were assembled according to manufacturer's instructions and buffer reservoirs filled with 1 x SDS-PAGE buffer. Samples were prepared by adding appropriate amount of 6x SDS-PAGE sample buffer on ice and centrifuged briefly (~15 s) at 12,000 g and RT. The samples were then boiled for 5 min at 100°C and centrifuged again briefly to collect the whole sample at the bottom of the tube. The wells were washed by pipeting SDS-PAGE buffer several times using gel loading tips. The samples were loaded onto gel using gel loading pipette tips. SDS-PAGE electrophoresis unit was aligned as per the colour coded banana plug and jacks. 200V voltage of was applied until the bromophenol blue dye front nearly elutes from the gel. The electrophoresis

unit was disassembled according to manufacturer's instructions and was processed to transfer proteins from gel to a PVDF membrane by immunoblotting.

Reference: (Gallagher, 1999)

2.7.5.20 Electrotransfer and Western Blot

Protocol: The stacking gel was cut off and transferred into 100 ml ice-cold transfer buffer (10 mM $NaHCO_3$ + 3 mM Na_2CO_3) and incubated with gentle agitation for 1 h at 4ºC. Whatman 3MM papers were incubated in ice-cold transfer buffer and PVDF membrane onto ~ 50 ml methanol. Once the PVDF membrane was completely wetted, it was transferred to transfer buffer for ~15 min. The gel sandwich was prepared by placing cassette with the gray side down on a clean surface followed by one pre-wetted fiber pad. A sheet of Whatman 3MM paper was placed onto the equilibrated gel to match all edges exactly. Whatman 3MM paper carrying the gel was placed onto the fiber pad with the gel facing up. Any air bubbles between the Whatman 3M paper and the gel were removed by rolling a Pasteur pipette gently over the gel. Pre-wetted PVDF membrane was placed on the gel removing any air bubbles. The sandwich was completed by placing a sheet of Whatman 3MM paper onto the PVDF membrane and pre-wetted fiber pad onto the Whatman 3MM paper. The cassette was firmly closed and locked with the white latch. Magnetic stirrer was added in the tank. The gray side of each cassette was placed facing the cathode (-pole). The transfer unit was placed into a large plastic a glass tray placed on a stir plate in the cold laboratory. The tank was filled completely with ice-cold transfer buffer. The lid was put on and cables were plugged into the power supply. Transfer was started by setting the voltage to 30 V with stirring of the transfer buffer for overnight. Upon completion of the run, membrane was removed by disassembling the blotting sandwich.

Western Blot: The membranes were transformed into plastic trays containing PBST (PBS + 0.1% (v/v) tween 20) + 5% (w/v) skim milk powder and incubate 1 h at RT with shaking (~50-60 rpm). The membranes were transferred into a 50 ml centrifuge tube containing 50 μl/cm^2 PBST + 2.5% (w/v) skim milk powder + primary antibody (Anti-HA antibody, Roche 12CA5, 100 ng/ml; Anti-PGK, Molecular Probes, 2mg/ml) removing any air bubbles between the tube walls and the membrane and incubated 1

h at RT with rotation. The membranes were then washed four times with PBST by incubating for 5 min at RT with shaking. The membranes were then incubated with PBST + 2.5% (w/v) skim milk powder + secondary antibody (anti-mouse IgG-POD-(Fab')2;Roche #60530, 1:300 dilution) for 1 h at RT with rotation. The membranes were washed with PBST four times for 5 min each at RT with shaking. The blots were developed using ECL kit (GE Healthcare).

References: (Gallagher et al., 1997; Towbin et al., 1979)

Chapter 3

Destabilised β-galactosidase reporters:

Construction, validation & transcriptional regulation of URS1 controlled early meiotic genes

3.1 *CYC1-lacZ* reporters for monitoring transcriptional activity under nutrient-rich conditions

Meiosis is negatively regulated in the presence of glucose and nitrogen sources and this has been extensively studied. However, the direct regulation of meiosis by nitrogen abundance is not very well understood. *S. cerevisiae* diploid cells under nitrogen starvation and in the presence of non-fermentable carbon sources undergo meiosis (Herskowitz, 1988; Kupiec et al., 1997). The onset of the meiotic program is marked by induction of the early meiotic genes. The bZIP transcription factor Hac1[i]p is a negative regulator of early meiotic genes under nitrogen replete conditions (Schröder et al., 2000) through the upstream repression site 1 (URS1, TCGGCGGCT), present in most of the early meiotic genes. The negative regulation of early meiotic genes is shown by an increase in the mRNA levels of early meiotic genes in the absence of Hac1[i]p and repression in the presence of Hac1[i]p under nitrogen starved conditions (Schröder et al., 2004). Further evidence comes from the use of *CYC1-lacZ* reporters, which are routinely used for measuring transcriptional activity. In the *CYC1-lacZ* reporters, the *Escherichia coli lacZ* gene is fused to the *CYC1* promoter [**Figure 3.1** and (Guarente and Mason, 1983; Kadosh and Struhl, 1997; Wu et al., 2001; Zhang et al., 1998)]. Schröder et al., 2004 used URS1-*CYC1-lacZ* reporters, derivatives of *CYC1-lacZ* reporters (known as pLGΔ312SΔSS in **Figure 3.1B**) without any upstream activating sequences of the *CYC1* promoter to study URS1-controlled transcriptional repression by Hac1[i]p under meiotic growth conditions. Hac1[i]p was constitutively expressed in these experiments, which repressed the activation of β-galactosidase from URS1-*CYC1-lacZ* reporter. However, the regulation that underlies nutrient-rich/mitotic growth conditions could not be shown directly because pLGΔ312SΔSS constructs show barely detectable levels of β-galactosidase under nutrient rich conditions and are only induced under meiotic conditions. I wanted to directly demonstrate whether the negative regulation of Hac1[i]p on URS1-controlled genes can be recapitulated in nutrient rich conditions. In order to test this we wanted to employ a system that firstly elevates expression of a reporter gene mediated through URS1 and secondly it is easily detected in large number of samples. Early meiotic genes are repressed in nutrient rich conditions and so their mRNA cannot be detected easily (Kupiec et al., 1997). Moreover early meiotic gene transcripts are highly unstable when expressed during vegetative

growth or sporulation (Surosky and Esposito, 1992). Analysis by reporter system allows monitoring specific changes at transcriptional level as compared to techniques like quantitative real time RT-PCR, which also depends on mRNA stability rather than transcription initiation. Therefore we decided to use heterologous promoter to elevate expression of a reporter gene that can be used to measure transcriptional activity with relative ease. β-Galactosidase reporter assays are routinely used for testing transcriptional activity at a promoter element of interest. Transcriptional activity regulated by cis acting element can be studied by cloning in a heterologous promoter upstream of *lacZ*. The transcriptional regulation can be detected by colorimetric estimation of β-galactosidase activity without having to detect mRNA transcripts in multiple samples. The principal advantage of these assays is their high sensitivity, reliability, convenience, inexpensive and adaptability to large-scale measurements. β-Galactosidase reporter employs an enzyme assay as compared to non-enzymatic fluorescence based reporters and therefore allows quantitative study of transcriptional induction and repression phenomenon. Advances in microplate technology have allowed both assay miniaturization and the possibility to save time, reagents and increase dramatically the number of samples analysed. The use of β-galactosidase reporter enzymes allows a more rapid and equally sensitive method for detection of transcription than the analysis of specific transgene transcripts within the cells. Construction of a control reporter where introduction of point mutations in URS1, can prevent binding of Ume6p is convenient in comparison to manipulation of URS1 in the endogenous genes. Since β-Galactosidase reporter also can be applied to a wide variety of other experimental uses, construction of destabilised reporters is useful as well as a technical advancement in the field. The pLGΔ312SΔSS constructs without any *CYC1* upstream activating sequences have barely detectable levels of β-galactosidase in nutrient-rich vegetative (mitotic) growth conditions, precluding the use of pLGΔ312SΔSS based plasmids to investigate whether Hac1[i]p represses on URS1 in vegetative growth conditions (Bowdish and Mitchell, 1993; Kadosh and Struhl, 1997; Schröder et al., 2004). Therefore we needed a reporter system that was elevated under nutrient rich conditions. **Figure 3.1** shows various derivatives of *CYC1-lacZ* reporters widely used to study transcriptional activity driving the expression of β-galactosidase by heterologous promoter elements. pLGΔ312S-based plasmids, which contains *CYC1* upstream activating sequences and show robust mitotic expression suited the purpose of the study (**Figure 3.1A**). The *CYC1*

fragment -324 to +141, which includes two UAS$_{CYC1}$ and the TATA region, is fused to β-galactosidase encoded by the *lacZ* region (Guarente and Mason, 1983). The plasmid pLGΔ312S-INO1 contains one URS1 element from *INO1* gene and pLGΔ312S-IME2 contains two URS1 elements from *IME2* gene and are located in the *CYC1* promoter immediately upstream of UAS$_{CYC1}$ [**Figure 3.1C** and (Kadosh and Struhl, 1997)]. I employed the URS1 containing *CYC1-lacZ* reporters to test the transcriptional activity mediated on URS1 elements in vegetative growth conditions.

S. cerevisiae WT strains were transformed with pLGΔ312S, pLGΔ312S-INO1 and pLGΔ312S-IME2 and their transcriptional activity was monitored in cells grown in nutrient-rich synthetic acetate medium (PSP2 medium) and harvested at exponential phase to measure β-galactosidase levels. The steady state levels of URS1-*CYC1-lacZ* reporters expressed under the *CYC1* promoter containing 0, 1 or 2 URS1 sites is shown in **Figure 3.2**. β-Galactosidase is expressed at elevated levels from URS1-*CYC1-lacZ* reporter plasmids with or without any URS1 under nutrient-rich conditions. The mitotic repression is not remarkable with one URS1 site but in presence of two URS1 sites there is a repressing trend in nutrient rich conditions.

The URS1-*CYC1-lacZ* reporters show elevated expression in nutrient-rich conditions without any URS1 sites, making them appropriate to study transcriptional regulation at URS1 in nutrient abundance as compared to UAS-less *CYC1-lacZ* reporters. Under mitotic growth conditions the URS1 site is repressed by an array of proteins recruited by Ume6p to repress early meiotic genes, but this repression is relieved under meiotic conditions allowing transcription of early meiotic genes (Kupiec et al., 1997). pLGΔ312ΔSS-based plasmids used in the study by Schröder, et al., 2004 have shown that constitutively expressing *HAC1^i* under nitrogen starved conditions represses β-galactosidase levels through URS1 but in the presence of nitrogen no clear conclusion could be implied due to weak expression of these reporter plasmids. However, deletion of *HAC1* derepresses this regulation in nitrogen-rich conditions. This may be because *HAC1^i* splicing occurs at basal levels in vegetatively growing cells and may induce some repression through URS1. In order to demonstrate negative regulation by Hac1^{i}p through URS1, ectopic Hac1^{i}p expression may be necessary in nutrient-rich conditions. Therefore, induced expression of *HAC1^i* would suit the purpose of the experiment to capture the repression mediated by Hac1^{i}p.
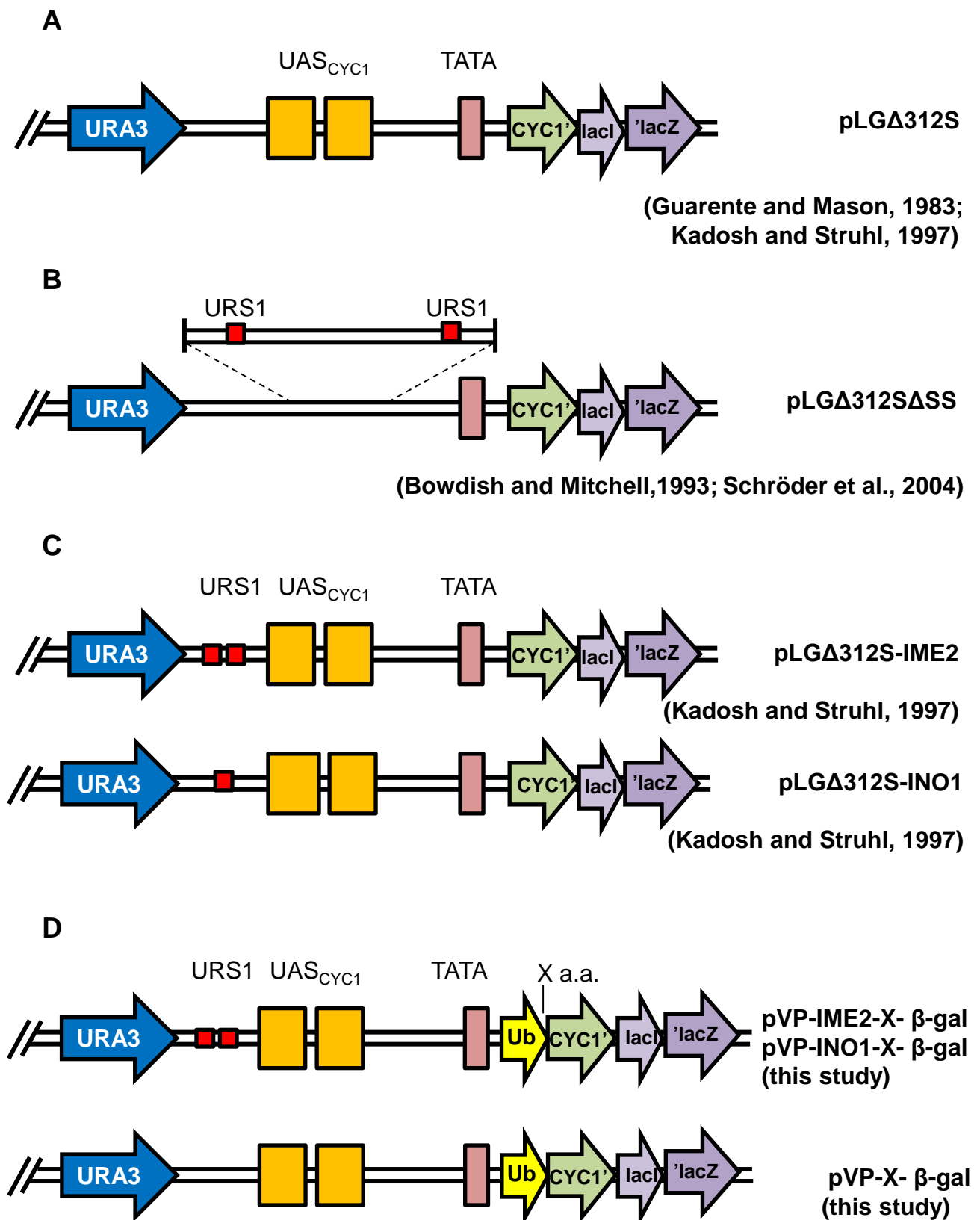
Figure 3.1. *CYC1-lacZ* reporter constructs used to study transcriptional activity. List of *CYC1-lacZ* constructs containing UAS$_{CYC1}$ and URS1 used in this study and various other studies for measuring transcriptional activity mediated via URS1. URS1-upstream repressing site 1;UAS-upstream activating sequence; X a.a.-N-terminal amino acid of *lacI*. CYC1' denotes the one codon fused to *lacI*. The arrows indicate open reading frames and their direction of transcription. C and D have been referred in the text as URS1-*CYC1-lacZ* and URS1-*CYC1*-Ub-X-*lacZ* reporters respectively.

A
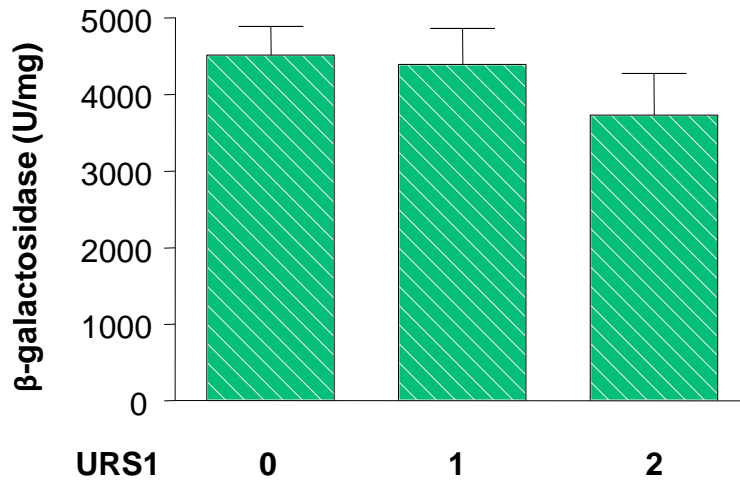
B
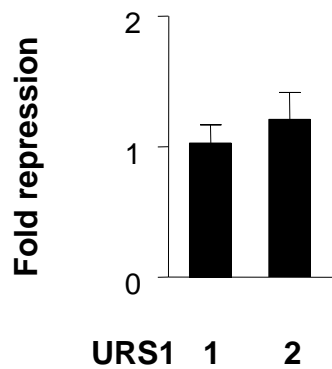
Figure 3.2. Steady state levels of β-galactosidase encoded by URS1-*CYC1-lacZ* containing zero, one and two URS1 sites expressed in vegetative growth medium. (A) WT strains MSY138-17 and MSY 133-34 were transformed with pLGΔ312S, pLGΔ312S-INO1 and pLGΔ312S-IME2 and grown in synthetic acetate medium (PSP2 medium) and harvested at exponential phase to measure β-galactosidase levels. **(B)** The fold repression is defined as the ratio of β-galactosidase expressed from plasmid with zero URS1 sites to one or two URS1 sites. The average and standard error from at least three independent transformants are shown.

3.2 Demonstration of Hac1[i]p-mediated negative regulation of EMGs through URS1

The splicing of *HAC1* mRNA increases in response to the high nitrogen levels and lead to synthesis of Hac1[i]p and activate a basal UPR, while splicing ceases under nitrogen starvation (Schröder, 2000). When Hac1[i]p was overexpressed it had little or no effect on *IME1* mRNA levels but repressed *IME2* levels including other meiotic and non-meiotic genes containing URS1 (Schröder et al., 2000; Schröder et al., 2004). Overexpression of Hac1[i]p represses through URS1 under nitrogen starvation conditions and when *HAC1* was deleted, expression of genes containing URS1 derepressed modestly (~2 fold). However, we wanted to investigate whether Hac1[i]p negatively regulates through URS1 in nutrient rich conditions. The results in **figure 3.2** show that URS1-*CYC1-lacZ* reporters have elevated expression under nitrogen-rich conditions and repressing trend in the presence of URS1, which allows these reporters to study regulation under nitrogen-rich conditions. To investigate the Hac1[i]p -mediated repression on EMGs via URS1 in nitrogen-rich conditions, I decided to use URS1-*CYC1-lacZ* reporters (**Figure 3.1A** and **C**).

In nitrogen-rich conditions a basal UPR is active, which splices *HAC1* mRNA leading to some repression (Bicknell et al., 2007; Kuhn et al., 2001; Schröder et al., 2000). Constitutively expressing spliced form of *HAC1[i]* slows the growth of the cells and is toxic to the cells (Mori et al., 2000). Therefore ectopic expression of *HAC1[i]* from an inducible system addresses the potential problem of repression by Hac1[i]p synthesized from basal UPR activation and toxicity to cells. The expression of Hac1[i]p was induced from pRS423-GRE3-HA-*HAC1[i]*, which contains three glucocorticoid response elements and expression is induced only in the presence of glucocorticoid receptor (pG-N795) (Schena et al., 1991) and steroids. Hac1[i]p is successfully induced under the control of glucocorticoid response elements in the presence of the steroid deoxycorticosterone (DOC) and the rat glucocorticoid receptor expressed constitutively in yeast (**Figure 3.3B**) and (Schröder et al., 2004). In figure 3.3B, the Western blot was carried out on supernatant of Sin3p immunoprecipitation samples and blocking peptide used here competes with Sin3p for binding to anti-Sin3 antibody. Blocking peptide does not affect detection of non-Sin3p bound Hac1[i]p, which is overexpressed here and therefore present in molar excess as compared to Sin3p. The levels of β-galactosidase, when Hac1[i]p was induced by DOC were mostly unchanged in the presence of URS1 elements (**Figure 3.3A**).

The levels of β-galactosidase remain unchanged in the strains containing one or two URS1 sites as compared to no URS1 site in the presence of induced Hac1^{i}p. The repression of *IME2* and *INO1* mRNA levels seen in the Northern blot analysis by overexpression of *HAC1^i* could not be seen with the URS1-*CYC1-lacZ* reporters (Schröder, 2004). The expression of Hac1^{i}p which is induced from inducible plasmid pRS423-GRE3-HA-*HAC1^i* on addition of 50 µM DOC for 1 hour in the presence of glucocorticoid receptor expressed from pG-N795 was checked by Western blot (**Figure 3.3B**) and (Schröder et al., 2004). If the repression on β-galactosidase levels is caused by Hac1^{i}p synthesized from basal UPR activation, the inducible system would not allow any further repression by Hac1^{i}p expression. The other possibility is that the long half-life of the reporter protein β-galactosidase masks any dynamic changes in transcriptional activity caused by inducible expression of *HAC1^i*. In the presence of Hac1^{i}p, any transcriptional repression caused by Hac1^{i}p on URS1-controlled β-galactosidase expression may be masked owing to the longer half-life of β-galactosidase (>30 h). Thus data from **figure 3.2** and **figure 3.3** suggests that an inducible expression of Hac1^{i}p did not repress the β-galactosidase levels possibly due to already present Hac1^{i}p from basal UPR activation and may be due to residual activity of β-galactosidase due to its long half-life, which may hinder the testing of transcriptional regulation under vegetative growth conditions. One problem with β-galactosidase reporter systems is the relatively long half-life, which prevents monitoring of dynamic changes during gene regulation. Background expression due to preexisting reporter molecules present within the cells before the actual experiment cause a low signal-to-noise ratio. Therefore use of destabilized reporter system can give a low background as pre-existing β-galactosidase molecules are rapidly degraded and this can provide a broad dynamic range to the assay. Therefore, to test the possibility that β-galactosidase half-life and therefore residual activity hinders monitoring of transcriptional activity I decided to reduce the half-life of β-galactosidase.

A

β-galactosidase (U/mg) — y-axis ranges from 0 to 8000

Legend: ☐ - DOC, ▨ + DOC

URS1: 0, 1, 2 (pRS423); 0, 1, 2 (pRS423-GRE3-HA-HAC1^i)

B

| DOC (50 µm) | – | – | + | + |
| Blocking peptide | – | + | – | + |

anti-HA

anti-PGK

1 2 3 4
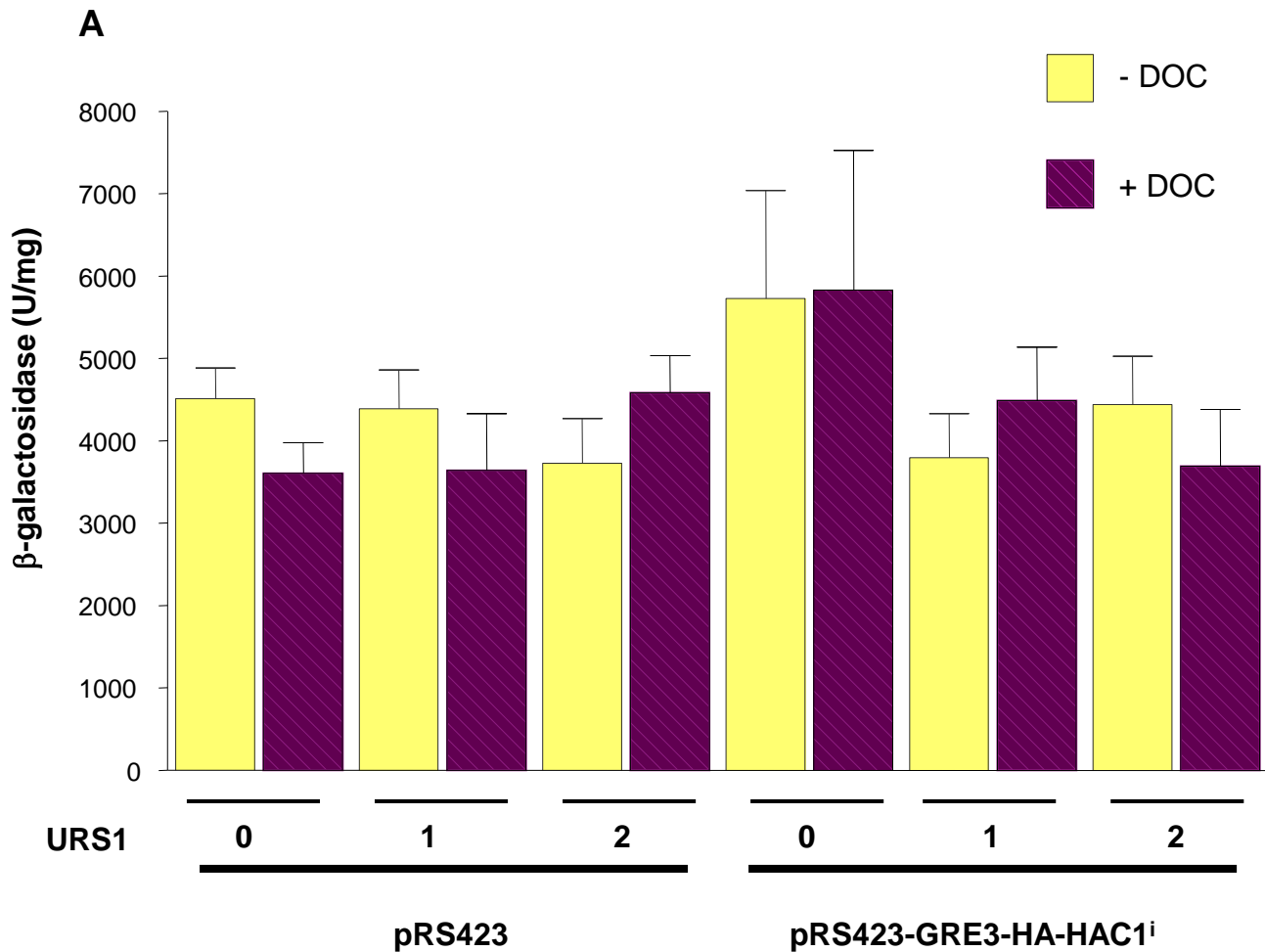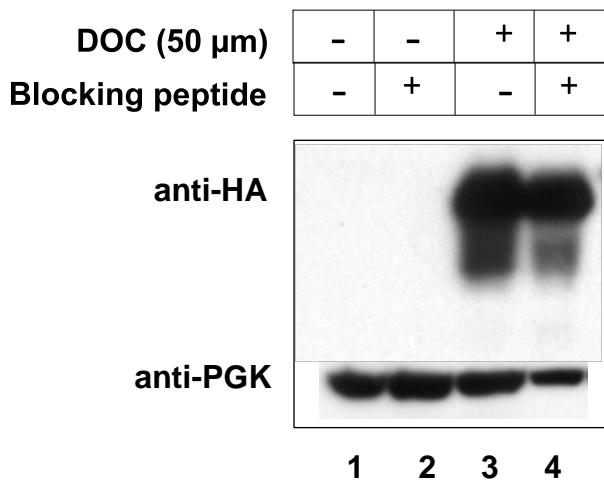
Figure 3.3. Inducible expression of Hac1^{i}p does not repress β-galactosidase driven by URS1 encoded by URS1-*CYC1-lacZ* reporters. **(A)** Expression of URS1-*CYC1-lacZ* in the presence of Hac1^{i}p induced by 50 µM DOC for one h in strains grown in PSP2 medium. The average and standard error from at least three independent transformants are shown. **(B)** HA tagged Hac1^{i}p is induced by DOC for 1 h in lane 3 and 4 as detected by Western blot. Supernatant of the samples used for immunoprecipitation with anti-Sin3 antibody were used here. The blocking peptide in lane 2 and 4 competes with Sin3p for binding to anti-Sin3 antibody. HA tagged Hac1^{i}p was detected by anti-HA antibody and phosphoglycerate kinase (PGK) was detected as loading control.

3.3 Construction of URS1-*CYC1*-Ub-X-*lacZ* reporters

The β-galactosidase with higher half-life may mask the transcriptional activity mediated by URS1. In order to remove the background β-galactosidase rapidly we decided to decrease the half-life of β-galactosidase so that we can use URS1-*CYC1-lacZ* reporters to measure transcriptional repression. The N-terminal amino acid residue can determine the stability of the protein and this pathway is called the N-end rule (Varshavsky, 1997). Features that confer metabolic instability to the protein are called degrons. In eukaryotes, the N-degron consists of three determinants: a destabilizing N-terminal amino acid of the protein substrate, the internal lysine residue which forms the anchor for the ubiquitin chain and the conformationally flexible region in the vicinity of the other determinants required for ubiquitylation and/or degradation (Hu et al., 2006). The destabilizing residues are recognized by N-recognins and the N-end rule substrates are tagged with ubiquitin to allow degradation by the 26S proteosome (Hu et al., 2006). When a chimeric gene encoding the ubiquitin-β-galactosidase fusion protein is expressed in yeast, ubiquitin is cleaved off the nascent polypeptide exposing the amino acid residue present at the ubiquitin-β-galactosidase junction, thereby making it possible to express a β-galactosidase protein with different amino acid residues on its amino-terminus. These β-galactosidase proteins can have a varied half-life from less than 3 min to more than 30 hours depending on the β-galactosidase amino acid residue exposed after cleavage of ubiquitin. Thus, an amino acid residue at the N-terminus of the protein can decide the stability of the protein (Bachmair et al., 1986; Bachmair and Varshavsky, 1989). The metabolic instability of engineered N-end rule substrates is due to degradation signals called degrons, which are recognised by N-recognins (E3 ubiquitin ligases). Decrease in half life of β-galactosidase protein based on N-end rule relies on post-translational removal of the ubiquitin moiety by proteases (Bachmair et al., 1986). Since techniques like Northern Blot and highly sensitive quantitative real time RT-PCR detect all the lacZ mRNA transcripts irrespective of destabilisation of β-galactosidase protein, use of enzymatic detection of β-galactosidase as transcriptional output give more dynamicity to the assay.

The pUB23 and pLGΔ312S series of plasmids were used to construct URS1-*CYC1*-Ub-X-*lacZ* reporters (Bachmair et al., 1986; Bachmair and Varshavsky, 1989; Guarente and Mason, 1983). The Ub-X-*lacZ* reporter plasmids (pUB23) contain the ubiquitin moiety which is fused to β-galactosidase coding region and the amino acid after ubiquitin coding region is changed from methionine to a destabilizing residue. This allows the first amino acid of the β-galactosidase coding region to be changed to any amino acid substituting methionine. Expression of Ub-β-gal fusion proteins is driven by the inducible *GAL1,10* promoter [(Bachmair and Varshavsky, 1989) and (**Figure 3.4**)]. In order to use these reporters to monitor transcriptional activity through URS1, the *GAL1,10* promoter has to be replaced by a constitutive promoter carrying URS1 elements. The reporter plasmids with URS1 containing promoter sequences cloned upstream of UAS$_{CYC1}$ were used to replace the *GAL1,10* promoter (**Figure 3.1** and **Figure 3.4**). The sequence encoding ubiquitin moiety with different amino acid residue was amplified by PCR from pUB23M, pUB23K, pUB23L and pUB23R plasmids (Bachmair and Varshavsky, 1989) using primers A1 and A2. The B1 and B2 primers were used to amplify a fragment from pLGΔ312S-IME2 or pLGΔ312S-INO1 or pLGΔ312S that would amplify a region spanning the *URA3* region, URS1 sequence and the *lacZ* region. The primers A2 and B2 were designed to have an overhang complementary to each other to get a fusion PCR product as shown in **Figure 3.4**. Primers A1 and B1 were designed to amplify fragments that would contain *Nar*I and *Psp*OMI sites respectively, so that the resulting fusion PCR product could be digested using these restriction enzymes and cloned into pLGΔ312S-IME2. As shown in **Figure 3.4** this would result in a PCR product having the sequence *URA3*-URS1 (2, 1 or 0)-P'*CYC1*-ubiquitin-X amino acid-*lacI*-*lacZ*. The cloning of the fusion product into pLGΔ312S plasmids using restriction enzyme *Nar*I and *Psp*OMI only yielded pVP-IME2-M-β-gal and pVP-IME2-L-β-gal. One reason was that digestion of vector with *Nar*I and *Psp*OMI was inefficient. The other reason could be inefficient digestion of PCR product. Therefore, the fusion products were first cloned into pSTBlue-1 blunt vector. Cloning of fusion products released from pSTBlue-1 vector by digestion with *Nar*I and *Psp*OMI into pLGΔ312S was not successful either. Therefore I resorted to gap repair method of homologous recombination in yeast, which does not depend on requirement of sticky ends of DNA for ligation but only requires homologous sequences in the vector and insert (Ma et al., 1987). **Figure 3.5** shows the strategy used to clone the fusion products by the

gap repair method. The fusion product released with *EcoR*I from pSTBlue-1 Blunt vector and *Bam*HI-digested pLGΔ312S plasmid fragment have homologous regions at *URA3* and *lacI*. Co-transformation of these fragments into *S. cerevisiae* allows homologous recombination to yield the final plasmid as shown in **figure 3.5**. Formation of functional *URA*3 metabolic marker in the plasmid constructed by homologous recombination allowed selection in a *ura3* strain on uracil dropout plates. Plasmids were extracted from yeast and transformed into *E. coli*. The reporters with isoleucine and glutamine were obtained by site-directed mutagenesis of the constructed plasmids (**Table 3.1**). These reporters are now referred to as URS1-*CYC1*-Ub-X-*lacZ* reporters which contain 0, 1 (from *INO1*) or 2 URS1 (from *IME2*) and the N-terminal amino acid of β-galactosidase exposed is denoted by 'X', which is methionine, lysine, leucine, arginine, isoleucine or glutamine. The individual plasmids as shown in **figure 3.1** are designated as pVP-IME2-X- β-gal containing two URS1 sites, pVP-INO1-X- β-gal containing one URS site and pVP-X- β-gal containing no URS1 site. As a result the destabilized URS1-*CYC1*-Ub-X-*lacZ* reporters would encode β-galactosidase with lower half lives that may be useful to achieve dynamic and tighter monitoring of the transcriptional regulation by Hac1[i]p.
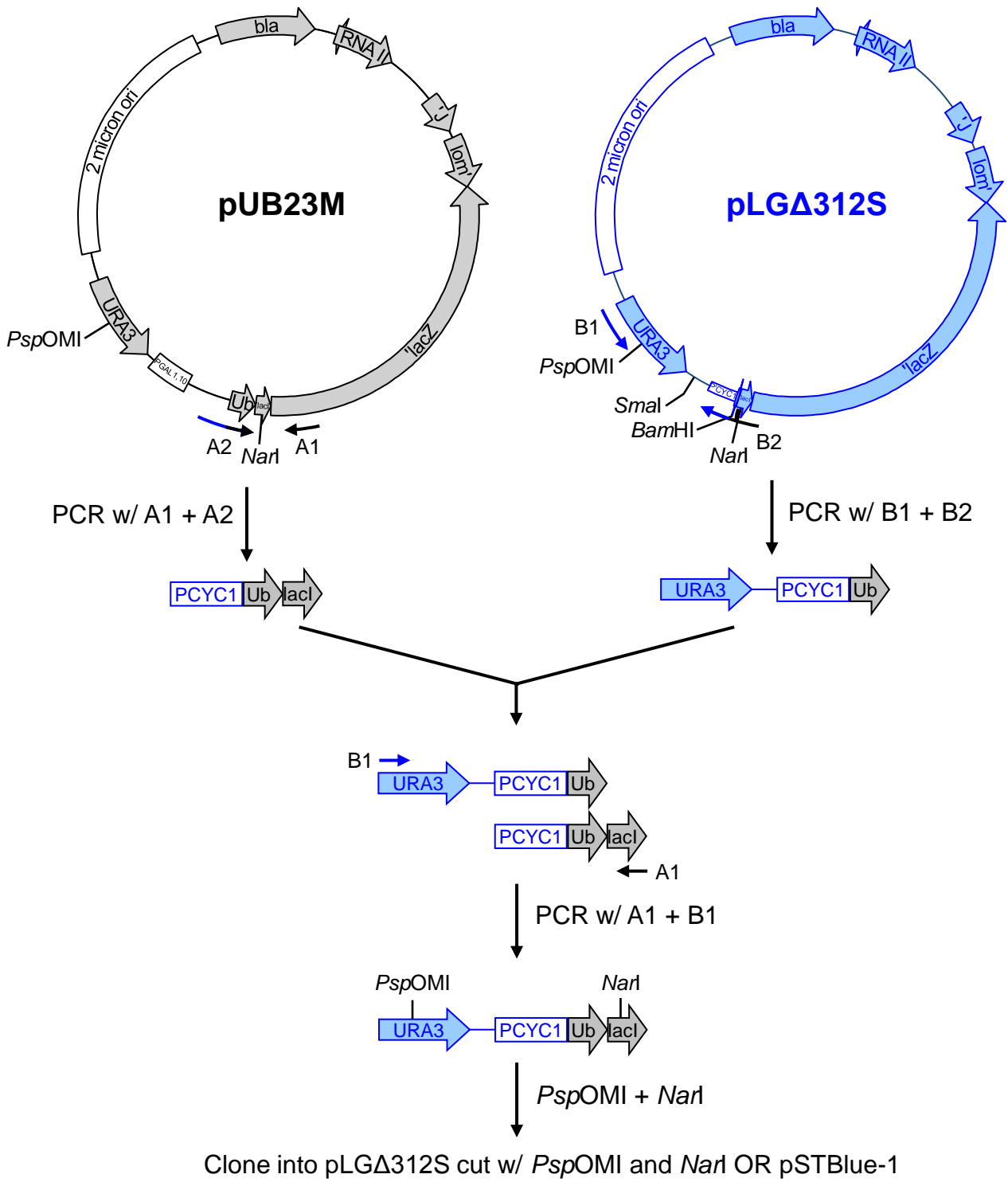
Figure 3.4. Cloning strategy for URS1-*CYC1*-Ub-X-*lacZ* reporter plasmids. The fusion product was amplified using A1 and B1 primers and was cloned into pLGΔ312S or pST-Blue1 vector.
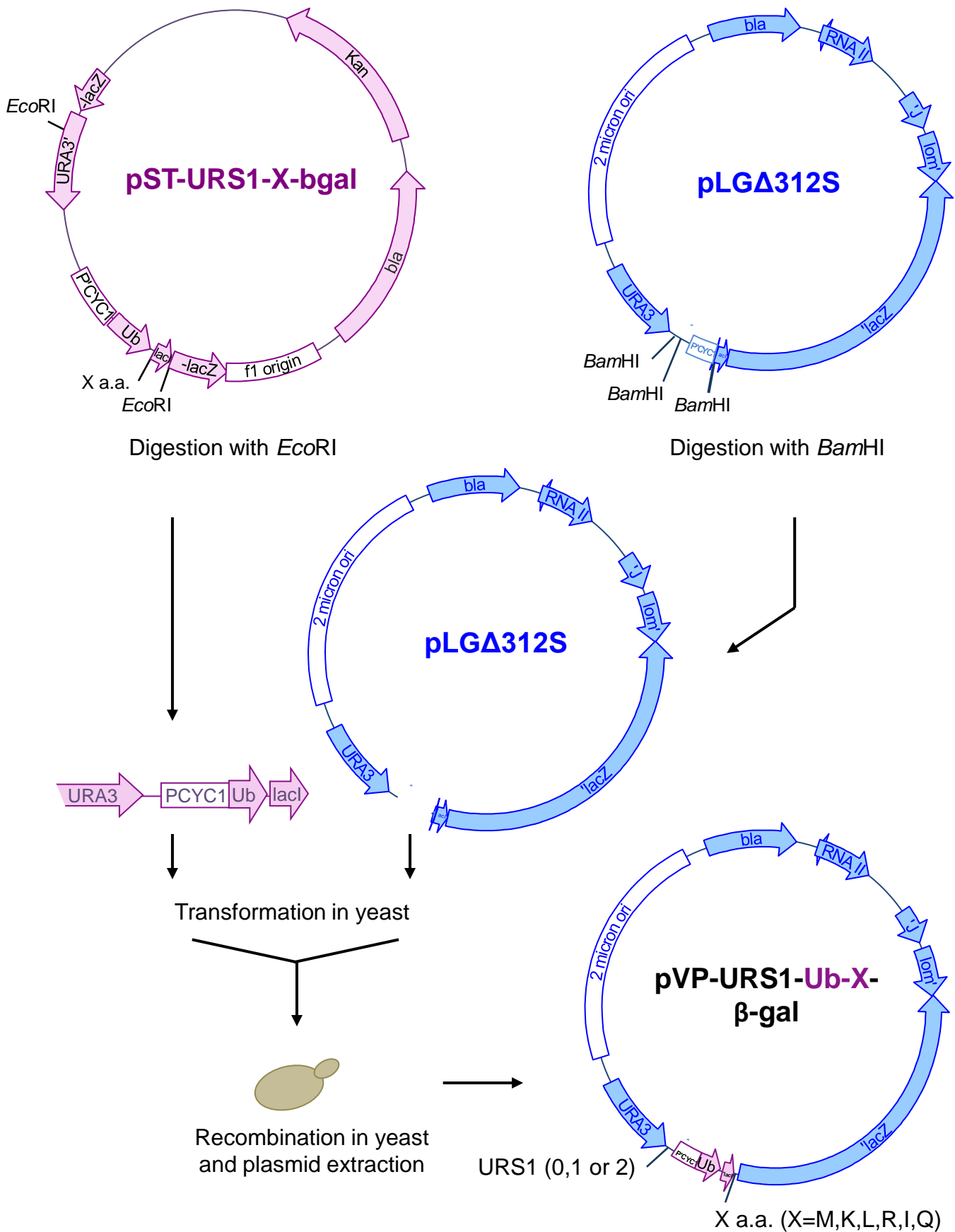
Figure 3.5. Cloning strategy for URS1-*CYC1*-Ub-X-*lacZ* reporter plasmids using gap repair in yeast. The fusion product released with *Eco*RI from pST-Blue1 Blunt vector and the *Bam*HI-digested pLGΔ312S plasmid are transformed into *S. cerevisiae* to derive constructs by homologous recombination.

Table 3.1. List of cloning strategies for the construction of destabilized URS1-*CYC1*-Ub-X-*lacZ* reporters.

| Sr. No.	Plasmid	Method
1.	pVP-IME2-M-β-gal & pVP-IME2-L-β-gal	Fusion PCR and cloning into pLGΔ312S-IME2 at *Nar*I and *Psp*OMI
2.	pVP-IME2-K-β-gal pVP-IME2-R-β-gal pVP-INO1-M-β-gal pVP-INO1-K-β-gal pVP-INO1-L-β-gal pVP-INO1-R-β-gal pVP-M-β-gal pVP-K-β-gal pVP-L-β-gal pVP-R-β-gal	Fusion PCR, cloning into pSTBlue-1 vector, Gap repair
3.	pVP-IME2-I-β-gal pVP-IME2-Q-β-gal	Site-directed mutagenesis of pVP-IME2-R-β-gal using I-β-gal and Q-β-gal oligonucleotides containing silent restriction site *Bau*I
	pVP-INO1-I-β-gal pVP-INO1-Q-β-gal	Site-directed mutagenesis of pVP-INO1-R-β-gal using I-β-gal and Q-β-gal oligonucleotides containing silent restriction site *Bau*I
	pVP-I-β-gal pVP-Q-β-gal	Site-directed mutagenesis of pVP-M-β-gal using I-β-gal and Q-β-gal oligonucleotides containing silent restriction site *Bau*I

The URS1-*CYC1*-Ub-X-*lacZ* reporters were digested with *Eco*RV and *Bam*HI to confirm the predicted fragments. Restriction digestion analysis (**Figure 3.6A-F**) showed expected fragments. The selected clones were checked for the N-terminal amino acid of β-galactosidase in each construct by sequencing. **Figure 3.6G** shows the sequences of the constructed plasmids compared with the original plasmid used

for plasmid construction. URS1-*CYC1*-Ub-X-*lacZ* reporters show different amino acid residues at the N-terminus. The silent restriction site *Bau*I introduced in isoleucine and glutamine plasmid constructs by site directed mutagenesis produced an extra band and this was checked by restriction enzyme digestion with *Bau*I (**Figure 3.6E-F**) and then confirmed by sequencing (**Figure 3.6G**). The silent restriction site, *Bau*I can be seen in the sequences of pVP-I-β-gal and pVP-Q-β-gal plasmids.
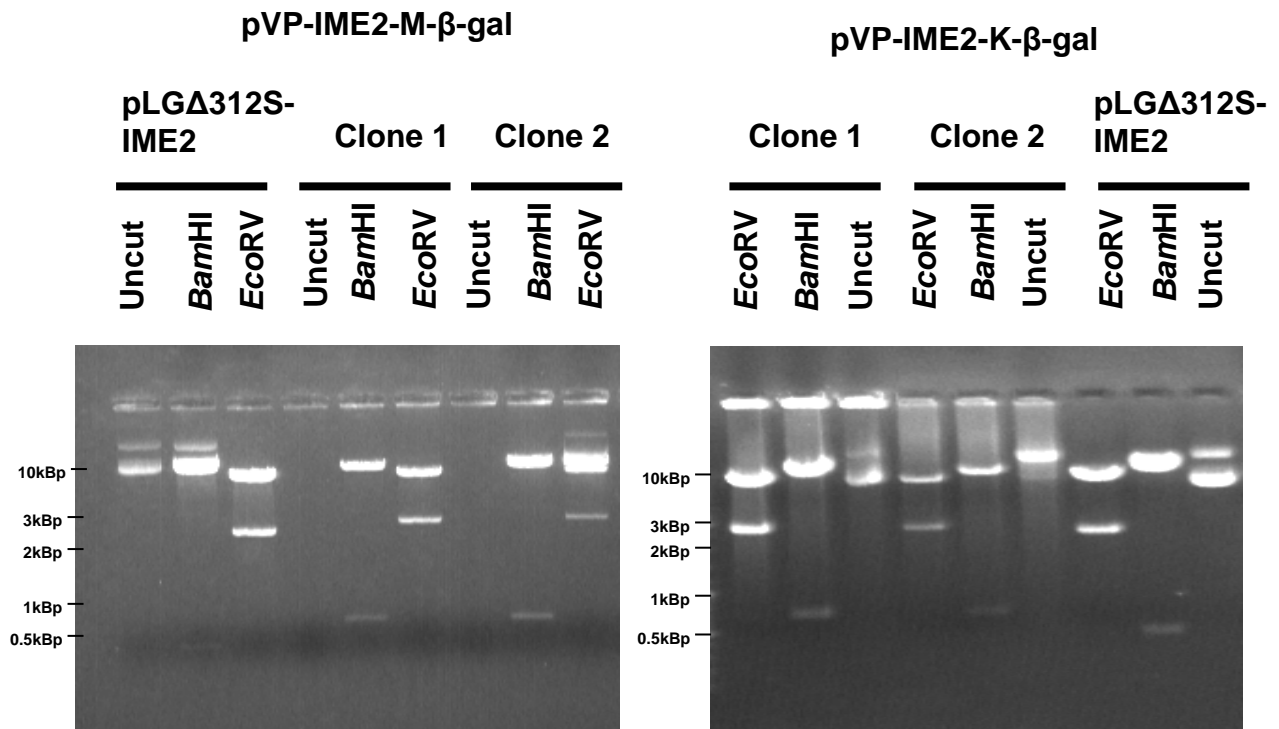
Expected fragment sizes

Plasmid	Enzyme	Predicted fragments
pLGΔ312S-IME2	*Bam*HI	9664 bp + 445 bp
	*Eco*RV	7785 bp + 2370
pVP-IME2-M-β-gal **pVP-IME2-K-β-gal**	*Bam*HI	9664 bp + 673 bp
	*Eco*RV	7785 bp + 2598

Figure 3.6A. Confirmation of pVP-IME2-M-β-gal and pVP-IME2-K-β-gal reporter plasmids by restriction digestion analysis. The plasmids digested with *Bam*HI and *Eco*RV showing the expected fragment sizes were confirmed by sequencing.

pVP-IME2-L-β-gal
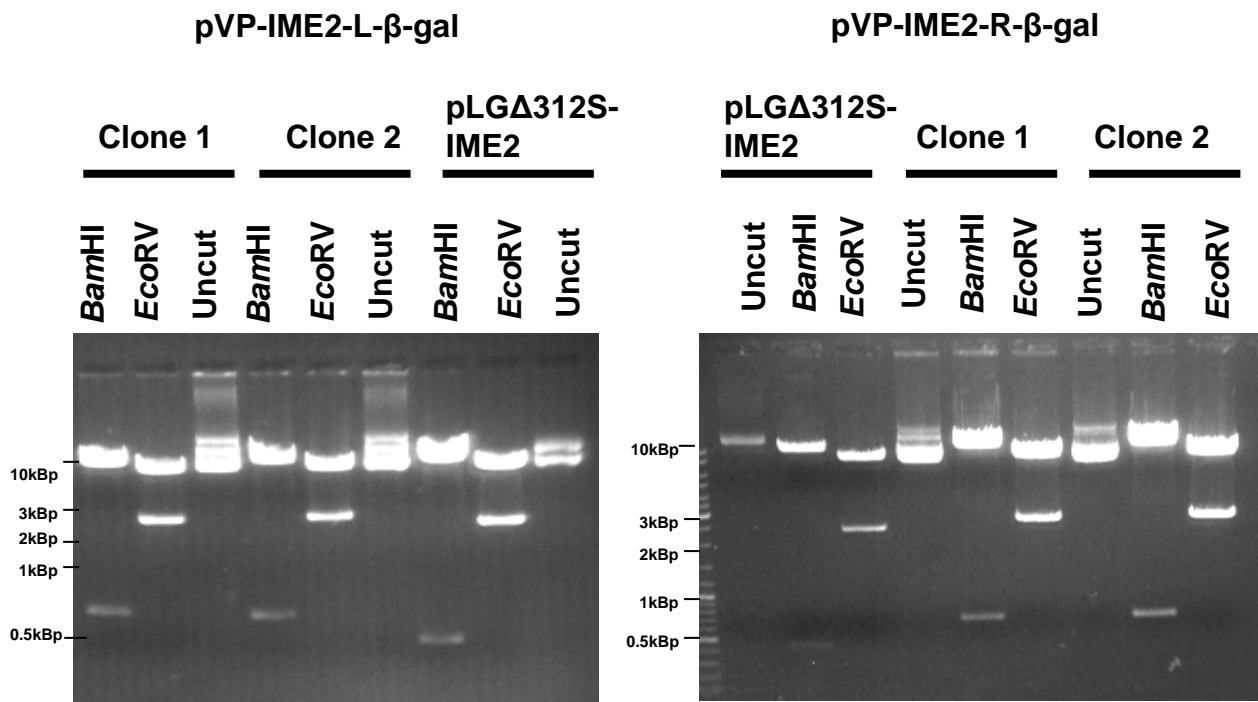
pVP-IME2-R-β-gal

Expected fragment sizes

Plasmid	Enzyme	Predicted fragments
pLGΔ312S-IME2	*Bam*HI	9664 bp + 445 bp
	*Eco*RV	7785 bp + 2370
pVP-IME2-L-β-gal **pVP-IME2-R-β-gal**	*Bam*HI	9664 bp + 673 bp
	*Eco*RV	7785 bp + 2598

Figure 3.6B. **Confirmation of pVP-IME2-L-β-gal and pVP-IME2-R-β-gal reporter plasmids.** The plasmids digested with *Bam*HI and *Eco*RV showing the expected fragment sizes were confirmed by sequencing.

Figure 3.6C. **Confirmation of pVP-INO1-M-β-gal, pVP-INO1-K-β-gal, pVP-INO1-L-β-gal and pVP-INO1-R-β-gal reporter plasmids.** The plasmids digested with *Bam*HI and *Eco*RV showing the expected fragment sizes were confirmed by sequencing.

Expected fragment sizes

Plasmid	Enzyme	Predicted fragments
pLGΔ312S-INO1	*Bam*HI	9664 bp + 448 bp
	*Eco*RV	7785 bp + 2327
pVP-INO1-M- β-gal	*Bam*HI	9664 bp + 676 bp
pVP-INO1-K- β-gal	*Eco*RV	7785 bp + 2555 bp
pVP-INO1-L- β-gal		
pVP-INO1-R- β-gal		

Figure 3.6D. **Confirmation of pVP-M-β-gal, pVP-K-β-gal, pVP-L-β-gal and pVP-R-β-gal reporter plasmids.** The plasmids digested with *Bam*HI and *Eco*RV showing the expected fragment sizes were confirmed by sequencing.

Expected fragment sizes

Plasmid	Enzyme	Predicted fragments
pLGΔ312S	*Bam*HI	10063 bp
	*Eco*RV	7785 bp + 2278 bp
pVP-M- β-gal	*Bam*HI	10291 bp
pVP-K- β-gal	*Eco*RV	7785 bp + 2506 bp
pVP-L- β-gal		
pVP-R- β-gal		
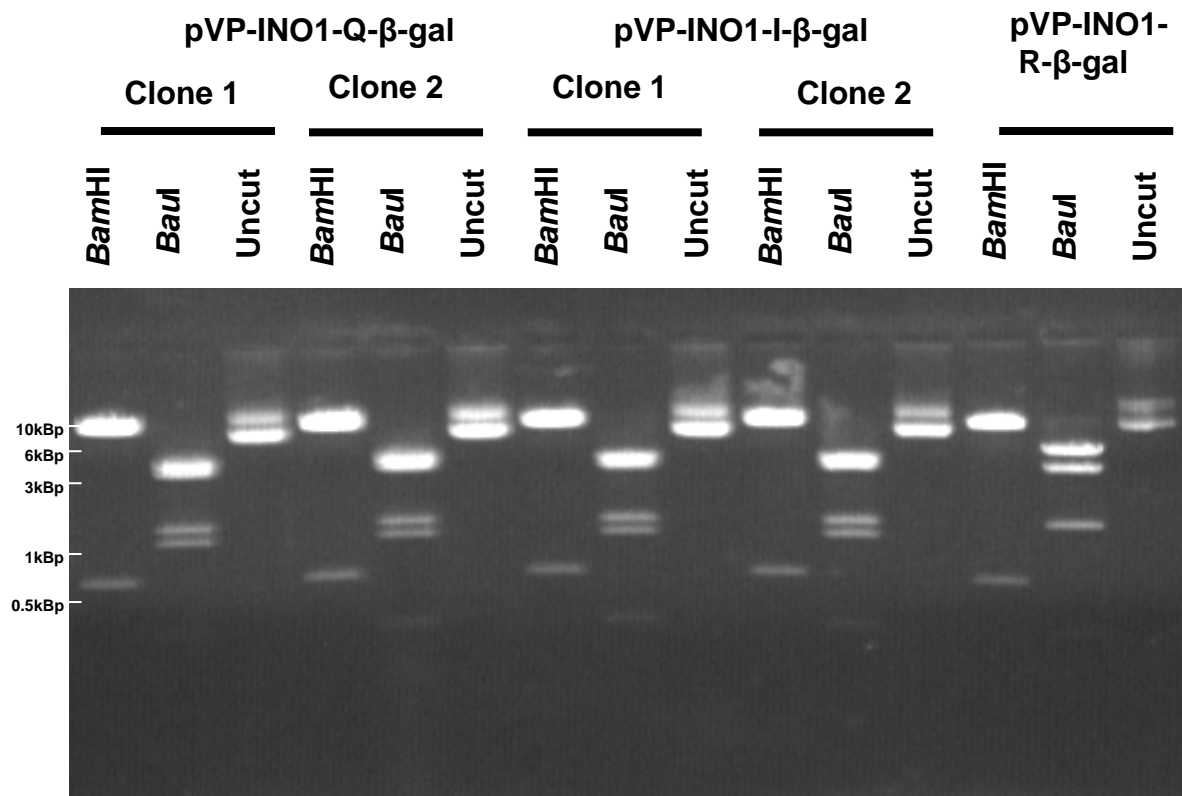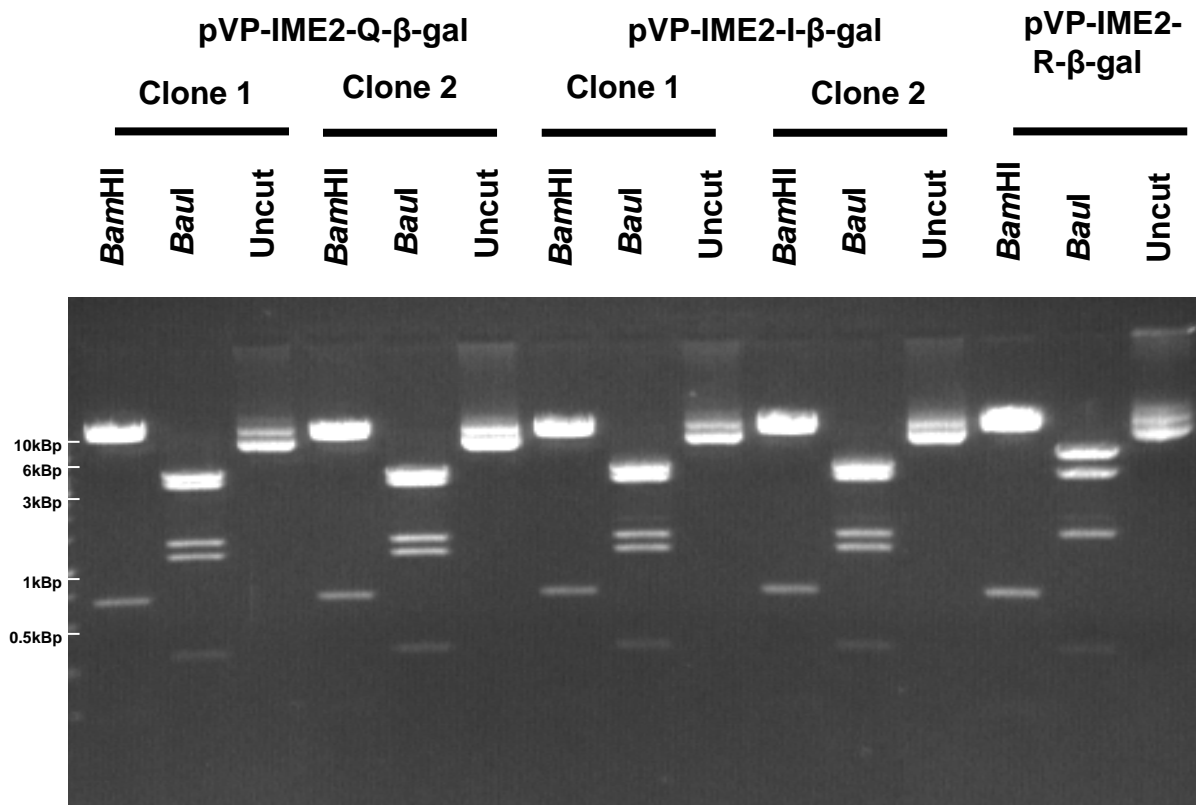
Figure 3.6E. Confirmation of pVP-IME2-Q-β-gal, pVP-IME2-I-β-gal, pVP-INO1-Q-β-gal and pVP-INO1-I-β-gal reporter plasmids. The plasmids digested with *Bam*HI and *Eco*RV showing the expected fragment sizes were confirmed by sequencing.
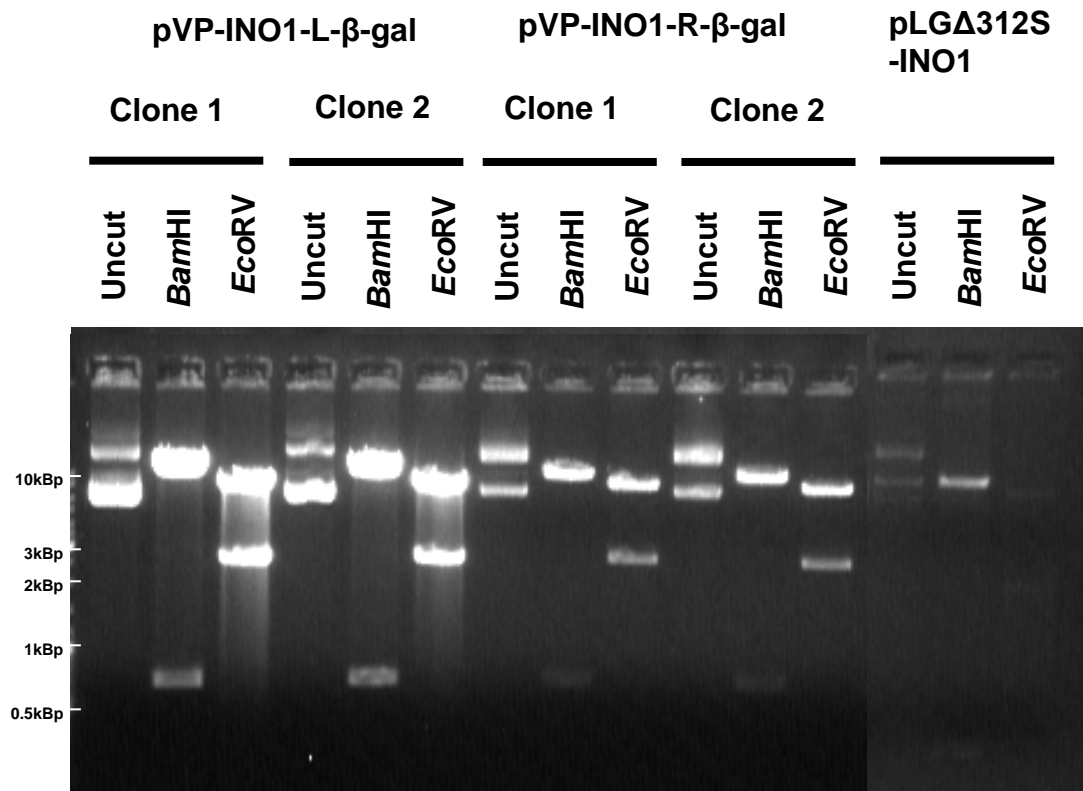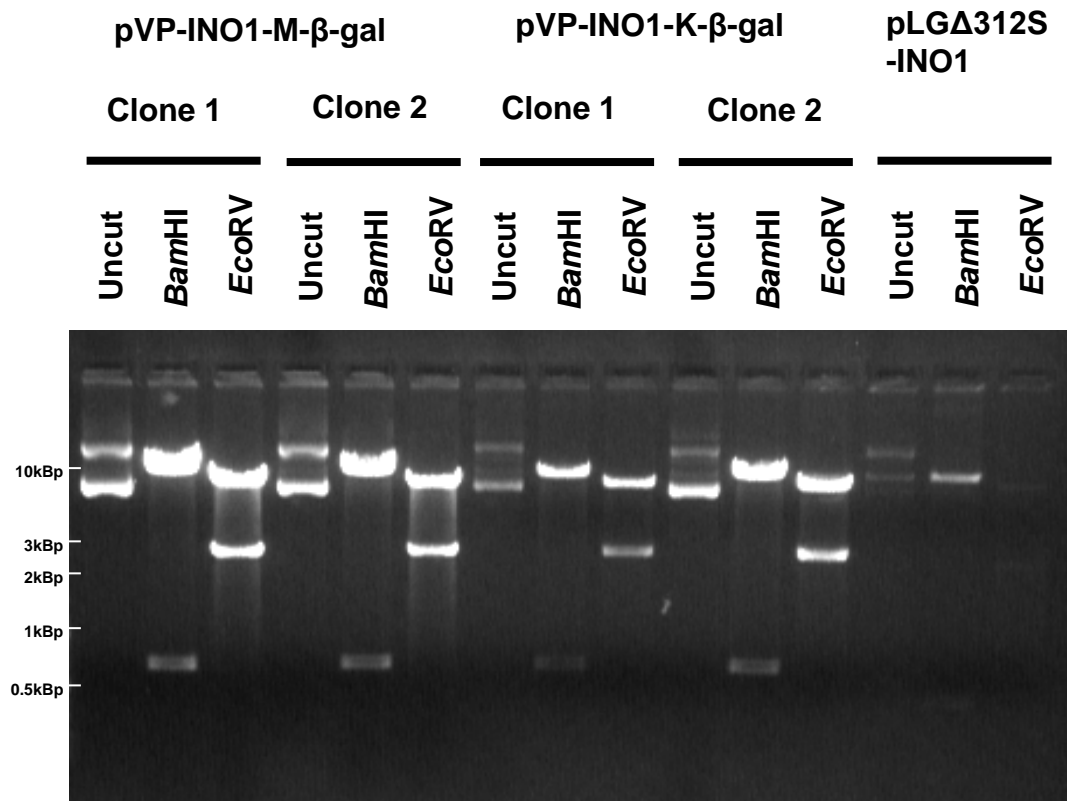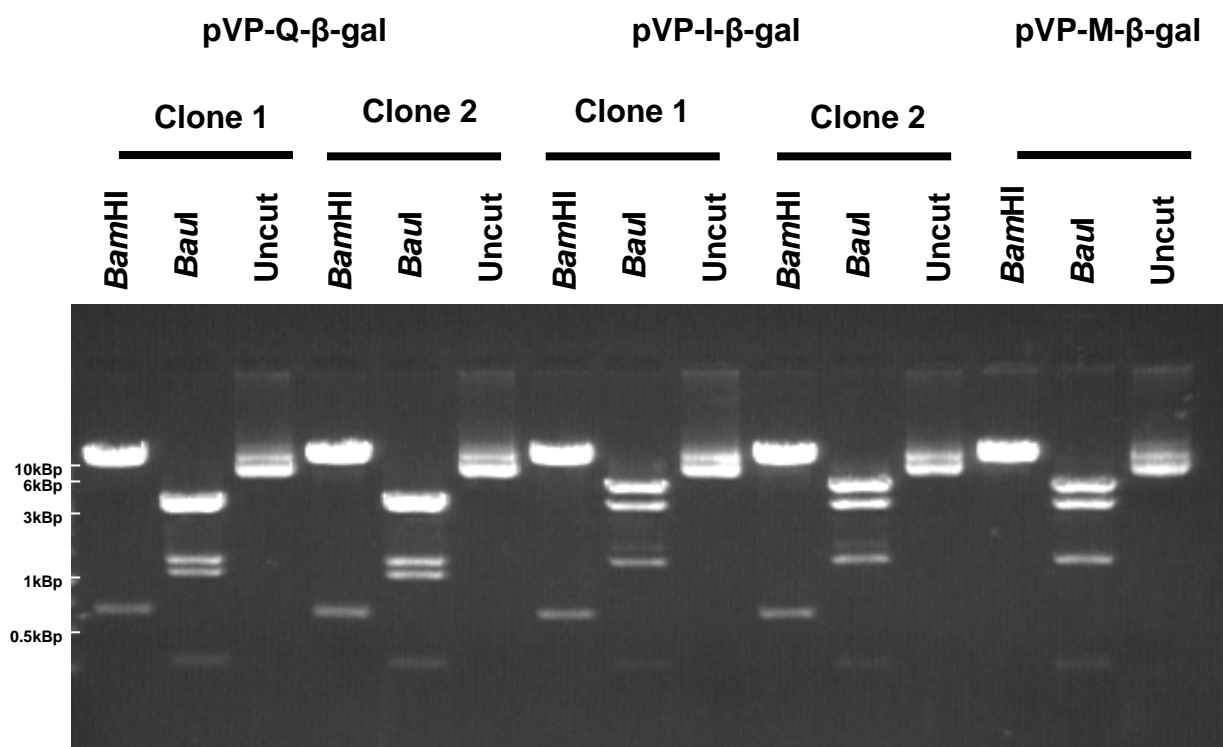
Expected fragment sizes

Plasmid	Enzyme	Predicted fragments
pVP-IME2-R-β-gal	*Bam*HI	9664bp + 673bp
	*Bau*I	5250bp + 3442bp + 1384bp + 307bp
pVP-IME2-I-β-gal	*Bam*HI	9664bp + 673bp
pVP-IME2-Q-β-gal	*Bau*I	4092bp + 3442bp + 1384bp + 1158bp + 307bp
pVP-INO1-R-β-gal	*Bam*HI	9664bp + 676bp
	*Bau*I	5207bp + 3442bp + 1384bp + 307bp
pVP-INO1-I-β-gal	*Bam*HI	9664bp + 676bp
pVP-INO1-Q-β-gal	*Bau*I	4049bp + 3442bp + 1384bp + 1158bp + 307bp
pVP-M-β-gal	*Bam*HI	10337bp
	*Bau*I	5158bp + 3442bp + 1384bp + 307bp
pVP-I-β-gal	*Bam*HI	9664bp + 673bp
pVP-Q-β-gal	*Bau*I	4000bp + 3442bp + 1384bp + 1158bp + 307bp

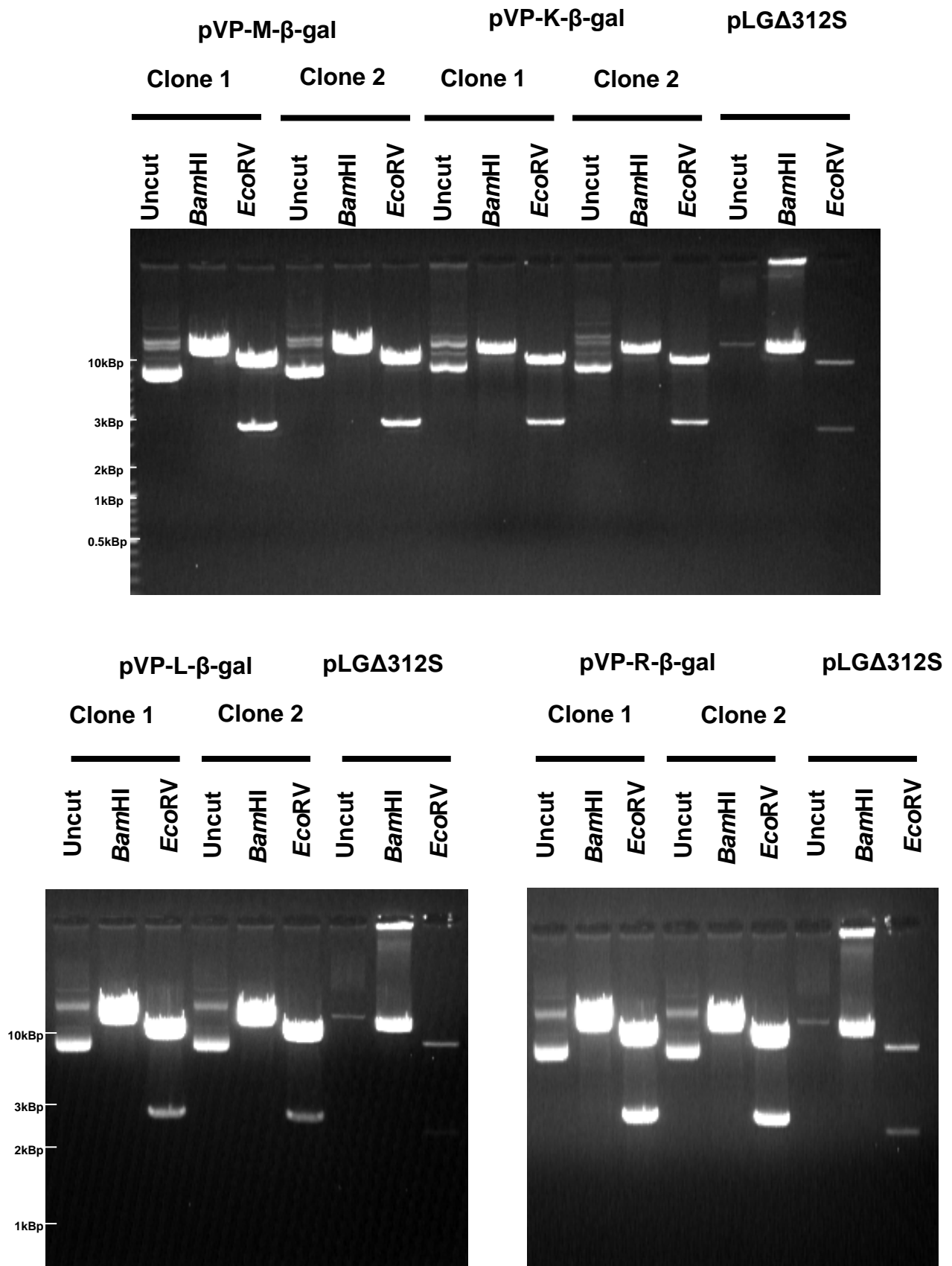**Figure 3.6F. Confirmation of pVP-Q-β-gal and pVP-I-β-gal reporter plasmids.** The plasmids digested with *Bam*HI and *Eco*RV showing the expected fragment sizes were confirmed by sequencing.
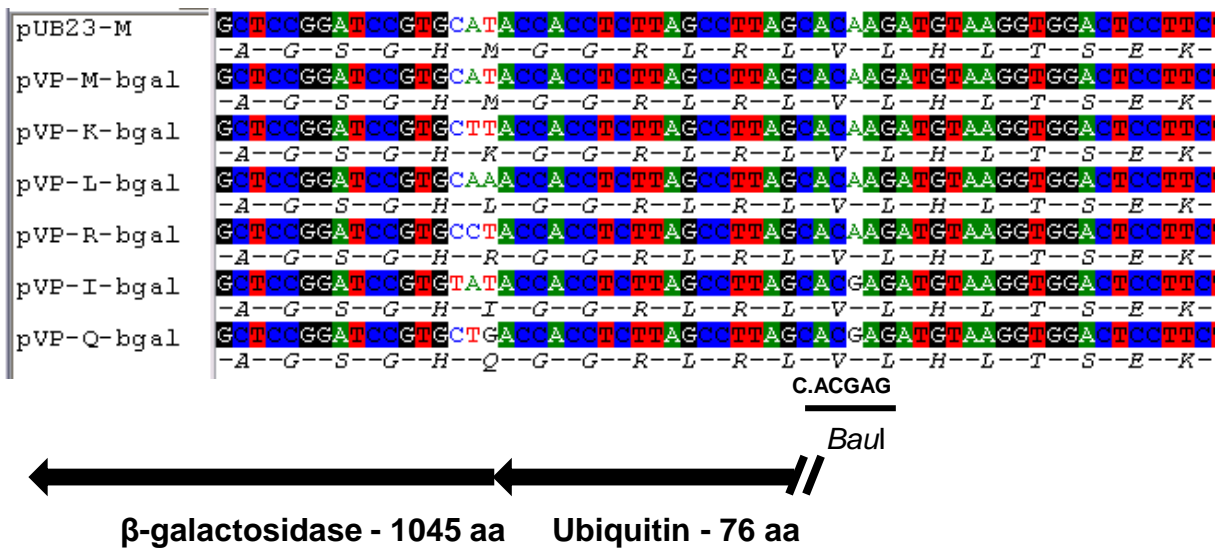
Figure 3.6G. Comparison of *lacZ* N-terminal amino acid residues of URS1-*CYC1*-Ub-X-*lacZ* reporter plasmids. URS1-*CYC1*-Ub-X-*lacZ* reporter plasmids were sequenced and confirmed for the N-terminal amino acid by comparing it to the original plasmids; pUB23-M and pLGΔ312S. pVP-I-β-gal and pVP-Q-β-gal plasmid sequences with *Bau*I silent restriction site introduced by site-directed mutagenesis. DNA bases are colour coded and amino acids are black colour.

3.4 Validation of URS1-*CYC1*-Ub-X-*lacZ* reporters

The newly constructed reporters (now called URS1-*CYC1*-Ub-X-*lacZ* reporter) express chimeric ubiquitin-β-galactosidase protein, which is designed to have a decreased half-life due to destabilizing amino acid residues at the N-terminal end of the β-galactosidase. Expression of β-galactosidase from URS1-*CYC1*-Ub-X-*lacZ* reporter is driven by the *CYC1* promoter and is expected to be mitotically repressed through URS1. β-Galactosidase with decreased half-life are expected to increase the dynamic range of the assay and validate the use of these reporters to monitor the transcriptional repression via URS1. To test whether the half-lives of destabilized β-galactosidase has been decreased and validate the mitotic repression in newly constructed reporter plasmids, we measured the steady state levels of β-galactosidase in wild type strains. The URS1-*CYC1*-Ub-X-*lacZ* reporter plasmids were transformed into a wild type strain and grown in synthetic acetate (PSP2) medium, harvested in the exponential growth phase and frozen at -20$^{\mathrm{o}}$C before using them for the β-galactosidase assays. The decreased steady state levels of the destabilised β-galactosidase protein due to decreased half lives can be seen in **Figure 3.7**. In the strains containing the plasmid with 0 URS1 sites, the β-galactosidase levels have decreased ~five fold with leucine and arginine and ~15 fold with glutamine at N-terminal amino acid as compared to the methionine residue at the N-terminus. The β-galactosidase levels exposing destabilising N-terminal amino acid residues (Q, L and R) have decreased steady state levels reflecting the lower half-life as compared to β-galactosidase with methionine at the N-terminal end (compare zero URS1 sites). The β-galactosidase levels for isoleucine were very low and so were omitted in the later experiments. On comparing β-galactosidase levels exposing methionine residues without URS1 sites, there was ~three fold repression with URS1 (compare zero URS1 to one and two URS1 with methionine residues). There was ~1.5-2.5 fold repression with leucine and arginine amino acids containing one and two URS1 as compared to zero URS1 (compare zero to one and two URS1 for leucine and arginine). There was no remarkable increase in repression with an increase in the number of URS1 elements with methionine, leucine and arginine residues (compare one and two URS1).

The steady state levels have decreased when chimeric proteins start with destabilising N-terminal amino acid residues. But surprisingly the presence of

ubiquitin moiety in the chimeric β-galactosidase led to repression in levels of β-galactosidase exposing methionine residues (**Figure 3.7**) when compared to β-galactosidase levels in **figure 3.2**. De-ubiquitination of the nascent ubiquitin-β-galactosidase chimera was not affected by the type of amino acid at the ubiquitin-β-galactosidase junction (Bachmair et al., 1986). Same study also showed that the half life of the ubiquitin-Met-β-galactosidase and control β-galactosidase, which was not fused to ubiquitin were comparable. This indicates that fusing ubiquitin to β-galactosidase N-terminal end does not affect half life and therefore steady state levels. However the variation in degradation of β-galactosidase encoded from slightly different URS1-*CYC1*-Ub-*lacZ* reporters due ubiquitin moiety cannot be excluded completely. It should be noted that while the repression in ubiquitin-Met-β-galactosidase was reproducible, the magnitude of this repression was variable. This is possibly caused due to protease susceptibility of ubiquitin-Met-β-galactosidase. However, quantitatively more reproducible data was achieved by addition of protease inhibitors to the extraction buffer. This is evident in the subsequent experiments, where mitotic repression is reproducible and not over 1.5 fold (**Figure 3.8** and **3.9**).

The β-galactosidase levels are repressed in the presence of URS1, which corroborates that the early meiotic gene promoters containing URS1 are maintained in a repressed state under mitotic growth conditions and validating the assay system. We selected the destabilised β-galactosidase reporters with leucine and arginine as the N-terminal amino acid for further experiments as these constructs show lowered steady state levels and repression in the presence of URS1.

A
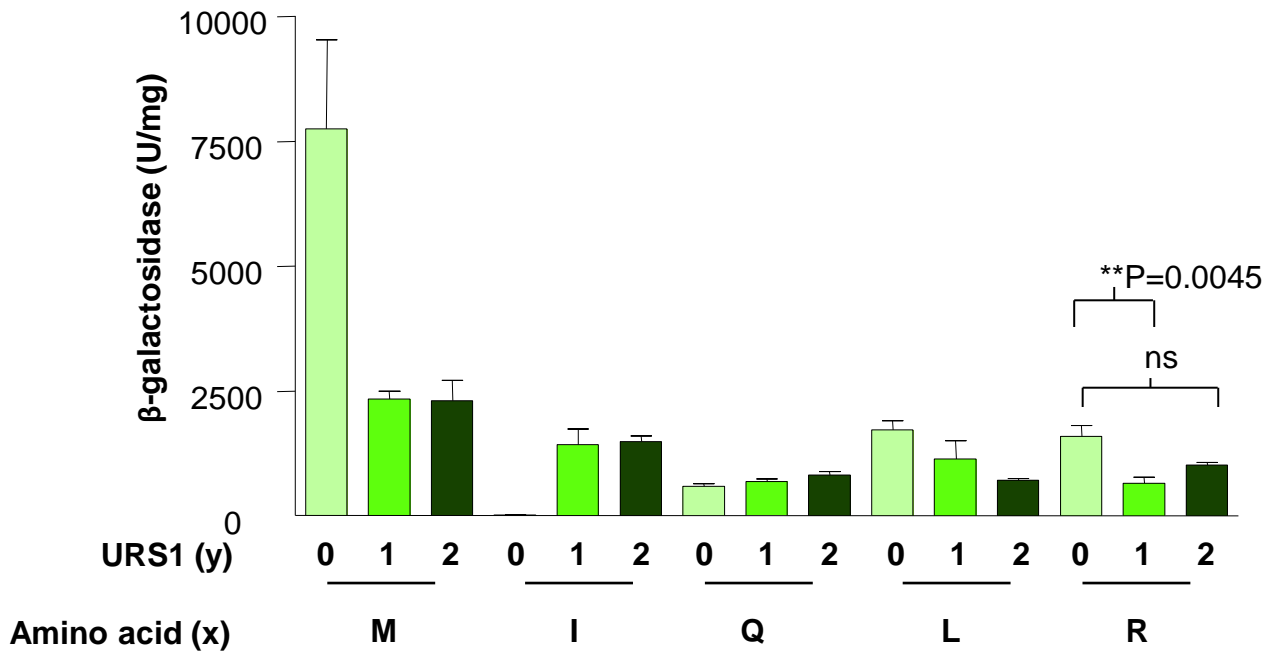
B
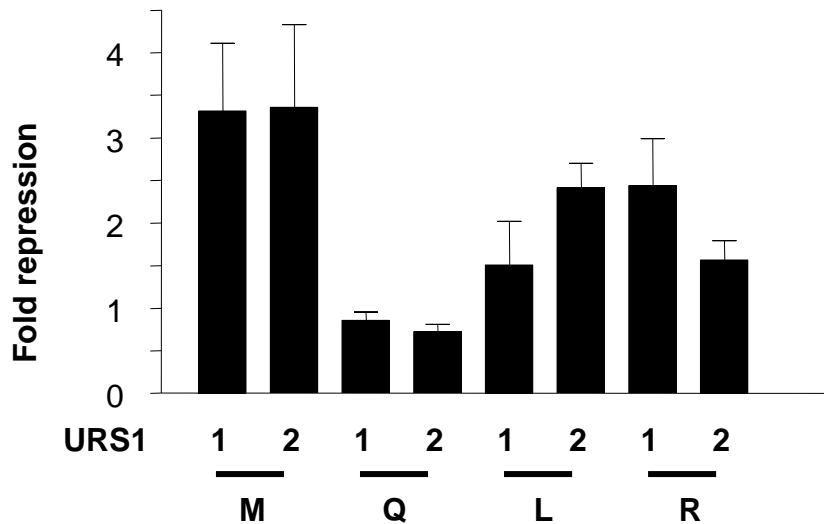
Figure 3.7. Decreased steady state levels of β-galactosidase expressed by URS1-*CYC1*-Ub-X-*lacZ* reporters and repression by URS1 in vegetative growth conditions. Wild type strain (MSY 134-36) strain was transformed with the reporters plasmids and grown to exponential phase and used for the assay. The average and standard error from at least three independent transformants are shown. (**B**) Fold repression is defined here as the ratio of β-galactosidase expressed from a plasmid without URS1 sites to β-galactosidase expressed from a plasmid with one or two URS1 sites.

3.5 Discussion

In order to study the transcriptional repression by Hac1^{i}p at URS1, I first looked at the expression of URS1-*CYC1-lacZ* reporters in nitrogen-rich conditions. Kadosh and Struhl, 1997 have demonstrated mitotic repression on URS1 with URS1-*CYC1-lacZ* reporters based plasmids. Expression of β-galactosidase from *CYC1-lacZ* reporters showed robust expression (**figure 3.2**) as compared to UAS-less reporters (Schröder et al., 2004). Since URS1 is a mitotically repressed site, the level of β-galactosidase containing URS1 under mitotic growth conditions should be lowered. When plasmids containing two URS1 sites were compared to plasmids containing no URS1 site, the repression in β-galactosidase levels directed by URS1 was not remarkable, but there was a repressing trend (**Figure 3.2**). This indicates that URS1 sites in the *CYC1* promoter do not show robust mitotic repression. Induced expression of Hac1^{i}p didn't cause any further repression possibly due to long half-life of β-galactosidase (**Figure 3.3**). Therefore, β-galactosidase was destabilized using N-end rule. As a result, URS1-*CYC1*-Ub-X-*lacZ* reporters were created and steady state levels of β-galactosidase were decreased due to mitotic repression at URS1 (**figure 3.7**).

3.6 Demonstration of Hac1[i]p-mediated negative regulation of EMGs through URS1 using URS1-*CYC1*-Ub-X-*lacZ* reporters

In order to circumvent the potential problem caused by the long half-life of β-galactosidase (>30 h) and masking of transcriptional repression mediated by URS1, we used the destabilised URS1-*CYC1*-Ub-X-*lacZ* reporters. The leucine and arginine amino acid residues at the N-terminal end of the *lacZ* coding region decreased the half-life of β-galactosidase to three min and two min, respectively [(Bachmair and Varshavsky, 1989; Balzi et al., 1990; Gonda et al., 1989) and **Figure 3.7**]. The levels of β-galactosidase were also decreased in the presence of URS1 sites depicting the repression under mitotic growth conditions (**Figure 3.7**). I employed URS1-*CYC1*-Ub-X-*lacZ* reporters encoding β-galactosidase with decreased half-lives to test whether Hac1[i]p represses through URS1 under nitrogen-rich conditions. In order to do this Hac1[i]p was constitutively expressed from pRS314-*HAC1[i]* driven by its endogenous promoter (Schröder et al., 2004). I chose plasmid constructs with methionine, leucine and arginine at the ubiquitin-β-galactosidase junction to drive the expression of β-galactosidase from URS1 sites. A WT strain was co-transformed with URS1-*CYC1*-Ub-X-*lacZ* reporter (either containing zero or two URS1 sites) and pRS314-*HAC1[i]*. Plasmid pRS314 was transformed as a vector control. The strains carrying the combinations of the plasmids were grown in vegetative growth medium and harvested at exponential phase of growth to measure β-galactosidase levels. In the presence of Hac1[i]p, the URS1-*CYC1*-Ub-X-*lacZ* reporters with methionine and leucine do not show any repression (**Figure 3.8**). Mitotic repression in the presence of URS1 can be still seen (~1.3 fold for the methionine plasmid and ~three fold for the leucine plasmid). β-Galactosidase levels expressed from arginine constructs donot show remarkable mitotic repression seen in other constructs but show ~1.7 fold repression in the presence of Hac1[i]p. Expression of Hac1[i]p does not cause any decrease of β-galcatosidase levels. Therefore Hac1[i]p-mediated repression cannot be concluded as expression of Hac1[i]p does not repress β-galactosidase URS1. β-Galactosidase levels measured for constructs with arginine at the N-terminus of β-galactosidase protein were barely detectable when the same number of cells were used as for other constructs possibly due to decreased half-life of ~two min. This causes variation in β-galactosidase assay and therefore a difficulty in using arginine constructs.

The negative regulation of Hac1^{i}p on early meiotic genes mediated by URS1 could not be corroborated when URS1-*CYC1*-Ub-X-*lacZ* reporters were expressed in the presence of Hac1^{i}p expressed from its endogenous promoter in nitrogen-rich conditions. The constitutive expression of Hac1^{i}p from pRS314-*HAC1^i* has been shown by Schröder et al, 2004.
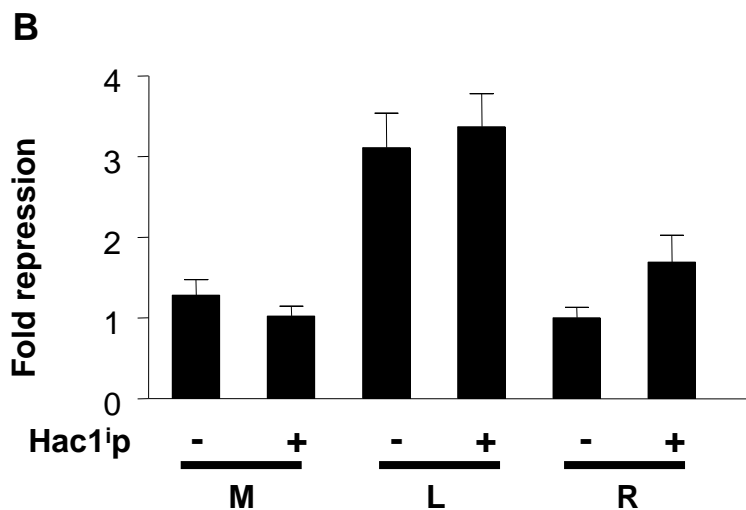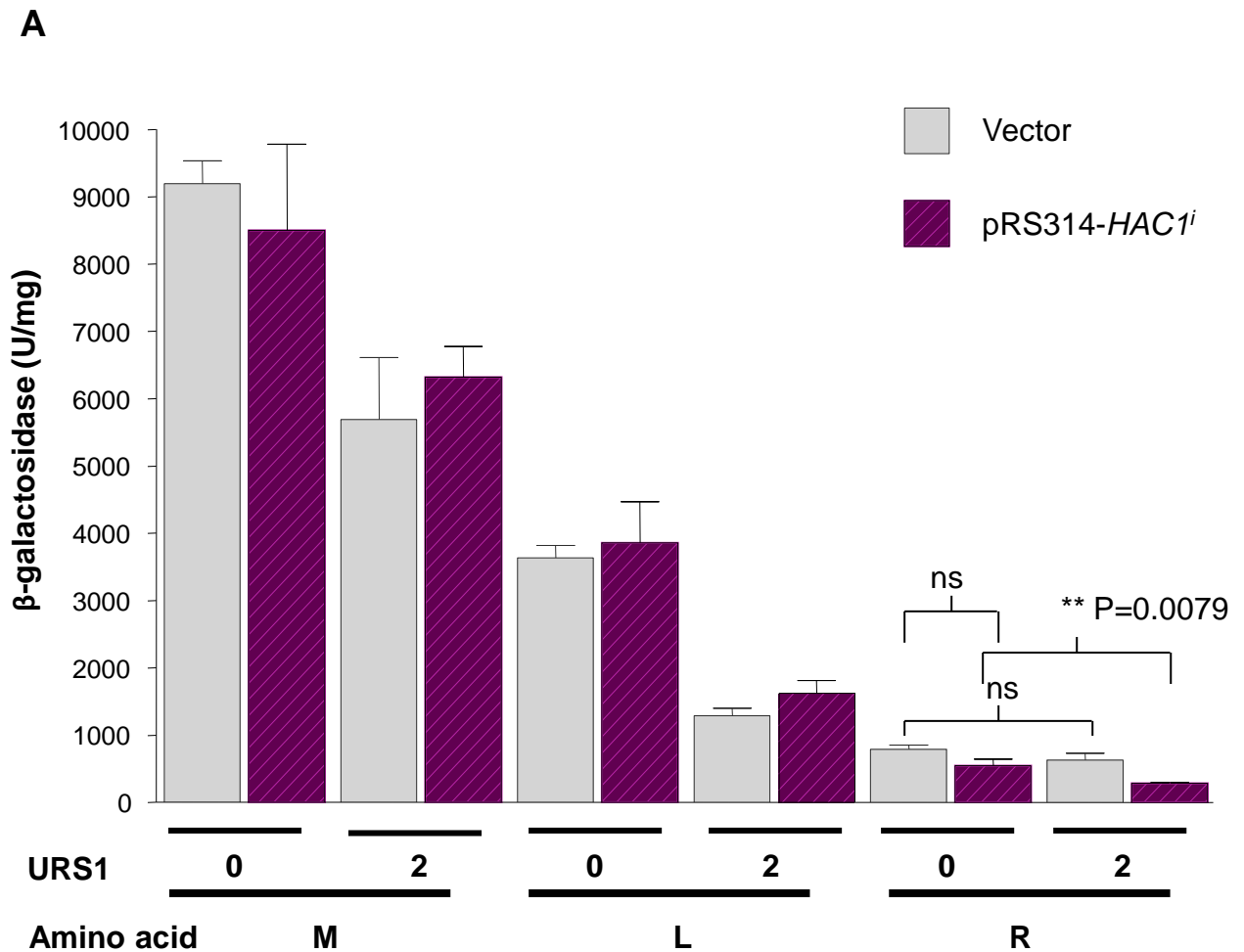
Figure 3.8. Expression of URS1-*CYC1*-Ub-X-*lacZ* reporters in the presence of Hac1[i]p. URS1-CYC1-Ub-X-lacZ reporters (X= M, L or R; URS1=0,1 or 2) are expressed in the presence of Hac1[i]p expressed from pRS314-*HAC1[i]* in WT strain (MSY 134-36). The fold repression is the ratio of β-galactosidase levels expressed from a plasmid with zero URS1 to β-galactosidase levels expressed from a plasmid with two URS1 sites. The average and standard error from at least three independent transformants are shown. (**B**) Fold repression is defined here as the ratio of β-galactosidase levels expressed from a plasmid without URS1 sites to β-galactosidase levels expressed from a plasmid with two URS1 sites.

3.7 Disruption of Hac1[i]p-mediated negative regulation in *hac1Δ*

The destabilisation of β-galactosidase in the URS1-*CYC1*-Ub-X-*lacZ* reporters did not reveal repression mediated by Hac1[i]p through URS1 (**Figure 3.8**). This is surprising because induced expression of Hac1[i]p repressed transcription of EMGs and β-galactosidase levels from UAS less *CYC1-lacZ* reporters under nitrogen starvation conditions suggested negative regulation of EMGs through URS1 (Schröder et al., 2000; Schröder et al., 2004). An alternative explanation is that endogenously spliced Hac1[i]p under vegetative growth may be enough to mediate repression through URS1 on early meiotic genes. To test whether endogenously spliced Hac1[i]p under vegetative growth is sufficient to repress through URS1, I decided to delete *HAC1* and test URS1-*CYC1*-Ub-X-*lacZ* reporters in the *hac1Δ* strains.

In order to demonstrate the repression caused by Hac1[i]p synthesized in vegetatively growing cells, the URS1-*CYC1*-Ub-X-*lacZ* reporters were transformed into a *HAC1* null mutant (*hac1Δ*) strain and a WT strain and grown under vegetative growth conditions (synthetic minimal acetate medium; PSP2). β-Galactosidase levels were measured from cells harvested at exponential phase (**Figure 3.9**). The methionine plasmids show moderate mitotic repression (~1.5 fold) in the WT strain. When *HAC1* was deleted, β-galactosidase levels were activated moderately (~0.68 fold) in the presence of two URS1 sites. The β-galactosidase reporters with leucine as N-terminal amino acid showed ~two fold repression in the presence of URS1 sites in the WT strain. But in the absence of Hac1[i]p (*hac1Δ*) the leucine constructs showed ~0.17 fold activation in β-galactosidase levels (**Figure 3.9B**). When the WT strain was compared to *hac1Δ* (**Figure 3.9C**), deletion of *HAC1* leads to ~2.5 fold activation with methionine plasmids and ~13 fold activation of β-galactosidase levels with leucine plasmids. So the mitotic repression at URS1 is abolished in absence of Hac1[i]p.

The repression by Hac1[i]p via URS1 is relieved when Hac1[i]p is deleted in *HAC1* null mutant suggesting the disruption of negative regulatory mechanism on URS1. The activation of β-galactosidase levels under nitrogen-rich conditions in *hac1Δ* strains indicates that Hac1[i]p also regulates URS1-controlled genes in nutrient-rich conditions to repress meiosis.
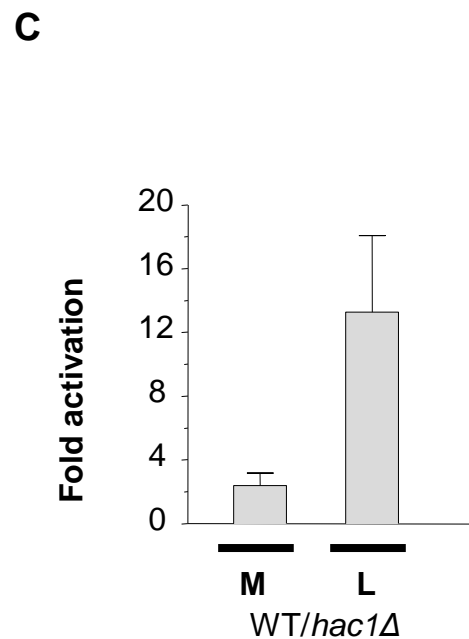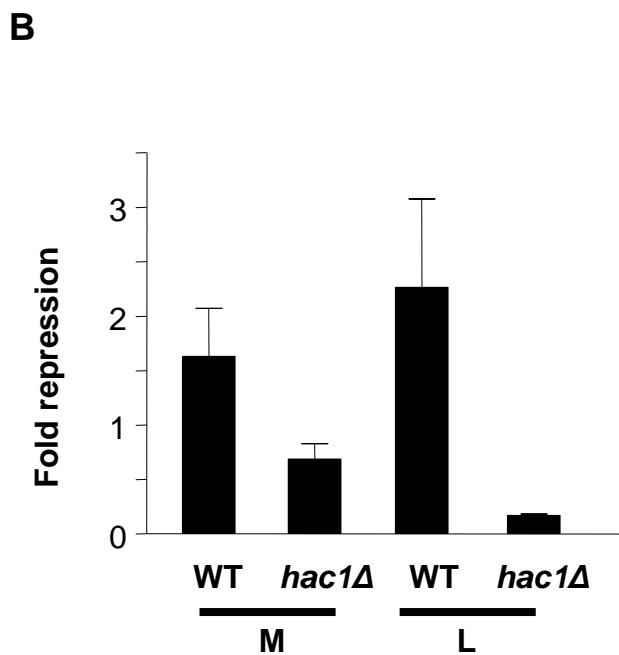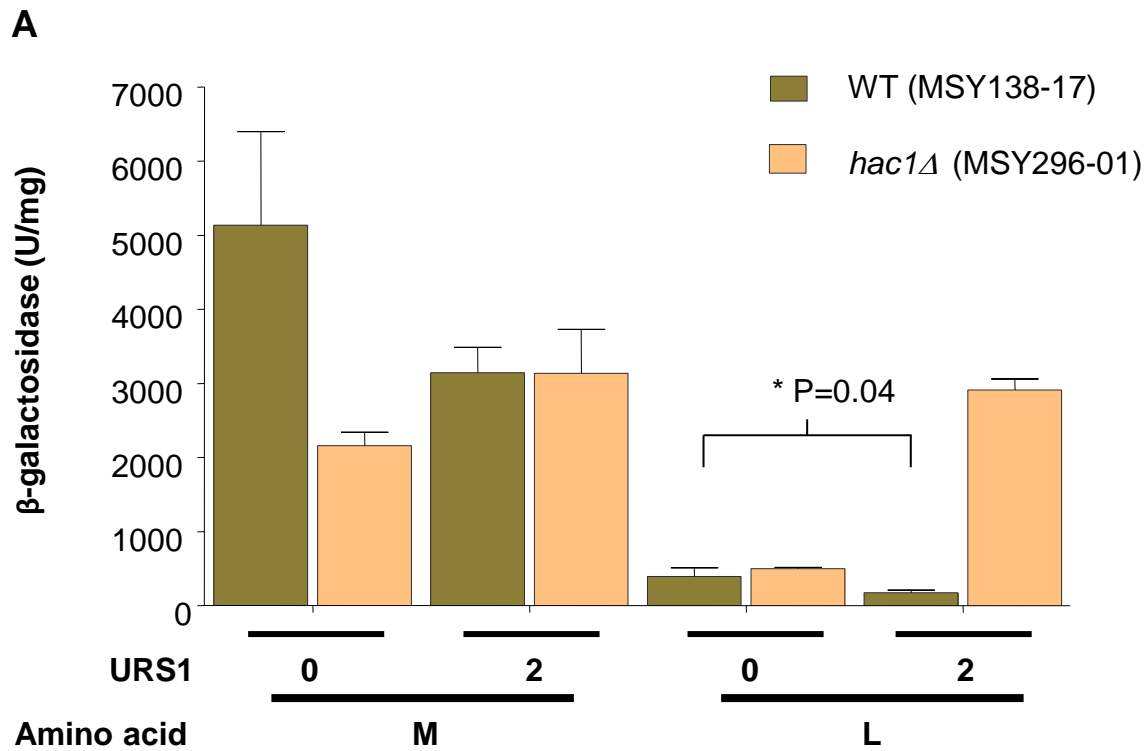
Figure 3.9 Repression is relieved in the absence of Hac1[i]p. Expression of URS1-
CYC1-Ub-X-*lacZ* reporters in a *HAC1* null mutant (*hac1Δ*) and WT strain in minimal
synthetic acetate (PSP2) medium. The amino acid residues at the N-terminus of β-
galactosidase are methionine (M) and leucine (L). The average and standard error
from at least three independent transformants are shown. (**B**) The fold repression
depicts mitotic repression by URS1 sites. Fold repression is the ratio of β-
galactosidase levels from a plasmid with zero URS1 sites to β-galactosidase levels
from a plasmid with two URS1 sites and fold activation is the ratio of β-galactosidase
levels from a plasmid with two URS1 sites to β-galactosidase levels from a plasmid
with zero URS1 sites. (**C**) Activation of β-galactosidase levels is calculated as the ratio
of the fold repression of WT to *hac1Δ*.

3.8 Discussion

URS1-*CYC1*-Ub-X-*lacZ* reporters encoding β-galactosidase with decreased half lives were tested in the presence of constitutively expressed Hac1[i]p. The negative regulation of Hac1[i]p on early meiotic genes mediated by URS1 could not be seen in URS1-*CYC1*-Ub-X-*lacZ* reporters (**Figure 3.8**). The cells in this experiment were grown in minimal acetate medium (PSP2). PSP2 contains acetate as the sole source of carbon. The level of *HAC1* mRNA splicing is reported to be higher in the presence of acetate as carbon source (2% acetate in YPAc) as compared to other carbon sources tested (Schröder et al., 2000). Thus the abundance of Hac1[i]p under these conditions (minimal acetate vegetative medium; 1% acetate) may be enough to achieve constitutive repression on URS1 under mitotic growth conditions, which may mask the repression that may be otherwise caused solely by Hac1[i]p expressed from pRS314-*HAC1*[i]. When Hac1[i]p was deleted, β-galactosidase levels were derepressed (**Figure 3.9C**), suggesting negative regulation at URS1. However, an experiment in which *HAC1*[i] is ectopically expressed in *hac1Δ* strains would substantiate these data. The URS1-*CYC1*-Ub-*X*-*lacZ* reporters studied here can be used in nutrient-rich conditions to study transcriptional regulation on URS1-controlled genes in future work.

Chapter 4

Transcriptional regulation of metabolic genes under nutrient rich condition

4.1 Ume6p in regulation of URS1-controlled genes

Using URS1-*CYC1*-Ub-**L**-*lacZ* reporter with leucine residue at the N-terminal end of β-galactosidase I showed that insertion of the URS1 sites decreases steady state level of β-galactosidase. However this was not seen convincingly earlier with methionine plasmids. It is known that the URS1 site is occupied by Ume6p/Sin3p/Rpd3p repressing the transcription in vegetative growth conditions (Schröder et al., 2004). The *ISW2-ITC1* chromatin remodelling complex is also recruited by Ume6p under mitotic growth in a parallel pathway to *RPD3-SIN3* HDAC complex (Goldmark et al., 2000). To validate if the repression of URS1-*CYC1*-Ub-**L**-*lacZ* reporter can be attributed to the known repressing mechanism of URS1 where recruitment of *ISW2-ITC1* and *RPD3-SIN3* by Ume6p to URS1 site leads to repression in vegetatively growing cells, I looked at the URS1-controlled *lacZ* expression by expressing URS1-*CYC1*-Ub-L-*lacZ* reporters in an *ume6Δ* strain. The WT strain showed ~2.5 fold mitotic repression through URS1. However, deletion of *UME6* led to a ~4.5 fold increased levels of β-galactosidase as compared to WT in the presence or absence of URS1 (**Figure 4.1**). Thus, *ume6Δ* leads to elevated expression of URS1-*CYC1*-Ub-L-*lacZ* reporters, which suggests that either Ume6p negatively regulates components of an activating mechanism/binding of these components to URS1 or other *cis*-acting sites in the *CYC1* promoter. It is also possible that deletion of Ume6p causes disruption of Ume6p/Rpd3p/Sin3p repressing unit which leads to recruitment of histone modifying complexes that activate the transcription at URS1.
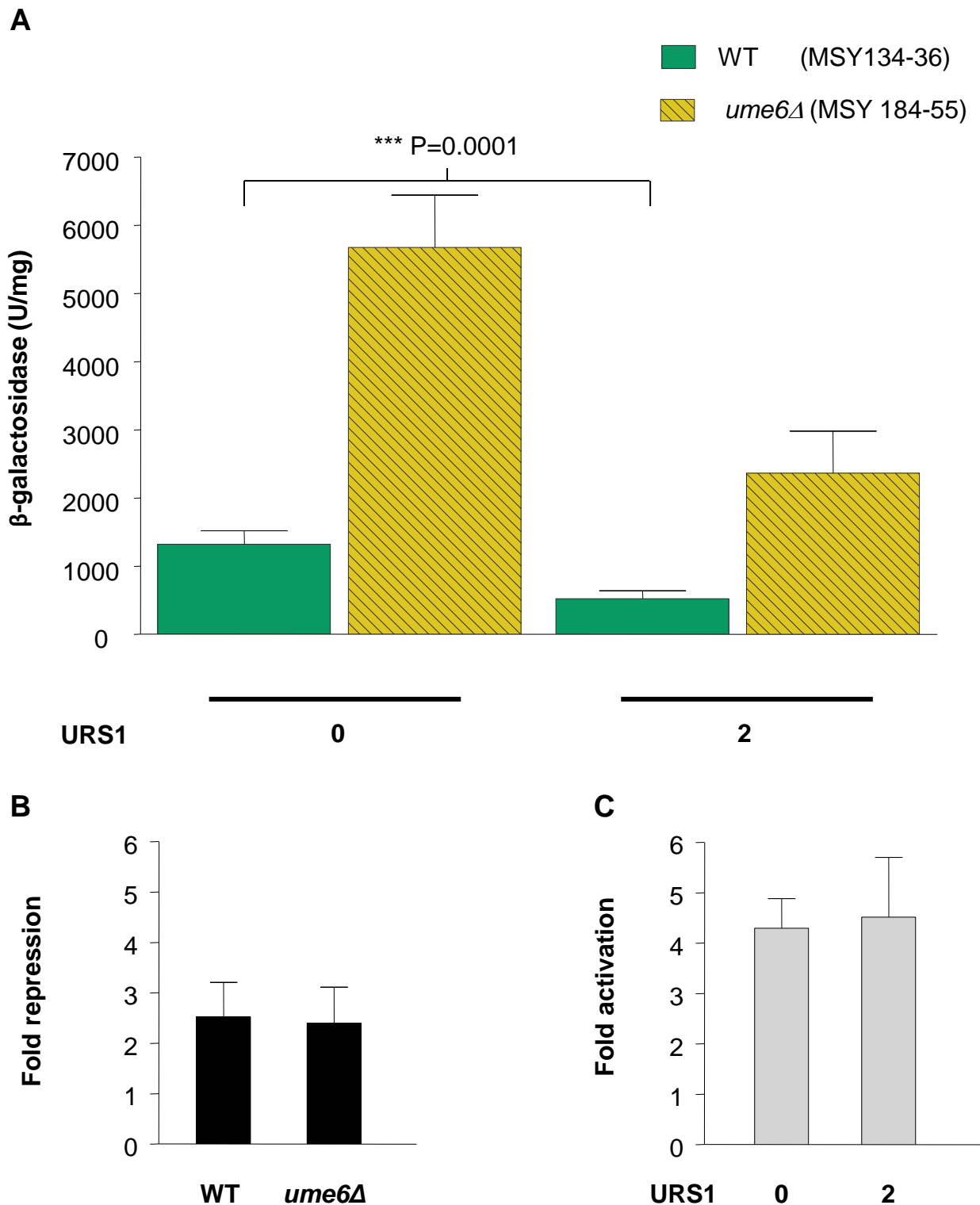
Figure 4.1 Ume6p in the regulation of URS1 controlled genes. URS1-CYC1-Ub-X-lacZ (X= L; leucine) reporters were expressed in *ume6Δ* strain and WT. The average and standard error from at least three independent transformants are shown. (**B**) The fold repression depicts mitotic repression by URS1 sites. Fold repression is calculated as the ratio of β-galactosidase levels from a plasmid with zero URS1 sites to β-galactosidase levels from a plasmid with two URS1 sites in the strains indicated. (**C**) Fold activation is the ratio of β-galactosidase levels from WT to β-galactosidase levels from *ume6Δ.*

4.2 *RPD3-SIN3* histone deacetylase complex in regulation of URS1-controlled genes under nutrient-rich conditions

The transcriptional repression of early meiotic genes involves function of the *RPD3-SIN3* histone deacetylase (HDAC) complex and the *ISW2-ITC1* chromatin remodelling complex. The *RPD3-SIN3* HDAC is a large multiprotein complex involved in regulation of a wide range of genes in meiosis, metabolism, osmotic stress, telomere boundary regulation and anaerobic growth (De Nadal et al., 2004; Ehrentraut et al., 2010; Kadosh and Struhl, 1997; Rundlett et al., 1998; Vidal and Gaber, 1991). Rpd3p functions as histone deacetylase and Sin3p is a co-repressor which is recruited by Ume6p to the promoters of early meiotic genes (Kadosh and Struhl, 1997). Schröder et al., 2004 showed that Hac1[i]p interacts physically with Rpd3p-Sin3p HDAC to mediate nitrogen-mediated negative regulation of EMG transcription and that the catalytic activity of Rpd3p is required for this negative regulation. They also showed that the Ume6p binding site URS1 is the site of Hac1[i]p-mediated repression. To test whether the *RPD3-SIN3* complex is involved in regulation of URS1-*CYC1*-Ub-*X*-*lacZ* reporters as reported for URS1-controlled EMGs under nitrogen-rich conditions, we expressed URS1-*CYC1*-Ub-*X*-*lacZ* reporters in a strain deleted for *RPD3* on minimal synthetic medium (PSP2).

The WT strain shows ~2 fold repression in the presence of URS1 (**Figure 4.2**). But in the absence of Rpd3p (*rpd3Δ*), β-galactosidase levels are not only decreased (~2.5 fold) with URS1 but also when compared to WT (**Figure 4.2B**). This was surprising as Kadosh and Struhl, 1997 have shown using URS1-*CYC1*-*lacZ* reporters that the deletion of Rpd3p showed moderate derepression (~four fold). Next I looked at Sin3p which is a component of Rpd3p-Sin3p HDAC multiprotein complex involved in transcriptional repression at EMGs. Sin3p, which acts as a co-repressor is recruited to URS1 by Ume6p. Sin3p then targets Rpd3p HDAC to deacetylate early meiotic gene promoters and to mediate transcriptional repression. To test whether the known function of Sin3p is involved in regulation of URS1-*CYC1*-Ub-*X*-*lacZ* reporters, I expressed URS1-*CYC1*-Ub-*X*-*lacZ* reporters in *sin3Δ* strains under vegetative growth conditions. In the presence of Sin3p (WT), the β-galactosidase levels decreased in the plasmids containing URS1 (~2.5 fold), but when Sin3p was deleted the β-galactosidase levels elevated not only in the presence of URS1, but also in the absence of URS1 (**Figure 4.3**). When the WT strain is compared to *sin3Δ* strain, β-

galactosidase levels elevated to ~three fold (**Figure 4.3C**). Thus, the mitotic repression seen in the WT strain (~2.5 fold) is not seen in *sin3Δ* strain and deletion of Sin3p elevated β-galactosidase levels in absence or presence of URS1.

A
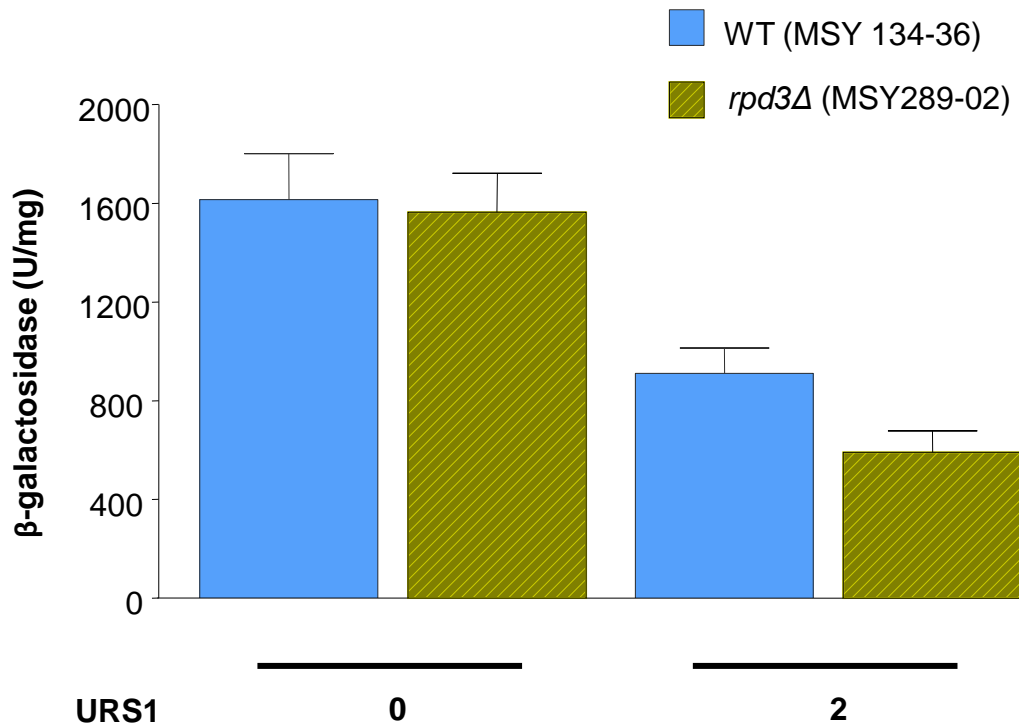
B
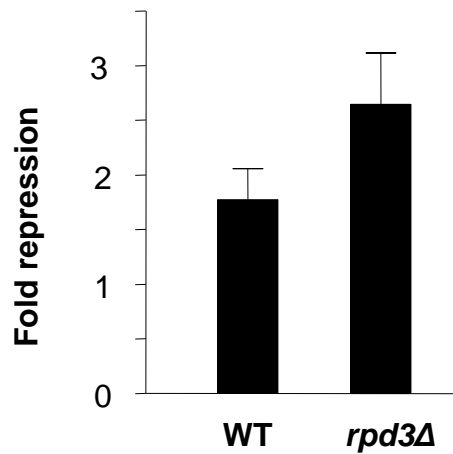
Figure 4.2. Role of Rpd3p in regulation of URS1. URS1-*CYC1*-Ub-X-*lacZ* reporters (X= L; leucine) were expressed in *rpd3Δ* strain and WT strain in synthetic minimal media. The average and standard error from at least three independent transformants are shown. (**B**) The fold repression depicts mitotic repression by URS1 sites. Fold repression is calculated as the ratio of β-galactosidase levels expressed from a plasmid with zero URS1 sites to β-galactosidase levels expressed from a plasmid with two URS1 sites in the strains indicated.

Figure 4.3 Role of Sin3p in regulation of URS1-*CYC1*-Ub-X-*lacZ* reporters. URS1-*CYC1*-Ub-X-*lacZ* reporters (X= L; leucine) were expressed in the absence of Sin3p (*sin3Δ*) in minimal synthetic medium. **(B)** The fold repression depicts mitotic repression by URS1. Fold repression is calculated as the ratio of β-galactosidase levels expressed from a plasmid with zero URS1 sites to β-galactosidase levels expressed from a plasmid with two URS1 sites. (**C**) Activation of β-galactosidase levels is calculated as the ratio of the fold repression of WT to the fold repression of *sin3Δ* from (**B**). The β-galactosidase levels shown are an average and standard error from at least three independent transformants.

4.3 Role of *ISW2-ITC1* chromatin remodelling complex in regulation of URS1-controlled genes

ISW2 and *ITC1*, which are components of the Isw2p-Itc1p ATP dependent chromatin remodelling complex are recruited by *UME6* to repress early meiotic genes (Goldmark et al., 2000) and other non-meiotic genes like *INO1* (Sugiyama and Nikawa, 2001). The Isw2p complex creates a nuclease inaccessible chromatin structure upstream of the Ume6p binding site in target promoters (Goldmark et al., 2000). The Itc1p-Isw2p chromatin remodelling complex was not involved in Hac1[i]p-mediated repression under nitrogen starvation conditions (Schröder et al., 2004). However, I wanted to investigate and validate the role of the chromatin remodelling complex *ISW2-ITC1* in repression at URS1 of URS1-*CYC1*-Ub-X-*lacZ* reporters under nutrient-rich conditions. In order to test whether the same mechanism of repression by *ISW2* and *ITC1* on URS1-controlled genes in mitotic growth conditions as reported is also functional on the URS1-*CYC1*-Ub-X-*lacZ* reporters we transformed URS1-*CYC1*-Ub-X-*lacZ* reporters into *isw2Δ* cells. The cells were harvested at exponential growth phase and after lysis, β-galactosidase assays were performed. WT strain shows ~2.5 fold repression and *isw2Δ* strain shows ~1.2 fold repression in the presence of URS1 (**Figure 4.4B**). Deletion of Isw2p led to ~fourfold and ~tenfold elevated expression of β-galactosidase in absence and presence of URS1 respectively (**Figure 4.4A**). This suggests that *ISW2* may be negatively affecting transcription of the URS1-*CYC1*-Ub-X-*lacZ* reporter at sites other than URS1. Itc1p is also a component of *ISW2-ITC1* complex and so I wanted to test whether Itc1p was responsible for repression of β-galactosidase levels of URS1-*CYC1*-Ub-X-*lacZ* reporters. Levels of β-galactosidase expressed from URS1-*CYC1*-Ub-X-*lacZ* reporters in *itc1Δ* strains were measured. WT strain shows ~2.5 fold mitotic repression, while this repression is lost when *ITC1* was deleted (**Figure 4.5B**). Deletion of *itc1Δ* led to ~three fold activation in presence of URS1 but there was no change in absence of URS1 (**Figure 4.5**), which indicates that *ITC1* is involved in repression at URS1 in URS1-*CYC1*-Ub-X-*lacZ* reporters as has been reported earlier. The elevated levels of β-galactosidase in the presence or absence of URS1 in **figure 4.4** indicates that this activation may be independent of URS1. When Itc1p is deleted, β-galactosidase levels are derepressed only in presence of URS1, indicating that *ITC1* is involved in the repression machinery at the URS1 site. Thus deletion of

ITC1 shows that repression at URS1 of URS1-*CYC1*-Ub-X-*lacZ* reporters is lost, but when *ISW2* is deleted, β-galactosidase levels are elevated even in the absence of URS1 indicating that *ISW2* may be acting independently of *ITC1*.
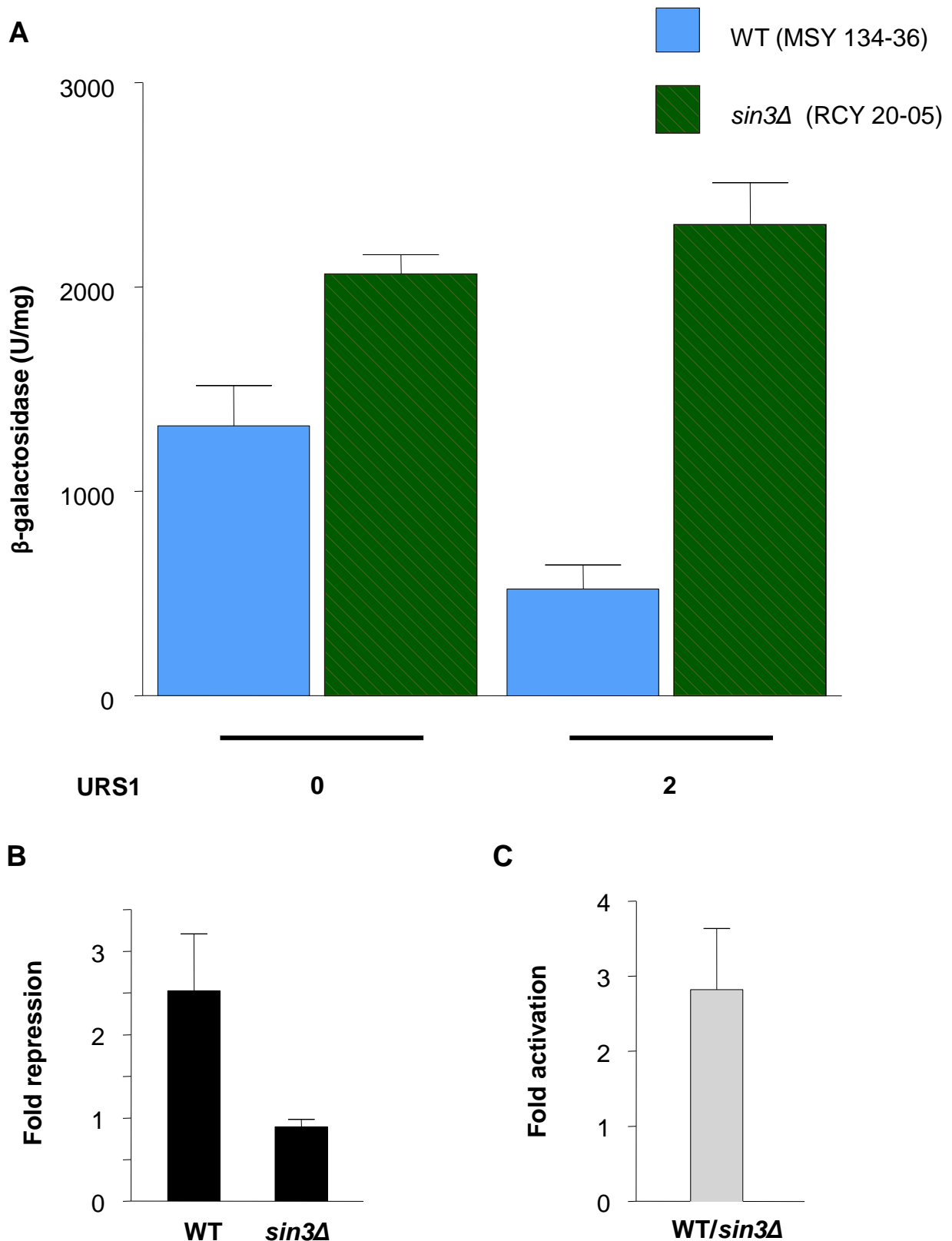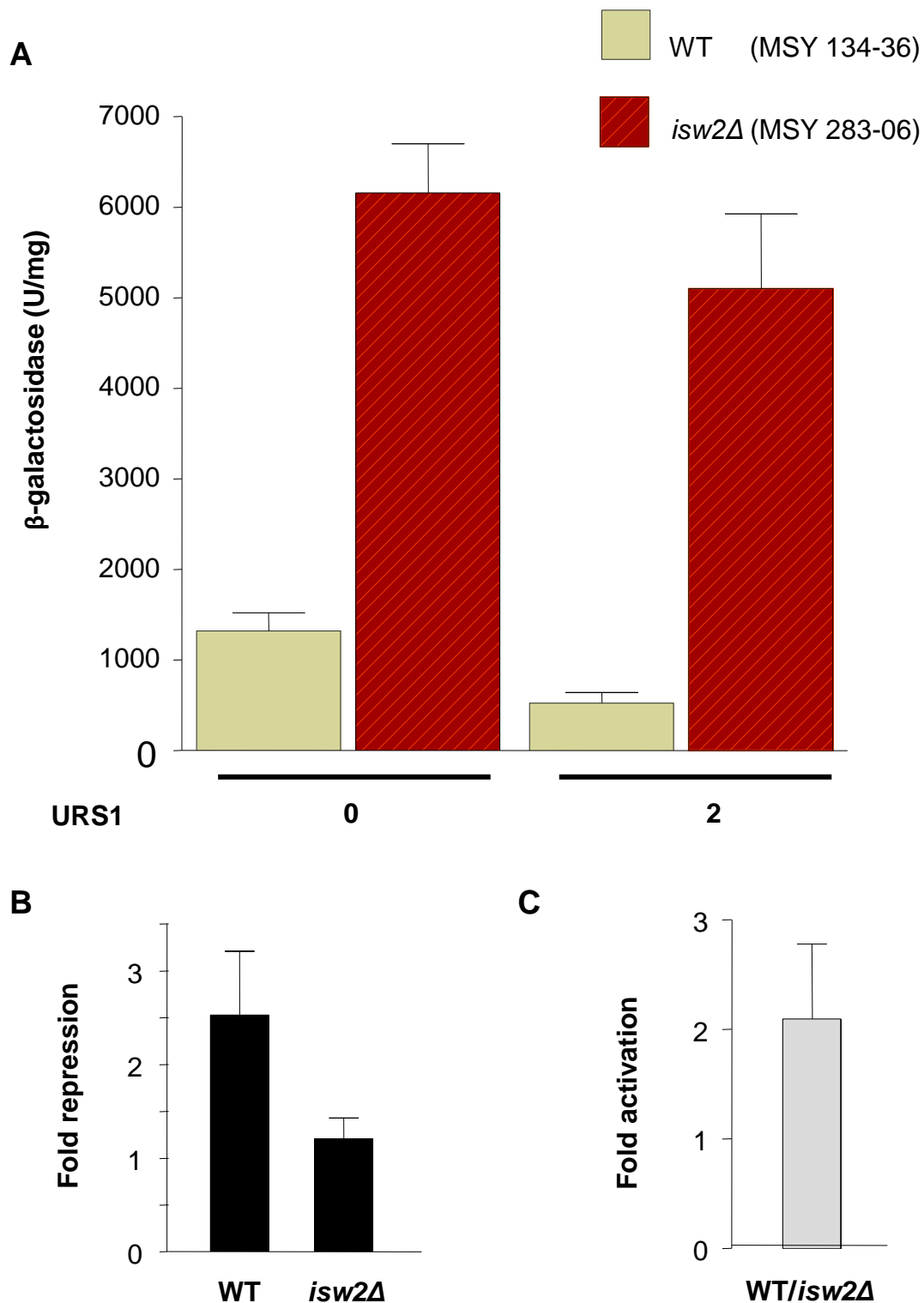
Figure 4.4. Role of Isw2p in regulation of URS1 mediated repression. URS1-*CYC1*-Ub-X-*lacZ* reporters (X= L;leucine) were expressed in *isw2Δ* strain and WT strain. (**B**)The fold repression depicts mitotic repression. Fold repression is calculated as the ratio of β-galactosidase levels expressed from a plasmid with zero URS1 sites to β-galactosidase levels expressed from a plasmid with two URS1 sites. (**C**) Fold activation is calculated as the ratio of fold repression of WT to fold repression of *isw2Δ* levels from (**B**). The β-galactosidase levels are an average and standard error of at least three independent transformants.
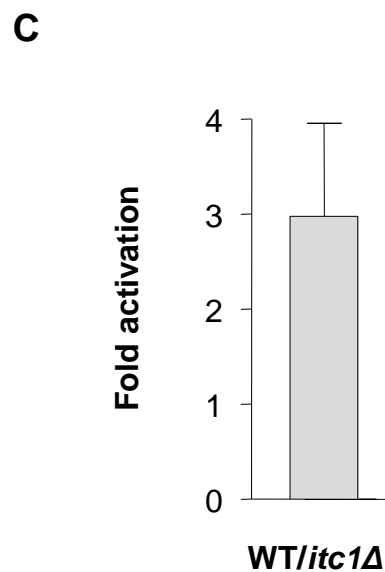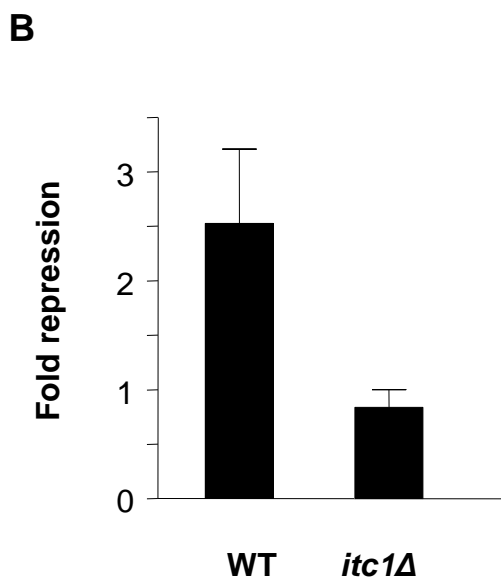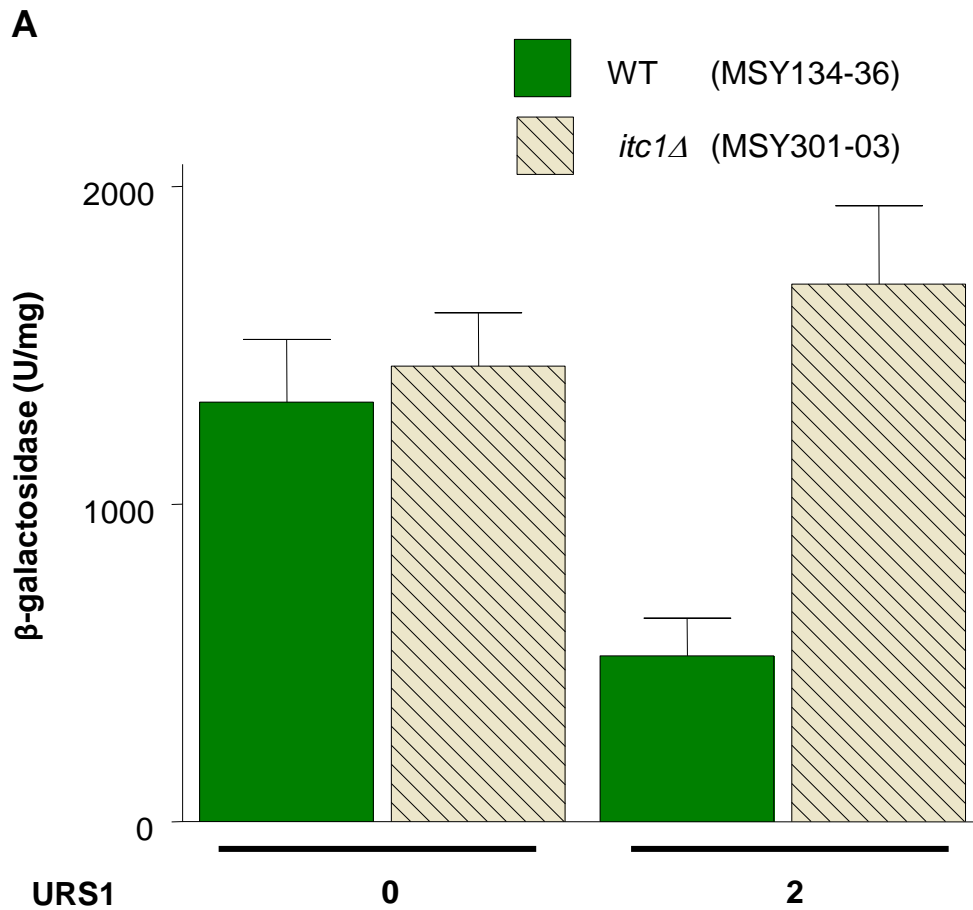
Figure 4.5 Itc1p is involved in regulation of URS1 mediated repression. URS1-*CYC1*-Ub-X-*lacZ* (X= L;leucine) reporters were expressed in *itc1Δ* strain. (**B**) The fold repression depicts mitotic repression by URS1. Fold repression is calculated as the ratio of β-galactosidase levels expressed from a plasmid with zero URS1 to β-galactosidase levels expressed from a plasmid with two URS1. (**C**) Fold activation of β-galactosidase levels is calculated as the ratio of the fold repression of WT to the fold repression of *itc1Δ* from values in (**B**). The average and standard error from at least three independent transformants are shown.

4.4 Discussion

Deletion of Ume6p leads to activation of β-galactosidase in the absence of URS1 (**Figure 4.1**) suggesting that Ume6p may be regulating other sites causing activation of URS1-*CYC1*-Ub-*X*-*lacZ* reporters without URS1. The URS1-*CYC1*-Ub-*X*-*lacZ* reporters used in this study contains the *CYC1* fragment from -324 to +141 that includes two UAS$_{CYC1}$ sites, the TATA region and URS1 elements cloned immediately upstream of UAS$_{CYC1}$ [(Guarente and Mason, 1983; Kadosh and Struhl, 1997) and **Figure 3.1C**]. UAS$_{CYC1}$ from the promoter region of the *CYC1* gene encoding iso-1-cytochrome *c* is tightly regulated by levels of intracellular heme (Guarente and Mason, 1983). *CYC1* is also induced by oxygen and lactate, and repressed by glucose (Boss et al., 1980; Guarente and Hoar, 1984; Guarente and Mason, 1983; Hortner et al., 1982). Induction of oxygen occurs through binding of the transcription factor Hap1p to UAS1 in the *CYC1* promoter (Pfeifer et al., 1987), while repression in the presence of glucose is mediated by binding of Mig1p and the CCAAT-binding activator complex subunits Hap2p, Hap3p, Hap4p and Hap5p to UAS2 in the *CYC1* promoter (Olesen et al., 1987; Treitel and Carlson, 1995). It is likely that regulation of Hap1p or Hap2p-3p-4p-5p complex on UAS$_{CYC1}$ is somehow negatively regulated by Ume6p, because *UME6* is not only a meiosis specific regulator but also regulates genes involved in arginine catabolism (Strich et al., 1994), peroxisomal function (*FOX3*) (Einerhand et al., 1995) and DNA repair genes (*PHR1*) (Sweet et al., 1997). Microarray data show that *HAP1* gene was derepressed in *ume6Δ* (**Table 4.1**). The *HAP4* gene, whose gene expression provides transcriptional activation domain to the Hap2p-3p-4p-5p complex showed a small increase in transcription (Williams et al., 2002). So it can be conceived that *HAP1* encoding a zinc finger transcription factor, which requires homodimerization for high affinity DNA-binding to UAS1 may be regulated by *UME6*. Other regulatory mechanisms barring the transcriptional level regulation by Ume6p cannot be excluded for regulation at UAS$_{CYC1}$.

It can be conceived that Ume6p is involved in activation of URS1-*CYC1*-Ub-X-*lacZ* reporters also through UAS$_{CYC1}$ and looking at the genes regulated by Hap1p in *ume6Δ* strains may throw more light on understanding of *UME6* targets. Also understanding the UAS$_{CYC1}$ regulatory mechanism promises to be of particular

interest as the core *CYC1* promoter is used in investigation of transcriptional activation and repression.

Table 4.1. Microarray data showing expression of *HAP* genes in *UME6* and *ume6Δ* strains of SK1 genetic background [data from (Williams et al., 2002)]

Sr. No	Gene	Normalized intensity	
		UME6	*ume6Δ*
1.	*HAP1*	144	237
2.	*HAP2*	87	508
3.	*HAP3*	587	311
4.	*HAP4*	2380	2603
5.	*HAP5*	205	498
6.	*CYC1*	2097	2762

In the absence of Rpd3p (*rpd3Δ*), there was a decrease in the levels of β-galactosidase as compared to wild type, but when Sin3p was deleted the repression on URS1 was derepressed. The behaviour of *rpd3Δ* cells may be not that surprising as Kadosh and Struhl, 1997 suggested that *sin3Δ* strain lost URS1-dependent transcriptional repression to a larger degree than in *rpd3Δ* strain. Moreover the effect of deletion of Rpd3p on repression could be compensated by other related HDAC (Rundlett et al., 1996) with Sin3p (**Figure 4.2**). The elevated expression of β-galactosidase in *sin3Δ* strains in the absence of URS1 sites indicates that Sin3p regulates another site in URS1-*CYC1*-Ub-*X*-*lacZ* reporters (**Figure 4.3**). The data also suggests that Sin3p may have repressing function as β-galactosidase levels are elevated in *sin3Δ*. The contribution of transcriptional repression by Sin3p has been earlier suggested to be minor (Kadosh and Struhl, 1997), but the data here shows that the contribution of Sin3p is not minor. Presumably other sites in the *CYC1* promoter region of URS1-*CYC1*-Ub-*X*-*lacZ* reporters exist where Sin3p mediates repression. Mutations in Sin3p or Sin3p binding sites in *CYC1* promoter region that may be responsible for this repression can provide more insight into Sin3p mediated repression.

Deletion of *ISW2* results in mitotic transcriptional derepression of many genes normally induced under meiosis (Goldmark et al., 2000). Deletion of *ISW2* here elevated expression of β-galactosidase from URS1-*CYC1*-Ub-*X*-*lacZ* reporters even without URS1 (**Figure 4.4**) suggesting that Isw2p acts on other sites in this reporter. *ISW1,* another member of imitation switch (ISWI) class and *ISW2* act redundantly with Chd1p in regulation of *CYC1* (Alén et al., 2002). It can be speculated from this data that *ISW2* may be repressing on sites other than URS1, which may be activated when *ISW2* is deleted because Hap1p binding to UAS1 in the *CYC1* promoter region was restored in *isw2Δ* strains because of loss of nucleosome positioning (Morohashi et al., 2007). Therefore, deletion of *ISW2* may open chromatin structure around the *CYC1* promoter region in URS1-*CYC1*-Ub-X-*lacZ* reporters which may lead to activation of β-galactosidase. Isw2p and Itc1p have been suggested to act in the same pathway (Gelbart et al., 2001), but when *ITC1* was deleted β-galactosidase were elevated only in the presence of URS1. This suggests negative regulation was lost at URS1 when *ITC1* was deleted. Therefore elevated β-galactosidase levels in the absence of URS1 in *isw2Δ* strain, suggests that *ISW2* may be acting independently of *ITC1* at sites other than URS1 in URS1-*CYC1*-Ub-*X*-*lacZ* reporters. The *itc1Δ* strain shows that the regulation on URS1 is lost (**Figure 4.5**) and this can be explained by the fact that a population of Itc1p preferentially interacts with Ume6p besides its interaction with Ume6p and Isw2p (Goldmark et al., 2000).

Chapter 5

Pseudohyphal growth on non-fermentable carbon sources

5.1 Pseudohyphal growth on non-fermentable carbon sources

The yeast *S. cerevisiae* show different growth patterns including yeast and pseudohyphal forms depending on the environmental cues and cell type. Under nitrogen deplete conditions and in the presence of fermentable carbon sources, *S. cerevisiae* differentiate to form pseudohyphae, which is characterized by an elongated cell shape, unipolar budding, symmetric cell division, adhesion of cells to each other after cell division is completed and invasion of solid growth media (Gimeno et al., 1992; Kron et al., 1994). The formation of pseudohyphal growth requires coordination of at least two signalling pathways, the mating and filamentation mitogen activated protein kinase (MAPK) signalling cascade and the cAMP-dependent protein kinase A (PKA) pathway. These pathways may act in a parallel and partially overlapping manner. The unfolded protein response (UPR) represses pseudohyphal growth and meiosis under nitrogen-rich conditions. However, when the UPR pathway is compromised under sporulation-inducing conditions the cells respond inappropriately by switching to pseudohyphal growth. *ire1Δ/ire1Δ* and *hac1Δ/hac1Δ* diploids also showed increased pseudohyphal growth and expression of spliced Hac1[i]p repressed pseudohyphal growth. The splicing of *HAC1* mRNA was higher in the presence of acetate as non-fermentable carbon source compared to other carbon sources (Schröder et al., 2000), suggesting that repression of pseudohyphal growth by the UPR is especially an effect of non-fermentable carbon source. So non-fermentable carbon sources repress pseudohyphal growth and presence of acetate under pseudohyphal growth conditions (glucose and nitrogen limiting) may affect the cell's response. Therefore, we tested whether **a**/α diploid cells under pseudohyphal growth-inducing conditions were affected by the presence of acetate in the SK1 genetic background. The pseudohyphal growth conditions, in the presence of glucose and nitrogen limiting conditions (SLAD plates; glucose and 50 µM ammonium sulfate) induced moderate pseudohyphal growth, characterized by branching chains of cells extruding away from the centre of the colony (**Figure 5.1**). Surprisingly, when acetate was included in the media containing glucose and limiting ammonium sulphate, **a**/α diploid cells show enhanced pseudohyphal growth (**Figure 5.1**). Besides acetate other non-fermentable carbon sources are also utilised to generate energy through respiration and so we wanted to check whether other non-fermentable carbon sources also showed a

similar effect on pseudohyphal growth. L-lactate, pyruvate, glycerol and ethanol were added to glucose and tested for pseudohyphal growth. Pseudohyphal growth was also enhanced in the presence of other non-fermentable carbon sources as well (**Figure 5.1**). Enhanced pseudohyphal growth in the presence of acetate and other non-fermentable carbon sources under pseudohyphal growth inducing conditions was surprising for two reasons. Firstly, the utilization of non-fermentable carbon sources is repressed in the presence of glucose (Gancedo, 1998; Schüller, 2003) and secondly non-fermentable carbon sources have been shown to induce meiosis and not pseudohyphal growth (Gimeno et al., 1992; Kupiec et al., 1997). These observations should be noted with the background information that pseudohyphal growth is widely investigated in Σ1278b strain background (Gimeno et al., 1992), while SK1, which is an efficiently sporulating strain (Kane and Roth, 1974) is employed in studying meiosis. In contrast to SK1 strain nonfermentable carbon sources inhibit pseudohyphal growth in Σ1278b WT strain (Strudwick et al., 2010).

The presence of glucose represses several enzymes of citric acid cycle and respiratory chain (Schüller, 2003). However, the nitrogen limiting conditions on SLA plates may derepress genes encoding citric acid cycle enzymes as reported for rapamycin treated cells grown on glucose (Hardwick et al., 1999). Therefore it is possible that non-fermentable carbon sources require the metabolic and respiratory function to induce pseudohyphal growth. To test whether respiratory function is required for inducing pseudohyphal growth in presence of non-fermentable carbon sources respiration deficient petite mutants were created. The respiration deficiency was checked by the inability of petite mutants to grow on plates containing only non-fermentable carbon source like acetate as seen in **figure 5.1A**. The petite mutants were grown on glucose supplemented with various non-fermentable carbon sources. Pseudohyphal growth was unchanged in respiration-deficient petite mutants compared to a wild type strain, indicating that respiration is not required for induction of pseudohyphal growth by non-fermentable sources in the SK1 genetic background (**Figure 5.1**). These results also suggest that moderate pseudohyphal growth on glucose may be caused by fermentation by-products like ethanol, since ethanol also stimulates pseudohyphal growth [(**Figure 5.1**) (Lorenz et al., 2000a)]. *S. cerevisiae* cells may be detecting its own metabolic by-products to sense the environment and evoke signalling to decide the cell fate. However, there is evidence that petite

mutants in Σ1278b background are unable to undergo filamentous growth and require mitochondrial function (Kang and Jiang, 2005).
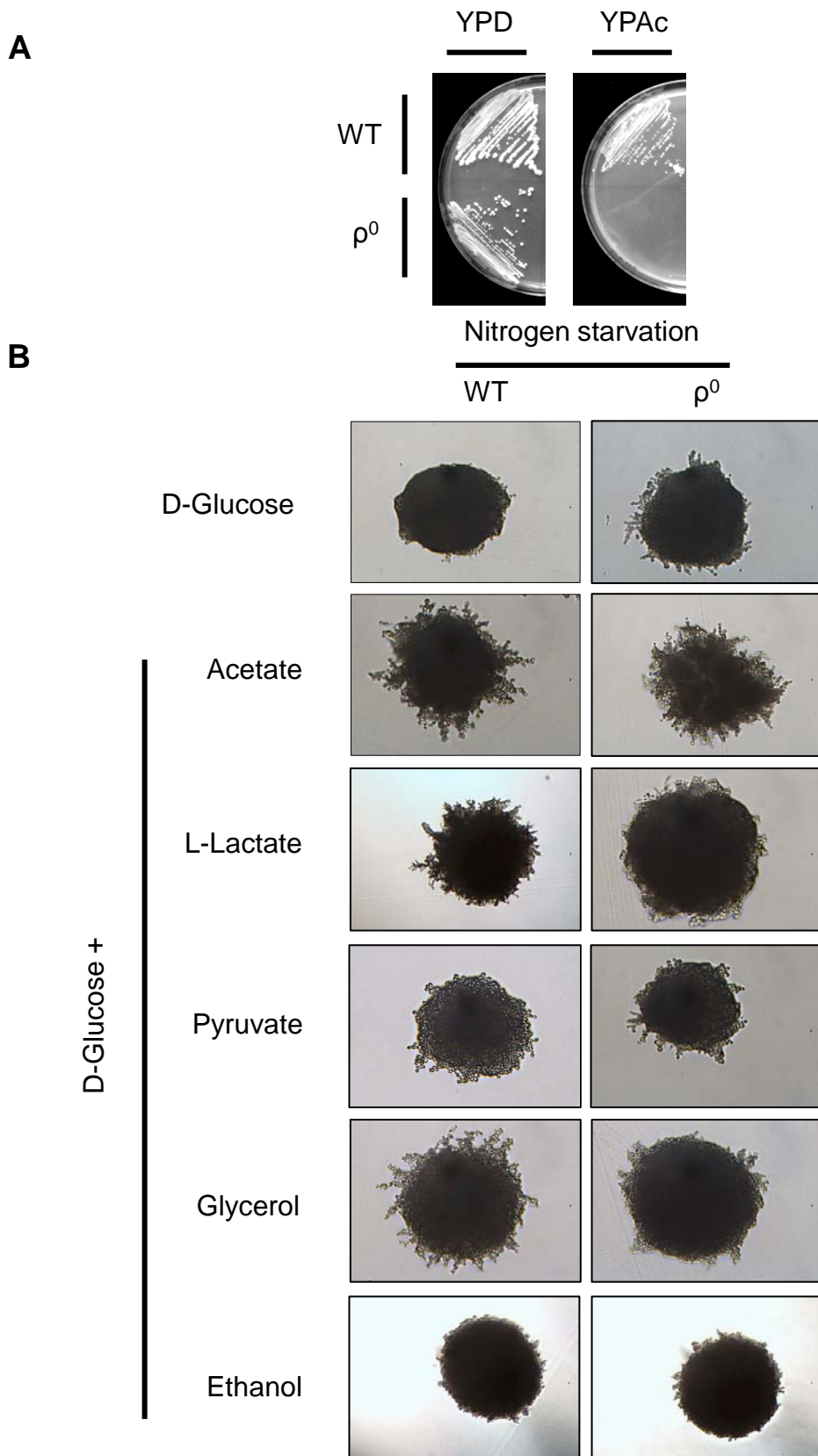
Figure 5.1 Non-fermentable carbon sources induce pseudohyphal growth and respiratory function is not required for induction of pseudohyphal growth. (A) Growth of WT (AMP109) and a petit mutant (ρ^0) on acetate as carbon source. **(B)** AMP109 strain was grown on SLA agar plates containing 50 µM $(NH_4)_2SO_4$, yeast nitrogen base without amino acids and $(NH_4)_2SO_4$, different carbon sources as indicated and amino acids to complement amino acid auxotrophy. The colony morphology after 7 d growth is shown.

5.2 Role of mitochondrial retrograde signalling pathway in regulation of pseudohyphal growth

The non-fermentable carbon sources therefore induce pseudohyphal growth independent of their use as respiratory energy source. The SLAD plates used here lack glutamate and so cells need to synthesize glutamate, which is the main precursor of other amino acids. Glutamate and its metabolite glutamine are a source of all nitrogen utilized by yeast in biosynthetic reactions (Magasanik and Kaiser, 2002). Growth under pseudohyphal growth conditions in the presence of non-fermentable carbon sources and absence of glutamate (**Figure 5.1**) suggests that early steps of the TCA cycle must be activated to meet the demand for glutamate. Mitochondrial retrograde (RTG) signalling is closely associated with the carbon and nitrogen metabolism in yeast cells and the main function of the RTG signalling pathway is to maintain glutamate levels in the cell (Magasanik and Kaiser, 2002). Rapamycin inhibits TOR kinases and induces expression of *RTG*-dependent target genes (Komeili et al., 2000), which increases the pool of glutamine and glutamate. *RTG* genes induce expression of the first three steps of the TCA cycle, *CIT2* (citrate synthase) involved in the glyoxylate cycle and *DLD3* (D-lactate dehydrogenase). *CIT2* is an enzyme in the glyoxylate cycle that enables yeast cells to utilize acetate and ethanol as sole carbon source. The transcript profiles of genes regulated by the RTG pathway in SK1 genetic background strain were found upregulated as compared to Σ1278b strain background (**Table 5.1**). Σ1278b is normally used to study pseudohyphal growth and non-fermentable carbon sources inhibit pseudohyphal growth in this strain background (Gimeno et al., 1992; Strudwick et al.). To test whether activation of *RTG* genes in the SK1 background are responsible for induction of pseudohyphal growth in the presence of glucose and acetate, we created *rtg* deletion strains and tested their growth on plates containing low nitrogen, glucose in the presence or absence of non-fermentable carbon sources. Pseudohyphal growth was unchanged in *rtg2Δ* and *rtg3Δ* strains compared to WT showing that RTG pathway here is not involved in regulation of pseudohyphal growth on non-fermentable carbon sources (**Figure 5.2**). There was no difference in the WT and the mutants in the presence of glucose. Deletion of *RTG* genes leads to glutamate auxotrophy. The *rtg1Δ* strains I used were also arginine auxotrophs.

Therefore, *rtg1Δ* strains did not grow on SLA plates, which lack glutamate and arginine and therefore could not be tested here.
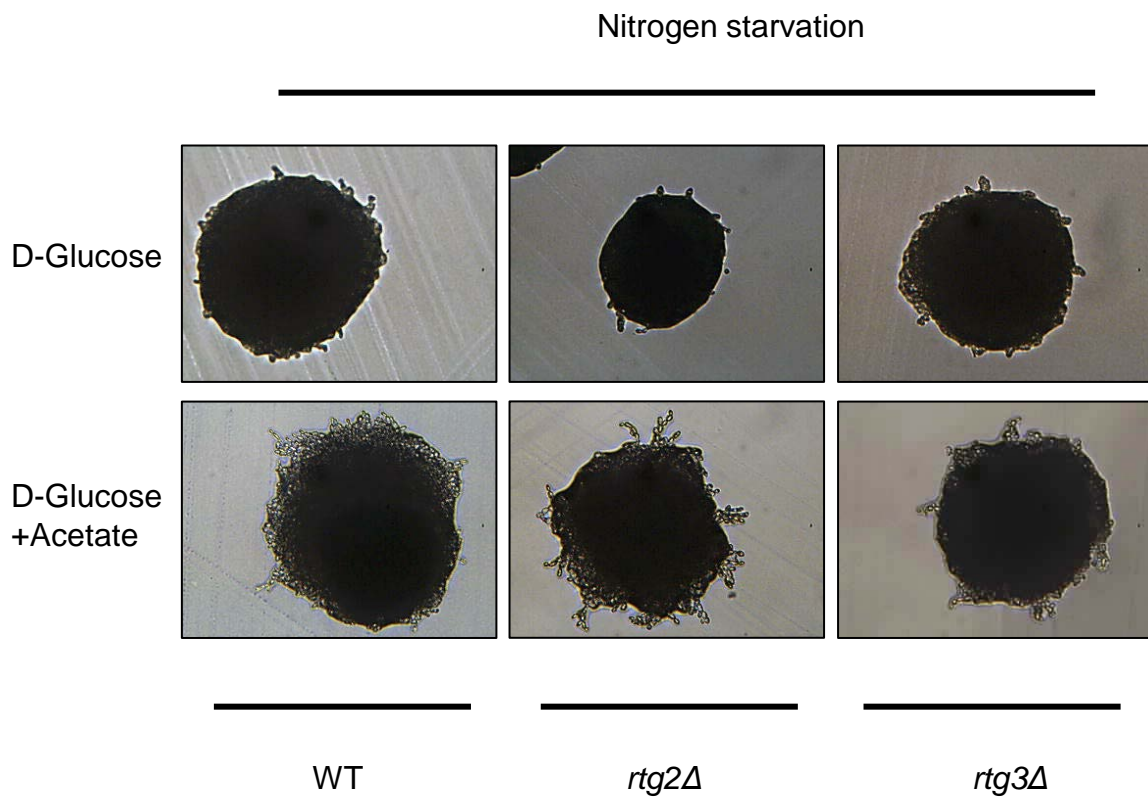
Figure 5.2 Role of RTG signalling pathway in induction of pseudohyphal growth on non-fermentable carbon source. Mitochondrial retrograde (RTG) signalling pathway mutants *rtg2Δ* and *rtg3Δ* strains were grown on nitrogen limiting conditions as in figure 6.1

5.3 Discussion

Non-fermentable carbon sources trigger pseudohyphal growth under nitrogen limiting conditions supplemented with glucose (**Figure 5.1**) in the SK1 genetic background. Stimulation of pseudohyphal growth in respiration deficient cells suggested that respiration function of the cell is not required for induction of pseudohyphal growth. These findings have partly been published in Strudwick et al, 2010. The difference in response to acetate stimuli in SK1 strain compared to Σ1278b strain is attributed differences in cyclic AMP (cAMP) signalling. Elevated cAMP signalling in Σ1278b background has been shown to inhibit pseudohyphal growth (Strich et al., 1994; Strudwick et al., 2010).

Deletion of mitochondrial RTG pathway components did not affect the enhanced growth stimulated by non-fermentable carbon sources (**Figure 5.2**). Pseudohyphal growth was unchanged when acetate was provided in addition to glucose in *rtg2Δ* and *rtg3Δ* indicating that RTG pathway may not be involved in regulation of pseudohyphal growth in the presence of non-fermentable carbon sources. The response to carbon source is regulated by a number of pathways but in the presence of glucose, utilization of alternate carbon sources is inhibited due to glucose repression. Non-fermentable carbon sources like ethanol and acetate are converted to acetyl-CoA which is catabolised by TCA cycle in mitochondria or assimilated in peroxisomes for gluconeogenesis. The *RTG* deletion strains growing on SLAD plates in the absence of glutamate indicates that glutamate prototrophy is achieved by expression of *ACO1*, *CIT1*, *CIT2*, *IDH1* and *IDH2* of TCA cycle and glyoxylate cycle, which are induced by *RTG* genes (Liao and Butow, 1993; Liu and Butow, 1999). The expression of genes, which encode the first three steps of the TCA cycle from oxaloacetate to α-ketoglutarate is under the regulation of Hap2-3-4-5p in full mitochondrial function, but switch their dependence to *RTG* genes in compromised mitochondrial function (Liu and Butow, 1999). When the cells respiratory function is reduced or lost these genes lose control by *HAP* genes and are under regulation by *RTG* genes. Glutamate negatively feeds back by inhibition of RTG signalling pathway. The dual regulation of early steps of TCA cycle by Hap2-3-4-5p and Rtg1-2-3p transcription complex allows cells to adapt to carbon source and mitochondrial state and ensures the availability of glutamate. Growth in glucose and acetate under nitrogen-limiting conditions despite deletion of *RTG* genes suggests that the Hap2-3-

4-5p complex regulates the expression of genes of first three steps of TCA cycle. Mitochondrial retrograde signalling pathway has been suggested to be a negative regulator of pseudohyphal growth in Σ1278b strain background (Jin et al., 2008). However, *rtg2Δ* and mitochondrial defect still induce intermediate pseudohyphal growth suggesting the possibility that other retrograde signalling pathways may be involved and cannot be excluded here (Epstein et al., 2001; Traven et al., 2001).

Table 5.1. Microarray data showing transcript profile in terms of raw intensity expressed from Σ1278b and SK1 genetic backgrounds (Strudwick et al., 2010).

Sr. No	Gene	Raw intensity	
		Σ1278b	SK1
1.	*CIT1*	-0.52	12.70
2.	*CIT2*	-0.91	13.20
3.	*DLD3*	-1.54	9.65
4.	*ACO1*	-0.41	12.78
5.	*IDH1*	-0.76	12.10
6.	*IDH2*	-0.97	12.19

Chapter 6

Conclusions and future work

6.1 Conclusions and future work:

In yeast *S. cerevisiae* the differentiation responses depend on the nutritional environment. Many studies have been carried out studying nitrogen starvation responses like meiosis and pseudohyphal growth. Nitrogen-rich conditions are known to repress these differentiation events in *S. cerevisiae*. In the current study the negative regulatory mechanism at early meiotic genes by Hac1[i]p in nitrogen-rich condition was investigated by using URS1-CYC1-Ub-X-lacZ reporters. **Figure 3.9** successfully demonstrates that Hac1[i]p negatively regulates at URS1 in nitrogen-rich conditions. The regulation of metabolic genes under nutrient rich conditions by Hac1[i]p, an important transcription factor of UPR signifies the importance of how UPR also functions as nutrient sensing pathway and thereby influencing the differentiation program. When the nitrogen is limiting, UPR is turned off and Hac1[i]p synthesis ceases. This can induce nitrogen starvation responses like pseudohyphal growth or meiosis based on the carbon source (**Figure 1.7**). When nitrogen is abundant, *HAC1* mRNA splicing is induced dramatically, repressing both the pathways. Therefore the information of nutritional state of the cell is sensed by UPR, which represses nitrogen starvation responses, promotes growth and decides the fate of developmental pathways. Hac1[i]p is a bZIP transcription factor, which activates transcription of genes containing UPR element and *INO1* gene (Chapman et al., 1998). According to the genome-wide two-hybrid interaction screen, Hac1[i]p does not interact with any other protein (Uetz et al., 2000). Future studies can be carried out to study mechanism of repression and targets of Hac1[i]p.

A poorly understood aspect of meiotic gene regulation is how transcriptional repression is maintained under nutrient rich conditions through URS1. The interactions between the URS1 regulatory element and its associating factors are complex. Experiments on individual mutants (*ume6Δ*, *rpd3Δ*, *sin3Δ*, *isw2Δ* and *itc1Δ*) of the mitotic repression machinery at URS1 under nitrogen rich conditions corroborate their role in regulation of early meiosis. These experiments also suggest regulation at additional sites in the minimal *CYC1* promoter other than URS1 of URS1-*CYC1*-Ub-X-*lacZ* reporters. Understanding regulation at UAS$_{CYC1}$ would be important in dissecting the transcriptional activity by Ume6p in core CYC1 promoter. Deletion of Rpd3p of *RPD3-SIN3* HDAC complex didn't considerably affect transcription at URS1, but deletion of Sin3p did suggesting that either Sin3p has

additional repressing functions or there are additional sites regulated by Sin3p (**Figure 4.2 and 4.3**). Identifying these additional sites could provide more insight into regulation at URS1-*CYC1*-Ub-X-*lacZ* reporter. This is useful, primarily because minimal CYC1 promoter is extensively used as heterologous promoter to study transcriptional regulation and other cell processes. Secondly these reporter systems have widespread uses in genetic screen and techniques like two-hybrid screen. URS1-CYC1-Ub-X-lacZ reporters constructed in this study show reduced steady state levels as compared to the WT β-galactosidase. These reporters are a technical advancement in the field of reporter system and can be widely used to study transcription. Rpd3p and Sin3p or Isw2p and Itc1p functions were separable as suggested by independent repression by Sin3p and Isw2p deletion. This will be useful to identify and understand the way deletion of proteins with stronger phenotypes act.

We tested the SK1 genetic background for pseudohyphal growth under nitrogen starvation conditions known to induce pseudohyphal growth. This induced moderate pseudohyphal growth due to glycolytic by products such as ethanol. Stimulation by nonfermentable carbon sources stimulated pseudohyphal growth and this stimulation didn't require the nonfermentable carbon source as respiratory energy source (**Figure 5.1B**). The results presented in **figure 5.2** also show that stimulation of pseudohyphal growth does not require mitochondrial RTG pathway. This work highlights the importance of different signaling cascades like MAPK signaling and cAMP signaling stimulated by different nutrient conditions. Studies on pathways functioning in pseudohyphal differentiation are important, because pathogenic yeasts also use these pathways for dimorphic switch to hyphal growth (Borges-Walmsley and Walmsley, 2000; Lengeler et al., 2000; Roman et al., 2007). The change to hyphal form is a virulence factor in many human and plant pathogenic yeasts. Insight into the signal transduction mechanisms that are necessary for the morphological change will contribute to an understanding of basic biological phenomena and of pathogenesis. Better understanding of these pathways and its elements can be used to develop novel drug targets.

A major challenge moving forward will be to better understand how simple eukaryotes such as yeast are able to precisely discriminate between different nutrient

signals and how they are able to generate a diversity of responses given that they use different but overlapping pathways in different contexts.

References

References:

Alén, C., Kent, N.A., Jones, H.S., O'Sullivan, J., Aranda, A. and Proudfoot, N.J. (2002) A role for chromatin remodeling in transcriptional termination by RNA polymerase II. *Mol Cell*, **10**, 1441-1452.

An, J.Y., Seo, J.W., Tasaki, T., Lee, M.J., Varshavsky, A. and Kwon, Y.T. (2006) Impaired neurogenesis and cardiovascular development in mice lacking the E3 ubiquitin ligases UBR1 and UBR2 of the N-end rule pathway. *Proc Natl Acad Sci U S A*, **103**, 6212-6217.

Anderson, S.F., Steber, C.M., Esposito, R.E. and Coleman, J.E. (1995) UME6, a negative regulator of meiosis in *Saccharomyces cerevisiae*, contains a C-terminal Zn_2Cys_6 binuclear cluster that binds the URS1 DNA sequence in a zinc-dependent manner. *Protein Sci*, **4**, 1832-1843.

Andreasson, C. and Ljungdahl, P.O. (2002) Receptor-mediated endoproteolytic activation of two transcription factors in yeast. *Genes Dev*, **16**, 3158-3172.

Aronova, S., Wedaman, K., Anderson, S., Yates, J., 3rd and Powers, T. (2007) Probing the membrane environment of the TOR kinases reveals functional interactions between TORC1, actin, and membrane trafficking in Saccharomyces cerevisiae. *Mol Biol Cell*, **18**, 2779-2794.

Ashrafi, K., Lin, S.S., Manchester, J.K. and Gordon, J.I. (2000) Sip2p and its partner snf1p kinase affect aging in S. cerevisiae. *Genes Dev*, **14**, 1872-1885.

Audhya, A., Loewith, R., Parsons, A.B., Gao, L., Tabuchi, M., Zhou, H., Boone, C., Hall, M.N. and Emr, S.D. (2004) Genome-wide lethality screen identifies new PI4,5P2 effectors that regulate the actin cytoskeleton. *Embo J*, **23**, 3747-3757.

Bachmair, A., Finley, D. and Varshavsky, A. (1986) In vivo half-life of a protein is a function of its amino-terminal residue. *Science*, **234**, 179-186.

Bachmair, A. and Varshavsky, A. (1989) The degradation signal in a short-lived protein. *Cell*, **56**, 1019-1032.

Back, S.H., Scheuner, D., Han, J., Song, B., Ribick, M., Wang, J., Gildersleeve, R.D., Pennathur, S. and Kaufman, R.J. (2009) Translation attenuation through eIF2alpha phosphorylation prevents oxidative stress and maintains the differentiated state in beta cells. *Cell Metab*, **10**, 13-26.

Baker, R.T., Tobias, J.W. and Varshavsky, A. (1992) Ubiquitin-specific proteases of Saccharomyces cerevisiae. Cloning of UBP2 and UBP3, and functional analysis of the UBP gene family. *J Biol Chem*, **267**, 23364-23375.

Baker, R.T. and Varshavsky, A. (1995) Yeast N-terminal amidase. A new enzyme and component of the N-end rule pathway. *J Biol Chem*, **270**, 12065-12074.

Balzi, E., Choder, M., Chen, W.N., Varshavsky, A. and Goffeau, A. (1990) Cloning and functional analysis of the arginyl-tRNA-protein transferase gene ATE1 of Saccharomyces cerevisiae. *J Biol Chem*, **265**, 7464-7471.

Bandyopadhyay, G.K., Yu, J.G., Ofrecio, J. and Olefsky, J.M. (2005) Increased p85/55/50 expression and decreased phosphotidylinositol 3-kinase activity in insulin-resistant human skeletal muscle. *Diabetes*, **54**, 2351-2359.

Bao, M.Z., Schwartz, M.A., Cantin, G.T., Yates, J.R., 3rd and Madhani, H.D. (2004) Pheromone-dependent destruction of the Tec1 transcription factor is required for MAP kinase signaling specificity in yeast. *Cell*, **119**, 991-1000.

Bardwell, L., Cook, J.G., Voora, D., Baggott, D.M., Martinez, A.R. and Thorner, J. (1998) Repression of yeast Ste12 transcription factor by direct binding of unphosphorylated Kss1 MAPK and its regulation by the Ste7 MEK. *Genes Dev*, **12**, 2887-2898.

Batlle, M., Lu, A., Green, D.A., Xue, Y. and Hirsch, J.P. (2003) Krh1p and Krh2p act downstream of the Gpa2p G(alpha) subunit to negatively regulate haploid invasive growth. *J Cell Sci*, **116**, 701-710.

Beck, T. and Hall, M.N. (1999) The TOR signalling pathway controls nuclear localization of nutrient-regulated transcription factors. *Nature*, **402**, 689-692.

Beeser, A.E. and Cooper, T.G. (2000) The dual-specificity protein phosphatase Yvh1p regulates sporulation, growth, and glycogen accumulation independently of catalytic activity in Saccharomyces cerevisiae via the cyclic AMP-dependent protein kinase cascade. *J Bacteriol*, **182**, 3517-3528.

Benjamin, K.R., Zhang, C., Shokat, K.M. and Herskowitz, I. (2003) Control of landmark events in meiosis by the CDK Cdc28 and the meiosis-specific kinase Ime2. *Genes Dev*, **17**, 1524-1539.

Bertolotti, A., Zhang, Y., Hendershot, L.M., Harding, H.P. and Ron, D. (2000) Dynamic interaction of BiP and ER stress transducers in the unfolded-protein response. *Nat Cell Biol*, **2**, 326-332.

Bianconi, M.L. (2003) Calorimetric determination of thermodynamic parameters of reaction reveals different enthalpic compensations of the yeast hexokinase isozymes. *J Biol Chem*, **278**, 18709-18713.

Bicknell, A.A., Babour, A., Federovitch, C.M. and Niwa, M. (2007) A novel role in cytokinesis reveals a housekeeping function for the unfolded protein response. *J Cell Biol*, **177**, 1017-1027.

Bilsland-Marchesan, E., Arino, J., Saito, H., Sunnerhagen, P. and Posas, F. (2000) Rck2 kinase is a substrate for the osmotic stress-activated mitogen-activated protein kinase Hog1. *Mol Cell Biol*, **20**, 3887-3895.

Birnboim, H.C. and Doly, J. (1979) A rapid alkaline extraction procedure for screening recombinant plasmid DNA. *Nucleic Acids Res*, **7**, 1513-1523.

Bloch, K.D. and Grossmann, B. (1995) Enzymatic manipulation of DNA and RNA. Restriction endonucleases. Digestion of DNA with restriction endonucleases. In Ausubel, F.M., Brent, R., Kingston, R.E., Moore, D.D., Seidman, C.E.,

Smith, J.A. and Struhl, K. (eds.), *Current Protocols in Molecular Biology*. John Wiley & Sons, New York, Vol. 1, pp. 3.1.1-21.

Boeckstaens, M., Andre, B. and Marini, A.M. (2007) The yeast ammonium transport protein Mep2 and its positive regulator, the Npr1 kinase, play an important role in normal and pseudohyphal growth on various nitrogen media through retrieval of excreted ammonium. *Mol Microbiol*, **64**, 534-546.

Bolte, M., Steigemann, P., Braus, G.H. and Irniger, S. (2002) Inhibition of APC-mediated proteolysis by the meiosis-specific protein kinase Ime2. *Proc Natl Acad Sci U S A*, **99**, 4385-4390.

Bonifacino, J.S., Dell'Angelica, E.C. and Springer, T.A. (1999) Analysis of proteins. Immunoprecipitation. In Ausubel, F.M., Brent, R., Kingston, R.E., Moore, D.D., Seidman, C.E., Smith, J.A. and Struhl, K. (eds.), *Current Protocols in Molecular Biology*. John Wiley & Sons, New York, Vol. 2, pp. 10.16.11-29.

Borges-Walmsley, M.I. and Walmsley, A.R. (2000) cAMP signalling in pathogenic fungi: control of dimorphic switching and pathogenicity. *Trends Microbiol*, **8**, 133-141.

Boss, J.M., Darrow, M.D. and Zitomer, R.S. (1980) Characterization of yeast iso-1-cytochrome c mRNA. *J Biol Chem*, **255**, 8623-8628.

Bowdish, K.S. and Mitchell, A.P. (1993) Bipartite structure of an early meiotic upstream activation sequence from Saccharomyces cerevisiae. *Mol Cell Biol*, **13**, 2172-2181.

Bowdish, K.S., Yuan, H.E. and Mitchell, A.P. (1995) Positive control of yeast meiotic genes by the negative regulator UME6. *Mol Cell Biol*, **15**, 2955-2961.

Broach, J.R. and Deschenes, R.J. (1990) The function of ras genes in Saccharomyces cerevisiae. *Adv Cancer Res*, **54**, 79-139.

Brush, M.H., Weiser, D.C. and Shenolikar, S. (2003) Growth arrest and DNA damage-inducible protein GADD34 targets protein phosphatase 1 alpha to the endoplasmic reticulum and promotes dephosphorylation of the alpha subunit of eukaryotic translation initiation factor 2. *Mol Cell Biol*, **23**, 1292-1303.

Bultynck, G., Heath, V.L., Majeed, A.P., Galan, J.M., Haguenauer-Tsapis, R. and Cyert, M.S. (2006) Slm1 and slm2 are novel substrates of the calcineurin phosphatase required for heat stress-induced endocytosis of the yeast uracil permease. *Mol Cell Biol*, **26**, 4729-4745.

Burgess, S.M., Ajimura, M. and Kleckner, N. (1999) GCN5-dependent histone H3 acetylation and RPD3-dependent histone H4 deacetylation have distinct, opposing effects on IME2 transcription, during meiosis and during vegetative growth, in budding yeast. *Proc Natl Acad Sci U S A*, **96**, 6835-6840.

Butow, R.A. and Avadhani, N.G. (2004) Mitochondrial signaling: the retrograde response. *Mol Cell*, **14**, 1-15.

Calfon, M., Zeng, H., Urano, F., Till, J.H., Hubbard, S.R., Harding, H.P., Clark, S.G. and Ron, D. (2002) IRE1 couples endoplasmic reticulum load to secretory capacity by processing the XBP-1 mRNA. *Nature*, **415**, 92-96.

Cardenas, M.E., Cutler, N.S., Lorenz, M.C., Di Como, C.J. and Heitman, J. (1999) The TOR signaling cascade regulates gene expression in response to nutrients. *Genes Dev*, **13**, 3271-3279.

Carrozza, M.J., Florens, L., Swanson, S.K., Shia, W.J., Anderson, S., Yates, J., Washburn, M.P. and Workman, J.L. (2005) Stable incorporation of sequence specific repressors Ash1 and Ume6 into the Rpd3L complex. *Biochim Biophys Acta*, **1731**, 77-87; discussion 75-76.

Casagrande, R., Stern, P., Diehn, M., Shamu, C., Osario, M., Zuniga, M., Brown, P.O. and Ploegh, H. (2000) Degradation of proteins from the ER of S. cerevisiae requires an intact unfolded protein response pathway. *Mol Cell*, **5**, 729-735.

Chapman, R., Sidrauski, C. and Walter, P. (1998) Intracellular signaling from the endoplasmic reticulum to the nucleus. *Annu Rev Cell Dev Biol*, **14**, 459-485.

Chapman, R.E. and Walter, P. (1997) Translational attenuation mediated by an mRNA intron. *Curr Biol*, **7**, 850-859.

Chavel, C.A., Dionne, H.M., Birkaya, B., Joshi, J. and Cullen, P.J. (2010) Multiple signals converge on a differentiation MAPK pathway. *PLoS Genet*, **6**, e1000883.

Cheatham, B., Vlahos, C.J., Cheatham, L., Wang, L., Blenis, J. and Kahn, C.R. (1994) Phosphatidylinositol 3-kinase activation is required for insulin stimulation of pp70 S6 kinase, DNA synthesis, and glucose transporter translocation. *Mol Cell Biol*, **14**, 4902-4911.

Chelstowska, A. and Butow, R.A. (1995) RTG genes in yeast that function in communication between mitochondria and the nucleus are also required for expression of genes encoding peroxisomal proteins. *J Biol Chem*, **270**, 18141-18146.

Chen, D.C., Yang, B.C. and Kuo, T.T. (1992) One-step transformation of yeast in stationary phase. *Curr Genet*, **21**, 83-84.

Chen, E.J. and Kaiser, C.A. (2003) LST8 negatively regulates amino acid biosynthesis as a component of the TOR pathway. *J Cell Biol*, **161**, 333-347.

Chen, H. and Fink, G.R. (2006) Feedback control of morphogenesis in fungi by aromatic alcohols. *Genes Dev*, **20**, 1150-1161.

Chen, R.E. and Thorner, J. (2010) Systematic Epistasis Analysis of the Contributions of PKA- and MAPK-dependent Signaling to Nutrient Limitation-evoked responses in the Yeast Saccharomyces cerevisiae. *Genetics*.

Chen, X., Shen, J. and Prywes, R. (2002) The luminal domain of ATF6 senses endoplasmic reticulum (ER) stress and causes translocation of ATF6 from the ER to the Golgi. *J Biol Chem*, **277**, 13045-13052.

Cherepanov, A.V. and de Vries, S. (2001) Binding of nucleotides by T4 DNA ligase and T4 RNA ligase: optical absorbance and fluorescence studies. *Biophys J*, **81**, 3545-3559.

Cherkasova, V.A. and Hinnebusch, A.G. (2003) Translational control by TOR and TAP42 through dephosphorylation of eIF2alpha kinase GCN2. *Genes Dev*, **17**, 859-872.

Choi, K.Y., Satterberg, B., Lyons, D.M. and Elion, E.A. (1994) Ste5 tethers multiple protein kinases in the MAP kinase cascade required for mating in S. cerevisiae. *Cell*, **78**, 499-512.

Chou, S., Huang, L. and Liu, H. (2004) Fus3-regulated Tec1 degradation through SCFCdc4 determines MAPK signaling specificity during mating in yeast. *Cell*, **119**, 981-990.

Chu, S., DeRisi, J., Eisen, M., Mulholland, J., Botstein, D., Brown, P.O. and Herskowitz, I. (1998) The transcriptional program of sporulation in budding yeast. *Science*, **282**, 699-705.

Clancy, M.J., Shambaugh, M.E., Timpte, C.S. and Bokar, J.A. (2002) Induction of sporulation in Saccharomyces cerevisiae leads to the formation of N6-methyladenosine in mRNA: a potential mechanism for the activity of the IME4 gene. *Nucleic Acids Res*, **30**, 4509-4518.

Clifton, D., Walsh, R.B. and Fraenkel, D.G. (1993) Functional studies of yeast glucokinase. *J Bacteriol*, **175**, 3289-3294.

Coffman, J.A., Rai, R., Cunningham, T., Svetlov, V. and Cooper, T.G. (1996) Gat1p, a GATA family protein whose production is sensitive to nitrogen catabolite repression, participates in transcriptional activation of nitrogen-catabolic genes in Saccharomyces cerevisiae. *Mol Cell Biol*, **16**, 847-858.

Colomina, N., Gari, E., Gallego, C., Herrero, E. and Aldea, M. (1999) G1 cyclins block the Ime1 pathway to make mitosis and meiosis incompatible in budding yeast. *Embo J*, **18**, 320-329.

Cooper, T.G. (2002) Transmitting the signal of excess nitrogen in Saccharomyces cerevisiae from the Tor proteins to the GATA factors: connecting the dots. *FEMS Microbiol Rev*, **26**, 223-238.

Cormack, B. (1997) Mutagenesis of cloned DNA. Directed mutagenesis using the polymerase chain reaction. In Ausubel, F.M., Brent, R., Kingston, R.E., Moore, D.D., Seidman, C.E., Smith, J.A. and Struhl, K. (eds.), *Current Protocols in Molecular Biology*. John Wiley & Sons, New York, Vol. 1, pp. 8.5.1-10.

Covitz, P.A., Herskowitz, I. and Mitchell, A.P. (1991) The yeast RME1 gene encodes a putative zinc finger protein that is directly repressed by a1-alpha 2. *Genes Dev*, **5**, 1982-1989.

Covitz, P.A. and Mitchell, A.P. (1993) Repression by the yeast meiotic inhibitor RME1. *Genes Dev*, **7**, 1598-1608.

Cox, J.S., Chapman, R.E. and Walter, P. (1997) The unfolded protein response coordinates the production of endoplasmic reticulum protein and endoplasmic reticulum membrane. *Mol Biol Cell*, **8**, 1805-1814.

Cox, J.S. and Walter, P. (1996) A novel mechanism for regulating activity of a transcription factor that controls the unfolded protein response. *Cell*, **87**, 391-404.

Crespo, J.L., Powers, T., Fowler, B. and Hall, M.N. (2002) The TOR-controlled transcription activators GLN3, RTG1, and RTG3 are regulated in response to intracellular levels of glutamine. *Proc Natl Acad Sci U S A*, **99**, 6784-6789.

Cullen, P.J., Sabbagh, W., Jr., Graham, E., Irick, M.M., van Olden, E.K., Neal, C., Delrow, J., Bardwell, L. and Sprague, G.F., Jr. . (2004) A signaling mucin at the head of the Cdc42- and MAPK-dependent filamentous growth pathway in yeast. *Genes Dev*, **18**, 1695-1708.

Cusi, K., Maezono, K., Osman, A., Pendergrass, M., Patti, M.E., Pratipanawatr, T., DeFronzo, R.A., Kahn, C.R. and Mandarino, L.J. (2000) Insulin resistance differentially affects the PI 3-kinase- and MAP kinase-mediated signaling in human muscle. *J Clin Invest*, **105**, 311-320.

Cutler, N.S., Pan, X., Heitman, J. and Cardenas, M.E. (2001) The TOR signal transduction cascade controls cellular differentiation in response to nutrients. *Mol Biol Cell*, **12**, 4103-4113.

Daquinag, A., Fadri, M., Jung, S.Y., Qin, J. and Kunz, J. (2007) The yeast PH domain proteins Slm1 and Slm2 are targets of sphingolipid signaling during the response to heat stress. *Mol Cell Biol*, **27**, 633-650.

Davenport, K.D., Williams, K.E., Ullmann, B.D. and Gustin, M.C. (1999) Activation of the Saccharomyces cerevisiae filamentation/invasion pathway by osmotic stress in high-osmolarity glycogen pathway mutants. *Genetics*, **153**, 1091-1103.

Davydov, I.V. and Varshavsky, A. (2000) RGS4 is arginylated and degraded by the N-end rule pathway in vitro. *J Biol Chem*, **275**, 22931-22941.

De Nadal, E., Zapater, M., Alepuz, P.M., Sumoy, L., Mas, G. and Posas, F. (2004) The MAPK Hog1 recruits Rpd3 histone deacetylase to activate osmoresponsive genes. *Nature*, **427**, 370-374.

De Silva-Udawatta, M.N. and Cannon, J.F. (2001) Roles of trehalose phosphate synthase in yeast glycogen metabolism and sporulation. *Mol Microbiol*, **40**, 1345-1356.

Deng, C. and Saunders, W.S. (2001) RIM4 encodes a meiotic activator required for early events of meiosis in Saccharomyces cerevisiae. *Mol Genet Genomics*, **266**, 497-504.

Deng, J., Lu, P.D., Zhang, Y., Scheuner, D., Kaufman, R.J., Sonenberg, N., Harding, H.P. and Ron, D. (2004) Translational repression mediates activation of nuclear factor kappa B by phosphorylated translation initiation factor 2. *Mol Cell Biol*, **24**, 10161-10168.

Dever, T.E. (2002) Gene-specific regulation by general translation factors. *Cell*, **108**, 545-556.

Dickinson, J.R. (1996) 'Fusel' alcohols induce hyphal-like extensions and pseudohyphal formation in yeasts. *Microbiology*, **142 (Pt 6)**, 1391-1397.

Dilova, I., Chen, C.Y. and Powers, T. (2002) Mks1 in concert with TOR signaling negatively regulates RTG target gene expression in S. cerevisiae. *Curr Biol*, **12**, 389-395.

Dirick, L., Goetsch, L., Ammerer, G. and Byers, B. (1998) Regulation of meiotic S phase by Ime2 and a Clb5,6-associated kinase in Saccharomyces cerevisiae. *Science*, **281**, 1854-1857.

Ditzel, M., Wilson, R., Tenev, T., Zachariou, A., Paul, A., Deas, E. and Meier, P. (2003) Degradation of DIAP1 by the N-end rule pathway is essential for regulating apoptosis. *Nat Cell Biol*, **5**, 467-473.

Donaton, M.C., Holsbeeks, I., Lagatie, O., Van Zeebroeck, G., Crauwels, M., Winderickx, J. and Thevelein, J.M. (2003) The Gap1 general amino acid permease acts as an amino acid sensor for activation of protein kinase A targets in the yeast Saccharomyces cerevisiae. *Mol Microbiol*, **50**, 911-929.

Donzeau, M. and Bandlow, W. (1999) The yeast trimeric guanine nucleotide-binding protein alpha subunit, Gpa2p, controls the meiosis-specific kinase Ime2p activity in response to nutrients. *Mol Cell Biol*, **19**, 6110-6119.

Draznin, B. (2006) Molecular mechanisms of insulin resistance: serine phosphorylation of insulin receptor substrate-1 and increased expression of p85alpha: the two sides of a coin. *Diabetes*, **55**, 2392-2397.

Duvel, K., Santhanam, A., Garrett, S., Schneper, L. and Broach, J.R. (2003) Multiple roles of Tap42 in mediating rapamycin-induced transcriptional changes in yeast. *Mol Cell*, **11**, 1467-1478.

Ehrentraut, S., Weber, J.M., Dybowski, J.N., Hoffmann, D. and Ehrenhofer-Murray, A.E. (2010) Rpd3-dependent boundary formation at telomeres by removal of Sir2 substrate. *Proc Natl Acad Sci U S A*, **107**, 5522-5527.

Einerhand, A.W., Kos, W., Smart, W.C., Kal, A.J., Tabak, H.F. and Cooper, T.G. (1995) The upstream region of the FOX3 gene encoding peroxisomal 3-oxoacyl-coenzyme A thiolase in Saccharomyces cerevisiae contains ABF1-

and replication protein A-binding sites that participate in its regulation by glucose repression. *Mol Cell Biol*, **15**, 3405-3414.

Eizirik, D.L., Cardozo, A.K. and Cnop, M. (2008) The role for endoplasmic reticulum stress in diabetes mellitus. *Endocr Rev,* **29**, 42-61.

Elbing, K. and Brent, R. (2002) *Escherichia coli*, plasmids, and bacteriophages. *Escherichia coli.* Growth in liquid media. In Ausubel, F.M., Brent, R., Kingston, R.E., Moore, D.D., Seidman, C.E., Smith, J.A. and Struhl, K. (eds.), *Current Protocols in Molecular Biology.* John Wiley & Sons, New York, Vol. 1, pp. 1.2.1-2.

Elouil, H., Bensellam, M., Guiot, Y., Vander Mierde, D., Pascal, S.M., Schuit, F.C. and Jonas, J.C. (2007) Acute nutrient regulation of the unfolded protein response and integrated stress response in cultured rat pancreatic islets. *Diabetologia*, **50**, 1442-1452.

Epstein, C.B., Waddle, J.A., Hale, W.t., Dave, V., Thornton, J., Macatee, T.L., Garner, H.R. and Butow, R.A. (2001) Genome-wide responses to mitochondrial dysfunction. *Mol Biol Cell*, **12**, 297-308.

Erdman, S., Lin, L., Malczynski, M. and Snyder, M. (1998) Pheromone-regulated genes required for yeast mating differentiation. *J Cell Biol*, **140**, 461-483.

Escote, X., Zapater, M., Clotet, J. and Posas, F. (2004) Hog1 mediates cell-cycle arrest in G1 phase by the dual targeting of Sic1. *Nat Cell Biol*, **6**, 997-1002.

Esposito, M.S. and Esposito, R.E. (1974) Genes controlling meiosis and spore formation in yeast. *Genetics*, **78**, 215-225.

Fadri, M., Daquinag, A., Wang, S., Xue, T. and Kunz, J. (2005) The pleckstrin homology domain proteins Slm1 and Slm2 are required for actin cytoskeleton organization in yeast and bind phosphatidylinositol-4,5-bisphosphate and TORC2. *Mol Biol Cell*, **16**, 1883-1900.

Fazzio, T.G., Kooperberg, C., Goldmark, J.P., Neal, C., Basom, R., Delrow, J. and Tsukiyama, T. (2001) Widespread collaboration of Isw2 and Sin3-Rpd3 chromatin remodeling complexes in transcriptional repression. *Mol Cell Biol*, **21**, 6450-6460.

Fazzio, T.G. and Tsukiyama, T. (2003) Chromatin remodeling in vivo: evidence for a nucleosome sliding mechanism. *Mol Cell*, **12**, 1333-1340.

Fitzgerald, D.J., DeLuca, C., Berger, I., Gaillard, H., Sigrist, R., Schimmele, K. and Richmond, T.J. (2004) Reaction cycle of the yeast Isw2 chromatin remodeling complex. *Embo J*, **23**, 3836-3843.

Foiani, M., Nadjar-Boger, E., Capone, R., Sagee, S., Hashimshoni, T. and Kassir, Y. (1996) A meiosis-specific protein kinase, Ime2, is required for the correct timing of DNA replication and for spore formation in yeast meiosis. *Mol Gen Genet*, **253**, 278-288.

Fonseca, S.G., Lipson, K.L. and Urano, F. (2007) Endoplasmic reticulum stress signaling in pancreatic beta-cells. *Antioxid Redox Signal*, **9**, 2335-2344.

Forsberg, H. and Ljungdahl, P.O. (2001) Sensors of extracellular nutrients in Saccharomyces cerevisiae. *Curr Genet*, **40**, 91-109.

Fox, T.D., Folley, L.S., Mulero, J.J., McMullin, T.W., Thorsness, P.E., Hedin, L.O. and Costanzo, M.C. (1991) Analysis and manipulation of yeast mitochondrial genes. *Methods Enzymol*, **194**, 149-165.

Friedlander, G., Joseph-Strauss, D., Carmi, M., Zenvirth, D., Simchen, G. and Barkai, N. (2006) Modulation of the transcription regulatory program in yeast cells committed to sporulation. *Genome Biol*, **7**, R20.

Friedlander, R., Jarosch, E., Urban, J., Volkwein, C. and Sommer, T. (2000) A regulatory link between ER-associated protein degradation and the unfolded-protein response. *Nat Cell Biol*, **2**, 379-384.

Fujita, A., Tonouchi, A., Hiroko, T., Inose, F., Nagashima, T., Satoh, R. and Tanaka, S. (1999) Hsl7p, a negative regulator of Ste20p protein kinase in the Saccharomyces cerevisiae filamentous growth-signaling pathway. *Proc Natl Acad Sci U S A*, **96**, 8522-8527.

Gailus-Durner, V., Xie, J., Chintamaneni, C. and Vershon, A.K. (1996) Participation of the yeast activator Abf1 in meiosis-specific expression of the HOP1 gene. *Mol Cell Biol*, **16**, 2777-2786.

Gallagher, S.R. (1999) Analysis of proteins. One-dimensional SDS gel electrophoresis of proteins. In Ausubel, F.M., Brent, R., Kingston, R.E., Moore, D.D., Seidman, C.E., Smith, J.A. and Struhl, K. (eds.), *Current Protocols in Molecular Biology*. John Wiley & Sons, New York, Vol. 2, pp. 10.12A.11-34.

Gallagher, S.R., Winston, S.E., Fuller, S.A. and Hurrell, J.G.R. (1997) Analysis of proteins. Detection of proteins. Immunoblotting and immunodetection. In Ausubel, F.M., Brent, R., Kingston, R.E., Moore, D.D., Seidman, C.E., Smith, J.A. and Struhl, K. (eds.), *Current Protocols in Molecular Biology*. John Wiley & Sons, New York, Vol. 2, pp. 10.18.11-21.

Gallego, C., Gari, E., Colomina, N., Herrero, E. and Aldea, M. (1997) The Cln3 cyclin is down-regulated by translational repression and degradation during the G1 arrest caused by nitrogen deprivation in budding yeast. *Embo J*, **16**, 7196-7206.

Gancedo, J.M. (1998) Yeast carbon catabolite repression. *Microbiol Mol Biol Rev*, **62**, 334-361.

Gancedo, J.M. (2001) Control of pseudohyphae formation in Saccharomyces cerevisiae. *FEMS Microbiol Rev*, **25**, 107-123.

Garreau, H., Hasan, R.N., Renault, G., Estruch, F., Boy-Marcotte, E. and Jacquet, M. (2000) Hyperphosphorylation of Msn2p and Msn4p in response to heat shock

and the diauxic shift is inhibited by cAMP in Saccharomyces cerevisiae. *Microbiology*, **146 (Pt 9)**, 2113-2120.

Gelbart, M.E., Rechsteiner, T., Richmond, T.J. and Tsukiyama, T. (2001) Interactions of Isw2 chromatin remodeling complex with nucleosomal arrays: analyses using recombinant yeast histones and immobilized templates. *Mol Cell Biol*, **21**, 2098-2106.

Gimeno, C.J. and Fink, G.R. (1994) Induction of pseudohyphal growth by overexpression of PHD1, a Saccharomyces cerevisiae gene related to transcriptional regulators of fungal development. *Mol Cell Biol*, **14**, 2100-2112.

Gimeno, C.J., Ljungdahl, P.O., Styles, C.A. and Fink, G.R. (1992) Unipolar cell divisions in the yeast S. cerevisiae lead to filamentous growth: regulation by starvation and RAS. *Cell*, **68**, 1077-1090.

Goldmark, J.P., Fazzio, T.G., Estep, P.W., Church, G.M. and Tsukiyama, T. (2000) The Isw2 chromatin remodeling complex represses early meiotic genes upon recruitment by Ume6p. *Cell*, **103**, 423-433.

Gonda, D.K., Bachmair, A., Wunning, I., Tobias, J.W., Lane, W.S. and Varshavsky, A. (1989) Universality and structure of the N-end rule. *J Biol Chem*, **264**, 16700-16712.

Gonzales, J.C., Gentile, C.L., Pfaffenbach, K.T., Wei, Y., Wang, D. and Pagliassotti, M.J. (2008) Chemical induction of the unfolded protein response in the liver increases glucose production and is activated during insulin-induced hypoglycaemia in rats. *Diabetologia*, **51**, 1920-1929.

Good, M., Tang, G., Singleton, J., Remenyi, A. and Lim, W.A. (2009) The Ste5 scaffold directs mating signaling by catalytically unlocking the Fus3 MAP kinase for activation. *Cell*, **136**, 1085-1097.

Graciet, E., Walter, F., Maoileidigh, D.O., Pollmann, S., Meyerowitz, E.M., Varshavsky, A. and Wellmer, F. (2009) The N-end rule pathway controls multiple functions during Arabidopsis shoot and leaf development. *Proc Natl Acad Sci U S A*.

Granot, D., Margolskee, J.P. and Simchen, G. (1989) A long region upstream of the IME1 gene regulates meiosis in yeast. *Mol Gen Genet*, **218**, 308-314.

Greenman, I.C., Gomez, E., Moore, C.E. and Herbert, T.P. (2007) Distinct glucose-dependent stress responses revealed by translational profiling in pancreatic beta-cells. *J Endocrinol*, **192**, 179-187.

Gregor, M.F., Yang, L., Fabbrini, E., Mohammed, B.S., Eagon, J.C., Hotamisligil, G.S. and Klein, S. (2009) Endoplasmic reticulum stress is reduced in tissues of obese subjects after weight loss. *Diabetes*, **58**, 693-700.

Guarente, L. and Hoar, E. (1984) Upstream activation sites of the CYC1 gene of Saccharomyces cerevisiae are active when inverted but not when placed downstream of the "TATA box". *Proc Natl Acad Sci U S A*, **81**, 7860-7864.

Guarente, L. and Mason, T. (1983) Heme regulates transcription of the CYC1 gene of S. cerevisiae via an upstream activation site. *Cell*, **32**, 1279-1286.

Gustin, M.C., Albertyn, J., Alexander, M. and Davenport, K. (1998) MAP kinase pathways in the yeast Saccharomyces cerevisiae. *Microbiol Mol Biol Rev*, **62**, 1264-1300.

Guttmann-Raviv, N., Boger-Nadjar, E., Edri, I. and Kassir, Y. (2001) Cdc28 and Ime2 possess redundant functions in promoting entry into premeiotic DNA replication in Saccharomyces cerevisiae. *Genetics*, **159**, 1547-1558.

Guttmann-Raviv, N., Martin, S. and Kassir, Y. (2002) Ime2, a meiosis-specific kinase in yeast, is required for destabilization of its transcriptional activator, Ime1. *Mol Cell Biol*, **22**, 2047-2056.

Hall, J.P., Cherkasova, V., Elion, E., Gustin, M.C. and Winter, E. (1996) The osmoregulatory pathway represses mating pathway activity in Saccharomyces cerevisiae: isolation of a FUS3 mutant that is insensitive to the repression mechanism. *Mol Cell Biol*, **16**, 6715-6723.

Hao, N., Nayak, S., Behar, M., Shanks, R.H., Nagiec, M.J., Errede, B., Hasty, J., Elston, T.C. and Dohlman, H.G. (2008) Regulation of cell signaling dynamics by the protein kinase-scaffold Ste5. *Mol Cell*, **30**, 649-656.

Harashima, T., Anderson, S., Yates, J.R., 3rd and Heitman, J. (2006) The kelch proteins Gpb1 and Gpb2 inhibit Ras activity via association with the yeast RasGAP neurofibromin homologs Ira1 and Ira2. *Mol Cell*, **22**, 819-830.

Harding, H.P., Zhang, Y., Bertolotti, A., Zeng, H. and Ron, D. (2000) Perk is essential for translational regulation and cell survival during the unfolded protein response. *Mol Cell*, **5**, 897-904.

Harding, H.P., Zhang, Y. and Ron, D. (1999) Protein translation and folding are coupled by an endoplasmic-reticulum-resident kinase. *Nature*, **397**, 271-274.

Hardwick, J.S., Kuruvilla, F.G., Tong, J.K., Shamji, A.F. and Schreiber, S.L. (1999) Rapamycin-modulated transcription defines the subset of nutrient-sensitive signaling pathways directly controlled by the Tor proteins. *Proc Natl Acad Sci U S A*, **96**, 14866-14870.

Harris, K., Lamson, R.E., Nelson, B., Hughes, T.R., Marton, M.J., Roberts, C.J., Boone, C. and Pryciak, P.M. (2001) Role of scaffolds in MAP kinase pathway specificity revealed by custom design of pathway-dedicated signaling proteins. *Curr Biol*, **11**, 1815-1824.

Haze, K., Yoshida, H., Yanagi, H., Yura, T. and Mori, K. (1999) Mammalian transcription factor ATF6 is synthesized as a transmembrane protein and activated by proteolysis in response to endoplasmic reticulum stress. *Mol Biol Cell*, **10**, 3787-3799.

Herbach, N., Rathkolb, B., Kemter, E., Pichl, L., Klaften, M., de Angelis, M.H., Halban, P.A., Wolf, E., Aigner, B. and Wanke, R. (2007) Dominant-negative

effects of a novel mutated Ins2 allele causes early-onset diabetes and severe beta-cell loss in Munich Ins2C95S mutant mice. *Diabetes*, **56**, 1268-1276.

Herman, P.K. and Rine, J. (1997) Yeast spore germination: a requirement for Ras protein activity during re-entry into the cell cycle. *Embo J*, **16**, 6171-6181.

Herschkovitz, A., Liu, Y.F., Ilan, E., Ronen, D., Boura-Halfon, S. and Zick, Y. (2007) Common inhibitory serine sites phosphorylated by IRS-1 kinases, triggered by insulin and inducers of insulin resistance. *J Biol Chem*, **282**, 18018-18027.

Herskowitz, I. (1988) Life cycle of the budding yeast Saccharomyces cerevisiae. *Microbiol Rev*, **52**, 536-553.

Herskowitz, I., Rine, J. and Strathern, J.N. (1992) Mating-type determination and mating-type interconversion in Saccharomyces cerevisiae. In Pringle, J.R., Broach, J.R. and Jones, E.W. (eds.), *The Molecular and Cellular Biology of the Yeast Saccharomyces: Gene Expression*. Cold Spring Harbor Laboratory Press, Plainview, N.Y., Vol. 2, pp. 583-656.

Hetz, C., Bernasconi, P., Fisher, J., Lee, A.H., Bassik, M.C., Antonsson, B., Brandt, G.S., Iwakoshi, N.N., Schinzel, A., Glimcher, L.H. and Korsmeyer, S.J. (2006) Proapoptotic BAX and BAK modulate the unfolded protein response by a direct interaction with IRE1alpha. *Science*, **312**, 572-576.

Heydrick, S.J., Gautier, N., Olichon-Berthe, C., Van Obberghen, E. and Le Marchand-Brustel, Y. (1995) Early alteration of insulin stimulation of PI 3-kinase in muscle and adipocyte from gold thioglucose obese mice. *Am J Physiol*, **268**, E604-612.

Hinnebusch, A.G. (2005) Translational regulation of GCN4 and the general amino acid control of yeast. *Annu Rev Microbiol*, **59**, 407-450.

Hinnebusch, A.G. and Natarajan, K. (2002) Gcn4p, a master regulator of gene expression, is controlled at multiple levels by diverse signals of starvation and stress. *Eukaryot Cell*, **1**, 22-32.

Hirschberg, J. and Simchen, G. (1977) Commitment to the mitotic cell cycle in yeast in relation to meiosis. *Exp Cell Res*, **105**, 245-252.

Hofman-Bang, J. (1999) Nitrogen catabolite repression in Saccharomyces cerevisiae. *Mol Biotechnol*, **12**, 35-73.

Hohmann, S. (2002) Osmotic stress signaling and osmoadaptation in yeasts. *Microbiol Mol Biol Rev*, **66**, 300-372.

Hollenhorst, P.C., Bose, M.E., Mielke, M.R., Muller, U. and Fox, C.A. (2000) Forkhead genes in transcriptional silencing, cell morphology and the cell cycle. Overlapping and distinct functions for FKH1 and FKH2 in Saccharomyces cerevisiae. *Genetics*, **154**, 1533-1548.

Hollien, J., Lin, J.H., Li, H., Stevens, N., Walter, P. and Weissman, J.S. (2009) Regulated Ire1-dependent decay of messenger RNAs in mammalian cells. *J Cell Biol*, **186**, 323-331.

Hong, S.P., Leiper, F.C., Woods, A., Carling, D. and Carlson, M. (2003) Activation of yeast Snf1 and mammalian AMP-activated protein kinase by upstream kinases. *Proc Natl Acad Sci U S A*, **100**, 8839-8843.

Hongay, C.F., Grisafi, P.L., Galitski, T. and Fink, G.R. (2006) Antisense transcription controls cell fate in Saccharomyces cerevisiae. *Cell*, **127**, 735-745.

Honigberg, S.M. (2004) Ime2p and Cdc28p: co-pilots driving meiotic development. *J Cell Biochem*, **92**, 1025-1033.

Honigberg, S.M., Conicella, C. and Espositio, R.E. (1992) Commitment to meiosis in Saccharomyces cerevisiae: involvement of the SPO14 gene. *Genetics*, **130**, 703-716.

Honigberg, S.M. and Esposito, R.E. (1994) Reversal of cell determination in yeast meiosis: postcommitment arrest allows return to mitotic growth. *Proc Natl Acad Sci U S A*, **91**, 6559-6563.

Honigberg, S.M. and Purnapatre, K. (2003) Signal pathway integration in the switch from the mitotic cell cycle to meiosis in yeast. *J Cell Sci*, **116**, 2137-2147.

Hori, O., Ichinoda, F., Yamaguchi, A., Tamatani, T., Taniguchi, M., Koyama, Y., Katayama, T., Tohyama, M., Stern, D.M., Ozawa, K., Kitao, Y. and Ogawa, S. (2004) Role of Herp in the endoplasmic reticulum stress response. *Genes Cells*, **9**, 457-469.

Hortner, H., Ammerer, G., Hartter, E., Hamilton, B., Rytka, J., Bilinski, T. and Ruis, H. (1982) Regulation of synthesis of catalases and iso-1-cytochrome c in Saccharomyces cerevisiae by glucose, oxygen and heme. *Eur J Biochem*, **128**, 179-184.

Hotamisligil, G.S. (2006) Inflammation and metabolic disorders. *Nature*, **444**, 860-867.

Hu, R.G., Brower, C.S., Wang, H., Davydov, I.V., Sheng, J., Zhou, J., Kwon, Y.T. and Varshavsky, A. (2006) Arginyltransferase, its specificity, putative substrates, bidirectional promoter, and splicing-derived isoforms. *J Biol Chem*, **281**, 32559-32573.

Hu, R.G., Sheng, J., Qi, X., Xu, Z., Takahashi, T.T. and Varshavsky, A. (2005) The N-end rule pathway as a nitric oxide sensor controlling the levels of multiple regulators. *Nature*, **437**, 981-986.

Huang, C.J., Lin, C.Y., Haataja, L., Gurlo, T., Butler, A.E., Rizza, R.A. and Butler, P.C. (2007) High expression rates of human islet amyloid polypeptide induce endoplasmic reticulum stress mediated beta-cell apoptosis, a characteristic of humans with type 2 but not type 1 diabetes. *Diabetes*, **56**, 2016-2027.

Inai, T., Yukawa, M. and Tsuchiya, E. (2007) Interplay between chromatin and trans-acting factors on the IME2 promoter upon induction of the gene at the onset of meiosis. *Mol Cell Biol*, **27**, 1254-1263.

Iwakoshi, N.N., Lee, A.H., Vallabhajosyula, P., Otipoby, K.L., Rajewsky, K. and Glimcher, L.H. (2003) Plasma cell differentiation and the unfolded protein response intersect at the transcription factor XBP-1. *Nat Immunol*, **4**, 321-329.

Jia, M.H., Larossa, R.A., Lee, J.M., Rafalski, A., Derose, E., Gonye, G. and Xue, Z. (2000) Global expression profiling of yeast treated with an inhibitor of amino acid biosynthesis, sulfometuron methyl. *Physiol Genomics*, **3**, 83-92.

Jiang, H.Y., Wek, S.A., McGrath, B.C., Lu, D., Hai, T., Harding, H.P., Wang, X., Ron, D., Cavener, D.R. and Wek, R.C. (2004) Activating transcription factor 3 is integral to the eukaryotic initiation factor 2 kinase stress response. *Mol Cell Biol*, **24**, 1365-1377.

Jiang, H.Y., Wek, S.A., McGrath, B.C., Scheuner, D., Kaufman, R.J., Cavener, D.R. and Wek, R.C. (2003) Phosphorylation of the alpha subunit of eukaryotic initiation factor 2 is required for activation of NF-kappaB in response to diverse cellular stresses. *Mol Cell Biol*, **23**, 5651-5663.

Jin, R., Dobry, C.J., McCown, P.J. and Kumar, A. (2008) Large-scale analysis of yeast filamentous growth by systematic gene disruption and overexpression. *Molecular Biology of the Cell*, **19**, 284-296.

Johnson, E.S., Gonda, D.K. and Varshavsky, A. (1990) cis-trans recognition and subunit-specific degradation of short-lived proteins. *Nature*, **346**, 287-291.

Johnston, M. (1999) Feasting, fasting and fermenting. Glucose sensing in yeast and other cells. *Trends Genet*, **15**, 29-33.

Jorgensen, P., Rupes, I., Sharom, J.R., Schneper, L., Broach, J.R. and Tyers, M. (2004) A dynamic transcriptional network communicates growth potential to ribosome synthesis and critical cell size. *Genes Dev*, **18**, 2491-2505.

Joshi, A.A. and Struhl, K. (2005) Eaf3 chromodomain interaction with methylated H3-K36 links histone deacetylation to Pol II elongation. *Mol Cell*, **20**, 971-978.

Kadosh, D. and Struhl, K. (1997) Repression by Ume6 involves recruitment of a complex containing Sin3 corepressor and Rpd3 histone deacetylase to target promoters. *Cell*, **89**, 365-371.

Kadosh, D. and Struhl, K. (1998) Targeted recruitment of the Sin3-Rpd3 histone deacetylase complex generates a highly localized domain of repressed chromatin in vivo. *Mol Cell Biol*, **18**, 5121-5127.

Kagalwala, M.N., Glaus, B.J., Dang, W., Zofall, M. and Bartholomew, B. (2004) Topography of the ISW2-nucleosome complex: insights into nucleosome spacing and chromatin remodeling. *Embo J*, **23**, 2092-2104.

Kamada, Y., Fujioka, Y., Suzuki, N.N., Inagaki, F., Wullschleger, S., Loewith, R., Hall, M.N. and Ohsumi, Y. (2005) Tor2 directly phosphorylates the AGC kinase Ypk2 to regulate actin polarization. *Mol Cell Biol*, **25**, 7239-7248.

Kane, S.M. and Roth, R. (1974) Carbohydrate metabolism during ascospore development in yeast. *J Bacteriol*, **118**, 8-14.

Kaneto, H., Nakatani, Y., Kawamori, D., Miyatsuka, T., Matsuoka, T.A., Matsuhisa, M. and Yamasaki, Y. (2006) Role of oxidative stress, endoplasmic reticulum stress, and c-Jun N-terminal kinase in pancreatic beta-cell dysfunction and insulin resistance. *Int J Biochem Cell Biol*, **38**, 782-793.

Kang, C.M. and Jiang, Y.W. (2005) Genome-wide survey of non-essential genes required for slowed DNA synthesis-induced filamentous growth in yeast. *Yeast*, **22**, 79-90.

Kassabov, S.R., Henry, N.M., Zofall, M., Tsukiyama, T. and Bartholomew, B. (2002) High-resolution mapping of changes in histone-DNA contacts of nucleosomes remodeled by ISW2. *Mol Cell Biol*, **22**, 7524-7534.

Kassir, Y., Adir, N., Boger-Nadjar, E., Raviv, N.G., Rubin-Bejerano, I., Sagee, S. and Shenhar, G. (2003) Transcriptional regulation of meiosis in budding yeast. *Int Rev Cytol*, **224**, 111-171.

Kassir, Y., Granot, D. and Simchen, G. (1988) IME1, a positive regulator gene of meiosis in S. cerevisiae. *Cell*, **52**, 853-862.

Kawahara, T., Yanagi, H., Yura, T. and Mori, K. (1997) Endoplasmic reticulum stress-induced mRNA splicing permits synthesis of transcription factor Hac1p/Ern4p that activates the unfolded protein response. *Mol Biol Cell*, **8**, 1845-1862.

Kent, N.A., Karabetsou, N., Politis, P.K. and Mellor, J. (2001) In vivo chromatin remodeling by yeast ISWI homologs Isw1p and Isw2p. *Genes Dev*, **15**, 619-626.

Keogh, M.C., Kurdistani, S.K., Morris, S.A., Ahn, S.H., Podolny, V., Collins, S.R., Schuldiner, M., Chin, K., Punna, T., Thompson, N.J., Boone, C., Emili, A., Weissman, J.S., Hughes, T.R., Strahl, B.D., Grunstein, M., Greenblatt, J.F., Buratowski, S. and Krogan, N.J. (2005) Cotranscriptional set2 methylation of histone H3 lysine 36 recruits a repressive Rpd3 complex. *Cell*, **123**, 593-605.

Kerouz, N.J., Horsch, D., Pons, S. and Kahn, C.R. (1997) Differential regulation of insulin receptor substrates-1 and -2 (IRS-1 and IRS-2) and phosphatidylinositol 3-kinase isoforms in liver and muscle of the obese diabetic (ob/ob) mouse. *J Clin Invest*, **100**, 3164-3172.

Khazak, V., Sadhale, P.P., Woychik, N.A., Brent, R. and Golemis, E.A. (1995) Human RNA polymerase II subunit hsRPB7 functions in yeast and influences stress survival and cell morphology. *Mol Biol Cell*, **6**, 759-775.

Klasson, H., Fink, G.R. and Ljungdahl, P.O. (1999) Ssy1p and Ptr3p are plasma membrane components of a yeast system that senses extracellular amino acids. *Mol Cell Biol*, **19**, 5405-5416.

Kobayashi, O., Yoshimoto, H. and Sone, H. (1999) Analysis of the genes activated by the FLO8 gene in Saccharomyces cerevisiae. *Curr Genet*, **36**, 256-261.

Komeili, A., Wedaman, K.P., O'Shea, E.K. and Powers, T. (2000) Mechanism of metabolic control. Target of rapamycin signaling links nitrogen quality to the activity of the Rtg1 and Rtg3 transcription factors. *J Cell Biol*, **151**, 863-878.

Korennykh, A.V., Egea, P.F., Korostelev, A.A., Finer-Moore, J., Zhang, C., Shokat, K.M., Stroud, R.M. and Walter, P. (2009) The unfolded protein response signals through high-order assembly of Ire1. *Nature*, **457**, 687-693.

Kraakman, L., Lemaire, K., Ma, P., Teunissen, A.W., Donaton, M.C., Van Dijck, P., Winderickx, J., de Winde, J.H. and Thevelein, J.M. (1999) A Saccharomyces cerevisiae G-protein coupled receptor, Gpr1, is specifically required for glucose activation of the cAMP pathway during the transition to growth on glucose. *Mol Microbiol*, **32**, 1002-1012.

Kramer, M.F. and Coen, D.M. (2001) The Polymerase chain reaction. Enzymatic amplification of DNA by PCR: Standard procedures and optimization. In Ausubel, F.M., Brent, R., Kingston, R.E., Moore, D.D., Seidman, C.E., Smith, J.A. and Struhl, K. (eds.), *Current Protocols in Molecular Biology*. John Wiley & Sons, New York, Vol. 2, pp. 15.11.11-14.

Kron, S.J. and Gow, N.A. (1995) Budding yeast morphogenesis: signalling, cytoskeleton and cell cycle. *Curr Opin Cell Biol*, **7**, 845-855.

Kron, S.J., Styles, C.A. and Fink, G.R. (1994) Symmetric cell division in pseudohyphae of the yeast Saccharomyces cerevisiae. *Mol Biol Cell*, **5**, 1003-1022.

Kruckeberg, A.L., Walsh, M.C. and Van Dam, K. (1998) How do yeast cells sense glucose? *Bioessays*, **20**, 972-976.

Kübler, E., Mosch, H.U., Rupp, S. and Lisanti, M.P. (1997) Gpa2p, a G-protein alpha-subunit, regulates growth and pseudohyphal development in Saccharomyces cerevisiae via a cAMP-dependent mechanism. *J Biol Chem*, **272**, 20321-20323.

Kuchin, S., Vyas, V.K. and Carlson, M. (2002) Snf1 protein kinase and the repressors Nrg1 and Nrg2 regulate FLO11, haploid invasive growth, and diploid pseudohyphal differentiation. *Mol Cell Biol*, **22**, 3994-4000.

Kuhn, K.M., DeRisi, J.L., Brown, P.O. and Sarnow, P. (2001) Global and specific translational regulation in the genomic response of Saccharomyces cerevisiae to a rapid transfer from a fermentable to a nonfermentable carbon source. *Mol Cell Biol*, **21**, 916-927.

Kupiec, M., Byers, B., Esposito, R.E. and Mitchell, A.P. (1997) Meiosis and sporulation in Saccharomyces cerevisiae. In Pringle, J.R., Broach, J.R. and Jones, E.W. (eds.), *The Molecular and Cellular Biology of the Yeast Saccharomyces.* Cold Spring Harbor Laboratory Press, Plainview, N.Y., Vol. 3, pp. 889-1036.

Kwon, Y.T., Balogh, S.A., Davydov, I.V., Kashina, A.S., Yoon, J.K., Xie, Y., Gaur, A., Hyde, L., Denenberg, V.H. and Varshavsky, A. (2000) Altered activity, social behavior, and spatial memory in mice lacking the NTAN1p amidase and the asparagine branch of the N-end rule pathway. *Mol Cell Biol*, **20**, 4135-4148.

Kwon, Y.T., Kashina, A.S., Davydov, I.V., Hu, R.G., An, J.Y., Seo, J.W., Du, F. and Varshavsky, A. (2002) An essential role of N-terminal arginylation in cardiovascular development. *Science*, **297**, 96-99.

Kwon, Y.T., Kashina, A.S. and Varshavsky, A. (1999) Alternative splicing results in differential expression, activity, and localization of the two forms of arginyl-tRNA-protein transferase, a component of the N-end rule pathway. *Mol Cell Biol*, **19**, 182-193.

Kwon, Y.T., Xia, Z., An, J.Y., Tasaki, T., Davydov, I.V., Seo, J.W., Sheng, J., Xie, Y. and Varshavsky, A. (2003) Female lethality and apoptosis of spermatocytes in mice lacking the UBR2 ubiquitin ligase of the N-end rule pathway. *Mol Cell Biol*, **23**, 8255-8271.

Lamb, T.M., Xu, W., Diamond, A. and Mitchell, A.P. (2001) Alkaline response genes of Saccharomyces cerevisiae and their relationship to the RIM101 pathway. *J Biol Chem*, **276**, 1850-1856.

Laybutt, D.R., Preston, A.M., Akerfeldt, M.C., Kench, J.G., Busch, A.K., Biankin, A.V. and Biden, T.J. (2007) Endoplasmic reticulum stress contributes to beta cell apoptosis in type 2 diabetes. *Diabetologia*, **50**, 752-763.

Leberer, E., Wu, C., Leeuw, T., Fourest-Lieuvin, A., Segall, J.E. and Thomas, D.Y. (1997) Functional characterization of the Cdc42p binding domain of yeast Ste20p protein kinase. *Embo J*, **16**, 83-97.

Lee, A.H., Chu, G.C., Iwakoshi, N.N. and Glimcher, L.H. (2005a) XBP-1 is required for biogenesis of cellular secretory machinery of exocrine glands. *Embo J*, **24**, 4368-4380.

Lee, A.H., Iwakoshi, N.N. and Glimcher, L.H. (2003) XBP-1 regulates a subset of endoplasmic reticulum resident chaperone genes in the unfolded protein response. *Mol Cell Biol*, **23**, 7448-7459.

Lee, M.J., Tasaki, T., Moroi, K., An, J.Y., Kimura, S., Davydov, I.V. and Kwon, Y.T. (2005b) RGS4 and RGS5 are in vivo substrates of the N-end rule pathway. *Proc Natl Acad Sci U S A*, **102**, 15030-15035.

Lee, R.H. and Honigberg, S.M. (1996) Nutritional regulation of late meiotic events in Saccharomyces cerevisiae through a pathway distinct from initiation. *Mol Cell Biol*, **16**, 3222-3232.

Lengeler, K.B., Davidson, R.C., D'Souza, C., Harashima, T., Shen, W.C., Wang, P., Pan, X., Waugh, M. and Heitman, J. (2000) Signal transduction cascades regulating fungal development and virulence. *Microbiol Mol Biol Rev*, **64**, 746-785.

Lesage, P., Yang, X. and Carlson, M. (1996) Yeast SNF1 protein kinase interacts with SIP4, a C6 zinc cluster transcriptional activator: a new role for SNF1 in the glucose response. *Mol Cell Biol*, **16**, 1921-1928.

Liao, X. and Butow, R.A. (1993) RTG1 and RTG2: two yeast genes required for a novel path of communication from mitochondria to the nucleus. *Cell*, **72**, 61-71.

Lin, K.I., Lin, Y. and Calame, K. (2000) Repression of c-myc is necessary but not sufficient for terminal differentiation of B lymphocytes in vitro. *Mol Cell Biol*, **20**, 8684-8695.

Liu, C.Y., Xu, Z. and Kaufman, R.J. (2003) Structure and intermolecular interactions of the luminal dimerization domain of human IRE1alpha. *J Biol Chem*, **278**, 17680-17687.

Liu, H., Styles, C.A. and Fink, G.R. (1996) Saccharomyces cerevisiae S288C has a mutation in FLO8, a gene required for filamentous growth. *Genetics*, **144**, 967-978.

Liu, Z. and Butow, R.A. (1999) A transcriptional switch in the expression of yeast tricarboxylic acid cycle genes in response to a reduction or loss of respiratory function. *Mol Cell Biol*, **19**, 6720-6728.

Liu, Z. and Butow, R.A. (2006) Mitochondrial retrograde signaling. *Annu Rev Genet*, **40**, 159-185.

Lo, H.J., Kohler, J.R., DiDomenico, B., Loebenberg, D., Cacciapuoti, A. and Fink, G.R. (1997) Nonfilamentous C. albicans mutants are avirulent. *Cell*, **90**, 939-949.

Lo, W.S. and Dranginis, A.M. (1998) The cell surface flocculin Flo11 is required for pseudohyphae formation and invasion by Saccharomyces cerevisiae. *Mol Biol Cell*, **9**, 161-171.

Lobo, Z. and Maitra, P.K. (1977) Physiological role of glucose-phosphorylating enzymes in Saccharomyces cerevisiae. *Arch Biochem Biophys*, **182**, 639-645.

Loeb, J.D., Kerentseva, T.A., Pan, T., Sepulveda-Becerra, M. and Liu, H. (1999) Saccharomyces cerevisiae G1 cyclins are differentially involved in invasive and pseudohyphal growth independent of the filamentation mitogen-activated protein kinase pathway. *Genetics*, **153**, 1535-1546.

Loewith, R., Jacinto, E., Wullschleger, S., Lorberg, A., Crespo, J.L., Bonenfant, D., Oppliger, W., Jenoe, P. and Hall, M.N. (2002) Two TOR complexes, only one of which is rapamycin sensitive, have distinct roles in cell growth control. *Mol Cell*, **10**, 457-468.

Lorenz, M.C., Cutler, N.S. and Heitman, J. (2000a) Characterization of alcohol-induced filamentous growth in Saccharomyces cerevisiae. *Mol Biol Cell*, **11**, 183-199.

Lorenz, M.C. and Heitman, J. (1997) Yeast pseudohyphal growth is regulated by GPA2, a G protein alpha homolog. *Embo J*, **16**, 7008-7018.

Lorenz, M.C. and Heitman, J. (1998a) The MEP2 ammonium permease regulates pseudohyphal differentiation in Saccharomyces cerevisiae. *Embo J*, **17**, 1236-1247.

Lorenz, M.C. and Heitman, J. (1998b) Regulators of pseudohyphal differentiation in Saccharomyces cerevisiae identified through multicopy suppressor analysis in ammonium permease mutant strains. *Genetics*, **150**, 1443-1457.

Lorenz, M.C., Pan, X., Harashima, T., Cardenas, M.E., Xue, Y., Hirsch, J.P. and Heitman, J. (2000b) The G protein-coupled receptor gpr1 is a nutrient sensor that regulates pseudohyphal differentiation in Saccharomyces cerevisiae. *Genetics*, **154**, 609-622.

Lowry, O.H., Rosebrough, N.J., Farr, A.L. and Randall, R.J. (1951) Protein measurement with the Folin phenol reagent. *J Biol Chem*, **193**, 265-275.

Lu, P.D., Harding, H.P. and Ron, D. (2004) Translation reinitiation at alternative open reading frames regulates gene expression in an integrated stress response. *J Cell Biol*, **167**, 27-33.

Ma, H., Kunes, S., Schatz, P.J. and Botstein, D. (1987) Plasmid construction by homologous recombination in yeast. *Gene*, **58**, 201-216.

Ma, K., Vattem, K.M. and Wek, R.C. (2002) Dimerization and release of molecular chaperone inhibition facilitate activation of eukaryotic initiation factor-2 kinase in response to endoplasmic reticulum stress. *J Biol Chem*, **277**, 18728-18735.

Ma, Y. and Hendershot, L.M. (2003) Delineation of a negative feedback regulatory loop that controls protein translation during endoplasmic reticulum stress. *J Biol Chem*, **278**, 34864-34873.

Madhani, H.D. and Fink, G.R. (1998) The riddle of MAP kinase signaling specificity. *Trends Genet*, **14**, 151-155.

Madhani, H.D., Galitski, T., Lander, E.S. and Fink, G.R. (1999) Effectors of a developmental mitogen-activated protein kinase cascade revealed by expression signatures of signaling mutants. *Proc Natl Acad Sci U S A*, **96**, 12530-12535.

Madhani, H.D., Styles, C.A. and Fink, G.R. (1997) MAP kinases with distinct inhibitory functions impart signaling specificity during yeast differentiation. *Cell*, **91**, 673-684.

Madura, K. and Varshavsky, A. (1994) Degradation of G alpha by the N-end rule pathway. *Science*, **265**, 1454-1458.

Maeda, T., Takekawa, M. and Saito, H. (1995) Activation of yeast PBS2 MAPKK by MAPKKKs or by binding of an SH3-containing osmosensor. *Science*, **269**, 554-558.

Magasanik, B. and Kaiser, C.A. (2002) Nitrogen regulation in Saccharomyces cerevisiae. *Gene*, **290**, 1-18.

Malathi, K., Xiao, Y. and Mitchell, A.P. (1997) Interaction of yeast repressor-activator protein Ume6p with glycogen synthase kinase 3 homolog Rim11p. *Mol Cell Biol*, **17**, 7230-7236.

Malathi, K., Xiao, Y. and Mitchell, A.P. (1999) Catalytic roles of yeast GSK3beta/shaggy homolog Rim11p in meiotic activation. *Genetics*, **153**, 1145-1152.

Maleri, S., Ge, Q., Hackett, E.A., Wang, Y., Dohlman, H.G. and Errede, B. (2004) Persistent activation by constitutive Ste7 promotes Kss1-mediated invasive growth but fails to support Fus3-dependent mating in yeast. *Mol Cell Biol*, **24**, 9221-9238.

Mallory, M.J., Cooper, K.F. and Strich, R. (2007) Meiosis-specific destruction of the Ume6p repressor by the Cdc20-directed APC/C. *Mol Cell*, **27**, 951-961.

Mandel, S., Robzyk, K. and Kassir, Y. (1994) Ime1 gene encodes a transcription factor which is required to induce meiosis in *Saccharomyces cerevisiae*. *Dev Genet*, **15**, 139-147.

Marion, R.M., Regev, A., Segal, E., Barash, Y., Koller, D., Friedman, N. and O'Shea, E.K. (2004) Sfp1 is a stress- and nutrient-sensitive regulator of ribosomal protein gene expression. *Proc Natl Acad Sci U S A*, **101**, 14315-14322.

Marston, A.L. and Amon, A. (2004) Meiosis: cell-cycle controls shuffle and deal. *Nat Rev Mol Cell Biol*, **5**, 983-997.

Matsumoto, K., Uno, I. and Ishikawa, T. (1983) Initiation of meiosis in yeast mutants defective in adenylate cyclase and cyclic AMP-dependent protein kinase. *Cell*, **32**, 417-423.

McConnell, A.D., Gelbart, M.E. and Tsukiyama, T. (2004) Histone fold protein Dls1p is required for Isw2-dependent chromatin remodeling in vivo. *Mol Cell Biol*, **24**, 2605-2613.

Miled, C., Mann, C. and Faye, G. (2001) Xbp1-mediated repression of CLB gene expression contributes to the modifications of yeast cell morphology and cell cycle seen during nitrogen-limited growth. *Mol Cell Biol*, **21**, 3714-3724.

Miller, J.H. (1972) *Assay of β-galactosidase in Experiments in molecular genetics*. Cold Spring Harbor Laboratory Press, [Cold Spring Harbor N.Y.].

Mitchell, A.P., Driscoll, S.E. and Smith, H.E. (1990) Positive control of sporulation-specific genes by the IME1 and IME2 products in Saccharomyces cerevisiae. *Mol Cell Biol*, **10**, 2104-2110.

Mori, K., Kawahara, T., Yoshida, H., Yanagi, H. and Yura, T. (1996) Signalling from endoplasmic reticulum to nucleus: transcription factor with a basic-leucine zipper motif is required for the unfolded protein-response pathway. *Genes Cells*, **1**, 803-817.

Mori, K., Ogawa, N., Kawahara, T., Yanagi, H. and Yura, T. (1998) Palindrome with spacer of one nucleotide is characteristic of the cis-acting unfolded protein response element in Saccharomyces cerevisiae. *J Biol Chem*, **273**, 9912-9920.

Mori, K., Ogawa, N., Kawahara, T., Yanagi, H. and Yura, T. (2000) mRNA splicing-mediated C-terminal replacement of transcription factor Hac1p is required for efficient activation of the unfolded protein response. *Proc Natl Acad Sci U S A*, **97**, 4660-4665.

Mori, K., Sant, A., Kohno, K., Normington, K., Gething, M.J. and Sambrook, J.F. (1992) A 22 bp cis-acting element is necessary and sufficient for the induction of the yeast KAR2 (BiP) gene by unfolded proteins. *Embo J*, **11**, 2583-2593.

Moriya, H., Shimizu-Yoshida, Y., Omori, A., Iwashita, S., Katoh, M. and Sakai, A. (2001) Yak1p, a DYRK family kinase, translocates to the nucleus and phosphorylates yeast Pop2p in response to a glucose signal. *Genes Dev*, **15**, 1217-1228.

Morohashi, N., Nakajima, K., Kurihara, D., Mukai, Y., Mitchell, A.P. and Shimizu, M. (2007) A nucleosome positioned by alpha2/Mcm1 prevents Hap1 activator binding in vivo. *Biochem Biophys Res Commun*, **364**, 583-588.

Mösch, H.U. and Fink, G.R. (1997) Dissection of filamentous growth by transposon mutagenesis in Saccharomyces cerevisiae. *Genetics*, **145**, 671-684.

Mösch, H.U., Kubler, E., Krappmann, S., Fink, G.R. and Braus, G.H. (1999) Crosstalk between the Ras2p-controlled mitogen-activated protein kinase and cAMP pathways during invasive growth of Saccharomyces cerevisiae. *Mol Biol Cell*, **10**, 1325-1335.

Mueller, P.P. and Hinnebusch, A.G. (1986) Multiple upstream AUG codons mediate translational control of GCN4. *Cell*, **45**, 201-207.

Mulet, J.M., Martin, D.E., Loewith, R. and Hall, M.N. (2006) Mutual antagonism of target of rapamycin and calcineurin signaling. *J Biol Chem*, **281**, 33000-33007.

Murakami, Y., Tatebayashi, K. and Saito, H. (2008) Two adjacent docking sites in the yeast Hog1 mitogen-activated protein (MAP) kinase differentially interact with the Pbs2 MAP kinase kinase and the Ptp2 protein tyrosine phosphatase. *Mol Cell Biol*, **28**, 2481-2494.

Murray, L.E., Rowley, N., Dawes, I.W., Johnston, G.C. and Singer, R.A. (1998) A yeast glutamine tRNA signals nitrogen status for regulation of dimorphic growth and sporulation. *Proc Natl Acad Sci U S A*, **95**, 8619-8624.

Nakatani, Y., Kaneto, H., Kawamori, D., Yoshiuchi, K., Hatazaki, M., Matsuoka, T.A., Ozawa, K., Ogawa, S., Hori, M., Yamasaki, Y. and Matsuhisa, M. (2005) Involvement of endoplasmic reticulum stress in insulin resistance and diabetes. *J Biol Chem*, **280**, 847-851.

Nandi, A., Kitamura, Y., Kahn, C.R. and Accili, D. (2004) Mouse models of insulin resistance. *Physiol Rev*, **84**, 623-647.

Natarajan, K., Meyer, M.R., Jackson, B.M., Slade, D., Roberts, C., Hinnebusch, A.G. and Marton, M.J. (2001) Transcriptional profiling shows that Gcn4p is a master regulator of gene expression during amino acid starvation in yeast. *Mol Cell Biol*, **21**, 4347-4368.

Nath, N., McCartney, R.R. and Schmidt, M.C. (2003) Yeast Pak1 kinase associates with and activates Snf1. *Mol Cell Biol*, **23**, 3909-3917.

Nelson, B., Parsons, A.B., Evangelista, M., Schaefer, K., Kennedy, K., Ritchie, S., Petryshen, T.L. and Boone, C. (2004) Fus1p interacts with components of the Hog1p mitogen-activated protein kinase and Cdc42p morphogenesis signaling pathways to control cell fusion during yeast mating. *Genetics*, **166**, 67-77.

Nishitoh, H., Matsuzawa, A., Tobiume, K., Saegusa, K., Takeda, K., Inoue, K., Hori, S., Kakizuka, A. and Ichijo, H. (2002) ASK1 is essential for endoplasmic reticulum stress-induced neuronal cell death triggered by expanded polyglutamine repeats. *Genes Dev*, **16**, 1345-1355.

O'Rourke, S.M. and Herskowitz, I. (1998) The Hog1 MAPK prevents cross talk between the HOG and pheromone response MAPK pathways in Saccharomyces cerevisiae. *Genes Dev*, **12**, 2874-2886.

O'Rourke, S.M. and Herskowitz, I. (2004) Unique and redundant roles for HOG MAPK pathway components as revealed by whole-genome expression analysis. *Mol Biol Cell*, **15**, 532-542.

Ohkuni, K. and Yamashita, I. (2000) A transcriptional autoregulatory loop for KIN28-CCL1 and SRB10-SRB11, each encoding RNA polymerase II CTD kinase-cyclin pair, stimulates the meiotic development of S. cerevisiae. *Yeast*, **16**, 829-846.

Olesen, J., Hahn, S. and Guarente, L. (1987) Yeast HAP2 and HAP3 activators both bind to the CYC1 upstream activation site, UAS2, in an interdependent manner. *Cell*, **51**, 953-961.

Olson, K.A., Nelson, C., Tai, G., Hung, W., Yong, C., Astell, C. and Sadowski, I. (2000) Two regulators of Ste12p inhibit pheromone-responsive transcription by separate mechanisms. *Mol Cell Biol*, **20**, 4199-4209.

Ozawa, K., Miyazaki, M., Matsuhisa, M., Takano, K., Nakatani, Y., Hatazaki, M., Tamatani, T., Yamagata, K., Miyagawa, J., Kitao, Y., Hori, O., Yamasaki, Y. and Ogawa, S. (2005) The endoplasmic reticulum chaperone improves insulin resistance in type 2 diabetes. *Diabetes*, **54**, 657-663.

Özcan, S., Dover, J., Rosenwald, A.G., Wolfl, S. and Johnston, M. (1996) Two glucose transporters in Saccharomyces cerevisiae are glucose sensors that generate a signal for induction of gene expression. *Proc Natl Acad Sci U S A*, **93**, 12428-12432.

Ozcan, S. and Johnston, M. (1999) Function and regulation of yeast hexose transporters. *Microbiol Mol Biol Rev*, **63**, 554-569.

Özcan, U., Cao, Q., Yilmaz, E., Lee, A.H., Iwakoshi, N.N., Ozdelen, E., Tuncman, G., Gorgun, C., Glimcher, L.H. and Hotamisligil, G.S. (2004) Endoplasmic reticulum stress links obesity, insulin action, and type 2 diabetes. *Science*, **306**, 457-461.

Özcan, U., Yilmaz, E., Ozcan, L., Furuhashi, M., Vaillancourt, E., Smith, R.O., Gorgun, C.Z. and Hotamisligil, G.S. (2006) Chemical chaperones reduce ER stress and restore glucose homeostasis in a mouse model of type 2 diabetes. *Science*, **313**, 1137-1140.

Page, S.L. and Hawley, R.S. (2004) The genetics and molecular biology of the synaptonemal complex. *Annu Rev Cell Dev Biol*, **20**, 525-558.

Pak, J. and Segall, J. (2002) Regulation of the premiddle and middle phases of expression of the NDT80 gene during sporulation of Saccharomyces cerevisiae. *Mol Cell Biol*, **22**, 6417-6429.

Palecek, S.P., Parikh, A.S. and Kron, S.J. (2000) Genetic analysis reveals that FLO11 upregulation and cell polarization independently regulate invasive growth in Saccharomyces cerevisiae. *Genetics*, **156**, 1005-1023.

Pan, X. and Heitman, J. (1999) Cyclic AMP-dependent protein kinase regulates pseudohyphal differentiation in Saccharomyces cerevisiae. *Mol Cell Biol*, **19**, 4874-4887.

Pan, X. and Heitman, J. (2000) Sok2 regulates yeast pseudohyphal differentiation via a transcription factor cascade that regulates cell-cell adhesion. *Mol Cell Biol*, **20**, 8364-8372.

Pan, X. and Heitman, J. (2002) Protein kinase A operates a molecular switch that governs yeast pseudohyphal differentiation. *Mol Cell Biol*, **22**, 3981-3993.

Park, S.W., Zhou, Y., Lee, J., Lu, A., Sun, C., Chung, J., Ueki, K. and Ozcan, U. (2010) The regulatory subunits of PI3K, p85alpha and p85beta, interact with XBP-1 and increase its nuclear translocation. *Nat Med*, **16**, 429-437.

Parviz, F. and Heideman, W. (1998) Growth-independent regulation of CLN3 mRNA levels by nutrients in Saccharomyces cerevisiae. *J Bacteriol*, **180**, 225-230.

Peter, M., Neiman, A.M., Park, H.O., van Lohuizen, M. and Herskowitz, I. (1996) Functional analysis of the interaction between the small GTP binding protein Cdc42 and the Ste20 protein kinase in yeast. *Embo J*, **15**, 7046-7059.

Pfeifer, K., Arcangioli, B. and Guarente, L. (1987) Yeast HAP1 activator competes with the factor RC2 for binding to the upstream activation site UAS1 of the CYC1 gene. *Cell*, **49**, 9-18.

Pitoniak, A., Birkaya, B., Dionne, H.M., Vadaie, N. and Cullen, P.J. (2009) The signaling mucins Msb2 and Hkr1 differentially regulate the filamentation mitogen-activated protein kinase pathway and contribute to a multimodal response. *Mol Biol Cell*, **20**, 3101-3114.

Posas, F. and Saito, H. (1997) Osmotic activation of the HOG MAPK pathway via Ste11p MAPKKK: scaffold role of Pbs2p MAPKK. *Science*, **276**, 1702-1705.

Primig, M., Williams, R.M., Winzeler, E.A., Tevzadze, G.G., Conway, A.R., Hwang, S.Y., Davis, R.W. and Esposito, R.E. (2000) The core meiotic transcriptome in budding yeasts. *Nat Genet*, **26**, 415-423.

Purnapatre, K., Gray, M., Piccirillo, S. and Honigberg, S.M. (2005) Glucose inhibits meiotic DNA replication through SCFGrr1p-dependent destruction of Ime2p kinase. *Mol Cell Biol*, **25**, 440-450.

Purnapatre, K. and Honigberg, S.M. (2002) Meiotic differentiation during colony maturation in Saccharomyces cerevisiae. *Curr Genet*, **42**, 1-8.

Purnapatre, K., Piccirillo, S., Schneider, B.L. and Honigberg, S.M. (2002) The CLN3/SWI6/CLN2 pathway and SNF1 act sequentially to regulate meiotic initiation in Saccharomyces cerevisiae. *Genes Cells*, **7**, 675-691.

Radcliffe, P.A., Binley, K.M., Trevethick, J., Hall, M. and Sudbery, P.E. (1997) Filamentous growth of the budding yeast Saccharomyces cerevisiae induced by overexpression of the WHi2 gene. *Microbiology*, **143 (Pt 6)**, 1867-1876.

Rahner, A., Scholer, A., Martens, E., Gollwitzer, B. and Schuller, H.J. (1996) Dual influence of the yeast Cat1p (Snf1p) protein kinase on carbon source-dependent transcriptional activation of gluconeogenic genes by the regulatory gene CAT8. *Nucleic Acids Res*, **24**, 2331-2337.

Randez-Gil, F., Bojunga, N., Proft, M. and Entian, K.D. (1997) Glucose derepression of gluconeogenic enzymes in Saccharomyces cerevisiae correlates with phosphorylation of the gene activator Cat8p. *Mol Cell Biol*, **17**, 2502-2510.

Rao, H., Uhlmann, F., Nasmyth, K. and Varshavsky, A. (2001) Degradation of a cohesin subunit by the N-end rule pathway is essential for chromosome stability. *Nature*, **410**, 955-959.

Reimold, A.M., Iwakoshi, N.N., Manis, J., Vallabhajosyula, P., Szomolanyi-Tsuda, E., Gravallese, E.M., Friend, D., Grusby, M.J., Alt, F. and Glimcher, L.H. (2001) Plasma cell differentiation requires the transcription factor XBP-1. *Nature*, **412**, 300-307.

Reinke, A., Anderson, S., McCaffery, J.M., Yates, J., 3rd, Aronova, S., Chu, S., Fairclough, S., Iverson, C., Wedaman, K.P. and Powers, T. (2004) TOR complex 1 includes a novel component, Tco89p (YPL180w), and cooperates

with Ssd1p to maintain cellular integrity in Saccharomyces cerevisiae. *J Biol Chem*, **279**, 14752-14762.

Reiser, V., Salah, S.M. and Ammerer, G. (2000) Polarized localization of yeast Pbs2 depends on osmostress, the membrane protein Sho1 and Cdc42. *Nat Cell Biol*, **2**, 620-627.

Remenyi, A., Good, M.C., Bhattacharyya, R.P. and Lim, W.A. (2005) The role of docking interactions in mediating signaling input, output, and discrimination in the yeast MAPK network. *Mol Cell*, **20**, 951-962.

Robertson, L.S. and Fink, G.R. (1998) The three yeast A kinases have specific signaling functions in pseudohyphal growth. *Proc Natl Acad Sci U S A*, **95**, 13783-13787.

Rohde, J.R., Campbell, S., Zurita-Martinez, S.A., Cutler, N.S., Ashe, M. and Cardenas, M.E. (2004) TOR controls transcriptional and translational programs via Sap-Sit4 protein phosphatase signaling effectors. *Mol Cell Biol*, **24**, 8332-8341.

Rolland, F., Winderickx, J. and Thevelein, J.M. (2001) Glucose-sensing mechanisms in eukaryotic cells. *Trends Biochem Sci*, **26**, 310-317.

Rolland, F., Winderickx, J. and Thevelein, J.M. (2002) Glucose-sensing and -signalling mechanisms in yeast. *FEMS Yeast Res*, **2**, 183-201.

Roman, E., Arana, D.M., Nombela, C., Alonso-Monge, R. and Pla, J. (2007) MAP kinase pathways as regulators of fungal virulence. *Trends Microbiol*, **15**, 181-190.

Ron, D. and Walter, P. (2007) Signal integration in the endoplasmic reticulum unfolded protein response. *Nat Rev Mol Cell Biol*, **8**, 519-529.

Roosen, J., Engelen, K., Marchal, K., Mathys, J., Griffioen, G., Cameroni, E., Thevelein, J.M., De Virgilio, C., De Moor, B. and Winderickx, J. (2005) PKA and Sch9 control a molecular switch important for the proper adaptation to nutrient availability. *Mol Microbiol*, **55**, 862-880.

Rose, M., Albig, W. and Entian, K.D. (1991) Glucose repression in Saccharomyces cerevisiae is directly associated with hexose phosphorylation by hexokinases PI and PII. *Eur J Biochem*, **199**, 511-518.

Rosenthal, N. (1987) Identification of regulatory elements of cloned genes with functional assays. *Methods Enzymol*, **152**, 704-720.

Rossi, R., Montecucco, A., Ciarrocchi, G. and Biamonti, G. (1997) Functional characterization of the T4 DNA ligase: a new insight into the mechanism of action. *Nucleic Acids Res*, **25**, 2106-2113.

Rubin-Bejerano, I., Mandel, S., Robzyk, K. and Kassir, Y. (1996) Induction of meiosis in Saccharomyces cerevisiae depends on conversion of the transcriptional

represssor Ume6 to a positive regulator by its regulated association with the transcriptional activator Ime1. *Mol Cell Biol*, **16**, 2518-2526.

Rundlett, S.E., Carmen, A.A., Kobayashi, R., Bavykin, S., Turner, B.M. and Grunstein, M. (1996) HDA1 and RPD3 are members of distinct yeast histone deacetylase complexes that regulate silencing and transcription. *Proc Natl Acad Sci U S A*, **93**, 14503-14508.

Rundlett, S.E., Carmen, A.A., Suka, N., Turner, B.M. and Grunstein, M. (1998) Transcriptional repression by UME6 involves deacetylation of lysine 5 of histone H4 by RPD3. *Nature*, **392**, 831-835.

Rupp, S., Summers, E., Lo, H.J., Madhani, H. and Fink, G. (1999) MAP kinase and cAMP filamentation signaling pathways converge on the unusually large promoter of the yeast FLO11 gene. *Embo J*, **18**, 1257-1269.

Rutherford, J.C., Chua, G., Hughes, T., Cardenas, M.E. and Heitman, J. (2008) A Mep2-dependent transcriptional profile links permease function to gene expression during pseudohyphal growth in Saccharomyces cerevisiae. *Mol Biol Cell*, **19**, 3028-3039.

Sagee, S., Sherman, A., Shenhar, G., Robzyk, K., Ben-Doy, N., Simchen, G. and Kassir, Y. (1998) Multiple and distinct activation and repression sequences mediate the regulated transcription of IME1, a transcriptional activator of meiosis-specific genes in Saccharomyces cerevisiae. *Mol Cell Biol*, **18**, 1985-1995.

Saito, H. and Tatebayashi, K. (2004) Regulation of the osmoregulatory HOG MAPK cascade in yeast. *J Biochem*, **136**, 267-272.

Saltiel, A.R. and Kahn, C.R. (2001) Insulin signalling and the regulation of glucose and lipid metabolism. *Nature*, **414**, 799-806.

Saltiel, A.R. and Pessin, J.E. (2002) Insulin signaling pathways in time and space. *Trends Cell Biol*, **12**, 65-71.

Sambrook, J.F.E.F.M.T. (1989) *Molecular cloning : a laboratory manual*. Cold Spring Harbor Laboratory, Cold Spring Harbor, N.Y.

Sari, F., Heinrich, M., Meyer, W., Braus, G.H. and Irniger, S. (2008) The C-terminal region of the meiosis-specific protein kinase Ime2 mediates protein instability and is required for normal spore formation in budding yeast. *J Mol Biol*, **378**, 31-43.

Schena, M., Picard, D. and Yamamoto, K.R. (1991) Vectors for constitutive and inducible gene expression in yeast. *Methods Enzymol*, **194**, 389-398.

Scherens, B., Feller, A., Vierendeels, F., Messenguy, F. and Dubois, E. (2006) Identification of direct and indirect targets of the Gln3 and Gat1 activators by transcriptional profiling in response to nitrogen availability in the short and long term. *FEMS Yeast Res*, **6**, 777-791.

Scheuner, D. and Kaufman, R.J. (2008) The unfolded protein response: a pathway that links insulin demand with beta-cell failure and diabetes. *Endocr Rev*, **29**, 317-333.

Scheuner, D., Song, B., McEwen, E., Liu, C., Laybutt, R., Gillespie, P., Saunders, T., Bonner-Weir, S. and Kaufman, R.J. (2001) Translational control is required for the unfolded protein response and in vivo glucose homeostasis. *Mol Cell*, **7**, 1165-1176.

Schindler, K., Benjamin, K.R., Martin, A., Boglioli, A., Herskowitz, I. and Winter, E. (2003) The Cdk-activating kinase Cak1p promotes meiotic S phase through Ime2p. *Mol Cell Biol*, **23**, 8718-8728.

Schindler, K. and Winter, E. (2006) Phosphorylation of Ime2 regulates meiotic progression in Saccharomyces cerevisiae. *J Biol Chem*, **281**, 18307-18316.

Schröder, M., Chang, J.S. and Kaufman, R.J. (2000) The unfolded protein response represses nitrogen-starvation induced developmental differentiation in yeast. *Genes Dev*, **14**, 2962-2975.

Schröder, M., Clark, R., Liu, C.Y. and Kaufman, R.J. (2004) The unfolded protein response represses differentiation through the RPD3-SIN3 histone deacetylase. *Embo J*, **23**, 2281-2292.

Schröder, M. and Kaufman, R.J. (2005) The mammalian unfolded protein response. *Annu Rev Biochem*, **74**, 739-789.

Schüller, H.J. (2003) Transcriptional control of nonfermentative metabolism in the yeast Saccharomyces cerevisiae. *Curr Genet*, **43**, 139-160.

Schwartz, M.A. and Madhani, H.D. (2004) Principles of MAP kinase signaling specificity in Saccharomyces cerevisiae. *Annu Rev Genet*, **38**, 725-748.

Schwartz, M.A. and Madhani, H.D. (2006) Control of MAPK signaling specificity by a conserved residue in the MEK-binding domain of the yeast scaffold protein Ste5. *Curr Genet*, **49**, 351-363.

Seidman, C.E., Struhl, K., Sheen, J. and Jessen, T. (1997a) *Escherichia coli*, plasmids, and bacteriophages. Vectors derived from plasmids. Introduction of plasmid DNA into cells. In Ausubel, F.M., Brent, R., Kingston, R.E., Moore, D.D., Seidman, C.E., Smith, J.A. and Struhl, K. (eds.), *Current Protocols in Molecular Biology*. John Wiley & Sons, New York, Vol. 1, pp. 1.8.4-7.

Seidman, C.E., Struhl, K., Sheen, J. and Jessen, T. (1997b) *Escherichia coli*, plasmids, and bacteriophages. Vectors derived from plasmids. Introduction of plasmid DNA into cells. In Ausubel, F.M., Brent, R., Kingston, R.E., Moore, D.D., Seidman, C.E., Smith, J.A. and Struhl, K. (eds.), *Current Protocols in Molecular Biology*. John Wiley & Sons, New York, Vol. 1, pp. 1.8.1-4.

Shaffer, A.L., Shapiro-Shelef, M., Iwakoshi, N.N., Lee, A.H., Qian, S.B., Zhao, H., Yu, X., Yang, L., Tan, B.K., Rosenwald, A., Hurt, E.M., Petroulakis, E., Sonenberg, N., Yewdell, J.W., Calame, K., Glimcher, L.H. and Staudt, L.M. (2004) XBP1,

downstream of Blimp-1, expands the secretory apparatus and other organelles, and increases protein synthesis in plasma cell differentiation. *Immunity*, **21**, 81-93.

Shah, J.C. and Clancy, M.J. (1992) IME4, a gene that mediates MAT and nutritional control of meiosis in Saccharomyces cerevisiae. *Mol Cell Biol*, **12**, 1078-1086.

Shamu, C.E. and Walter, P. (1996) Oligomerization and phosphorylation of the Ire1p kinase during intracellular signaling from the endoplasmic reticulum to the nucleus. *Embo J*, **15**, 3028-3039.

Sharma, P.M., Egawa, K., Huang, Y., Martin, J.L., Huvar, I., Boss, G.R. and Olefsky, J.M. (1998) Inhibition of phosphatidylinositol 3-kinase activity by adenovirus-mediated gene transfer and its effect on insulin action. *J Biol Chem*, **273**, 18528-18537.

Shefer-Vaida, M., Sherman, A., Ashkenazi, T., Robzyk, K. and Kassir, Y. (1995) Positive and negative feedback loops affect the transcription of IME1, a positive regulator of meiosis in Saccharomyces cerevisiae. *Dev Genet*, **16**, 219-228.

Shenhar, G. and Kassir, Y. (2001) A positive regulator of mitosis, Sok2, functions as a negative regulator of meiosis in Saccharomyces cerevisiae. *Mol Cell Biol*, **21**, 1603-1612.

Sherman, F. and Roman, H. (1963) Evidence for two types of allelic recombination in yeast. *Genetics*, **48**, 255-261.

Sherriff, J.A., Kent, N.A. and Mellor, J. (2007) The Isw2 chromatin-remodeling ATPase cooperates with the Fkh2 transcription factor to repress transcription of the B-type cyclin gene CLB2. *Mol Cell Biol*, **27**, 2848-2860.

Shimizu, M., Takahashi, K., Lamb, T.M., Shindo, H. and Mitchell, A.P. (2003) Yeast Ume6p repressor permits activator binding but restricts TBP binding at the HOP1 promoter. *Nucleic Acids Res*, **31**, 3033-3037.

Shirra, M.K. and Arndt, K.M. (1999) Evidence for the involvement of the Glc7-Reg1 phosphatase and the Snf1-Snf4 kinase in the regulation of INO1 transcription in Saccharomyces cerevisiae. *Genetics*, **152**, 73-87.

Shock, T.R., Thompson, J., Yates, J.R., 3rd and Madhani, H.D. (2009) Hog1 mitogen-activated protein kinase (MAPK) interrupts signal transduction between the Kss1 MAPK and the Tec1 transcription factor to maintain pathway specificity. *Eukaryot Cell*, **8**, 606-616.

Shoelson, S.E., Lee, J. and Goldfine, A.B. (2006) Inflammation and insulin resistance. *J Clin Invest*, **116**, 1793-1801.

Shulman, G.I. (1999) Cellular mechanisms of insulin resistance in humans. *Am J Cardiol*, **84**, 3J-10J.

Sia, R.A. and Mitchell, A.P. (1995) Stimulation of later functions of the yeast meiotic protein kinase Ime2p by the IDS2 gene product. *Mol Cell Biol*, **15**, 5279-5287.

Sidrauski, C., Cox, J.S. and Walter, P. (1996) tRNA ligase is required for regulated mRNA splicing in the unfolded protein response. *Cell*, **87**, 405-413.

Sidrauski, C. and Walter, P. (1997) The transmembrane kinase Ire1p is a site-specific endonuclease that initiates mRNA splicing in the unfolded protein response. *Cell*, **90**, 1031-1039.

Simchen, G., Pinon, R. and Salts, Y. (1972) Sporulation in Saccharomyces cerevisiae: premeiotic DNA synthesis, readiness and commitment. *Exp Cell Res*, **75**, 207-218.

Smith, H.E., Driscoll, S.E., Sia, R.A., Yuan, H.E. and Mitchell, A.P. (1993) Genetic evidence for transcriptional activation by the yeast *IME1* gene product. *Genetics*, **133**, 775-784.

Smith, H.E. and Mitchell, A.P. (1989) A transcriptional cascade governs entry into meiosis in Saccharomyces cerevisiae. *Mol Cell Biol*, **9**, 2142-2152.

Sopko, R., Raithatha, S. and Stuart, D. (2002) Phosphorylation and maximal activity of Saccharomyces cerevisiae meiosis-specific transcription factor Ndt80 is dependent on Ime2. *Mol Cell Biol*, **22**, 7024-7040.

Soushko, M. and Mitchell, A.P. (2000) An RNA-binding protein homologue that promotes sporulation-specific gene expression in Saccharomyces cerevisiae. *Yeast*, **16**, 631-639.

Spencer, J.F. and Spencer, D.M. (1996) Meiotic analysis. *Methods Mol Biol*, **53**, 51-58.

Sriburi, R., Jackowski, S., Mori, K. and Brewer, J.W. (2004) XBP1: a link between the unfolded protein response, lipid biosynthesis, and biogenesis of the endoplasmic reticulum. *J Cell Biol*, **167**, 35-41.

Stanbrough, M. and Magasanik, B. (1996) Two transcription factors, Gln3p and Nil1p, use the same GATAAG sites to activate the expression of GAP1 of Saccharomyces cerevisiae. *J Bacteriol*, **178**, 2465-2468.

Stanbrough, M., Rowen, D.W. and Magasanik, B. (1995) Role of the GATA factors Gln3p and Nil1p of Saccharomyces cerevisiae in the expression of nitrogen-regulated genes. *Proc Natl Acad Sci U S A*, **92**, 9450-9454.

Stanhill, A., Schick, N. and Engelberg, D. (1999) The yeast ras/cyclic AMP pathway induces invasive growth by suppressing the cellular stress response. *Mol Cell Biol*, **19**, 7529-7538.

Steber, C.M. and Esposito, R.E. (1995) UME6 is a central component of a developmental regulatory switch controlling meiosis-specific gene expression. *Proc Natl Acad Sci U S A*, **92**, 12490-12494.

Stoy, J., Edghill, E.L., Flanagan, S.E., Ye, H., Paz, V.P., Pluzhnikov, A., Below, J.E., Hayes, M.G., Cox, N.J., Lipkind, G.M., Lipton, R.B., Greeley, S.A., Patch, A.M., Ellard, S., Steiner, D.F., Hattersley, A.T., Philipson, L.H. and Bell, G.I. (2007) Insulin gene mutations as a cause of permanent neonatal diabetes. *Proc Natl Acad Sci U S A*, **104**, 15040-15044.

Strich, R., Surosky, R.T., Steber, C., Dubois, E., Messenguy, F. and Esposito, R.E. (1994) UME6 is a key regulator of nitrogen repression and meiotic development. *Genes Dev*, **8**, 796-810.

Strudwick, N., Brown, M., Parmar, V.M. and Schroder, M. (2010) Ime1 and Ime2 are required for pseudohyphal growth of Saccharomyces cerevisiae on nonfermentable carbon sources. *Mol Cell Biol*, **30**, 5514-5530.

Stuart, D. and Wittenberg, C. (1998) CLB5 and CLB6 are required for premeiotic DNA replication and activation of the meiotic S/M checkpoint. *Genes Dev*, **12**, 2698-2710.

Su, S.S. and Mitchell, A.P. (1993a) Identification of functionally related genes that stimulate early meiotic gene expression in yeast. *Genetics*, **133**, 67-77.

Su, S.S. and Mitchell, A.P. (1993b) Molecular characterization of the yeast meiotic regulatory gene RIM1. *Nucleic Acids Res*, **21**, 3789-3797.

Sugiyama, M. and Nikawa, J. (2001) The Saccharomyces cerevisiae Isw2p-Itc1p complex represses INO1 expression and maintains cell morphology. *J Bacteriol*, **183**, 4985-4993.

Suka, N., Suka, Y., Carmen, A.A., Wu, J. and Grunstein, M. (2001) Highly specific antibodies determine histone acetylation site usage in yeast heterochromatin and euchromatin. *Mol Cell*, **8**, 473-479.

Surosky, R.T. and Esposito, R.E. (1992) Early meiotic transcripts are highly unstable in Saccharomyces cerevisiae. *Mol Cell Biol*, **12**, 3948-3958.

Sweet, D.H., Jang, Y.K. and Sancar, G.B. (1997) Role of UME6 in transcriptional regulation of a DNA repair gene in Saccharomyces cerevisiae. *Mol Cell Biol*, **17**, 6223-6235.

Tabor, S. (1987) Enzymatic manipulation of DNA and RNA. Phosphatases and kinases. In Ausubel, F.M., Brent, R., Kingston, R.E., Moore, D.D., Seidman, C.E., Smith, J.A. and Struhl, K. (eds.), *Current Protocols in Molecular Biology*. John Wiley & Sons, New York, Vol. 1, pp. 3.10.11-15.

Tamaki, H., Miwa, T., Shinozaki, M., Saito, M., Yun, C.W., Yamamoto, K. and Kumagai, H. (2000) GPR1 regulates filamentous growth through FLO11 in yeast Saccharomyces cerevisiae. *Biochem Biophys Res Commun*, **267**, 164-168.

Taniguchi, C.M., Emanuelli, B. and Kahn, C.R. (2006) Critical nodes in signalling pathways: insights into insulin action. *Nat Rev Mol Cell Biol*, **7**, 85-96.

Tanti, J.F., Gual, P., Gremeaux, T., Gonzalez, T., Barres, R. and Le Marchand-Brustel, Y. (2004) Alteration in insulin action: role of IRS-1 serine phosphorylation in the retroregulation of insulin signalling. *Ann Endocrinol (Paris)*, **65**, 43-48.

Tasaki, T. and Kwon, Y.T. (2007) The mammalian N-end rule pathway: new insights into its components and physiological roles. *Trends Biochem Sci*, **32**, 520-528.

Tatebayashi, K., Tanaka, K., Yang, H.Y., Yamamoto, K., Matsushita, Y., Tomida, T., Imai, M. and Saito, H. (2007) Transmembrane mucins Hkr1 and Msb2 are putative osmosensors in the SHO1 branch of yeast HOG pathway. *Embo J*, **26**, 3521-3533.

Tatebayashi, K., Yamamoto, K., Tanaka, K., Tomida, T., Maruoka, T., Kasukawa, E. and Saito, H. (2006) Adaptor functions of Cdc42, Ste50, and Sho1 in the yeast osmoregulatory HOG MAPK pathway. *Embo J*, **25**, 3033-3044.

Teige, M., Scheikl, E., Reiser, V., Ruis, H. and Ammerer, G. (2001) Rck2, a member of the calmodulin-protein kinase family, links protein synthesis to high osmolarity MAP kinase signaling in budding yeast. *Proc Natl Acad Sci U S A*, **98**, 5625-5630.

ter Linde, J.J., Liang, H., Davis, R.W., Steensma, H.Y., van Dijken, J.P. and Pronk, J.T. (1999) Genome-wide transcriptional analysis of aerobic and anaerobic chemostat cultures of Saccharomyces cerevisiae. *J Bacteriol*, **181**, 7409-7413.

Thevelein, J.M. (1991) Fermentable sugars and intracellular acidification as specific activators of the RAS-adenylate cyclase signalling pathway in yeast: the relationship to nutrient-induced cell cycle control. *Mol Microbiol*, **5**, 1301-1307.

Thevelein, J.M. (1992) The RAS-adenylate cyclase pathway and cell cycle control in Saccharomyces cerevisiae. *Antonie Van Leeuwenhoek*, **62**, 109-130.

Thevelein, J.M., Gelade, R., Holsbeeks, I., Lagatie, O., Popova, Y., Rolland, F., Stolz, F., Van de Velde, S., Van Dijck, P., Vandormael, P., Van Nuland, A., Van Roey, K., Van Zeebroeck, G. and Yan, B. (2005) Nutrient sensing systems for rapid activation of the protein kinase A pathway in yeast. *Biochem Soc Trans*, **33**, 253-256.

Tobias, J.W., Shrader, T.E., Rocap, G. and Varshavsky, A. (1991) The N-end rule in bacteria. *Science*, **254**, 1374-1377.

Tobias, J.W. and Varshavsky, A. (1991) Cloning and functional analysis of the ubiquitin-specific protease gene UBP1 of Saccharomyces cerevisiae. *J Biol Chem*, **266**, 12021-12028.

Towbin, H., Staehelin, T. and Gordon, J. (1979) Electrophoretic transfer of proteins from polyacrylamide gels to nitrocellulose sheets: procedure and some applications. *Proc Natl Acad Sci U S A*, **76**, 4350-4354.

Traven, A., Wong, J.M., Xu, D., Sopta, M. and Ingles, C.J. (2001) Interorganellar communication. Altered nuclear gene expression profiles in a yeast mitochondrial dna mutant. *J Biol Chem*, **276**, 4020-4027.

Travers, K.J., Patil, C.K., Wodicka, L., Lockhart, D.J., Weissman, J.S. and Walter, P. (2000) Functional and genomic analyses reveal an essential coordination between the unfolded protein response and ER-associated degradation. *Cell*, **101**, 249-258.

Treco, D.A. and Lundblad, V. (1993) Yeast. Basic techniques of yeast genetics. Preparation and inoclation of frozen stock. In Ausubel, F.M., Brent, R., Kingston, R.E., Moore, D.D., Seidman, C.E., Smith, J.A. and Struhl, K. (eds.), *Current Protocols in Molecular Biology*. John Wiley & Sons, New York, Vol. 2, p. 13.11.16.

Treco, D.A. and Winston, F. (1997) Yeast. Basic techniques of yeast genetics. Growth and manipulation of yeast. In Ausubel, F.M., Brent, R., Kingston, R.E., Moore, D.D., Seidman, C.E., Smith, J.A. and Struhl, K. (eds.), *Current Protocols in Molecular Biology*. John Wiley & Sons, New York, Vol. 2, pp. 13.12.11-13.12.12.

Treinin, M. and Simchen, G. (1993) Mitochondrial activity is required for the expression of IME1, a regulator of meiosis in yeast. *Curr Genet*, **23**, 223-227.

Treitel, M.A. and Carlson, M. (1995) Repression by SSN6-TUP1 is directed by MIG1, a repressor/activator protein. *Proc Natl Acad Sci U S A*, **92**, 3132-3136.

Tsukiyama, T., Palmer, J., Landel, C.C., Shiloach, J. and Wu, C. (1999) Characterization of the imitation switch subfamily of ATP-dependent chromatin-remodeling factors in Saccharomyces cerevisiae. *Genes Dev*, **13**, 686-697.

Turner, G.C., Du, F. and Varshavsky, A. (2000) Peptides accelerate their uptake by activating a ubiquitin-dependent proteolytic pathway. *Nature*, **405**, 579-583.

Tyson, J.R. and Stirling, C.J. (2000) LHS1 and SIL1 provide a lumenal function that is essential for protein translocation into the endoplasmic reticulum. *Embo J*, **19**, 6440-6452.

Uetz, P., Giot, L., Cagney, G., Mansfield, T.A., Judson, R.S., Knight, J.R., Lockshon, D., Narayan, V., Srinivasan, M., Pochart, P., Qureshi-Emili, A., Li, Y., Godwin, B., Conover, D., Kalbfleisch, T., Vijayadamodar, G., Yang, M., Johnston, M., Fields, S. and Rothberg, J.M. (2000) A comprehensive analysis of protein-protein interactions in Saccharomyces cerevisiae. *Nature*, **403**, 623-627.

Urano, F., Bertolotti, A. and Ron, D. (2000a) IRE1 and efferent signaling from the endoplasmic reticulum. *J Cell Sci*, **113**, 3697-3702.

Urano, F., Wang, X., Bertolotti, A., Zhang, Y., Chung, P., Harding, H.P. and Ron, D. (2000b) Coupling of stress in the ER to activation of JNK protein kinases by transmembrane protein kinase IRE1. *Science*, **287**, 664-666.

Urban, J., Soulard, A., Huber, A., Lippman, S., Mukhopadhyay, D., Deloche, O., Wanke, V., Anrather, D., Ammerer, G., Riezman, H., Broach, J.R., De Virgilio, C., Hall, M.N. and Loewith, R. (2007) Sch9 is a major target of TORC1 in Saccharomyces cerevisiae. *Mol Cell*, **26**, 663-674.

Uren, A.G., Beilharz, T., O'Connell, M.J., Bugg, S.J., van Driel, R., Vaux, D.L. and Lithgow, T. (1999) Role for yeast inhibitor of apoptosis (IAP)-like proteins in cell division. *Proc Natl Acad Sci U S A*, **96**, 10170-10175.

Van de Velde, S. and Thevelein, J.M. (2008) Cyclic AMP-protein kinase A and Snf1 signaling mechanisms underlie the superior potency of sucrose for induction of filamentation in Saccharomyces cerevisiae. *Eukaryot Cell*, **7**, 286-293.

Van Nuland, A., Vandormael, P., Donaton, M., Alenquer, M., Lourenco, A., Quintino, E., Versele, M. and Thevelein, J.M. (2006) Ammonium permease-based sensing mechanism for rapid ammonium activation of the protein kinase A pathway in yeast. *Mol Microbiol*, **59**, 1485-1505.

Vander Mierde, D., Scheuner, D., Quintens, R., Patel, R., Song, B., Tsukamoto, K., Beullens, M., Kaufman, R.J., Bollen, M. and Schuit, F.C. (2007) Glucose activates a protein phosphatase-1-mediated signaling pathway to enhance overall translation in pancreatic beta-cells. *Endocrinology*, **148**, 609-617.

Varshavsky, A. (1997) The N-end rule pathway of protein degradation. *Genes Cells*, **2**, 13-28.

Varshavsky, A. (2003) The N-end rule and regulation of apoptosis. *Nat Cell Biol*, **5**, 373-376.

Vattem, K.M. and Wek, R.C. (2004) Reinitiation involving upstream ORFs regulates ATF4 mRNA translation in mammalian cells. *Proc Natl Acad Sci U S A*, **101**, 11269-11274.

Vidal, M. and Gaber, R.F. (1991) RPD3 encodes a second factor required to achieve maximum positive and negative transcriptional states in Saccharomyces cerevisiae. *Mol Cell Biol*, **11**, 6317-6327.

Vidan, S. and Mitchell, A.P. (1997) Stimulation of yeast meiotic gene expression by the glucose-repressible protein kinase Rim15p. *Mol Cell Biol*, **17**, 2688-2697.

Vincent, J.A., Kwong, T.J. and Tsukiyama, T. (2008) ATP-dependent chromatin remodeling shapes the DNA replication landscape. *Nat Struct Mol Biol*, **15**, 477-484.

Vogelstein, B. and Gillespie, D. (1979) Preparative and analytical purification of DNA from agarose. *Proc Natl Acad Sci U S A*, **76**, 615-619.

Voytas, D. (2000) Prepation and analysis of DNA. Resolution and recovery of large DNA fragments. Agarose gel electrophoresis. In Ausubel, F.M., Brent, R., Kingston, R.E., Moore, D.D., Seidman, C.E., Smith, J.A. and Struhl, K. (eds.), *Current Protocols in Molecular Biology*. John Wiley & Sons, New York, Vol. 1, pp. 2.5A.1-9.

Walsh, R.B., Kawasaki, G. and Fraenkel, D.G. (1983) Cloning of genes that complement yeast hexokinase and glucokinase mutants. *J Bacteriol*, **154**, 1002-1004.

Wang, H. and Jiang, Y. (2003) The Tap42-protein phosphatase type 2A catalytic subunit complex is required for cell cycle-dependent distribution of actin in yeast. *Mol Cell Biol*, **23**, 3116-3125.

Wang, Y., Abu Irqeba, A., Ayalew, M. and Suntay, K. (2009) Sumoylation of transcription factor Tec1 regulates signaling of mitogen-activated protein kinase pathways in yeast. *PLoS One*, **4**, e7456.

Ward, M.P., Gimeno, C.J., Fink, G.R. and Garrett, S. (1995) SOK2 may regulate cyclic AMP-dependent protein kinase-stimulated growth and pseudohyphal development by repressing transcription. *Mol Cell Biol*, **15**, 6854-6863.

Washburn, B.K. and Esposito, R.E. (2001) Identification of the Sin3-binding site in Ume6 defines a two-step process for conversion of Ume6 from a transcriptional repressor to an activator in yeast. *Mol Cell Biol*, **21**, 2057-2069.

Wedaman, K.P., Reinke, A., Anderson, S., Yates, J., 3rd, McCaffery, J.M. and Powers, T. (2003) Tor kinases are in distinct membrane-associated protein complexes in Saccharomyces cerevisiae. *Mol Biol Cell*, **14**, 1204-1220.

Welihinda, A.A., Tirasophon, W., Green, S.R. and Kaufman, R.J. (1997) Gene induction in response to unfolded protein in the endoplasmic reticulum is mediated through Ire1p kinase interaction with a transcriptional coactivator complex containing Ada5p. *Proc Natl Acad Sci U S A*, **94**, 4289-4294.

Welihinda, A.A., Tirasophon, W. and Kaufman, R.J. (2000) The transcriptional co-activator ADA5 is required for HAC1 mRNA processing in vivo. *J Biol Chem*, **275**, 3377-3381.

Wellen, K.E. and Hotamisligil, G.S. (2005) Inflammation, stress, and diabetes. *J Clin Invest*, **115**, 1111-1119.

Westfall, P.J. and Thorner, J. (2006) Analysis of mitogen-activated protein kinase signaling specificity in response to hyperosmotic stress: use of an analog-sensitive HOG1 allele. *Eukaryot Cell*, **5**, 1215-1228.

Williams, R.M., Primig, M., Washburn, B.K., Winzeler, E.A., Bellis, M., Sarrauste de Menthiere, C., Davis, R.W. and Esposito, R.E. (2002) The Ume6 regulon coordinates metabolic and meiotic gene expression in yeast. *Proc Natl Acad Sci U S A*, **99**, 13431-13436.

Winnay, J.N., Boucher, J., Mori, M.A., Ueki, K. and Kahn, C.R. (2010) A regulatory subunit of phosphoinositide 3-kinase increases the nuclear accumulation of X-box-binding protein-1 to modulate the unfolded protein response. *Nat Med*, **16**, 438-445.

Wright, R.M., Repine, T. and Repine, J.E. (1993) Reversible pseudohyphal growth in haploid Saccharomyces cerevisiae is an aerobic process. *Curr Genet*, **23**, 388-391.

Wu, C., Whiteway, M., Thomas, D.Y. and Leberer, E. (1995) Molecular characterization of Ste20p, a potential mitogen-activated protein or extracellular signal-regulated kinase kinase (MEK) kinase kinase from Saccharomyces cerevisiae. *J Biol Chem*, **270**, 15984-15992.

Wu, J., Suka, N., Carlson, M. and Grunstein, M. (2001) TUP1 utilizes histone H3/H2B-specific HDA1 deacetylase to repress gene activity in yeast. *Mol Cell*, **7**, 117-126.

Xella, B., Goding, C., Agricola, E., Di Mauro, E. and Caserta, M. (2006) The ISWI and CHD1 chromatin remodelling activities influence ADH2 expression and chromatin organization. *Mol Microbiol*, **59**, 1531-1541.

Xiao, Y. and Mitchell, A.P. (2000) Shared roles of yeast glycogen synthase kinase 3 family members in nitrogen-responsive phosphorylation of meiotic regulator Ume6p. *Mol Cell Biol*, **20**, 5447-5453.

Xie, Y. and Varshavsky, A. (1999) The E2-E3 interaction in the N-end rule pathway: the RING-H2 finger of E3 is required for the synthesis of multiubiquitin chain. *Embo J*, **18**, 6832-6844.

Xue, Y., Batlle, M. and Hirsch, J.P. (1998) GPR1 encodes a putative G protein-coupled receptor that associates with the Gpa2p Galpha subunit and functions in a Ras-independent pathway. *Embo J*, **17**, 1996-2007.

Yang, H.Y., Tatebayashi, K., Yamamoto, K. and Saito, H. (2009) Glycosylation defects activate filamentous growth Kss1 MAPK and inhibit osmoregulatory Hog1 MAPK. *Embo J*, **28**, 1380-1391.

Yoneda, T., Imaizumi, K., Oono, K., Yui, D., Gomi, F., Katayama, T. and Tohyama, M. (2001) Activation of caspase-12, an endoplastic reticulum (ER) resident caspase, through tumor necrosis factor receptor-associated factor 2-dependent mechanism in response to the ER stress. *J Biol Chem*, **276**, 13935-13940.

Yoshida, H., Matsui, T., Yamamoto, A., Okada, T. and Mori, K. (2001) XBP1 mRNA is induced by ATF6 and spliced by IRE1 in response to ER stress to produce a highly active transcription factor. *Cell*, **107**, 881-891.

Yoshida, H., Okada, T., Haze, K., Yanagi, H., Yura, T., Negishi, M. and Mori, K. (2000) ATF6 activated by proteolysis binds in the presence of NF-Y (CBF) directly to the *cis*-acting element responsible for the mammalian unfolded protein response. *Mol Cell Biol*, **20**, 6755-6767.

Yoshida, H., Oku, M., Suzuki, M. and Mori, K. (2006) pXBP1(U) encoded in XBP1 pre-mRNA negatively regulates unfolded protein response activator pXBP1(S) in mammalian ER stress response. *J Cell Biol*, **172**, 565-575.

Yoshida, S., Ito, M., Callis, J., Nishida, I. and Watanabe, A. (2002) A delayed leaf senescence mutant is defective in arginyl-tRNA:protein arginyltransferase, a component of the N-end rule pathway in Arabidopsis. *Plant J*, **32**, 129-137.

Yu, J., Angelin-Duclos, C., Greenwood, J., Liao, J. and Calame, K. (2000) Transcriptional repression by blimp-1 (PRDI-BF1) involves recruitment of histone deacetylase. *Mol Cell Biol*, **20**, 2592-2603.

Yuan, Y.L. and Fields, S. (1991) Properties of the DNA-binding domain of the Saccharomyces cerevisiae STE12 protein. *Mol Cell Biol*, **11**, 5910-5918.

Yun, C.W., Tamaki, H., Nakayama, R., Yamamoto, K. and Kumagai, H. (1997) G-protein coupled receptor from yeast Saccharomyces cerevisiae. *Biochem Biophys Res Commun*, **240**, 287-292.

Yun, C.W., Tamaki, H., Nakayama, R., Yamamoto, K. and Kumagai, H. (1998) Gpr1p, a putative G-protein coupled receptor, regulates glucose-dependent cellular cAMP level in yeast Saccharomyces cerevisiae. *Biochem Biophys Res Commun*, **252**, 29-33.

Zaman, S., Lippman, S.I., Schneper, L., Slonim, N. and Broach, J.R. (2009) Glucose regulates transcription in yeast through a network of signaling pathways. *Mol Syst Biol*, **5**, 245.

Zaragoza, O. and Gancedo, J.M. (2000) Pseudohyphal growth is induced in Saccharomyces cerevisiae by a combination of stress and cAMP signalling. *Antonie Van Leeuwenhoek*, **78**, 187-194.

Zenvirth, D., Loidl, J., Klein, S., Arbel, A., Shemesh, R. and Simchen, G. (1997) Switching yeast from meiosis to mitosis: double-strand break repair, recombination and synaptonemal complex. *Genes Cells*, **2**, 487-498.

Zhang, K., Wong, H.N., Song, B., Miller, C.N., Scheuner, D. and Kaufman, R.J. (2005) The unfolded protein response sensor IRE1α is required at 2 distinct steps in B cell lymphopoiesis. *J Clin Invest*, **115**, 268-281.

Zhang, Y., Sun, Z.W., Iratni, R., Erdjument-Bromage, H., Tempst, P., Hampsey, M. and Reinberg, D. (1998) SAP30, a novel protein conserved between human and yeast, is a component of a histone deacetylase complex. *Mol Cell*, **1**, 1021-1031.

Zhang, Z., Smith, M.M. and Mymryk, J.S. (2001) Interaction of the E1A oncoprotein with Yak1p, a novel regulator of yeast pseudohyphal differentiation, and related mammalian kinases. *Mol Biol Cell*, **12**, 699-710.

Zhu, G., Spellman, P.T., Volpe, T., Brown, P.O., Botstein, D., Davis, T.N. and Futcher, B. (2000) Two yeast forkhead genes regulate the cell cycle and pseudohyphal growth. *Nature*, **406**, 90-94.

Zitomer, R.S. and Lowry, C.V. (1992) Regulation of gene expression by oxygen in Saccharomyces cerevisiae. *Microbiol Rev*, **56**, 1-11.

Zurita-Martinez, S.A. and Cardenas, M.E. (2005) Tor and cyclic AMP-protein kinase A: two parallel pathways regulating expression of genes required for cell growth. *Eukaryot Cell*, **4**, 63-71.

APPENDIX I

Ime1 and Ime2 Are Required for Pseudohyphal Growth of *Saccharomyces cerevisiae* on Nonfermentable Carbon Sources[▽]

Natalie Strudwick, Max Brown, Vipul M. Parmar, and Martin Schröder*

Durham University, School of Biological and Biomedical Sciences, Durham DH1 3LE, United Kingdom

Pseudohyphal growth and meiosis are two differentiation responses to nitrogen starvation of diploid *Saccharomyces cerevisiae*. Nitrogen starvation in the presence of fermentable carbon sources is thought to induce pseudohyphal growth, whereas nitrogen and sugar starvation induces meiosis. In contrast to the genetic background routinely used to study pseudohyphal growth (Σ1278b), nonfermentable carbon sources stimulate pseudohyphal growth in the efficiently sporulating strain SK1. Pseudohyphal SK1 cells can exit pseudohyphal growth to complete meiosis. Two stimulators of meiosis, Ime1 and Ime2, are required for pseudohyphal growth of SK1 cells in the presence of nonfermentable carbon sources. Epistasis analysis suggests that Ime1 and Ime2 act in the same order in pseudohyphal growth as in meiosis. The different behaviors of strains SK1 and Σ1278b are in part attributable to differences in cyclic AMP (cAMP) signaling. In contrast to Σ1278b cells, hyperactivation of cAMP signaling using constitutively active Ras2^{G19V} inhibited pseudohyphal growth in SK1 cells. Our data identify the SK1 genetic background as an alternative genetic background for the study of pseudohyphal growth and suggest an overlap between signaling pathways controlling pseudohyphal growth and meiosis. Based on these findings, we propose to include exit from pseudohyphal growth and entry into meiosis in the life cycle of *S. cerevisiae*.

Diploid cells of the budding yeast *Saccharomyces cerevisiae* choose between two developmental responses to nitrogen starvation, namely, pseudohyphal growth and meiosis (30). Pseudohyphal growth allows sessile *S. cerevisiae* cells to forage for nutrients and is a growth form distinct from the vegetative, yeast-like growth form. Pseudohyphal growth is induced by nitrogen starvation in the presence of fermentable carbon sources (30). Pseudohyphal growth is characterized by an elongated cell shape, adhesion of cells to each other after cell division has been completed, a switch from a bipolar to a unipolar budding pattern, and prolongation of the G$_2$ phase of the cell cycle to allow daughter cells to grow to the size of their mothers (45). This increased cell size allows newly born pseudohyphal daughters to immediately enter the cell cycle and to bud in synchrony with their mothers. Starvation for nitrogen and fermentable carbon sources is a prerequisite for induction of meiosis. In meiosis (also called sporulation), single diploid cells form an ascus containing four haploid, stress- and starvation-resistant spores. Meiosis is temporally divided into at least early, middle, and late phases of gene expression (16, 74). After premeiotic DNA replication, cells go through two meiotic divisions (meiosis I and II), initiation of prospore wall growth at sites near the spindle pole bodies (SPBs), nuclear division, and maturation of the spore walls to form mature asci (47).

The protein kinase A (PKA) pathway and the mating and filamentation mitogen-activated protein kinase (MAPK) pathway control pseudohyphal growth. Both pathways stimulate pseudohyphal growth by stimulating expression of the cell surface flocculin Flo11 (51). The PKA pathway is activated by the glucose sensor Gpr1 (55, 102) and by the high-affinity ammonium permease Mep2 (7, 53, 83). Gpa2 activates adenylate cyclase, which in turn activates PKA (46, 54). In *S. cerevisiae*, three catalytic subunits of PKA, Tpk1, Tpk2, and Tpk3, regulate pseudohyphal growth. Tpk2 directly interacts with and inhibits the transcriptional repressor of *FLO11*, Sfl1 (77). Phosphorylation of the transcription factor Flo8 by Tpk2 stimulates binding of Flo8 to the *FLO11* promoter and activation of *FLO11* (71, 72). In contrast to *TPK2*, deletion of *TPK1* or *TPK3* enhances pseudohyphal growth (71, 77), suggesting that Tpk1 and Tpk3 are inhibitors of pseudohyphal growth. Substrates for Tpk1 or Tpk3 involved in repression of pseudohyphal growth have not been identified. The mating and filamentation MAPK cascade (56), consisting of the MAPK kinase kinase Ste11, the MAPK kinase Ste7, the MAPK Kss1, and the scaffold Ste5, is regulated by the cell surface mucin Msb2 (20). Msb2 recruits general signaling proteins, such as Sho1, the isoprenylated, plasma membrane-tethered protein Cdc42, and its p21-activated kinase, Ste20, to the filamentation MAPK cascade (20). The MAPK pathway controls the activity of the heterodimeric transcription factor Ste12-Tec1 (29, 82), which activates expression of *FLO11* and regulates cell elongation.

Entry into meiosis is governed by a transcriptional cascade controlling expression of early meiotic genes (EMGs) (47). Starvation induces expression of *IME1* (85). Ime1 carries a transcriptional activation domain (98), which activates transcription of EMGs (99), including *IME2*, after binding of Ime1 to the DNA-binding protein Ume6 (11, 79). A two-hybrid interaction between Ume6 and Ime1 is stimulated by several protein kinases, including the glycogen synthase kinase 3β ho-

---

TABLE 1. Plasmids used for this study

Plasmid	Features	Reference
pCITE-4a(+)-HA-UME6	*UME6*-His₆ *bla*	Schröder and Kaufman, unpublished data
pHS103	2μm *URA3 IME1 bla*	99
pHS105	2μm *URA3 IME2 bla*	99
pIL30	*FG(TyA)lacZ::URA3*	66
pKB193	2μm *URA3* T99N-*UME6-lexA bla*	11
pMW2	*CEN URA3 RAS2^{G19V} bla*	108
pRS316	*CEN6 ARSH4 URA3 bla*	97
pRS316-*UME6-lexA*	*CEN6 ARSH4 URA3 UME6-lexA bla*	This study
pRS316-T99N-*UME6-lexA*	*CEN6 ARSH4 URA3 T99N-UME6-lexA bla*	This study

mologs Rim11, Mck1, and Mrk1 and the protein kinase Rim15 (57, 58, 106, 110). Binding of Ime1 to Ume6 induces degradation of Ume6 (59). The protein kinase Ime2 is required for full expression of EMGs (99), stimulates its own expression through an upstream activating site (96), and promotes meiotic DNA replication by directly phosphorylating Rfa2 (17, 18). Sic1 phosphorylation by Ime2 triggers its proteasomal destruction and entry into meiotic S phase (21, 89). *IME2* is also required for expression of middle meiotic genes (4, 64, 69) and for reestablishment of repression of EMGs in the middle meiotic phase (47). Nutrient-rich conditions repress transcription of *IME1*. The PKA pathway represses expression of *IME1* in the presence of glucose (60, 62) and inhibits phosphorylation of Ime1 by Rim11 (80). Cells expressing constitutively active Ras2^{G19V}, Gpa2^{R273A}, or Gpa2^{G132V} (22, 105, 111) or deleted for the regulatory subunit of PKA, *BCY1*, do not sporulate (12).

Using an efficiently sporulating strain, SK1 (42), we report that elements of the early meiotic cascade, such as Ime1, binding of Ime1 to Ume6, and Ime2, are required for pseudohyphal growth of SK1 cells. In contrast to the genetic background routinely used to study pseudohyphal growth, i.e., strain Σ1278b (30), nonfermentable carbon sources stimulate pseudohyphal growth of SK1 cells independent of their utilization in respiration. Pseudohyphal SK1 cells can complete meiosis. Differences in cyclic AMP (cAMP) signaling may explain, in part, the different behaviors of these two strains. Whereas constitutively active Ras2^{G19V} stimulates pseudohyphal growth of Σ1278b cells, it inhibits pseudohyphal growth of SK1 cells. Our work establishes the SK1 genetic background as a tool for the study of mechanisms controlling the life choice decision between pseudohyphal growth and sporulation of dimorphic yeasts and filamentous fungi.

MATERIALS AND METHODS

Plasmid constructions. To obtain plasmid pRS316-T99N-*UME6*-lexA, the ~4.4-kbp SpeI/HindIII fragment of pKB193 (11) was cloned into SpeI- and HindIII-digested pRS316 (97). To cure the T99N mutation in *UME6*, the 263-bp BamHI/NheI fragment of pRS316-*T99N-UME6*-lexA was replaced with a similar fragment from pCITE-4a(+)-HA-*UME6* (M. Schröder and R. J. Kaufman, unpublished data) encoding wild-type (WT) Ume6. pMW2 (108) (*CEN URA3 RAS2^{G19V}*) was used to express constitutively active Ras2. The plasmids used for this study are listed in Table 1.

Yeast methods. Yeast strains (Table 2) were transformed by the LiOAc method (15). *IME1* and *IME2* were deleted by PCR-based gene deletion (32, 107), using the oligodeoxynucleotides listed in Table 3. Mating type was determined by PCR (38). Respiration-deficient ρ⁰ cells were generated by treatment

with 20 μg/ml ethidium bromide as described previously (24). Growth was monitored as described before (91). Pseudohyphal growth was assayed on synthetic low-ammonium (SLA) medium (91) plates containing a 2% (wt/vol) concentration of the indicated carbon source and, as required, amino acids or uracil to complement auxotrophies, at 5 to 10 mg/liter for SK1 cells. Ethanol was used in sealed containers containing a 2% (wt/vol) ethanol reservoir. WT and mutant strains were matched for auxotrophic mutations. In experiments in which mutant strains carried WT metabolic genes, the corresponding amino acids or uracil was added at the same concentration to plates for both the WT and mutant strains. Uracil was provided at 5 mg/liter in SLA plates for Σ1278b cells (30, 54, 55). Cells were streaked onto SLA plates to obtain single colonies. Pseudohyphal growth and agar invasion were scored after growth at 30°C for the times indicated in the figure legends. Pilot experiments revealed no difference in pseudohyphal growth on plates supplemented with 2.5 to 10 mg/liter of the amino acids or uracil required to complement auxotrophies. L-Lysine was included in all plates because the ho::LYS2 allele produces a weak Lys⁺ phenotype. cAMP (Calbiochem, Merck, Darmstadt, Germany) was used at 5 mM. To document the filamentation phenotype, pictures from at least four representative colonies were taken under bright-field illumination at a magnification of ×40 to ×100 with an inverted microscope (Inverso; Fisher Scientific), an eyepiece camera (Globecam D; Fisher Scientific), and imaging software (Image Driving software; Fisher Scientific). Pictures from asci were taken at a magnification of ×400. Time-lapse video microscopy was performed on the same microscope, using AMCap software. Plates were incubated at room temperature for time-lapse video microscopy. Wet tissues were placed into plates, and plates were sealed with Parafilm to minimize evaporation. Agar invasion was determined after washing away cells above the agar by gently scraping plates with a spreader under running distilled water for ~1 min. The remaining cells were photographed at a magnification of ×40 to ×100. Haploid invasive growth was assayed after growth for 3 days at 30°C on yeast extract-peptone-dextrose (YPD) plates. Plates were photographed before and after washing the cells from the agar surface to document total and invasive growth, respectively. Activity of the *FG(TyA)::lacZ* reporter was measured and standardized to total cellular protein activity as described before (66, 91). Cell length and width were measured using the straight tool in ImageJ. Bud and birth scars were stained as described before (25, 75). Briefly, cells were grown for 18 h on SLA acetate plates and washed off plates. A total of 1 × 10⁴ cells were resuspended in 25 μl of 1-mg/ml calcofluor white M2R (dissolved in water) and 50 μl of 1-mg/ml fluorescein isothiocyanate-wheat germ agglutinin (FITC-WGA) dissolved in phosphate-buffered saline (PBS; 4.3 mM Na₂HPO₄, 1.47 mM KH₂PO₄, 2.7 mM KCl, and 137 mM NaCl [pH 7.2]), incubated for 15 min at room temperature, and washed three times with PBS. Cells were visualized using a Nikon Eclipse TE 300 microscope and a 60× A/1.4 oil objective. Calcofluor white-stained bud scars were observed using a DAPI (4′,6-diamidino-2-phenylindole) filter, and FITC-WGA-stained birth and bud scars were observed using an FITC filter.

Measurement of sporulation. To determine sporulation, a fresh stationary-phase culture grown in rich medium (YPD; 2% [wt/vol] glucose, 2% [wt/vol] peptone, 1% [wt/vol] yeast extract) was used to inoculate rich acetate medium (YPAc; 2% [wt/vol] KOAc, 1% [wt/vol] yeast extract, 2% [wt/vol] peptone). These cells were grown to mid-log phase in baffled flasks, collected by centrifugation at 3,000 × g for 2 min, washed once with water, resuspended in complete sporulation medium (C-SPO) (106), and grown at 30°C with shaking for the required amount of time. Cells were visualized under a phase-contrast microscope, and the percentage of asci was determined for 3 replicates.

Tetrad dissection. Asci were washed off plates from areas containing small colonies consisting predominantly of asci formed by pseudohyphal cells by use of sterile water collected by centrifugation, and the cell wall was digested with Glusulase for 15 min at 30°C. Spores were dissected using a tetrad dissection microscope (Singer Instruments, Watchet, United Kingdom), placed onto a YPD plate, and allowed to germinate and grow for 2 days at 30°C. Pictures were taken with a GelDoc 2000 system (Bio-Rad Laboratories, Hemel Hempstead, United Kingdom).

Heat shock treatment. Cells were grown to mid-log phase in liquid YPD medium at 25°C (for glycogen and trehalose determinations) or 30°C (for Northern analysis) with shaking before being shifted to 37°C (for glycogen and trehalose determinations) or 39°C (for Northern analysis) for the indicated times. Samples were taken immediately and processed as described below.

Metabolite determinations. Glycogen and trehalose concentrations were determined as described by Parrou et al. (73). Briefly, cells were collected by centrifugation and washed once with ice-cold water, and the pellet was frozen immediately at −20°C. Cell pellets were resuspended in 250 μl 0.25 M Na₂CO₃ and heated at 95°C for 2 h with occasional mixing. The pH was adjusted to 5.2 by addition of 150 μl 1 M acetic acid and 600 μl 0.2 M sodium acetate buffer, pH

TABLE 2. Yeast strains used for this study[a]

Strain and genetic background	Genotype	Reference
SK1 genetic background		
AMP 109	**a**/α	10
AMP 115	**a**/α ime1-12::TRP1/ime1-12::TRP1	10
AMP 1618	α IME2-20-lacZ::LEU2 rme1Δ5::LEU2 met4	106
AMP 1619	**a** IME2-20-lacZ::LEU2 rme1Δ5::LEU2 arg6	91
KSY 162	**a**/α ime2-K97R-myc::TRP1/ime2-K97R-myc::TRP1 trp1ΔFA::hisG/trp1ΔFA::hisG his3-11,15/his3-11,15 ho::hisG/ho::hisG	65
KSY 187	**a**/α IME2-myc::TRP1/IME2-myc::TRP1 trp1ΔFA::hisG/trp1ΔFA::hisG his3-11,15/his3-11,15 ho::hisG/ho::hisG	65
MSY 133-29	**a** his3ΔSK rme1Δ5::LEU2	This study
MSY 133-34	**a** his3ΔSK rme1Δ5::LEU2	This study
MSY 135-12	**a** met4 rme1Δ5::LEU2	This study
MSY 135-43	**a** met4 rme1Δ5::LEU2	This study
MSY 136-40	α arg6 rme1Δ5::LEU2	92
MSY 138-17	α his3ΔSK rme1Δ5::LEU2	92
MSY 184-55	**a** arg6 rme1Δ5::LEU2 ume6-5::LEU2	This study
MSY 185-65	α his3ΔSK rme1Δ5::LEU2 ume6-5::LEU2	This study
MSY 186-68	α arg6 rme1Δ5::LEU2 ume6-5::LEU2	92
MSY 188-119	**a** his3ΔSK rme1Δ5::LEU2 ume6-5::LEU2	This study
MSY 202-14	α arg6 rme1Δ5::LEU2 ime2-2::LEU2	This study
MSY 203-22	**a** met4 rme1Δ5::LEU2 ime2-2::LEU2	This study
MSY 203-27	**a** met4 rme1Δ5::LEU2 ime2-2::LEU2	This study
MSY 203-33	**a** met4 rme1Δ5::LEU2 ime2-2::LEU2	This study
MSY 206-36	α his3ΔSK rme1Δ5::LEU2 ime2-2::LEU2	This study
MSY 552-17	α his3ΔSK rme1Δ5::LEU2 ime1Δ::hphMX4	This study
MSY 558-38	α his3ΔSK rme1Δ5::LEU2	This study
S497	**a**/α his3-11,15/his3-11,15 trp1ΔFA/trp1ΔFA ho::hisG/ho::hisG	88
S635	**a**/α IME2ΔC241-HA6-kanMX/IME2ΔC241-HA6-kanMX his3-11,15/his3-11,15 trp1ΔFA/trp1ΔFA ho::hisG/ho::hisG	88
Σ1278b genetic background		
MLY 61 **a**/α	**a**/α ura3-52/ura3-52	54
MLY 187 **a**/α	**a**/α ura3-52/ura3-52 ras2::G418/ras2::G418	55
MLY 232 **a**/α	**a**/α ura3-52/ura3-52 gpr1::G418/gpr1::G418	55
MSY 699-01 **a**/α	**a**/α ura3-52/ura3-52 ime1Δ::kanMX2/ime1Δ::hphMX4	This study
MSY 694-51 **a**/α	**a**/α ura3-52/ura3-52 ime2Δ::kanMX2/ime2Δ::hphMX4	This study

[a] All haploid SK1 strains have the additional alleles ura3, leu2::hisG, trp1::hisG, and lys-2 ho::LYS2, and all diploid SK1 strains are homozygous for these alleles, if not noted otherwise. The alleles arg6 (68), his3-11,15 (Saccharomyces Genome Database), his3ΔSK (68), ho::hisG (2), ho::LYS2 (2), ime1-12::TRP1 (99), ime2-2::LEU2 (64), ime2::kanMX (88), IME2-20-lacZ::LEU2 (106), IME2-myc::TRP1 (4), ime2-K97R-myc::TRP1 (4), IME2ΔC241-HA6-kanMX (88), leu2::hisG (2), lys2 (2), met4 (68), rme1Δ5::LEU2 (19), trp1::hisG (2), trp1ΔFA::hisG (37), ume6-5::LEU2 (101), ura3 (2), and ura3-52 (78) have been described before.

5.2. The suspension was split into two equal parts. The first of these was incubated overnight at 57°C with continuous shaking in the presence of 100 μg α-amyloglucosidase from *Aspergillus niger* (Sigma, St. Louis, MO), freshly prepared as a 10-mg/ml stock dissolved in 0.2 M sodium acetate buffer, pH 5.2. The second half of the suspension was incubated overnight at 37°C with 3 mU trehalase (0.25 U/ml; Sigma). Liberated glucose was measured using a GO glucose assay kit (Sigma) as directed. To measure the glucose concentration in plates, small sections of the most densely grown areas were cut out with a scalpel and placed into a syringe attached to a 0.22-μm filter. Liquid was expelled by applying pressure to the plunger. The glucose concentration was measured using a glucose meter (Roche Diagnostics).

cAMP assay. cAMP concentrations were measured essentially as described before (23, 67, 84, 90). In brief, cells grown to mid-log phase on acetate were collected by centrifugation and washed with ice-cold water. The cell pellet was resuspended in 6% ice-cold trichloroacetic acid. Acid-washed glass beads (diameter = 0.4 to 0.6 mm) were added before the suspension was snap-frozen in liquid nitrogen and thawed on ice. Cells were then lysed using a Precellys 24 homogenizer (Bertin Technologies, Montigny-le-Bretonneux, France) at 6,000 rpm twice for 30 s each, with a 1-min break between, at 4°C. Following removal of cell debris by centrifugation (2,000 × *g* for 15 min, 4°C), HCl was added to the supernatant to a final concentration of 10 mM. The sample was extracted four times with diethyl ether and subsequently dried in a speed vacuum. The lyophilized cAMP was resuspended in assay buffer from the cAMP Biotrak enzyme immunoassay (EIA) system (GE Healthcare, Little Chalfont, United Kingdom), and the cAMP concentration was measured by use of this kit as directed. Samples were standardized against the cell number.

Northern analysis. RNA analysis by Northern blotting was performed as described previously (92). Probes for *HSP12*, *HSP26*, *HSP82*, and *FLO11* (*MUC1*) were generated by PCR, using genomic DNA as the template. The probes for *HOP1*, *IME1*, *IME2*, *INO1*, *SPO13*, and the loading control pC4/2 have been described elsewhere (48, 92). All mRNAs were quantitated by phosphorimaging on a Typhoon 9400 system (GE Healthcare).

TABLE 3. Oligodeoxynucleotides used for this study

Oligonucleotide	Sequence
ime1Δ, 5′	GCTTTTCTATTCCTCTCCCCACAAACAAAATGCAAGCGGATATGCATGGACAGCTGAAGCTTCGTACGC
ime1Δ, 3′	TGAATGGATATATTTTGAGGGAAGGGGGGAAGATTGTAGTACTTTTCGAGAAGGCCACTAGTGGATCTG
ime2Δ, 5′	CGGTTAAGGTGGCTGTCTAGAGAATATAAACCTGTATTTATTTACCAGGCAGGCCACTAGTGGATCTG
ime2Δ, 3′	CTGAGCCGGGTAACCGAACACAAAGATCTCGTTCTACTTTTTTTGACCTCAAGCTTCGTACGCTGCAGG

RESULTS

Nonfermentable carbon sources stimulate pseudohyphal growth. We previously reported that **a**/α diploid cells defective in a nutrient-regulated signaling pathway respond inappropriately to a meiotic stimulus by initiating pseudohyphal growth (91). These observations prompted us to investigate whether diploid **a**/α WT cells with the SK1 genetic background induce pseudohyphal growth when exposed to starvation conditions known to induce meiosis. To test this hypothesis, we grew diploid **a**/α SK1 cells on plates containing nonfermentable carbon sources and a limiting ammonium sulfate concentration (50 μM). In these plate assays, pseudohyphal growth is characterized by multiple projections of cells radiating away from the colony center (30). Diploid WT SK1 cells formed few pseudohyphae and were modestly capable of invading the agar when grown on glucose (Fig. 1A and B). Nonfermentable carbon sources, such as acetate, glycerol, pyruvate, and L-lactate, stimulated formation of branched pseudohyphae and agar invasion (Fig. 1A and B). Pseudohypha formation and agar invasion were also enhanced on plates containing both glucose and a nonfermentable carbon source (Fig. 1A and B). This stimulation could be observed as early as 1 day after inoculation of the plates (not shown). Furthermore, ~1.6% (wt/vol) glucose remained even in the most densely grown areas of plates after 10 days of growth, suggesting that nonfermentable carbon sources stimulate pseudohyphal growth in the presence of glucose. Based on their appearance, pseudohyphae formed on nonfermentable carbon sources appear to share many morphological features with previously described pseudohyphae (30), such as cell adhesion after completion of cytokinesis, agar invasion, and directional growth (Fig. 1).

Glucose strongly inhibits utilization of alternative carbon sources by inhibiting expression of several enzymes of the citric acid cycle and the respiratory chain (93). However, limiting nitrogen concentrations under pseudohyphal growth conditions may derepress these genes. For example, rapamycin treatment, which mimics nitrogen starvation, induces glucose-repressible genes in glucose-grown cultures (35). To establish whether respiratory metabolism of nonfermentable carbon sources is required for stimulation of pseudohyphal growth by these carbon sources, we produced respiration-deficient petite cells. We confirmed the loss of respiratory function by the inability of petite cells to grow on plates containing only acetate as a carbon source. Acetate and pyruvate stimulated pseudohyphal growth in petite cells in the presence of glucose (Fig. 1D). In contrast, glycerol, ethanol, and L-lactate did not stimulate pseudohyphal growth of petite cells. These three carbon sources require NAD^+-dependent oxidation reactions in order to be metabolized (93), indicating that less efficient regeneration of NAD^+ from NADH may interfere with stimulation of pseudohyphal growth by these carbon sources in petite cells. Taken together, these data indicate that nonfermentable carbon sources stimulate pseudohyphal growth independent of their use as respiratory energy sources. These results also suggest that the less pronounced pseudohyphal growth seen on glucose as a sole carbon source (Fig. 1A) may be caused by the accumulation of glycolytic waste products, especially ethanol, during fermentative growth. In support of this hypothesis, we found that ethanol stimulates pseudohyphal growth and agar invasion (Fig. 1E) (52).

Microscopic examination of pseudohyphae on plates containing only nonfermentable carbon sources at a higher magnification revealed that pseudohyphal cells exited pseudohyphal growth and formed asci (Fig. 1C). Cells both above and below the agar surface sporulated as early as 3 days after inoculation of plates (not shown). All pseudohyphae of all colonies sporulated. All spores isolated from asci formed by pseudohyphal cells on acetate were viable (Fig. 1F). The mating type locus displayed a 2:2 segregation pattern (Fig. 1G), indicating normal execution of both meiotic divisions. No asci were observed in the presence of glucose. Asci sometimes displayed a linear arrangement of two to four spores, especially in cells grown on glycerol (Fig. 1C). All spores from linear asci were viable and displayed a 2:2 segregation pattern for the mating type locus (not shown). Taken together, these data show that nonfermentable carbon sources stimulate pseudohyphal growth and that pseudohyphal cells can enter and successfully complete meiosis.

Ime1 and the protein kinase activity of Ime2 are required for pseudohyphal growth on nonfermentable carbon sources. Sporulation of pseudohyphae precluded investigation of cellular characteristics of pseudohyphal cells, such as cell elongation. Both Ime1 and Ime2 control entry into meiosis. Sporulation of *ime1Δ/ime1Δ* and *ime2Δ/ime2Δ* cells is decreased several hundredfold compared to that of WT strains (43, 99). Functions for *IME1* or *IME2* outside meiosis have not been reported. Hence, we characterized pseudohypha formation and agar invasion of *ime1Δ/ime1Δ* and *ime2Δ/ime2Δ* strains. Surprisingly, pseudohypha formation was nearly completely absent in *ime1Δ/ime1Δ* cells (Fig. 2A). Deletion of *IME1* severely decreased the pseudohyphal morphology of nearly all colonies on a plate, independent of the position of the colony on the plate (Fig. 2A). However, *ime1Δ/ime1Δ* cells were able to invade the agar (Fig. 2C), showing that filamentation and agar invasion are genetically separable phenotypes. Similarly, filamentation, but not agar invasion, was defective in *ime2Δ/ime2Δ* cells grown on glucose, a mixture of glucose and acetate, or acetate, but not glycerol (Fig. 2B and D). Deletion of *IME2* decreased the pseudohyphal morphology of nearly all colonies on plates containing glucose, glucose plus acetate, or acetate as the carbon source (data not shown). However, the pseudohyphal growth defect of *ime2Δ/ime2Δ* cells was not as severe as the pseudohyphal growth defect of *ime1Δ/ime1Δ* cells (Fig. 2A and B). The roles of *IME1* and *IME2* in pseudohyphal growth were independent of the ability of yeast to respire (not shown). Overexpression of Ime1 and Ime2 from multicopy (2μm) plasmids enhanced pseudohyphal growth (Fig. 3A) and had no effect on agar invasion (Fig. 3D). This finding is consistent with decreased pseudohypha formation of *ime1Δ/ime1Δ* and *ime2Δ/ime2Δ* strains (Fig. 2). Cells carrying the protein kinase-defective *K97R-ime2* allele displayed a defect in pseudohypha formation similar to that with the *IME2* deletion (Fig. 2E and F), showing that the protein kinase activity of Ime2 is required for pseudohyphal growth and meiosis. Deletion of the C terminus of Ime2 (Ime2ΔC241), which controls the mitotic stability of Ime2 (88), did not affect pseudohyphal growth (not shown). Taken together, these data show that Ime1 and Ime2 are required for pseudohypha formation by SK1 cells.
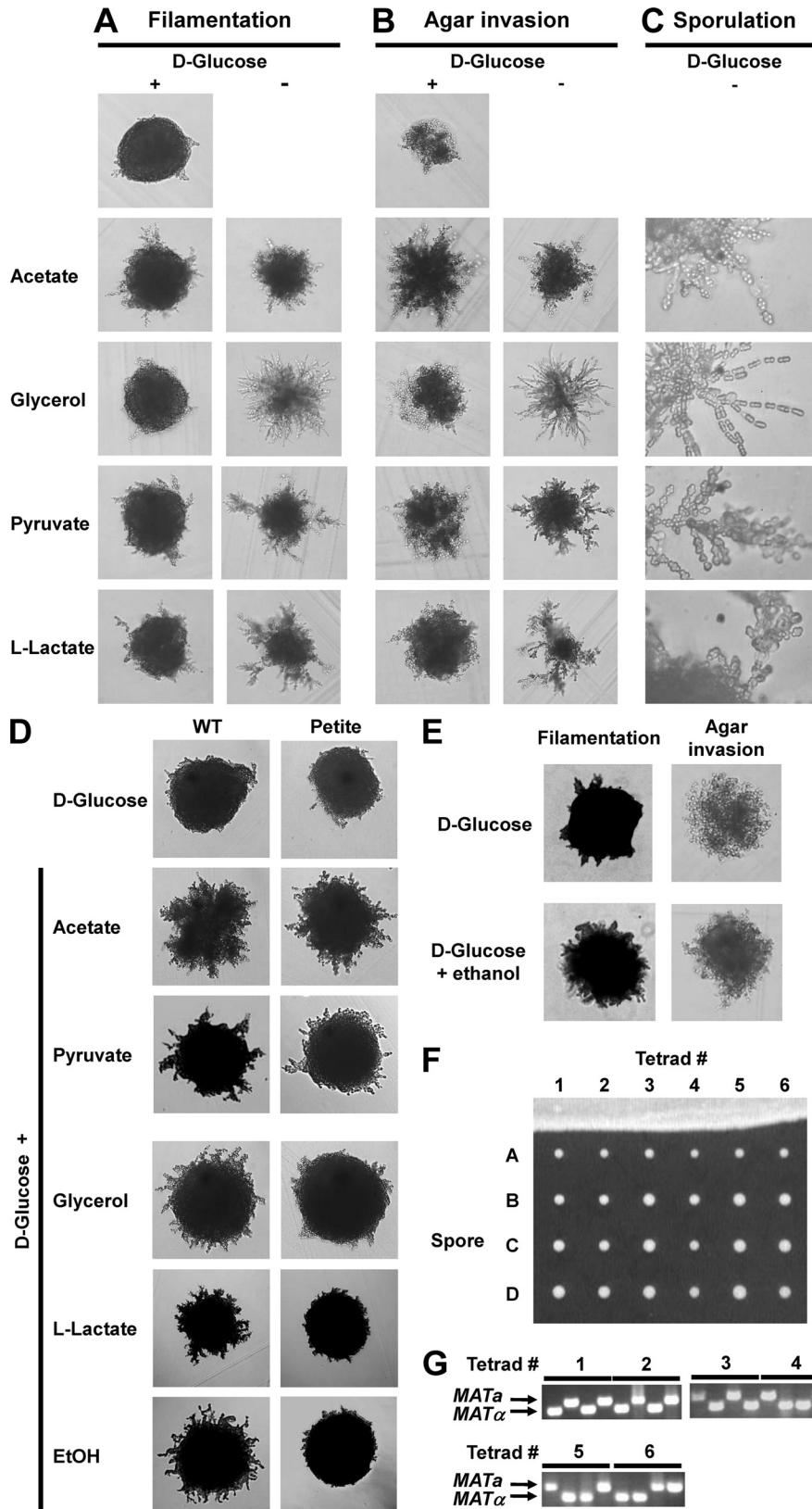
FIG. 1. Nonfermentable carbon sources stimulate pseudohyphal growth in WT **a**/α diploid SK1 strains (AMP 1618 × AMP 1619 transformed with pRS316). Identical results were obtained with another diploid WT strain (AMP 109) (cf. Fig. 1 and 2). Colony morphology (A), agar invasion (B), and ascus formation (C) are shown after growth for 7 days. (D) Stimulation of pseudohyphal growth in respiration-deficient petite cells. The colony morphology after 7 days of growth is shown. (E) Stimulation of pseudohyphal growth by ethanol. (F) Asci formed by pseudohyphal cells contain four viable spores. Asci formed by a WT strain (AMP109) on SLA medium supplemented with 2% KOAc were dissected with a tetrad dissection microscope, and spores were placed onto a YPD plate and allowed to germinate and grow for 2 days. (G) PCR genotyping of the mating type locus reveals a 2:2 segregation pattern for MAT**a** and MATα.
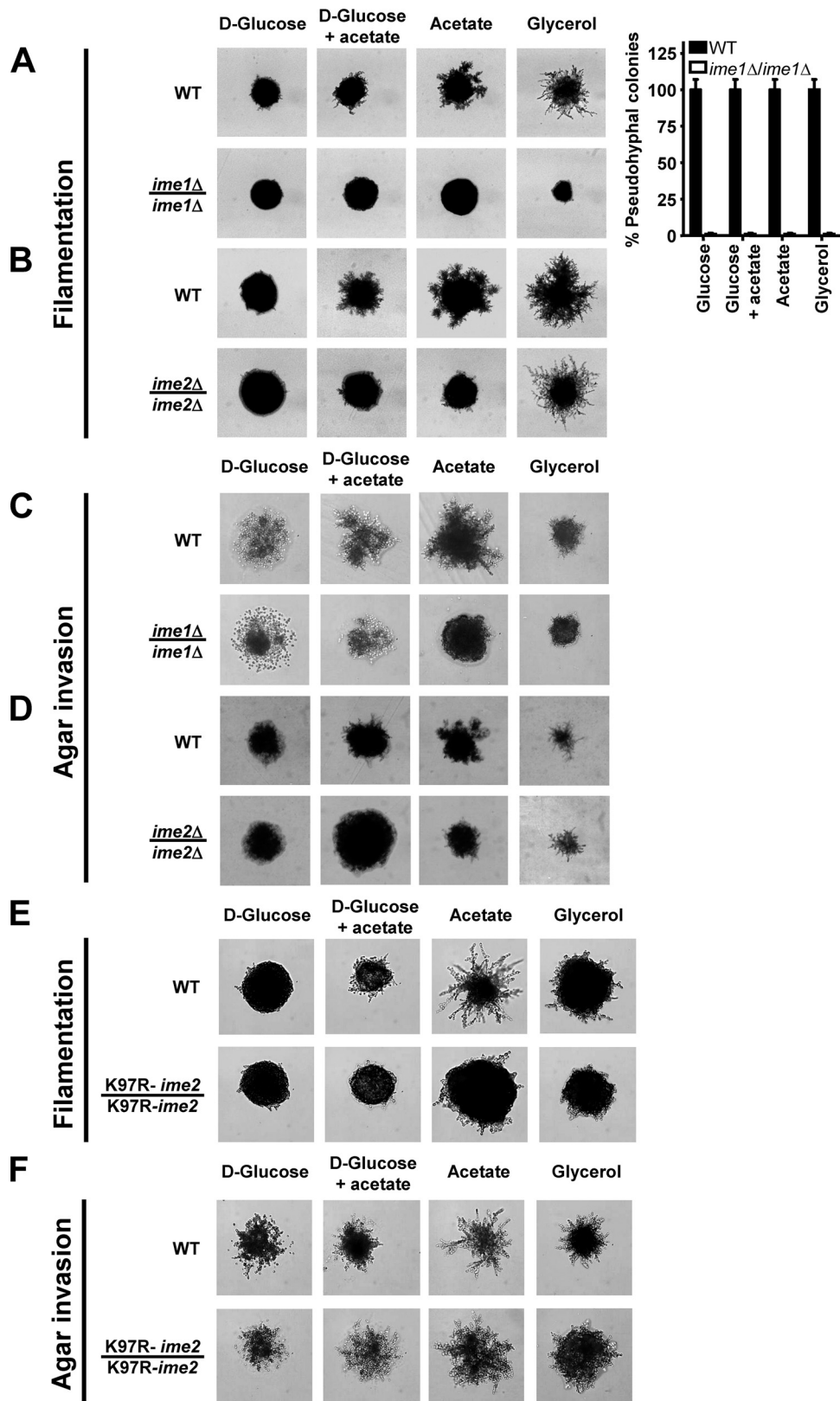
FIG. 2. Ime1 and the protein kinase activity of Ime2 are required for pseudohyphal growth. The colony morphology of WT (AMP 109) and *ime1Δ/ime1Δ* (AMP 115) strains (A) and of WT (MSY 135-43 × MSY 136-40) and *ime2Δ/ime2Δ* (MSY 202-14 × MSY 203-27) strains (B) is shown. Bar graphs show percentages of pseudohyphal colonies. For each strain and carbon source, >200 colonies were classified as pseudohyphal or nonpseudohyphal. Error bars represent standard errors. (C and D) Agar invasion by WT (AMP 109) and *ime1Δ/ime1Δ* (AMP 115) strains (C) and by WT (MSY 135-12 × MSY 138-17) and *ime2Δ/ime2Δ* (MSY 203-22 × MSY 206-36) strains (D). Filamentation (E) and agar invasion (F) of WT (KSY 187) and *K97R-ime2/K97R-ime2* (KSY 162) strains were scored after 7 days of growth.
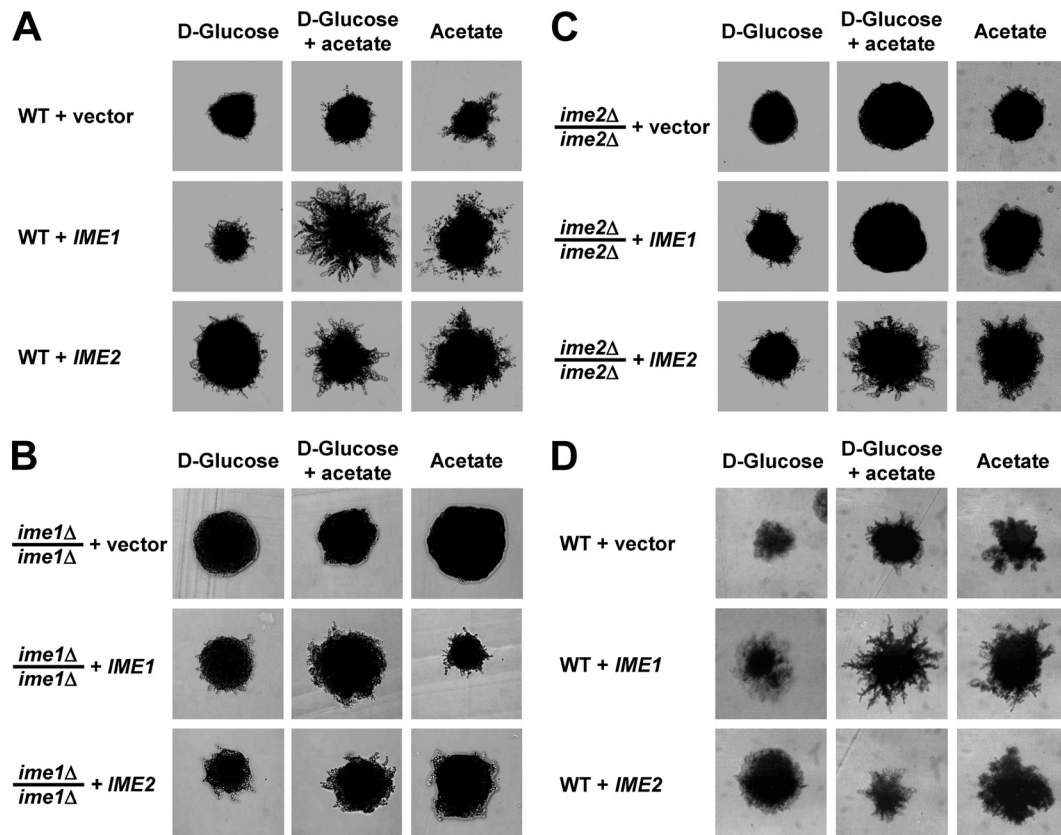
FIG. 3. *IME1* acts through *IME2* to stimulate pseudohyphal growth. Colony morphology is shown for WT (MSY 135-12 × MSY 138-17) (A), *ime1*Δ/*ime1*Δ (AMP 115) (B), and *ime2*Δ/*ime2*Δ (MSY 203-22 × MSY 206-36) (C) strains transformed with empty vector (pRS426) or 2μm plasmids expressing *IME1* (pHS103) or *IME2* (pHS105) from their endogenous promoters. Similar results were obtained with an *rme1*Δ/*rme1*Δ strain (MSY 135-12 × MSY 138-17) and an *RME1*/*RME1* strain (AMP 109). For simplicity, only MSY 135-12 × MSY 138-17 is shown in panel A. (D) Agar invasion of the strains in panel A. Filamentation and agar invasion were scored after 7 days of growth.

Ime1 acts through Ime2 to stimulate pseudohyphal growth. In meiosis, Ime1 activates transcription of EMGs, including *IME2*. Ime2 stimulates expression of EMGs, including its own expression, independent of *IME1* (64, 96). Ime2 is also a negative regulator of *IME1* expression (81, 95, 96, 99) and Ime1 stability (34). To establish whether *IME1* and *IME2* act in the same order in pseudohyphal growth and meiosis, we investigated whether overexpression of Ime1 or Ime2 from 2μm plasmids would rescue the pseudohyphal growth defects of *ime1*Δ/*ime1*Δ and *ime2*Δ/*ime2*Δ strains. Expression of Ime1 in *ime1*Δ/*ime1*Δ cells and of Ime2 in *ime2*Δ/*ime2*Δ cells restored pseudohyphal growth on nonfermentable carbon sources (Fig. 3B and C). Expression of Ime2 in *ime1*Δ/*ime1*Δ strains partially restored pseudohypha formation (Fig. 3B), whereas expression of Ime1 in *ime2*Δ/*ime2*Δ strains had no effect on acetate (Fig. 3C), suggesting that activation of *IME2* by Ime1 is required for pseudohyphal growth on acetate. The partial restoration of pseudohyphal growth by overexpression of Ime2 in *ime1*Δ/*ime1*Δ cells is consistent with an Ime2-independent function of Ime1 in pseudohyphal growth. The more severe pseudohyphal growth defects of *ime1*Δ/*ime1*Δ cells than those of *ime2*Δ/*ime2*Δ cells (Fig. 2) also suggest an Ime2-independent role for Ime1 in pseudohyphal growth. Agar invasion was not altered by overexpression of Ime1 or Ime2 in the WT, *ime1*Δ/*ime1*Δ, or *ime2*Δ/*ime2*Δ strain (Fig. 3D and not shown), providing addi-

tional evidence that Ime1 and Ime2 are not involved in regulation of agar invasion.

Evidence that binding of Ime1 to Ume6 is involved in pseudohyphal growth on nonfermentable carbon sources. Ime1 activates transcription of EMGs, including *IME2*, through the DNA-binding protein Ume6 (11, 59, 79). Ume6 also recruits two transcriptional repression complexes to EMG promoters, namely, the ISW2 chromatin remodeling complex (31) and the Rpd3-Sin3 histone deacetylase (HDAC) (41). Deletion of *UME6* derepresses EMG transcription, including that of *IME2*, under nutrient-rich conditions (92, 101, 109) but also abrogates activation of these genes during starvation. A T99N mutation in Ume6 interferes with activation of EMGs by Ime1. This mutation decreased the interaction between Ime1 and Ume6 ~35-fold in a two-hybrid assay (110). The T99N mutation interferes with association of Ime1 with EMG promoters (11, 39, 79, 92) and with degradation and removal of Ume6 from EMG promoters by Ime1 (59). These data suggested that Ume6 also has a role in pseudohyphal growth. Deletion of *UME6* derepressed filamentation (Fig. 4A). Agar invasion by *ume6*Δ/*ume6*Δ cells was enhanced compared to WT cells (Fig. 4A). This function of Ume6 in agar invasion is likely to be independent of *IME1* and *IME2*, because deletion or overexpression of these two genes had no effect on agar invasion (Fig. 2 and 3). Expression of WT Ume6 and T99N-
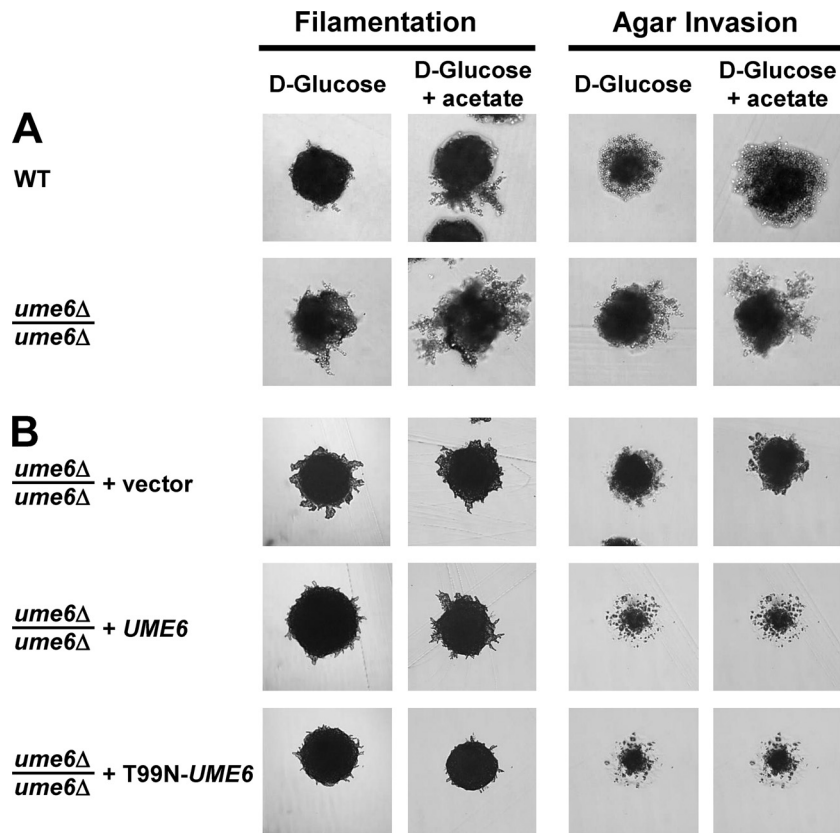
FIG. 4. Recruitment of Ime1 to early meiotic gene promoters, including the *IME2* promoter, by Ume6 is required for pseudohyphal growth. (A) Pseudohyphal growth is derepressed in a *ume6Δ/ume6Δ* (MSY 184-55 × MSY 185-65) strain compared to that in a WT strain (MSY 133-34 × MSY 136-40). (B) Abrogation of the interaction between Ume6 and Ime1 in cells expressing the *T99N-UME6* allele as the sole source of Ume6 results in a pseudohyphal growth defect. Filamentation and agar invasion phenotypes of *ume6Δ/ume6Δ* (MSY 186-68 × MSY 188-119) strains carrying empty vector (pRS316) or plasmids expressing WT Ume6 (pRS316-*UME6*-lexA) or T99N-Ume6 (pRS316-*T99N-UME6*-lexA) are shown. Filamentation and agar invasion were scored after 7 days of growth.

Ume6 complemented the enhanced agar invasion of *ume6Δ/ume6Δ* strains (Fig. 4B). T99N-Ume6 inhibited filamentation more severely than WT Ume6 did (Fig. 4B). This behavior of the T99N-Ume6 mutant is consistent with repression of *IME2* by the two transcriptional repression complexes recruited to the *IME2* promoter by Ume6 and, at the same time, with abrogation of the Ime1-Ume6 interaction by this mutation. These data indicate that the early meiotic cascade consisting of Ime1, recruitment of Ime1 to URS1 by Ume6, and Ime2 is required for both pseudohyphal growth and meiosis but not for agar invasion.

Ime1 is required for cell elongation, bud site selection, and budding of daughter cells before their mother cells. Next, we characterized cellular features that distinguish yeast-form and pseudohyphal cells to obtain more detailed insight into the roles of Ime1 and Ime2 in pseudohyphal growth. In contrast to yeast-form cells, pseudohyphal cells invade agar because they overexpress Flo11 (51). Compared to yeast-form cells, pseudohyphal cells are elongated, adhere to each other after cell division has been completed, and switch from a bipolar to a unipolar budding pattern. Yeast-form daughters are born smaller than their mothers. Pseudohyphal daughters are born with a size comparable to the size of their mothers, allowing

them to bud at the same time as, or even slightly before, their mothers (45).

Deletion of *IME1* or *IME2* did not affect agar invasion of diploid cells (Fig. 2), indicating that Ime1 and Ime2 act independent of Flo11. Flo11 is also required for haploid invasive growth (33). Deletion of *IME1* and *IME2* did not decrease haploid invasive growth (Fig. 5A). Northern blotting confirmed that *FLO11* expression was largely unperturbed in *ime1Δ/ime1Δ* cells (Fig. 5B). Consistent with these observations, we found that deletion of *IME1* or *IME2* did not significantly decrease expression of an *FG(TyA)::lacZ* reporter (not shown) whose activation correlates well with the activity of the filamentation MAPK cascade in pseudohyphal cells (66).

Microscopic examination of microcolonies revealed that *ime1Δ/ime1Δ* cells were not as elongated as WT cells when grown on SLA plates with glucose or acetate as the carbon source (Fig. 5C). Acetate enhanced cell elongation in both strains. *ime2Δ/ime2Δ* and *K97R-ime2/K97R-ime2* cells (Fig. 5D and data not shown) were also not as elongated as their corresponding WT cells. The elongation defects of the *ime2Δ/ime2Δ* and *K97R-ime2/K97R-ime2* strains were less severe than the elongation defect of the *ime1Δ/ime1Δ* strain. These elongation phenotypes are consistent with the less severe
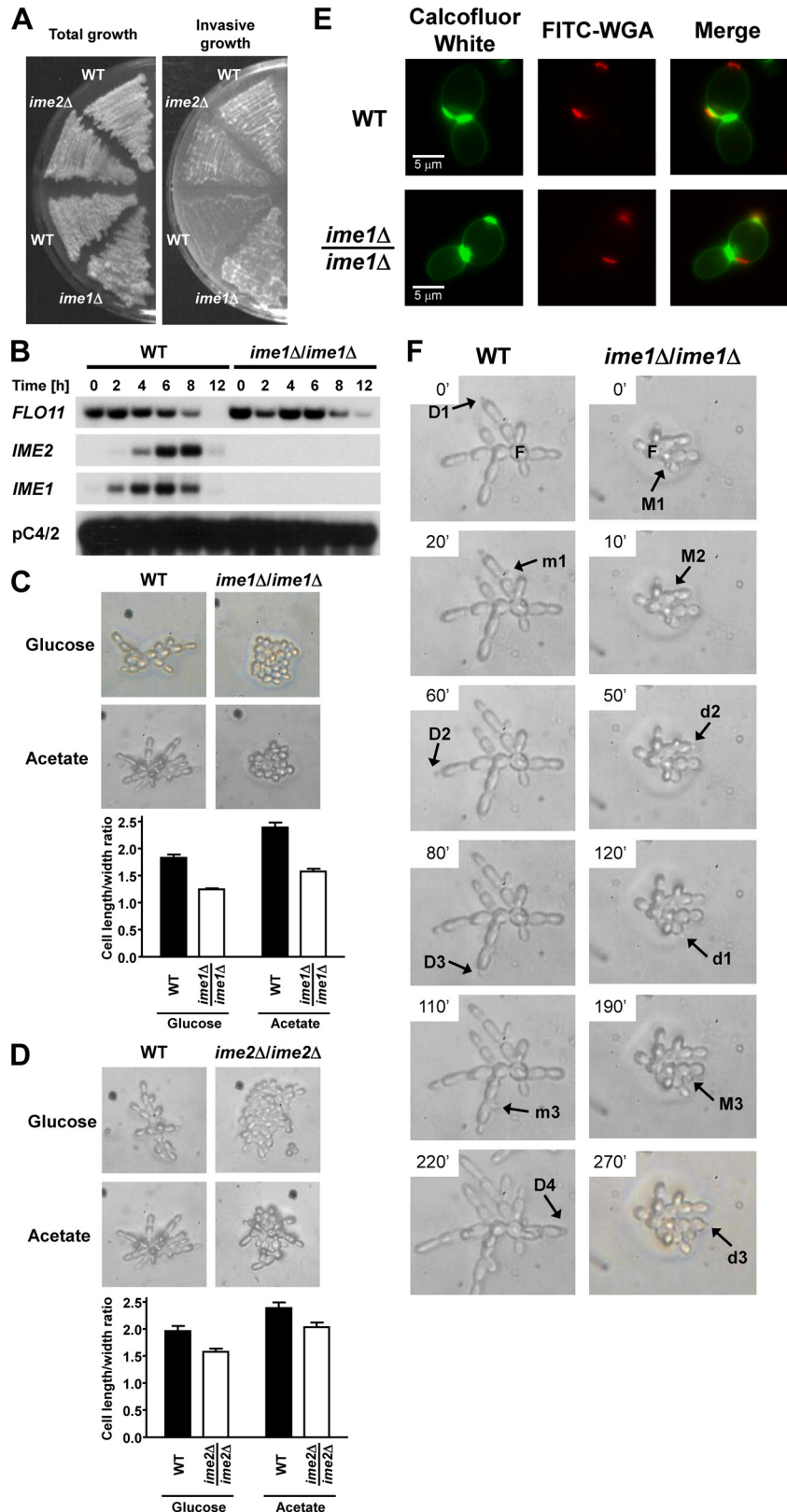
FIG. 5. Ime1 and Ime2 act independent of Flo11 expression and the filamentation MAPK cascade. (A) Haploid invasive growth is not defective in *ime1*Δ and *ime2*Δ strains. Invasive growth was scored after 3 days of growth on YPD plates. The strains used were upper WT (MSY 135-12), *ime2*Δ (MSY 203-27), lower WT (MSY 558-38), and *ime1*Δ (MSY 552-17). (B) Deletion of *IME1* does not affect transcription of *FLO11*. RNA samples isolated from a WT (AMP 109) or *ime1*Δ/*ime1*Δ (AMP 115) strain grown to mid-log phase on YPAc and shifted for the indicated times to C-SPO medium were analyzed by Northern blotting. (C and D) The microscopic appearance of microcolonies is shown for WT (AMP 109)

pseudohyphal growth phenotype of *ime2Δ/ime2Δ* colonies after growth for several days (Fig. 2A) and with the stimulation of pseudohyphal growth by acetate (Fig. 1A). These data show that *IME1* and *IME2* are required for elongation of pseudohyphal cells.

ime1Δ/ime1Δ and *ime2Δ/ime2Δ* microcolonies are more globular than microcolonies of WT cells. This suggested that another characteristic of pseudohyphal cells that contributes to directional growth is affected by deletion of *IME1* and *IME2*. To characterize whether the budding patterns of WT and *ime1Δ/ime1Δ* strains are bi- or unipolar, we stained bud scars with calcofluor white after growth of both strains for ~18 h on SLA acetate plates. For both strains, we observed cells with bud scars at both poles (not shown). Calcofluor white staining did not reveal a difference in bud site selection between the two strains (not shown). Bipolar budding cells display a strong bias toward the pole opposite their birth site in their first few divisions (14). For this reason, it may be difficult to distinguish between bi- and unipolar budding patterns by staining with calcofluor white only. To reveal more subtle differences in bud site selection, we costained cells with FITC-WGA. In addition to bud scars, FITC-WGA also stains birth scars (25). Identification of the birth scar allowed classification of budding events into events at the poles distal and proximal to the birth scar (Fig. 5E). This classification revealed that WT and *ime1Δ/ime1Δ* cells grown for 18 h on SLA acetate plates budded exclusively at the distal pole in their first division (Table 4). This bias for the distal pole persisted for the first few divisions in both strains. However, this bias appeared to decrease faster in the *ime1Δ/ime1Δ* strain. The second bud was formed at the birth pole in ~17% of *ime1Δ/ime1Δ* cells, whereas only ~4.7% of WT cells chose the birth pole for their second bud ($P <$ 0.05). This small increase in selection of the proximal pole in the second cell cycle may suffice to explain the more globular growth of *ime1Δ/ime1Δ* cells.

Time-lapse video microscopy revealed that pseudohyphal WT daughter cells budded before or around the same time as their mothers (12 of 14 mother-daughter pairs). Mothers could bud much later (>60 min) than their daughters (4 of 12 mother-daughter pairs in which the daughter budded first). In contrast, *ime1Δ/ime1Δ* daughter cells budded after their mothers (10 of 10 mother-daughter pairs) (Fig. 5F). This reversal in the budding order is a second factor that contributes to the globular growth of *ime1Δ/ime1Δ* cells.

Comparison of the roles of nonfermentable carbon sources in pseudohyphal growth in the SK1 and Σ1278b genetic backgrounds. Our data show that stimulation of pseudohyphal growth by nonfermentable carbon sources in the SK1 genetic background requires *IME1* and *IME2*. Next, we wished to

TABLE 4. Distribution of bud scars relative to the birth site in WT (AMP 109) and *ime1Δ/ime1Δ* (AMP 115) cells[a]

No. of bud scars on cells	No. of cells with only distal bud scars	No. of cells with ≥1 proximal bud scar	% of cells with only distal bud scars	% of cells with ≥1 proximal bud scar
WT cells				
1	157	0	100	0
2	61	3	95	4.7
3	15	12	56	44
4	5	6	45	55
5	0	3	0	100
6	0	3	0	100
ime1Δ/ime1Δ cells				
1	106	0	100	0
2	53	11	82	17
3	14	14	50	50
4	3	10	23	77
5	1	6	14	86
6	0	5	0	100
7	0	0		
8	0	1	0	100

[a] Cells were grown for 18 h on SLA acetate plates at 30°C. Cells were then stained with calcofluor white and FITC-WGA to reveal bud and birth scars, as described in Materials and Methods. Only the difference in selection of the second bud site was significantly different ($P < 0.05$, assuming that the number of bud scars formed at the proximal pole follows a Poisson distribution).

extend these findings to the Σ1278b genetic background, which is used more routinely to study pseudohyphal growth (30, 54). In contrast to the case for the SK1 genetic background, nonfermentable carbon sources inhibited pseudohyphal growth in diploid **a**/α Σ1278b WT cells (Fig. 6A). Likewise, *IME1* and *IME2* were not required for pseudohypha formation by diploid **a**/α Σ1278b WT cells on glucose (Fig. 6B).

Elevated cAMP signaling inhibits pseudohyphal growth on nonfermentable carbon sources. Stimulation of pseudohyphal growth in the presence of nonfermentable carbon sources in SK1 cells is different from the behavior of Σ1278b cells (Fig. 1 and 6A). To explore explanations for the different behaviors of these two genetic backgrounds, we decided to focus on the PKA pathway. The PKA pathway is a signaling pathway responding to the quality of the carbon source, is activated by glucose (87), and is involved in the regulation of pseudohyphal growth (26). The PKA pathway is hyperactive in Σ1278b cells compared to another genetic background, SP1 (100). Strains with high constitutive PKA activity fail to express *IME1* (60, 62), and PKA signaling inhibits Ime1 (80) and Ime2 (22, 76). These data suggest that elevated cAMP signaling in Σ1278b cells interferes with activation of Ime1 and Ime2, resulting in a pseudohyphal growth defect on nonfermentable carbon

and *ime1Δ/ime1Δ* (AMP 115) strains (C) and for WT (MSY 136-40 × MSY 135-12) and *ime2Δ/ime2Δ* (MSY 202-14 × MSY 203-27) strains (D) grown for 12 to 24 h on SLA plates containing glucose or acetate as a carbon source. The *P* values for all pairwise strain and medium comparisons are <0.01. (E) Examples of bud site selection in WT (AMP 109) and *ime1Δ/ime1Δ* (AMP 115) cells grown on SLA acetate plates at 30°C for 18 h. Bud scars were stained with calcofluor white and are false-colored in green. Bud and birth scars stained with FITC-WGA are false-colored in red to reveal the polarity of the cells. Note that calcofluor white does not stain the birth scar and that FITC-WGA does not stain the chitin ring between the mother and its growing bud. (F) Order of budding of mother and daughter cells in WT (AMP 109) and *ime1Δ/ime1Δ* (AMP 115) strains grown on SLA acetate plates. Abbreviations: D, daughter; M, mother. Uppercase letters represent the cell budding first, and lowercase letters represent the cell budding last. The numbers identify mother-daughter pairs. The cells from which the colonies originated are labeled with an "F." These cells are spherical and display a random, nonpolar budding pattern.
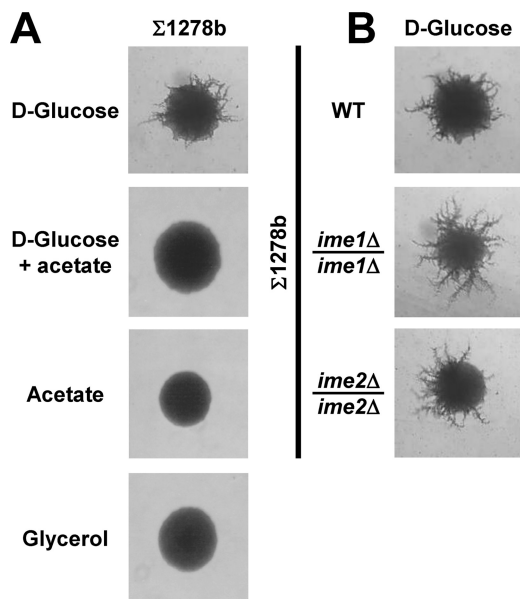
FIG. 6. Characterization of the roles of *IME1* and *IME2* in pseudohyphal growth in the Σ1278b background. (A) Inhibition of pseudohyphal growth by nonfermentable carbon sources in the Σ1278b genetic background. The strain used was MLY 61 **a**/α. (B) *IME1* (MSY 699-01 **a**/α) and *IME2* (MSY 694-51 **a**/α) are not required for pseudohyphal growth on glucose in Σ1278b cells. In both panels, the colony morphologies after 7 days of growth on the indicated carbon sources are shown.

sources. To test this hypothesis, we first confirmed that cAMP signaling is constitutively elevated in Σ1278b cells compared to SK1 cells. Consistent with elevated cAMP signaling in Σ1278b cells, we found that growth on nonfermentable carbon sources, sporulation, induction of heat shock genes, and accumulation of storage carbohydrates upon heat shock were decreased in Σ1278b cells (Fig. 7A to D). All of these phenotypes are known to be inhibited by elevated cAMP signaling (13, 100, 104). Deletion of cAMP signaling components such as *GPR1* or *RAS2* elevated sporulation and storage carbohydrate accumulation in heat-shocked Σ1278b cells (Fig. 7F, H, and J). Expression of constitutively active Ras2^{G19V} in SK1 cells inhibited sporulation and storage carbohydrate accumulation during heat shock (Fig. 7E, G, and I). These data confirm that cAMP signaling contributes to the magnitude of these phenotypes in Σ1278b and SK1 cells. cAMP levels were elevated in Σ1278b cells compared to those in SK1 cells (4.5 ± 0.3 pmol/10^7 cells versus 3.5 ± 0.2 pmol/10^7 cells). These data confirm that cAMP signaling is elevated in Σ1278b cells compared to SK1 cells. Steady-state *IME1* mRNA levels were significantly decreased in Σ1278b cells (Fig. 8A), consistent with repression of *IME1* by elevated cAMP signaling in Σ1278b cells. Addition of cAMP or expression of constitutively active Ras2^{G19V} inhibited pseudohyphal growth in SK1 cells (Fig. 8B and C). *FLO11*, whose expression is stimulated by an activated cAMP signaling pathway in Σ1278b cells, displayed strongly elevated mRNA levels in SK1 cells (Fig. 8A and D). Furthermore, acetate induced the expression of *FLO11* in SK1 cells (Fig. 8D) but not in Σ1278b cells (70), which may contribute to increased pseudohyphal growth and invasiveness of SK1 strains grown on

nonfermentable carbon sources (Fig. 1A and B). Deletion of *RAS2*, *GPR1*, or *GPA2* did not allow Σ1278b cells to form pseudohyphae on nonfermentable carbon sources (not shown), possibly because *FLO11* expression requires cAMP signaling in Σ1278b cells (71, 72, 77). Taken together, these data suggest that cAMP signaling inhibits pseudohyphal growth on nonfermentable carbon sources by inhibiting *IME1* and *IME2*.

DISCUSSION

Our work has shown that nonfermentable carbon sources stimulate pseudohyphal growth independent of respiratory function and that pseudohyphal cells formed in the absence of glucose exit pseudohyphal growth to successfully complete meiosis (Fig. 9). Two regulators of entry into meiosis, *IME1* and *IME2*, are required for stimulation of pseudohyphal growth by nonfermentable carbon sources. The use of a different genetic background, SK1, from that used routinely for investigation of pseudohyphal growth, Σ1278b, was critical for making these observations. Pseudohyphae formed by SK1 cells on nonfermentable carbon sources share several features with pseudohyphae formed by Σ1278b cells, for example, cell elongation, daughter cells budding before or at the same time as their mothers, and invasion of the agar. However, pseudohyphal SK1 cells appear to employ a bipolar budding pattern. Bipolar budding diploid cells display a strong bias toward budding at the pole opposite their birth site in the first few divisions (14). This bias (Table 4), together with daughters budding before their mothers (Fig. 5F), may allow SK1 cells to form pseudohyphae. Both of these features are affected by deletion of *IME1*. The budding order of daughter and mother cells is reversed in *ime1*Δ/*ime1*Δ cells (Fig. 5F). The bias for budding distal to the birth site is less pronounced in *ime1*Δ/*ime1*Δ cells, especially for the second budding event (Table 4). These buds and their first daughters are directed toward the origins of the colonies, thus explaining why *ime1*Δ/*ime1*Δ cells are defective in pseudohyphal growth.

Role of Ime1 and Ime2 in pseudohyphal growth. Studies on Ime1 and Ime2 in meiosis provide clues regarding the extent to which these two proteins may act through the same or similar downstream targets to stimulate pseudohyphal growth on nonfermentable carbon sources. Ime1 acts through Ume6 to activate EMGs, including *IME2* (11, 59, 79, 98). Ume6 serves dual, opposing roles on EMG promoters. Under nutrient-rich conditions, it represses EMGs via recruitment of the Rpd3-Sin3 HDAC (41) and the ISW2 chromatin remodeling complex (31), whereas in starvation its interaction with Ime1 is required for activation of EMGs, either because Ime1 bound to EMG promoters via Ume6 provides a transcriptional activation domain (11, 79, 98) or because the interaction between these two proteins is required to remove Ume6 from EMGs (59). To investigate whether this transcriptional switch also operates in pseudohyphal growth, we turned to a T99N mutation in Ume6. This mutation decreases the interaction of Ume6 with Ime1 in a two-hybrid assay (~35-fold) but does not derepress expression of EMGs prior to induction of meiosis (11), suggesting that the T99N mutation does not affect interaction of Ume6 with the Rpd3-Sin3 HDAC or the ISW2 chromatin remodeling complex. Cells expressing T99N-Ume6 formed less pseudohyphal colonies than cells deleted for *UME6* (Fig. 4B).
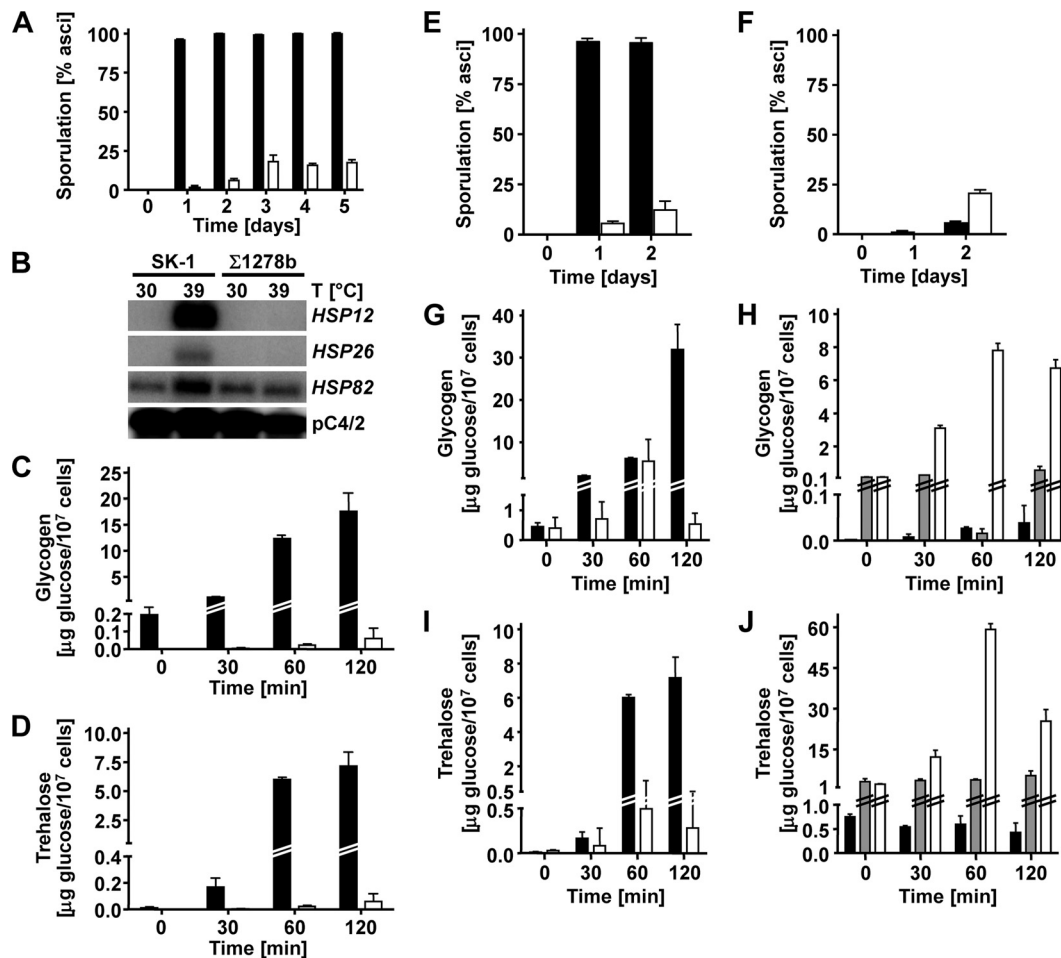
FIG. 7. cAMP signaling is hyperactive in Σ1278b cells compared to SK1 cells. (A) Sporulation of **a**/α diploid SK1 (AMP 109; filled bars) and Σ1278b (MLY 61 **a**/α; open bars) cells. (B) Induction of heat shock genes in WT (AMP 109 and MLY 61 **a**/α) shifted from 30°C to 39°C for 30 min. (C and D) Accumulation of glycogen (C) and trehalose (D) in WT cells (AMP 109 [filled bars] and MLY 61 **a**/α [open bars]) shifted from 25°C to 37°C for the indicated times. (E) Expression of constitutively active Ras2^{G19V} from plasmid pMW2 in a WT **a**/α diploid SK1 strain (AMP 109) inhibits sporulation. Filled bars, AMP 109 plus pRS316; open bars, AMP 109 plus pMW2. (F) Deletion of *GPR1* in a WT **a**/α diploid Σ1278b strain (MLY 61 **a**/α) increases sporulation. Filled bars, WT (MLY 61 **a**/α); open bars, *gpr1Δ/gpr1Δ* strain (MLY 232 **a**/α). (G and H) Glycogen accumulation is shown for cells shifted from 25°C to 37°C for the indicated times. (G) AMP 109 transformed with pRS316 (filled bars) or pMW2 expressing Ras2^{G19V} (open bars). (H) MLY 61 **a**/α (black bars), MLY 232 **a**/α (*gpr1Δ/gpr1Δ*; gray bars), and MLY 187 **a**/α (*ras2Δ/ras2Δ*; open bars). (I and J) Trehalose accumulation in the cells shown in graphs G and H. For each measurement, the average and standard error for two replicates are shown.

This finding is consistent with the interpretation that derepression of *IME2* enhances pseudohyphal growth in *ume6Δ/ume6Δ* cells. T99N-Ume6 also interfered with pseudohypha formation compared to WT Ume6 (Fig. 4B), which can be explained by the inability of Ime1 to activate *IME2* in cells expressing T99N-Ume6. This effect of the T99N-Ume6 mutant was more pronounced on plates containing both glucose and acetate than on plates containing only glucose (Fig. 4B), which is consistent with elevated expression of *IME1* in cells grown on nonfermentable carbon sources (Fig. 8E) and after exponential growth on glucose (44). The pseudohyphal growth defect of the T99N-Ume6-expressing cells was also not as severe as the pseudohyphal growth defect displayed by *ime1Δ/ime1Δ* cells, either because of a residual interaction between T99N-Ume6 and Ime1 or because of the existence of additional, Ume6-independent Ime1 targets. Epistasis analysis (Fig. 3) supports

the idea that Ime1 acts largely through inducing expression of Ime2 to stimulate pseudohyphal growth. The behavior of the T99N-Ume6 mutant (Fig. 4B) provides further support for this view. At the same time, the pseudohyphal growth defect of *ime1Δ/ime1Δ* cells is more severe than the pseudohyphal growth defect of *ime2Δ/ime2Δ* cells (Fig. 2 and 5), showing that Ime1 also stimulates pseudohyphal growth independent of Ime2. This situation is similar to regulation of entry into meiosis by Ime1 and Ime2, where Ime1 also acts through Ime2 and independent of Ime2 to stimulate entry into meiosis (64). We conclude that all key elements of the early meiotic cascade function in pseudohyphal growth. The transcriptional targets of Ime1 in pseudohyphal growth remain to be identified, but EMGs and genes carrying the Ume6-binding site URS1 in their promoters are likely targets.

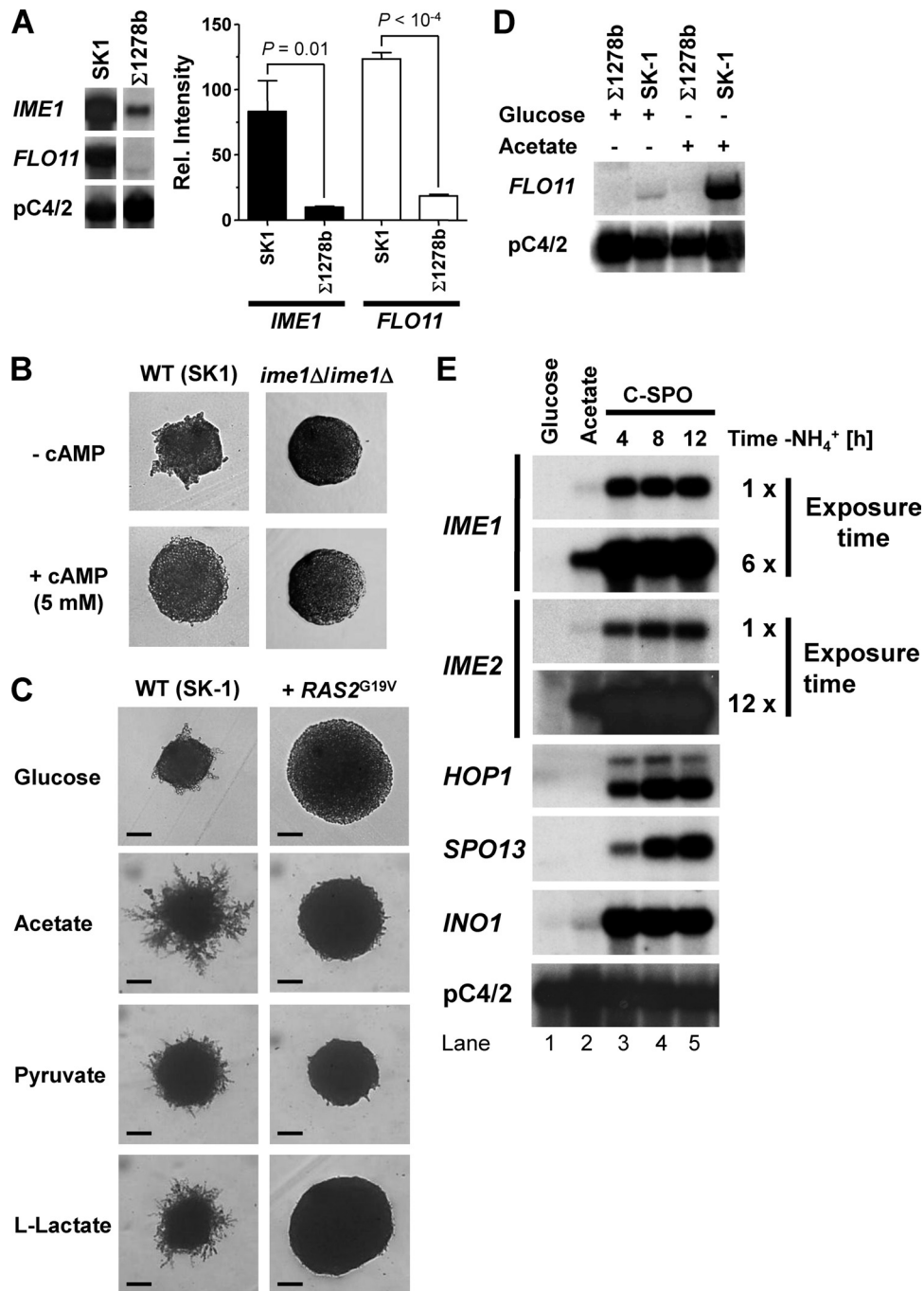Several substrates for Ime2 are known, including Sic1 (21,

FIG. 8. cAMP signaling represses pseudohyphal growth in SK1 cells. (A) Expression of *IME1* and *FLO11* in WT SK1 (AMP 109) and Σ1278b (MLY 61 **a**/α) strains grown on rich acetate medium (2% KOAc, 1% yeast extract, 2% peptone) to exponential growth phase. All bands are from the same blot. *P* values were derived from an unpaired, two-tailed *t* test (*n* = 6). (B and C) Addition of 5 mM cAMP to SLA glucose plates (B) or expression of constitutively active Ras2^{G19V} from plasmid pMW2 (C) inhibits pseudohyphal growth in SK1 cells (AMP 109). Filamentation and agar invasion were scored after 7 days of growth. Bars, 40 μm for glucose and 100 μm for the other carbon sources. (D) Acetate induces expression of *FLO11* in a WT SK1 strain (AMP 109). Cells were grown to mid-log phase on YPD or YPAc before isolation of RNA for Northern analysis. The Σ1278b strain was MLY 61 **a**/α. (E) Comparison of steady-state mRNA levels for *IME1*, *IME2*, the EMGs *HOP1* and *SPO13*, and the inositol biosynthetic gene *INO1* in an SK1 strain (AMP 1619) grown to exponential growth phase on glucose (lane 1) or acetate (lane 2) or 4, 8, or 12 h after being shifted to sporulation medium (C-SPO medium) (see Materials and Methods).

94), Cdh1 (8), the middle meiotic gene-specific transcription factor Ndt80 (4, 69), the repressor of middle meiotic genes Sum1 (65), and Rfa2 (17, 18). Stabilization of the G$_1$-S transition-promoting G$_1$ cyclins Cln1 to -3 in *grr1Δ/grr1Δ* cells stim-

ulates pseudohyphal growth (6). Consequently, pseudohyphal cells are characterized by a shortened G$_1$ and an extended G$_2$ phase (45). In meiosis, Ime2 substitutes for Cdc28 to trigger entry into meiotic S phase by phosphorylating Sic1 and trig-
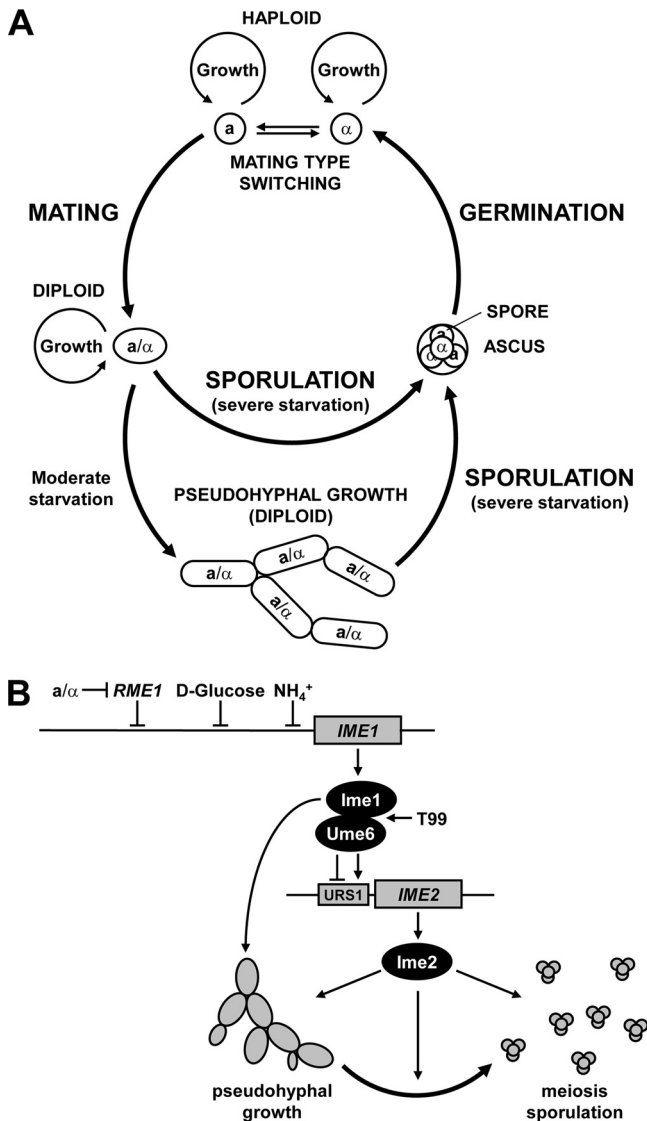
FIG. 9. Control of cell differentiation by the early meiotic cascade. (A) Revised life cycle of *S. cerevisiae* incorporating sporulation of pseudohyphal cells. Haploid **a** and α cells grow and divide in a nutrient-rich environment. Mating type switching allows **a** cells to switch to an α mating type and vice versa. **a** and α cells mate to form an **a**/α diploid cell when exposed to mating pheromones secreted by their opposite mating types. **a**/α diploid cells grow and divide in a nutrient-rich environment. Severe starvation triggers sporulation of **a**/α diploids and formation of an ascus harboring four haploid spores. Moderate starvation triggers pseudohyphal growth, which may allow yeasts to forage for nutrients. Severe starvation of pseudohyphae also induces sporulation. After exposure to nutrients and breakdown of the ascus wall, the spores germinate to form haploid **a** and α cells. (B) Model summarizing how the early meiotic cascade consisting of Ime1, Ume6, and Ime2 regulates cell differentiation in diploid *S. cerevisiae* cells. Starvation of **a**/α diploid cells induces expression of Ime1 and conversion of the transcriptional repressor Ume6 to an activator, leading to induction of early meiotic genes, including *IME2*. Activation of *IME1* and *IME2* is a general differentiation signal that promotes both pseudohyphal growth and meiosis. Induction of pseudohyphal growth or meiosis by Ime1 is abolished by a T99N mutation in Ume6. Modulation of the differentiation signal generated by *IME1* and *IME2* by other, uncharacterized events is expected to govern the choice between pseudohyphal growth and meiosis.

gering degradation of Sic1 (21), an inhibitor of Cdc28 and of the G_1-S transition, suggesting that Ime2 may stimulate pseudohyphal growth by stimulating Sic1 degradation. Nevertheless, future studies are required to identify the Ime2 substrates in pseudohyphal growth.

Sporulation of pseudohyphal cells. In the absence of glucose, pseudohyphae of SK1 cells exit pseudohyphal growth to successfully complete meiosis (Fig. 1). Several models for conversion of pseudohyphal cells into asci are imaginable. Pseudohyphal cells may exit pseudohyphal growth to form normal yeast- or vegetative-growth-form cells which then enter and execute meiosis. Alternatively, pseudohyphal cells may directly exit pseudohyphal growth and enter meiosis. Near-quantitative conversion of filaments into asci within 3 days and the requirement of *IME1* and *IME2* for pseudohyphal growth support the second model. Independent of the precise mechanism of switch from pseudohyphal growth to meiosis, the question arises of which stimulus triggers entry into meiosis by pseudohyphae. A further decrease in nutrient content of the medium caused by metabolic activity of the growing pseudohyphae may induce meiosis. Ascus formation by the tip cell of pseudohyphae (Fig. 1C) provides evidence against such a simple nutrient depletion model. Alternatively, entry into meiosis may be under temporal control. Detailed time-lapse studies will be necessary to establish whether pseudohyphal cells enter meiosis directly or via prior formation of yeast-form cells. Asci sometimes displayed a linear arrangement of two to four spores. This ascus morphology has been observed previously in *Saccharomyces ludwigii* (36) and after sporulation of newly formed zygotes of *S. cerevisiae* (103).

Role of cAMP signaling in pseudohyphal growth. Stimulation of pseudohyphal growth in the presence of nonfermentable carbon sources in SK1 cells contrasts with the behavior of Σ1278b cells, in which nonfermentable carbon sources inhibited pseudohyphal growth (Fig. 6A). cAMP signaling activity was elevated in Σ1278b cells compared to SK1 cells (Fig. 7), confirming an earlier report (100). Strains with high constitutive PKA activity fail to express *IME1* (60, 62). PKA signaling inhibits Ime1 (80) and Ime2 (22, 76). Therefore, Σ1278b cells may fail to form pseudohyphae on nonfermentable carbon sources because the activation of *IME1* and *IME2* is defective. Both *IME1* and *IME2* provide virtually essential functions for pseudohyphal growth on several nonfermentable carbon sources (Fig. 2). Attenuation of cAMP signaling by deletion of *RAS2*, *GPR1*, or *GPA2* did not rescue pseudohyphal growth of Σ1278b cells on nonfermentable carbon sources (not shown), possibly because *FLO11* expression requires an active cAMP signaling pathway in Σ1278b cells (71, 72, 77). In SK1 cells, *FLO11* expression was induced strongly by acetate (Fig. 8D). In contrast, acetate does not induce *FLO11* in Σ1278b cells (70). This potential uncoupling of *FLO11* expression from the PKA pathway in SK1 cells may allow SK1 cells to attenuate PKA signaling on nonfermentable carbon sources (5, 63) in order to activate *IME1* and *IME2*. Two isoforms of the catalytic subunit of PKA, Tpk1 and Tpk3, have negative roles in pseudohyphal growth (71, 77), indicating that Tpk1 or Tpk3 may target *IME1* or *IME2* to inhibit pseudohyphal growth on nonfermentable carbon sources.

Several lines of evidence suggest that Ime1 and Ime2 act independently of Flo11 in pseudohyphal growth. Haploid in-

vasive growth or agar invasion by diploid cells was not decreased by deletion of *IME1* or *IME2* (Fig. 5A). Deletion of *IME1* did not significantly affect *FLO11* mRNA levels (Fig. 5B). *ime1Δ/ime1Δ* cells and, to a lesser degree, *ime2Δ/ime2Δ* cells displayed cell elongation defects (Fig. 5C). Therefore, Ime1 and Ime2 may act independent of and in parallel to *FLO11* in pseudohyphal growth.

Implications for other yeast species. Ime2 belongs to a family of conserved MAPKs found in all eukaryotes (27, 28), including mammalian MAK, the *Schizosaccharomyces pombe* proteins Mde3 and Pit1, and the *Ustilago maydis* protein kinase Crk1. All family members may function in sexual development. MAK is expressed during spermatogenesis (40, 61), Mde3 and Pit1 are important for the timing of the meiotic divisions and spore morphogenesis (1), Crk1 is required for mating (28), and Ime2 is required for entry into meiotic S phase (21). Our finding that Ime2, Ime1, and Ume6 are required for pseudohyphal growth of *S. cerevisiae* suggests that Ime2 orthologs function in processes other than meiosis, for example, in hyphal development and filamentous growth of pathogenic yeasts, such as *Ustilago maydis*, *Magnaporthe grisea*, and *Candida* species, that undergo dimorphic transitions important for their virulence (9, 49, 50, 86). Indeed, Crk1 is required for hyperpolarized growth of *U. maydis* cells with defects in cAMP signaling (27) and for infection of maize plants (28), and Ume6 is required for hyphal extension in *Candida albicans* (3). Our work provides a motivation to investigate the roles of Ime2 orthologs, and possibly orthologs of other meiotic genes, in pseudohyphal and hyphal growth forms and in the virulence of pathogenic yeast species.

REFERENCES

1. **Abe, H., and C. Shimoda.** 2000. Autoregulated expression of *Schizosaccharomyces pombe* meiosis-specific transcription factor Mei4 and a genome-wide search for its target genes. Genetics **154:**1497–1508.
2. **Alani, E., L. Cao, and N. Kleckner.** 1987. A method for gene disruption that allows repeated use of *URA3* selection in the construction of multiply disrupted yeast strains. Genetics **116:**541–545.
3. **Banerjee, M., D. S. Thompson, A. Lazzell, P. L. Carlisle, C. Pierce, C. Monteagudo, J. L. Lopez-Ribot, and D. Kadosh.** 2008. *UME6*, a novel filament-specific regulator of *Candida albicans* hyphal extension and virulence. Mol. Biol. Cell **19:**1354–1365.
4. **Benjamin, K. R., C. Zhang, K. M. Shokat, and I. Herskowitz.** 2003. Control of landmark events in meiosis by the CDK Cdc28 and the meiosis-specific kinase Ime2. Genes Dev. **17:**1524–1539.
5. **Beullens, M., K. Mbonyi, L. Geerts, D. Gladines, K. Detremerie, A. W. Jans, and J. M. Thevelein.** 1988. Studies on the mechanism of the glucose-induced cAMP signal in glycolysis and glucose repression mutants of the yeast *Saccharomyces cerevisiae*. Eur. J. Biochem. **172:**227–231.
6. **Blacketer, M. J., P. Madaule, and A. M. Myers.** 1995. Mutational analysis of morphologic differentiation in *Saccharomyces cerevisiae*. Genetics **140:**1259–1275.
7. **Boeckstaens, M., B. Andre, and A. M. Marini.** 2007. The yeast ammonium transport protein Mep2 and its positive regulator, the Npr1 kinase, play an important role in normal and pseudohyphal growth on various nitrogen media through retrieval of excreted ammonium. Mol. Microbiol. **64:**534–546.
8. **Bolte, M., P. Steigemann, G. H. Braus, and S. Irniger.** 2002. Inhibition of APC-mediated proteolysis by the meiosis-specific protein kinase Ime2. Proc. Natl. Acad. Sci. U. S. A. **99:**4385–4390.
9. **Borges-Walmsley, M. I., and A. R. Walmsley.** 2000. cAMP signalling in pathogenic fungi: control of dimorphic switching and pathogenicity. Trends Microbiol. **8:**133–141.
10. **Bowdish, K. S., and A. P. Mitchell.** 1993. Bipartite structure of an early meiotic upstream activation sequence from *Saccharomyces cerevisiae*. Mol. Cell. Biol. **13:**2172–2181.
11. **Bowdish, K. S., H. E. Yuan, and A. P. Mitchell.** 1995. Positive control of yeast meiotic genes by the negative regulator UME6. Mol. Cell. Biol. **15:**2955–2961.
12. **Cameron, S., L. Levin, M. Zoller, and M. Wigler.** 1988. cAMP-independent control of sporulation, glycogen metabolism, and heat shock resistance in S. cerevisiae. Cell **53:**555–566.
13. **Cannon, J. F., and K. Tatchell.** 1987. Characterization of *Saccharomyces cerevisiae* genes encoding subunits of cyclic AMP-dependent protein kinase. Mol. Cell. Biol. **7:**2653–2663.
14. **Chant, J., and J. R. Pringle.** 1995. Patterns of bud-site selection in the yeast *Saccharomyces cerevisiae*. J. Cell Biol. **129:**751–765.
15. **Chen, D.-C., B.-C. Yang, and T.-T. Kuo.** 1992. One-step transformation of yeast in stationary phase. Curr. Genet. **21:**83–84.
16. **Chu, S., J. DeRisi, M. Eisen, J. Mulholland, D. Botstein, P. O. Brown, and I. Herskowitz.** 1998. The transcriptional program of sporulation in budding yeast. Science **282:**699–705.
17. **Clifford, D. M., S. M. Marinco, and G. S. Brush.** 2004. The meiosis-specific protein kinase Ime2 directs phosphorylation of replication protein A. J. Biol. Chem. **279:**6163–6170.
18. **Clifford, D. M., K. E. Stark, K. E. Gardner, S. Hoffmann-Benning, and G. S. Brush.** 2005. Mechanistic insight into the Cdc28-related protein kinase Ime2 through analysis of replication protein A phosphorylation. Cell Cycle **4:**1826–1833.
19. **Covitz, P. A., I. Herskowitz, and A. P. Mitchell.** 1991. The yeast *RME1* gene encodes a putative zinc finger protein that is directly repressed by a1-α2. Genes Dev. **5:**1982–1989.
20. **Cullen, P. J., W. Sabbagh, Jr., E. Graham, M. M. Irick, E. K. van Olden, C. Neal, J. Delrow, L. Bardwell, and G. F. Sprague, Jr.** 2004. A signaling mucin at the head of the Cdc42- and MAPK-dependent filamentous growth pathway in yeast. Genes Dev. **18:**1695–1708.
21. **Dirick, L., L. Goetsch, G. Ammerer, and B. Byers.** 1998. Regulation of meiotic S phase by Ime2 and a Clb5,6-associated kinase in *Saccharomyces cerevisiae*. Science **281:**1854–1857.
22. **Donzeau, M., and W. Bandlow.** 1999. The yeast trimeric guanine nucleotide-binding protein α subunit, Gpa2p, controls the meiosis-specific kinase Ime2p activity in response to nutrients. Mol. Cell. Biol. **19:**6110–6119.
23. **Eraso, P., and J. M. Gancedo.** 1984. Catabolite repression in yeasts is not associated with low levels of cAMP. Eur. J. Biochem. **141:**195–198.
24. **Fox, T. D., L. S. Folley, J. J. Mulero, T. W. McMullin, P. E. Thorsness, L. O. Hedin, and M. C. Costanzo.** 1991. Analysis and manipulation of yeast mitochondrial genes. Methods Enzymol. **194:**149–165.
25. **Frydlova, I., I. Malcova, P. Vasicova, and J. Hasek.** 2009. Deregulation of *DSE1* gene expression results in aberrant budding within the birth scar and cell wall integrity pathway activation in *Saccharomyces cerevisiae*. Eukaryot. Cell **8:**586–594.
26. **Gagiano, M., F. F. Bauer, and I. S. Pretorius.** 2002. The sensing of nutritional status and the relationship to filamentous growth in *Saccharomyces cerevisiae*. FEMS Yeast Res. **2:**433–470.
27. **Garrido, E., and J. Perez-Martin.** 2003. The *crk1* gene encodes an Ime2-related protein that is required for morphogenesis in the plant pathogen *Ustilago maydis*. Mol. Microbiol. **47:**729–743.
28. **Garrido, E., U. Voss, P. Müller, S. Castillo-Lluva, R. Kahmann, and J. Pérez-Martín.** 2004. The induction of sexual development and virulence in the smut fungus *Ustilago maydis* depends on Crk1, a novel MAPK protein. Genes Dev. **18:**3117–3130.
29. **Gavrias, V., A. Andrianopoulos, C. J. Gimeno, and W. E. Timberlake.** 1996. *Saccharomyces cerevisiae TEC1* is required for pseudohyphal growth. Mol. Microbiol. **19:**1255–1263.
30. **Gimeno, C. J., P. O. Ljungdahl, C. A. Styles, and G. R. Fink.** 1992. Unipolar cell divisions in the yeast S. cerevisiae lead to filamentous growth: regulation by starvation and RAS. Cell **68:**1077–1090.
31. **Goldmark, J. P., T. G. Fazzio, P. W. Estep, G. M. Church, and T. Tsukiyama.** 2000. The Isw2 chromatin remodeling complex represses early meiotic genes upon recruitment by Ume6p. Cell **103:**423–433.
32. **Goldstein, A. L., and J. H. McCusker.** 1999. Three new dominant drug resistance cassettes for gene disruption in *Saccharomyces cerevisiae*. Yeast **15:**1541–1553.
33. **Guo, B., C. A. Styles, Q. Feng, and G. R. Fink.** 2000. A Saccharomyces gene

family involved in invasive growth, cell-cell adhesion, and mating. Proc. Natl. Acad. Sci. U. S. A. **97:**12158–12163.

34. **Guttmann-Raviv, N., S. Martin, and Y. Kassir.** 2002. Ime2, a meiosis-specific kinase in yeast, is required for destabilization of its transcriptional activator, Ime1. Mol. Cell. Biol. **22:**2047–2056.

35. **Hardwick, J. S., F. G. Kuruvilla, J. K. Tong, A. F. Shamji, and S. L. Schreiber.** 1999. Rapamycin-modulated transcription defines the subset of nutrient-sensitive signaling pathways directly controlled by the Tor proteins. Proc. Natl. Acad. Sci. U. S. A. **96:**14866–14870.

36. **Hawthorne, D. C.** 1955. The use of linear asci for chromosome mapping in *Saccharomyces.* Genetics **40:**511–518.

37. **Horecka, J., and Y. Jigami.** 1999. The *trp1-ΔFA* designer deletion for PCR-based gene functional analysis in *Saccharomyces cerevisiae.* Yeast **15:**1769–1774.

38. **Huxley, C., E. D. Green, and I. Dunham.** 1990. Rapid assessment of *S. cerevisiae* mating type by PCR. Trends Genet. **6:**236.

39. **Inai, T., M. Yukawa, and E. Tsuchiya.** 2007. Interplay between chromatin and *trans*-acting factors on the *IME2* promoter upon induction of the gene at the onset of meiosis. Mol. Cell. Biol. **27:**1254–1263.

40. **Jinno, A., K. Tanaka, H. Matsushime, T. Haneji, and M. Shibuya.** 1993. Testis-specific Mak protein kinase is expressed specifically in the meiotic phase in spermatogenesis and is associated with a 210-kilodalton cellular phosphoprotein. Mol. Cell. Biol. **13:**4146–4156.

41. **Kadosh, D., and K. Struhl.** 1997. Repression by Ume6 involves recruitment of a complex containing Sin3 corepressor and Rpd3 histone deacetylase to target promoters. Cell **89:**365–371.

42. **Kane, S. M., and R. Roth.** 1974. Carbohydrate metabolism during ascospore development in yeast. J. Bacteriol. **118:**8–14.

43. **Kassir, Y., D. Granot, and G. Simchen.** 1988. *IME1*, a positive regulator gene of meiosis in S. cerevisiae. Cell **52:**853–862.

44. **Kawaguchi, H., M. Yoshida, and I. Yamashita.** 1992. Nutritional regulation of meiosis-specific gene expression in *Saccharomyces cerevisiae.* Biosci. Biotechnol. Biochem. **56:**289–297.

45. **Kron, S. J., C. A. Styles, and G. R. Fink.** 1994. Symmetric cell division in pseudohyphae of the yeast *Saccharomyces cerevisiae.* Mol. Biol. Cell **5:**1003–1022.

46. **Kübler, E., H. U. Mösch, S. Rupp, and M. P. Lisanti.** 1997. Gpa2p, a G-protein α-subunit, regulates growth and pseudohyphal development in *Saccharomyces cerevisiae* via a cAMP-dependent mechanism. J. Biol. Chem. **272:**20321–20323.

47. **Kupiec, M., B. Byers, R. E. Esposito, and A. P. Mitchell.** 1997. Meiosis and sporulation in Saccharomyces cerevisiae, p. 889–1036. *In* J. R. Pringle, J. R. Broach, and E. W. Jones (ed.), The molecular and cellular biology of the yeast Saccharomyces, vol. 3. Cold Spring Harbor Laboratory Press, Plainview, NY.

48. **Law, D. T., and J. Segall.** 1988. The *SPS100* gene of *Saccharomyces cerevisiae* is activated late in the sporulation process and contributes to spore wall maturation. Mol. Cell. Biol. **8:**912–922.

49. **Lee, N., C. A. D'Souza, and J. W. Kronstad.** 2003. Of smuts, blasts, mildews, and blights: cAMP signaling in phytopathogenic fungi. Annu. Rev. Phytopathol. **41:**399–427.

50. **Lengeler, K. B., R. C. Davidson, C. D'Souza, T. Harashima, W. C. Shen, P. Wang, X. Pan, M. Waugh, and J. Heitman.** 2000. Signal transduction cascades regulating fungal development and virulence. Microbiol. Mol. Biol. Rev. **64:**746–785.

51. **Lo, W. S., and A. M. Dranginis.** 1998. The cell surface flocculin Flo11 is required for pseudohyphae formation and invasion by *Saccharomyces cerevisiae.* Mol. Biol. Cell **9:**161–171.

52. **Lorenz, M. C., N. S. Cutler, and J. Heitman.** 2000. Characterization of alcohol-induced filamentous growth in *Saccharomyces cerevisiae.* Mol. Biol. Cell **11:**183–199.

53. **Lorenz, M. C., and J. Heitman.** 1998. The MEP2 ammonium permease regulates pseudohyphal differentiation in *Saccharomyces cerevisiae.* EMBO J. **17:**1236–1247.

54. **Lorenz, M. C., and J. Heitman.** 1997. Yeast pseudohyphal growth is regulated by GPA2, a G protein α homolog. EMBO J. **16:**7008–7018.

55. **Lorenz, M. C., X. Pan, T. Harashima, M. E. Cardenas, Y. Xue, J. P. Hirsch, and J. Heitman.** 2000. The G protein-coupled receptor Gpr1 is a nutrient sensor that regulates pseudohyphal differentiation in *Saccharomyces cerevisiae.* Genetics **154:**609–622.

56. **Madhani, H. D., and G. R. Fink.** 1998. The riddle of MAP kinase signaling specificity. Trends Genet. **14:**151–155.

57. **Malathi, K., Y. Xiao, and A. P. Mitchell.** 1999. Catalytic roles of yeast GSK3β/shaggy homolog Rim11p in meiotic activation. Genetics **153:**1145–1152.

58. **Malathi, K., Y. Xiao, and A. P. Mitchell.** 1997. Interaction of yeast repressor-activator protein Ume6p with glycogen synthase kinase 3 homolog Rim11p. Mol. Cell. Biol. **17:**7230–7236.

59. **Mallory, M. J., K. F. Cooper, and R. Strich.** 2007. Meiosis-specific destruction of the Ume6p repressor by the Cdc20-directed APC/C. Mol. Cell **27:**951–961.

60. **Matsumoto, K., I. Uno, and T. Ishikawa.** 1983. Initiation of meiosis in yeast mutants defective in adenylate cyclase and cyclic AMP-dependent protein kinase. Cell **32:**417–423.

61. **Matsushime, H., A. Jinno, N. Takagi, and M. Shibuya.** 1990. A novel mammalian protein kinase gene (*mak*) is highly expressed in testicular germ cells at and after meiosis. Mol. Cell. Biol. **10:**2261–2268.

62. **Matsuura, A., M. Treinin, H. Mitsuzawa, Y. Kassir, I. Uno, and G. Simchen.** 1990. The adenylate cyclase/protein kinase cascade regulates entry into meiosis in *Saccharomyces cerevisiae* through the gene *IME1.* EMBO J. **9:**3225–3232.

63. **Mbonyi, K., and J. M. Thevelein.** 1988. The high-affinity glucose uptake system is not required for induction of the RAS-mediated cAMP signal by glucose in cells of the yeast Saccharomyces cerevisiae. Biochim. Biophys. Acta **971:**223–226.

64. **Mitchell, A. P., S. E. Driscoll, and H. E. Smith.** 1990. Positive control of sporulation-specific genes by the *IME1* and *IME2* products in *Saccharomyces cerevisiae.* Mol. Cell. Biol. **10:**2104–2110.

65. **Moore, M., M. E. Shin, A. Bruning, K. Schindler, A. Vershon, and E. Winter.** 2007. Arg-Pro-X-Ser/Thr is a consensus phosphoacceptor sequence for the meiosis-specific Ime2 protein kinase in *Saccharomyces cerevisiae.* Biochemistry **46:**271–278.

66. **Mösch, H.-U., R. L. Roberts, and G. R. Fink.** 1996. Ras2 signals via the Cdc42/Ste20/mitogen-activated protein kinase module to induce filamentous growth in *Saccharomyces cerevisiae.* Proc. Natl. Acad. Sci. U. S. A. **93:**5352–5356.

67. **Nazar, R. N., H. G. Lawford, and J.-T. Wong.** 1970. An improved procedure for extraction and analysis of cellular nucleotides. Anal. Biochem. **35:**305–313.

68. **Neigeborn, L., and A. P. Mitchell.** 1991. The yeast *MCK1* gene encodes a protein kinase homolog that activates early meiotic gene expression. Genes Dev. **5:**533–548.

69. **Pak, J., and J. Segall.** 2002. Regulation of the premiddle and middle phases of expression of the *NDT80* gene during sporulation of *Saccharomyces cerevisiae.* Mol. Cell. Biol. **22:**6417–6429.

70. **Palecek, S. P., A. S. Parikh, J. H. Huh, and S. J. Kron.** 2002. Depression of *Saccharomyces cerevisiae* invasive growth on non-glucose carbon sources requires the Snf1 kinase. Mol. Microbiol. **45:**453–469.

71. **Pan, X., and J. Heitman.** 1999. Cyclic AMP-dependent protein kinase regulates pseudohyphal differentiation in *Saccharomyces cerevisiae.* Mol. Cell. Biol. **19:**4874–4887.

72. **Pan, X., and J. Heitman.** 2002. Protein kinase A operates a molecular switch that governs yeast pseudohyphal differentiation. Mol. Cell. Biol. **22:**3981–3993.

73. **Parrou, J. L., M. A. Teste, and J. François.** 1997. Effects of various types of stress on the metabolism of reserve carbohydrates in *Saccharomyces cerevisiae*: genetic evidence for a stress-induced recycling of glycogen and trehalose. Microbiology **143:**1891–1900.

74. **Primig, M., R. M. Williams, E. A. Winzeler, G. G. Tevzadze, A. R. Conway, S. Y. Hwang, R. W. Davis, and R. E. Esposito.** 2000. The core meiotic transcriptome in budding yeasts. Nat. Genet. **26:**415–423.

75. **Pringle, J. R.** 1991. Staining of bud scars and other cell wall chitin with calcofluor. Methods Enzymol. **194:**732–735.

76. **Purnapatre, K., M. Gray, S. Piccirillo, and S. M. Honigberg.** 2005. Glucose inhibits meiotic DNA replication through SCF^Grr1p-dependent destruction of Ime2p kinase. Mol. Cell. Biol. **25:**440–450.

77. **Robertson, L. S., and G. R. Fink.** 1998. The three yeast A kinases have specific signaling functions in pseudohyphal growth. Proc. Natl. Acad. Sci. U. S. A. **95:**13783–13787.

78. **Rose, M., and F. Winston.** 1984. Identification of a Ty insertion within the coding sequence of the *S. cerevisiae URA3* gene. Mol. Gen. Genet. **193:**557–560.

79. **Rubin-Bejerano, I., S. Mandel, K. Robzyk, and Y. Kassir.** 1996. Induction of meiosis in *Saccharomyces cerevisiae* depends on conversion of the transcriptional repressor Ume6 to a positive regulator by its regulated association with the transcriptional activator Ime1. Mol. Cell. Biol. **16:**2518–2526.

80. **Rubin-Bejerano, I., S. Sagee, O. Friedman, L. Pnueli, and Y. Kassir.** 2004. The in vivo activity of Ime1, the key transcriptional activator of meiosis-specific genes in *Saccharomyces cerevisiae*, is inhibited by the cyclic AMP/protein kinase A signal pathway through the glycogen synthase kinase 3-β homolog Rim11. Mol. Cell. Biol. **24:**6967–6979.

81. **Rubinstein, A., V. Gurevich, Z. Kasulin-Boneh, L. Pnueli, Y. Kassir, and R. Y. Pinter.** 2007. Faithful modeling of transient expression and its application to elucidating negative feedback regulation. Proc. Natl. Acad. Sci. U. S. A. **104:**6241–6246.

82. **Rupp, S., E. Summers, H. J. Lo, H. Madhani, and G. Fink.** 1999. MAP kinase and cAMP filamentation signaling pathways converge on the unusually large promoter of the yeast *FLO11* gene. EMBO J. **18:**1257–1269.

83. **Rutherford, J. C., G. Chua, T. Hughes, M. E. Cardenas, and J. Heitman.** 2008. An Mep2-dependent transcriptional profile links permease function to gene expression during pseudohyphal growth in *Saccharomyces cerevisiae.* Mol. Biol. Cell **19:**3028–3039.

84. **Sáez, M. J., and R. Lagunas.** 1976. Determination of intermediary metab-

olites in yeast. Critical examination of the effect of sampling conditions and recommendations for obtaining true levels. Mol. Cell. Biochem. **13:**73–78.

85. **Sagee, S., A. Sherman, G. Shenhar, K. Robzyk, N. Ben-Doy, G. Simchen, and Y. Kassir.** 1998. Multiple and distinct activation and repression sequences mediate the regulated transcription of *IME1*, a transcriptional activator of meiosis-specific genes in *Saccharomyces cerevisiae*. Mol. Cell. Biol. **18:**1985–1995.

86. **Sánchez-Martínez, C., and J. Pérez-Martín.** 2001. Dimorphism in fungal pathogens: *Candida albicans* and *Ustilago maydis*—similar inputs, different outputs. Curr. Opin. Microbiol. **4:**214–221.

87. **Santangelo, G. M.** 2006. Glucose signaling in *Saccharomyces cerevisiae*. Microbiol. Mol. Biol. Rev. **70:**253–282.

88. **Sari, F., M. Heinrich, W. Meyer, G. H. Braus, and S. Irniger.** 2008. The C-terminal region of the meiosis-specific protein kinase Ime2 mediates protein instability and is required for normal spore formation in budding yeast. J. Mol. Biol. **378:**31–43.

89. **Schindler, K., K. R. Benjamin, A. Martin, A. Boglioli, I. Herskowitz, and E. Winter.** 2003. The Cdk-activating kinase Cak1p promotes meiotic S phase through Ime2p. Mol. Cell. Biol. **23:**8718–8728.

90. **Schlanderer, G., and H. Dellweg.** 1974. Cyclic AMP and catabolite repression in yeasts. In *Schizosaccharomyces pombe* glucose lowers both intracellular adenosine 3′:5′-monophosphate levels and the activity of catabolite-sensitive enzymes. Eur. J. Biochem. **49:**305–316.

91. **Schröder, M., J. S. Chang, and R. J. Kaufman.** 2000. The unfolded protein response represses nitrogen-starvation induced developmental differentiation in yeast. Genes Dev. **14:**2962–2975.

92. **Schröder, M., R. Clark, C. Y. Liu, and R. J. Kaufman.** 2004. The unfolded protein response represses differentiation through the *RPD3-SIN3* histone deacetylase. EMBO J. **23:**2281–2292.

93. **Schüller, H. J.** 2003. Transcriptional control of nonfermentative metabolism in the yeast *Saccharomyces cerevisiae*. Curr. Genet. **43:**139–160.

94. **Sedgwick, C., M. Rawluk, J. Decesare, S. Raithatha, J. Wohlschlegel, P. Semchuk, M. Ellison, J. Yates III, and D. Stuart.** 2006. Saccharomyces cerevisiae Ime2 phosphorylates Sic1 at multiple PXS/T sites but is insufficient to trigger Sic1 degradation. Biochem. J. **399:**151–160.

95. **Shefer-Vaida, M., A. Sherman, T. Ashkenazi, K. Robzyk, and Y. Kassir.** 1995. Positive and negative feedback loops affect the transcription of Ime1, a positive regulator of meiosis in *Saccharomyces cerevisiae*. Dev. Genet. **16:**219–228.

96. **Sia, R. A. L., and A. P. Mitchell.** 1995. Stimulation of later functions of the yeast meiotic protein kinase Ime2p by the *IDS2* gene product. Mol. Cell. Biol. **15:**5279–5287.

97. **Sikorski, R. S., and P. Hieter.** 1989. A system of shuttle vectors and yeast host strains designed for efficient manipulation of DNA in *Saccharomyces cerevisiae*. Genetics **122:**19–27.

98. **Smith, H. E., S. E. Driscoll, R. A. L. Sia, H. E. Yuan, and A. P. Mitchell.** 1993. Genetic evidence for transcriptional activation by the yeast *IME1* gene product. Genetics **133:**775–784.

99. **Smith, H. E., and A. P. Mitchell.** 1989. A transcriptional cascade governs entry into meiosis in *Saccharomyces cerevisiae*. Mol. Cell. Biol. **9:**2142–2152.

100. **Stanhill, A., N. Schick, and D. Engelberg.** 1999. The yeast ras/cyclic AMP pathway induces invasive growth by suppressing the cellular stress response. Mol. Cell. Biol. **19:**7529–7538.

101. **Strich, R., R. T. Surosky, C. Steber, E. Dubois, F. Messenguy, and R. E. Esposito.** 1994. UME6 is a key regulator of nitrogen repression and meiotic development. Genes Dev. **8:**796–810.

102. **Tamaki, H., T. Miwa, M. Shinozaki, M. Saito, C. W. Yun, K. Yamamoto, and H. Kumagai.** 2000. *GPR1* regulates filamentous growth through *FLO11* in yeast *Saccharomyces cerevisiae*. Biochem. Biophys. Res. Commun. **267:**164–168.

103. **Thomas, J. H., and D. Botstein.** 1987. Ordered linear tetrads are produced by the sporulation of newly formed zygotes of *Saccharomyces cerevisiae*. Genetics **115:**229–232.

104. **Toda, T., S. Cameron, P. Sass, M. Zoller, J. D. Scott, B. McMullen, M. Hurwitz, E. G. Krebs, and M. Wigler.** 1987. Cloning and characterization of *BCY1*, a locus encoding a regulatory subunit of the cyclic AMP-dependent protein kinase in *Saccharomyces cerevisiae*. Mol. Cell. Biol. **7:**1371–1377.

105. **Toda, T., I. Uno, T. Ishikawa, S. Powers, T. Kataoka, D. Broek, S. Cameron, J. Broach, K. Matsumoto, and M. Wigler.** 1985. In yeast, RAS proteins are controlling elements of adenylate cyclase. Cell **40:**27–36.

106. **Vidan, S., and A. P. Mitchell.** 1997. Stimulation of yeast meiotic gene expression by the glucose-repressible protein kinase Rim15p. Mol. Cell. Biol. **17:**2688–2697.

107. **Wach, A., A. Brachat, R. Pöhlmann, and P. Philippsen.** 1994. New heterologous modules for classical or PCR-based gene disruptions in *Saccharomyces cerevisiae*. Yeast **10:**1793–1808.

108. **Ward, M. P., C. J. Gimeno, G. R. Fink, and S. Garrett.** 1995. *SOK2* may regulate cyclic AMP-dependent protein kinase-stimulated growth and pseudohyphal development by repressing transcription. Mol. Cell. Biol. **15:**6854–6863.

109. **Washburn, B. K., and R. E. Esposito.** 2001. Identification of the Sin3-binding site in Ume6 defines a two-step process for conversion of Ume6 from a transcriptional repressor to an activator in yeast. Mol. Cell. Biol. **21:**2057–2069.

110. **Xiao, Y., and A. P. Mitchell.** 2000. Shared roles of yeast glycogen synthase kinase 3 family members in nitrogen-responsive phosphorylation of meiotic regulator Ume6p. Mol. Cell. Biol. **20:**5447–5453.

111. **Xue, Y., M. Batlle, and J. P. Hirsch.** 1998. *GPR1* encodes a putative G protein-coupled receptor that associates with the Gpa2p Gα subunit and functions in a Ras-independent pathway. EMBO J. **17:**1996–2007.